Virus-Like Particles (VLPs) Platform for the Development of an Effective Melanoma Vaccine

---

A thesis submitted in fulfillment of the requirements for the degree of

Doctor of Philosophy in Clinical Medicine

Mona Omar Mohsen

Kellogg College

The Jenner Institute
Nuffield Department of Clinical Medicine
University of Oxford

Word Count ~ 39,467 (excl. References)

A word of Thanks

First and outmost, I would like to gratefully acknowledge the funding I have received towards my DPhil studies from Qatar Science Leadership Program (QRLP). QRLP gave me the chance to explore the world leading quality research of excellence at the University of Oxford.

Acknowledges to our role-model, Her Highness Sheikha Moza Bint Nasser Al-Missned and Her Excellency Sheikha Hind Bint Hamad Al Thani –The Chief Executive Officer of Qatar Foundation- for giving me the opportunity to be part of this capacity-building institute in Qatar aiming to produce homegrown scientists.

A special and sincere thanks to QRLP directors, managers and team; Dr. Aisha Al-Obaidly –Capacity Building Director-, Dr. Ayman Bassil –Head of Research Training- and Nuha Al-Okka - Senior Research Coordinator- for their continuous, nonstop support.

I am looking forward to making a contribution and an impact in cancer immunology research field in my country (State of Qatar).

Acknowledgement

I would like to express my truthful gratitude to my great supervisor Prof. Martin Bachmann for his continuous and constant support in my DPhil study. His motivation, patience, high standard of knowledge and guidance assisted me in my research and I could not have imagined having a greater mentor in my DPhil journey. Besides, I would like to thank my thesis committee: Prof. Helen McShane and Prof. Thomas Kündig for their intuitive and insightful encouragement and help.

I am very grateful to Prof. Robert Gilbert, the director of graduate studies at the Nuffield department of medicine, who has shown patience, remarkable support and helped me overcoming many obstacles through my studies.

I am also very indebted to Prof. Alexander Knuth and Dr. Said Demime at the National Center for Cancer Care and Research at Hamad Medical Corporation in Qatar.

Not to forget my colleagues at University of Oxford, Dr. Aadil El-Turabi, Dr. Gustavo Cabral-de Miranda and Ariane Gomes for their permanent help, stimulating discussion, the sleepless nights in the lab and the joyful moments we have spent together. They are a real family to me.

I would like to thank our collaborators at the University of Bern, who have contributed to this work and made it possible. Prof. Monique Vogel, who has welcomed me in the lab and facilitated my work by all possible means.

Moreover, I would thank my amazing colleagues at the University of Bern: Dr. Lisha Zha, Dr. Fabiana Leoratti, Caroline Krueger, Elisa Roesti, Federico Storni, Xinyue Chang, Paul Engeroff, Dr. Tasneem Arsiwala, Marianne Zwicker, David Mueller, Cyrill Lipp, Linda Johr, Elsbeth Keller, Flurin Caviezel and Marc Huldi. Also, my colleagues at University of Zurich: Dr. Antonia Gabriel_Fettelschoss, Dr. Franziska Thoms, Stefanie Haas, Michelle Daniel, Victoria Fettelschoss, Melano Maudrich and Florian Olomski.

Furthermore, I would like to acknowledge the scientists at the University of Oxford who contributed to my work, Dr. Nicola Ternette and Dr. Julius Muller for their expertise in conducting and analysing the data of immunopeptidomics and whole exome sequencing. Without their help, it would be had been hard to manage. A special thanks to Leanne Minall for her valuable advice on using Cu-free click chemistry as a coupling method. Also, Prof. Jens Stein from Theodor Kocher Institute at University of Bern and Marcos Sande from the Institute of anatomy at University of Bern for their expertise and contribution in all the imaging techniques we have done in this work. Daniel Speiser from University of Lausanne I am especially grateful to, as he guided me into the new field of cancer immunology.

I would like to thank Allergy Therapeutics ^{PLC} for their financial and scientific support to conduct part of the work in this thesis and their continuous support and encouraging discussions.

I am very grateful to Andris Zeltins to be an endless source of different VLPs and Paul Pumpens to open my eyes to the beauty of VLPs' symmetry.

A big and warm thank to my precious family, my amazing parents (Omar and Adiba), my brothers (Mahmoud, Ahmed and Dr. Mohammed), my sisters (Sahar and Maha) and my sisters in law (Dr. Alaa, Amoona and Amani) who supported me spiritually during this long and hard journey.

A very big hug to my father, who has been my true inspiration and motivation to pursue my DPhil studies and follow my dreams. A warmhearted thank to my beloved children (Mohammed, Gregor, Reema, Valerie, Rana and Jana). They are my supporting rocks and my stars and I dedicate this work to them. They gave me strength, made me laugh and reminded me always to feel proud for what I have achieved in my life and career.

Table of Content

Abstract

Melanoma is the least common type of skin-cancer but the deadliest one. Cancer immunotherapy is considered a powerful tool in cancer treatment. Nevertheless, therapeutic cancer vaccines have led so far to modest immune responses with little clinical impact. The first part of this work is focused on developing a personalized melanoma vaccine platform based on VLPs and copper-free click chemistry, enabling bedside production of personalized cancer vaccines. There is currently a debate in the field whether cancer-specific, non-mutated germ-line epitopes or mutated neo-epitopes are more powerful antigens for vaccination. To address this issue, we identified melanoma-specific germ-line T-cell epitopes by immunopeptidomic and neoantigens using exome sequencing. Different VLP-based vaccine cocktails were generated, and their immunogenecity was compared in melanoma murine models. We demonstrate that both neoantigens and germ-line epitopes can induce partial protection, but the best therapeutic effect is achieved when combining both. The second part of the thesis tested a new adjuvant microcrystalline tyrosine (MCT) in combination with VLP-based vaccine ($CuMV_{TT}$). MCT, is an adjuvant that has been used in licensed allergen-immunotherapy products for decades. The adjuvant potential of MCT was also compared to Alum and B-type CpGs. MCT was similarly potent as CpGs and clearly superior to Alum when $CD8^+$ T-cell responses and tumour protection were assessed. Combining a micron-sized adjuvant (MC) with nanoparticles ($CuMV_{TT}$) appears a particularly attractive strategy as it optimally harnesses the drainage properties of the immune system. Thus, MCT may not only be used in marketed allergy products but may also be promising for induction of protective CTL response. Finally, we focused on

delivering antigens and adjuvants in separate virus-like particles. This new technique would be beneficial when designing a personalized VLP-based vaccine as it would be handy to have a ready adjuvanted VLP which can be formulated with the patient' vaccine at bed-side.

Mona Mohsen, Kellogg College, Michaelmas Term 2018

Publications List

1) Delivering Adjuvants and Antigens in Separate Nanoparticles Eliminates the Need of Physical Linkage for Effective Vaccination

Mona O. Mohsen, Ariane C. Gomes, Gustavo Cabral-Miranda, Caroline C. Krueger, Fabiana MS Leoratti, Jens V. Stein, Martin F. Bachmann

Journal of control release, 2017 Apr 10;251:92-100. doi: 10.1016/j.jconrel.2017.02.031. Epub 2017 Feb 28.

2) Major Findings and Recent Advances in Virus–Like Particle (VLP)-Based Vaccines

Mona O. Mohsen, Lisha Zha, Gustavo Cabral-Miranda, Martin F. Bachmann

Seminars in Immunology, 2017 Dec;34:123-132. doi: 10.1016/j.smim.2017.08.014. Epub 2017 Sep 5

3) Interaction of Viral Capsid-Derived Virus-Like Particles (VLPs) with the Innate Immune System

Mona O. Mohsen, Ariane C. Gomes, Monique Vogel and Martin F. Bachmann

Vaccines, 2018 Jul 2;6(3). pii: E37. doi: 10.3390/vaccines6030037

4) Harnessing Nanoparticles for Immunomodulation and Vaccines

Ariane C. Gomes, **Mona Mohsen**, and Martin F. Bachmann

Vaccines, 2017 Mar; 5(1): 6. doi: 10.3390/vaccines5010006

5) Microcrystalline Tyrosine (MCT®): A Depot Adjuvant in Licensed Allergy Immunotherapy Offers New Opportunities in Malaria

Cabral-Miranda G, Heath MD, Gomes AC, **Mona O. Mohsen**, Montoya-Diaz E, Salman AM, Atcheson E, Skinner MA, Kramer MF, Reyes-Sandoval A, Bachmann MF

Vaccines, 2017 Sep 27;5(4). pii: E32. doi: 10.3390/vaccines5040032.

6)Virus-Like Particle (VLP) Plus Microcrystalline Tyrosine (MCT®) Adjuvants Enhance Vaccine Efficacy Improving T and B Cell Immunogenicity and Protection against Plasmodium berghei/vivax.

Cabral-Miranda G, Heath MD, **Mohsen MO**, Gomes AC, Engeroff P, Flaxman A, Leoratti FMS, El-Turabi A, Reyes-Sandoval A, Skinner MA, Kramer MF, Bachmann MF.
Vaccines, 2017 May 2;5(2). pii: E10. doi: 10.3390/vaccines5020010.

7) Therapeutic Silence of Pleiotrophin by Targeted Delivery of siRNA and its Effect on the Inhibition of Tumor Growth and Metastasis.
Zha L, He L, Xie W, Cheng J, Li T, **Mohsen MO**, Lei F, Storni F, Bachmann M, Chen H, Zhang Y.
PloS One. 2017 May 31;12(5):e0177964. doi: 10.1371/journal.pone.0177964. eCollection 2017.

8) An Unexpected Protective Role of Low-Affinity Allergen-Specific IgG through the Inhibitory Receptor FcγRIIb.
Zha L, Leoratti FMS, He L, **Mohsen MO**, Cragg M, Storni F, Vogel M, Bachmann MF.
Journal of Allergy and Clinical Immunology. 2018 Jan 31. pii: S0091-6749(18)30037-X. doi: 10.1016/j.jaci.2017.09.054.

9) New 3-Cyano-2-Substituted Pyridines Induce Apoptosis in MCF 7 Breast Cancer Cells (Master Degree)
Malki A, **Mohsen M**, Aziz H, Rizk O, Shaban O, El-Sayed M, Sherif ZA, Ashour H.
Molecules. 2016 Feb 18;21(2). pii: E230. doi: 10.3390/molecules21020230.

Potential additional publications from this thesis

1. Targeting germline and mutated epitopes enhances the immunogenicity of a preclinical model of personalized VLP-based vaccine

2. Vaccination with nanoparticles combined with micro-adjuvants protects against cancer

Overview over Experimental Chapters

Chapter 2: Targeting germline and mutated epitopes enhances the immunogenicity of a preclinical model of personalized VLP-based vaccine

This chapter describes the development of a platform for the generation of precision virus-like particle (VLP)-based cancer vaccines. Immunopeptidomics and whole exome sequencing approaches have been used to identify B16F10 melanoma specific T-cell epitopes (non-mutated germ-line and mutated neo-epitopes respectively). The identified epitopes were then prioritized by bioinformatics and *in vitro* T-cell experiments. Bio-orthogonal Cu-free click chemistry was used to couple the selected epitopes to Qβ-VLP loaded with B-type CpGs, a potent immune-stimulator. Different VLP-based vaccine cocktails have been prepared accordingly and their immunogenecity was compared in murine models bearing the aggressive B16F10p33 melanomas.

Chapter 3: Vaccination with nanoparticles combined with micro-adjuvants protects against cancer

This chapter studies the immunogenecity of $CuMV_{TT}$-VLP (Cucumber-mosaic virus genetically incorporating tetanus-toxoid universal T cell epitope) displaying p33 epitope and formulated with microcrystalline tyrosine (MCT®) adjuvant in inducing specific T-cell response in B16F10p33 murine melanoma model. The depot-forming effect of MCT adjuvant with/ without formulation with $CuMV_{TT}$-VLP vaccine was also studied. Furthermore, the adjuvant potential of MCT was compared to the widely used adjuvant Alum and the potent immunostimulatory molecules (B-type CpGs).

Chapter 4: Delivering adjuvants and antigens in separate nanoparticles eliminates the need of physical linkage for effective vaccination

This chapter assessed the efficiency of delivering adjuvants and antigens in separate nanoparticles and compared the obtained results to the conventional standard method which suggests that adjuvants and antigens should be in close proximity (physically linked) for optimal vaccination. The kinetics of mixed VLPs in the draining lymph node was assessed and again compared to the standard method. Furthermore, the induction of specific T-cell response in both methods was also assessed and compared.

Published: M.O. Mohsen et al. / Journal of Controlled Release 251 (2017) 92–100

List of Figures

List of Tables

List of Abbreviations

A

APC	Antigen-Presenting Cell
Alum	Aluminum Hydroxide
AF	Alexa Flour
Asp	Aspartic Acid
Asn	Asparagine
Ag	Antigen
Ab	Antibody
AP-1	Activator Protein-1

B

BMDC	Bone-Marrow Derived Dendritic Cell

C

cDC	Conventional Dendritic Cell
pDC	Plasmacytoid Dendritic Cell
CTL	Cytotoxic T-lymphocyte
Cu-free click chemistry	Copper-Free Click Chemistry
CMV	Cucumber-Mosaic Virus
$CuMV_{TT}$- VLP	Cucumber-Mosaic Virus incorporating Tetanus-Toxoid Epitope Virus-Like Particle
CCMV	Cowpea Chlorotic Mosaic Virus
CPMV	Cowpea Mosaic Virus
CpGs	Oligonucleotides Rich in CG Motifs
Cys	Cysteine

CTLA4	Cytotoxic T-Lymphocyte Associated Protein 4
ALVAC	Canarypox Virus Vector
D	
DC	Dendritic Cell
pDC	Plasmacytoid Dendritic Cell
cDC	Conventional Dendritic Cell
DBCO	Dibenzocyclooctyne
DMSO	Dimethyl Sulfoxide
DNA	Deoxyribonucleic Acid
DNase	Deoxyribonuclease
E	
E. coli	Escherichia Coli
ER	Endoplasmic Reticulum
G	
GL	Germ-Line
Glu	Glutamic Acid
Gln	Glutamine
GM-CSF	Granulocyte-Macrophage Colony-Stimulating Factor
H	
HLA	Human Leukocyte Antigen
HPV	Human Papilloma Virus
HBV	Hepatitis B-virus
HSV	Herpes Simplex Virus
I	

IFN-γ	Interferon Gamma
ITH	Intra-Tumour Heterogeneity
IL-2	Interleukin 2
irAEs	Immune-Related Adverse Events
IRF	Interferon Regulatory Factor
i.v.	Intravenous
K	
kDa	Kilo Dalton
L	
LN	Lymph Node
LCMV	Lymphocytic-Choriomeningitis Virus
Lys	Lysine
M	
MHC-I	Major-Histocompatibility Class I
MHC-II	Major-Histocompatibility Class II
MCT	Microcrystalline Tyrosine
M	Molar
Mg	Milligram
Mm	Millimeter
Ml	Milliliter
μm	Micrometer
μM	Micromolar
mM	Millimolar
MWCO	Molecular Weight Cut-Off
MTV	Multi-Target Vaccine

MDSC	Myeloid-Derived Suppressor Cell
MVA	Modified Vaccinia Ankara
mAb	Monoclonal Antibody
MITD	MHC-I Trafficking Domain
Mb	Megabase
N	
Nm	Nanometer
NF-κB	Nuclear Factor kappa-Light Chain Enhancer of Activated B cells
O	
ORR	Objective Response Rate
P	
PAMP	Pathogen-Associated Molecular Pattern
PASP	Pathogen-Associated Structural Pattern
PRR	Pathogen-Recognition Receptor
PET	Positron-Emission Tomography
PSA	Prostate-Specific Antigen
PD-1	Programmed Cell-Death Protein 1
PD-L1	Programmed Death Ligand 1
PBMC	Peripheral Blood Mononuclear Cell
pMHC	Peptide-Loaded MHC
R	
RNA	Ribonucleic acid
RNase	Ribonuclease
S	

SMPH	Succinimidyl-6-maleimidopropionamido hexanoate
SP	Signal Peptide
SNV	Single Nucleotide Variant
s.c.	Subcutaneous
T	
TAP	Transporters for Antigen Presentation
TLR	Toll-Like Receptor
TNF-α	Tumour-Necrosis Factor α
TILs	Tumour-Infiltrating Lymphocytes
TCEP	Tris (2-carboxyethyl) Phosphine Hydrochloride
TMV	Tobacco Mosaic Virus
TAP	Transporter-Associated with Antigen Processing
TT	Tetanus Toxoid
U	
µg	Microgram
V	
VLPs	Virus-Like Particles
W	
WES	Whole Exome Sequencing

Definitions of some endpoints in oncology

Term	Definition
(OS) Overall Survival	Time from randomization/treatment until death (due to any cause).
(PFS) Progression-Free Survival	Time from randomization/treatment until cancer progression or death.
(TTP) Time to Progression	Time from randomization/treatment until tumour progression (does not include death).
(TTF) Time to treatment Failure	Time from randomization/treatment until discontinuation of the treatment due to (tumour progression, toxicity or death).
(EFS) Event-free Survival	Time from randomization/treatment until tumour progression or death or discontinuation of the treatment due to (patient's preference, toxicity etc).
(ORR) Objective Response Rate	Proportion of patients with tumour reduction of a predefined amount.
(DoR) Duration of Response	Time from documenting a response to tumour progression.

((CDER), 2007)

http://www.fda.gov/downloads/Drugs/.../Guidances/ucm071590.pdf.

Ethical Framework

All procedures on animals in Oxford were approved and conducted in accordance with the (UK Animals Scientific Procedures Act of 1986). The procedures were permitted by the UK Home Office and University of Oxford Animal Care and Ethical Review Committee confirming the 2010/63/EU directives of European Union.

Animal procedures conducted at University of Bern were in accordance with the Swiss Animals Act (455.109.1) (September 2008, 5th) University of Bern.

1. Introduction

1.1 Melanoma

1.1.1. General background, pathophysiology and causes

Melanoma is defined as malignancy of the melanin-producing cells (melanocytes) located in the bottom layer of the epidermis (Rodriguez-Cerdeira et al., 2017). Melanin pigment is primarily responsible for the skin color. Melanoma can also occur in the ears, eyes, oral and genital membranes and gastrointestinal track (Institute, 2015). Melanoma constitutes only about 5% of all types of skin cancers, however its mortality is the highest as it tends to show early metastasis after loss of cellular adhesion in its primary location (Rodriguez-Cerdeira et al., 2017; Swetter, 2017).

Melanoma begins with the radial growth phase when melanocytes growth goes out of control. At an early stage the tumour is less than 1 mm thick and has not yet reached the bloodstream, therefore metastasis is unlikely at this stage. However, melanocytes behaviour dramatically changes as they start moving in different directions, vertically into the epidermis and the dermis. This is followed by the invasive radial growth phase when individual melanocytes start acquiring invasive potentials. Lastly, the vertical growth phase is the actual invasive melanoma stage in which melanocytes can grow in the surrounding tissues and organs and may spread into the body through blood or lymph. The tumour at this stage is more aggressive as it exceeds 1mm and would reach parts of the dermis (Figure 1.1) (Hershkovitz, Schachter, Treves, & Besser, 2010; Testa, Castelli, & Pelosi, 2017).

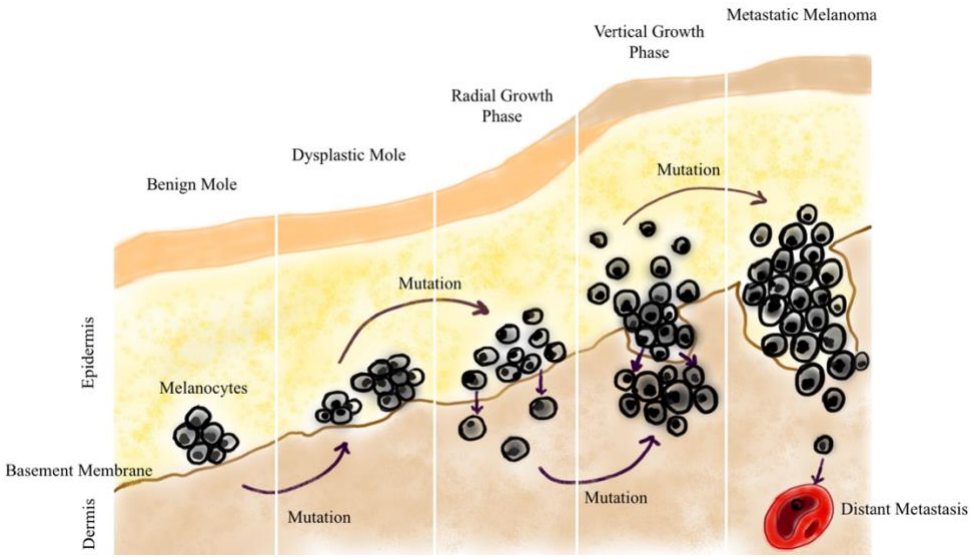

Figure 1. 1 Stages of Skin-Melanoma

Melanoma srats with a benign mole which develops to a dysplastic mole. The next stage is the radial growth phase characterized by surface spreading of the malignant cells. This is followed by the the vertical growth phase characterized by the appearance of a tumour papule and finally the metastatic phase in which the tumour can spread to other organs. Melanoma process involves several mutations including those in BRAF, NRAS, CDKN2A and loss of E-cadherin.

In general, the process of melanoma is poorly understood, it mainly involves progressive multistep mutations which alter cells differentiation, proliferation and death. Such processes are a result of an interaction between environmental and genetic factors. Environmental factors may include, exposure to ultraviolet radiation (considered the major risk factor), presence of evolving or changing moles, fair skin, older age color and poor tanning skin (Goldstein & Tucker, 2013; Rhodes, Weinstock, Fitzpatrick, Mihm, & Sober, 1987; Sober et al., 1979; Williams & Sagebiel, 1994). Family history reveals that there are some inherited genetic factors favouring cancer development. Several studies have shown that about 10% of melanoma cases report a family history in a first or second relative (Cherobin, Wainstein, Colosimo, Goulart, & Bittencourt, 2018;

Hayward, 2003). Most mutations found in melanoma and other cancers are, however, not inherited but rather accumulated within tumours, as they are genetically unstable.

Melanoma is a complex disease with the highest burden of somatic mutations in comparison to other types of solid tumours (Reddy, Miller, & Tsao, 2017). Several driver mutations can occur in different oncogenes leading to constitutive activation of signaling pathways that causes sustain tumougenesis. A driver mutation refers to a mutation that is necessary to promote and enhance malignancy (Mehnert & Kluger, 2012). Examples of the most common driver mutations in melanoma and their frequencies are listed hereunder (Table 1.1).

Table 1. 1 Melanoma mutations

Mutation	Frequency in Melanoma	Backgroud	References
BRAF	37-50%	BRAF is a gene encoding a protein involved in directing cell growth. Most BRAF mutations result in a missense mutation leading to a.a. substitution: ➢ 80-90% (V600E) Valine to Glutamic Acid. ➢ 5-12% (V600K) Valine to Lysine ➢ 5% (V600R) Valine to Arginine or (V600D) Valine to Aspartic Acid.	(Davies et al., 2002; Hodis et al., 2012; Lovly et al., 2012; Rubinstein et al., 2010)
NRAS	13-25%	NRAS is a gene encoding a protein involved in directing cell division and growth. Majority of NRAS mutations result in a misssense mutation leading	(Ball et al., 1994; Curtin et al., 2005; van 't Veer et al., 1989)

		to a.a. substitution in positions 12, 13 or 61.	
GNA11	1.2%	GNA11 is a gene encoding the alpha subunit of the G-protein. This protein is involved in cell signal transduction pathways. Most of GNA11 mutations are in the GTPase domain within exon 5.	(Patel, Kim, Lacey, & Hwu, 2016; Van Raamsdonk et al., 2010)
KIT	2-8%	KIT is a gene encoding the synthesis of receptor tyrosine kinase proteins family. These proteins are involved in cell signal transduction pathways. KIT mutations include somatic point mutations in the juxtamembrane domain or in the kinase domain.	(Beadling et al., 2008; Handolias et al., 2010)
MEK1	6-7%	MEK1 is a gene encoding proteins required for multiple biochemical signals in the cell. Most of the reported MEK1 mutations causes G>A and C>T a.a. substitution.	(Emery et al., 2009; Nikolaev et al., 2011)
CDKN2A	<2%	CDKN2A is a gene encoding two regulatory proteins of the cell cycle, $p16^{INK4a}$ and p14ARF. These proteins act as tumour suppressors. Mutation in CDKN2A gene is ~20-40% in melanoma-prone families Worldwide. Mutation in CDKN2A includes point mutation or deletion.	(Harland et al., 2014; Hayward, 2003; Hodis et al., 2012; Lesueur et al., 2008)

1.1.2. Stages of melanoma

Melanoma can be categorized into different stages based mainly on tumour characteristics such as thickness and the involvement of lymph nodes (LN) as

well as other organs. Three methods are used to stage melanoma; micro-staging, clinical staging and staging after investigation. Micro-staging refers to histopathology techniques, clinical staging examines local and enlarged LNs for evidence of tumour spread while staging after investigation uses imaging techniques such as MRI, CT and PET scan. The patient usually undergos two of the three staging methods. Once staging is defined, it will be described as a number ranging from (0-4) with a sub-stage from (a-d). The definition of each melanoma stage is described in the table (Table 1.2) (Australia, 2018; UK, 2016):

Table 1. 2 Melanoma stages and definition

Stage	Definition
Stage 0	Also called *in situ* melanoma. In this stage, melanoma is confined in the top layer of the skin (The epidermis) and has not spread to the deeper layer (The dermis).
Stage 1	Stage 1 can be divided into 2 categories: 2mm tumour with no ulceration, no LN involvement and no metastasis. The second category is 1mm tumour with ulceration and no LN involvement and no metastasis.
Stage 2	Stage 2 involves thickness and ulceration with no LN involvement and no metastasis.
Stage 3	In stage 3, melanoma can be of any thickness and LN are involved.
Stage 4	In stage 4, melanoma can be of any thickness and will spread to LN and organs such as lung, brain or bone.

1.1.3. Stage-specific overall survival of melanoma, incidence and mortality in Europe

There is limited information regarding the stage-specific overall survival of melanoma in Europe. A recent paper conducted a systemic literature review for 26 studies representing nine countries in Europe to identify the 5-year stage-specific overall survival of melanoma (Table 1.3). The study has covered 152,422 patients from 1978 to 2011 (Svedman et al., 2016).

Table 1. 3 Stage-speicifc overall survival of melanoma in Europe

Stage	5-year overall survival
Stage I	95-100 %
Stage II	65-92.8%
Stage III	41-71%
Stage IV	9-28%

Furthermore, there is a major gap in the epidemiological data about melanoma incidence and mortality in European countries. In general, the incidence of malignant melanoma has increased in several European countries at a rate of 3-7% when compared to U.S rate of 2.6%. Melanoma incidence in European countries varies considerably between 25.8 cases in Switzerland to 1.3 in Albania according to EUCAN in 2012 measured for 100,000 persons (Figure 1.2) (Forsea, Del Marmol, de Vries, Bailey, & Geller, 2012). Overall, 104,000 new cases and 22,000 deaths of melanoma have been reported in Europe in 2012 according to Globocan (cancer, 2012). A recent study has predicted the number of cancer death cases for the year 2017 in Europe by retrieving data of cancer death certificates from 1970-2012 using a joint-point regression model

(Malvezzi et al., 2017). The results showed that cancer mortality rates were forecast to decline in 2017 in both genders except for pancreatic cancer in both genders and lung cancer in women.

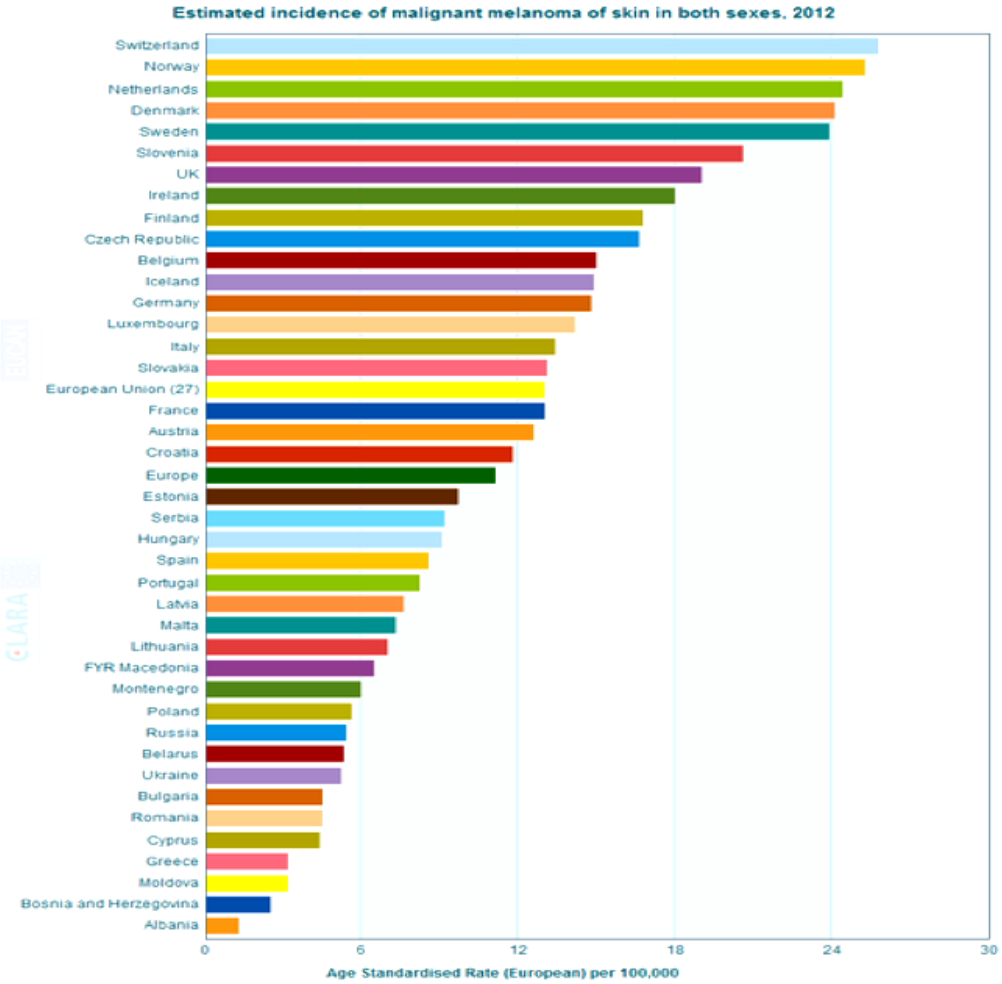

Figure 1. 2 Melanoma incidence in both sexes in 2012 in Europe. Retrieved from: http://www.melanomapatientnetworkeu.org/melanoma.html

1.1.4 Melanoma treatment

1.1.4.1 Conventional treatment

Treatment of melanoma varies according to its stage and location. Stages 0 and I are mainly treated by wide excision (surgery) while stage II is treated by wide excision and sentinel lymph node (LN) dissection. The physician may also recommend the addition of an adjuvant therapy for stage II melanoma. In stage

III/IV melanoma cells have generated metastases, therefore the treatment includes wide excision, eventually extended LN dissection, and therapies including irradiation, chemotherapy, type I interferon, IL-2, vaccines and immunotherapy (Society, 2016).

1.1.4.2 Immunotherapy

Since the beginning of the twentieth century, several important "immunotherapy" methods that harness the specificity of the immune system have been developed to eliminate cancer cells (Grabstald, 1965; Humphrey, Boehm, Jewell, & Boehm, 1972; Kelly et al., 2000; Mathe et al., 1969). Examples of early developed immunotherapeutic methods include, autologous dendritic cells based vaccine (Liau et al., 2000), treatment with IL-2 (Wanebo, Pace, Hargett, Katz, & Sando, 1986), treatment with oncolytic viruses (Roenigk, Deodhar, St Jacques, & Burdick, 1974), peptide-based vaccine (Stewart & Rosenberg, 2000) and DNA-based vaccine (Hawkins et al., 2000). Genetically engineered T-cell receptors lymphocytes (Fesnak, June, & Levine, 2016), chimeric antigen T-cells (CAR-T) (Sadelain, 2017) and checkpoint inhibitors (Gong, Chehrazi-Raffle, Reddi, & Salgia, 2018) have been developed recently (Restifo, Dudley, & Rosenberg, 2012; Rosenberg & Restifo, 2015; Sloan et al., 2000).

Immunotherapy in general may be considered nowadays an important tool for treating different types of cancers (including melanoma) usually combined with other conventional available therapies such as chemotherapy, radiation (Chae et al., 2018; Hu, Ott, & Wu, 2017) or targeted therapy (Karachaliou et al., 2017). Targeted therapy is a form of molecular medicine

that blocks cancer growth by interfering with specific molecules essential for tumour development and carcinogenesis (Huang, Shen, Ding, & Geng, 2014). Targeted therapy includes; small molecules "tyrosine-kinase inhibitors" such as Vemurafenib® used to treat metastatic melanoma cases harboring mutation in BRAF V600E (Chapman et al., 2011), "serine-threonine kinase inhibitors" and protein based drugs including monoclonal antibodies (mAb) such as Trastuzumab used to treat HER2 receptor positive breast cancer patients (Maximiano, Magalhaes, Guerreiro, & Morgado, 2016).

1.1.4.2.1 Checkpoint inhibitors

Immunotherapy with anti-CTLA4, anti-PD-1 or anti-PD-L1 has considerably improved the survival for melanoma patients (Chae et al., 2018; Tsao & Sober, 2005). Anti-CTLA4 mAb inhibits the binding of CTLA4 receptor to the co-stimulatory molecules B7-1 and B7-2 (CD80 and CD86 respectively) (Figure 1.3) on DCs and other APCs (Jazirehi, Lim, & Dinh, 2016). Ipilimumab® is the first FDA approved anti-CTLA4 mAb which has been tested extensively in phases II and III clinical trials and has shown to enhance the survival of melanoma patients (Geoerger et al., 2017). In a phase II study, 676 melanoma patients have been randomized to three groups. The first group was treated with 3mg/kg Ipilimumab and gp100 vaccine, the second group was treated with Ipilimumab with placebo and the last group with gp100 vaccine only. The results showed that the survival of the group treated with ipilimumab with placebo was 25% higher than the group treated with ipilimumab with gp100 19%. The study concluded that ipilimumab alone resulted in 2 years survival in one-fifth of the treated patients (D. McDermott et al., 2013).

Another study has shown that the effectivness of Ipilimumab in metastatic melanoma patients is dose-dependent in a range between 0.3 mg/kg and 10mg/kg. The results revealed an enhanced outcome of the drug at higher doses, however the side effects were severe (D. McDermott et al., 2013). FDA has approved Ipilumumab as a first and second line therapy for metastatic melanoma at 3mg/kg dose for 3 months period, administered every 3 weeks (Eggermont & Robert, 2011).

Anti-PD-1 mAb are designed to prevent PD-1 binding to PD-L1 ligand. Generally, the expression of PD-1 protein increases dramatically on the surface of activated T-cells, monocytes, DCs, B cells and tumour-infiltrating lymphocytes (TILs) upon antigen recognition, which also leads to increase secretion of cytokines (Figure 1.3). The secreted cytokines result in PD-L1 expression on tumour cells as well on APCs (Sun et al., 2015). Interaction between PD-1 on activated T-cells and PD-L1 result in T-cell exhaustion, dysfunction and secretion of the inhibitory cytokine IL-10 (Mahoney, Rennert, & Freeman, 2015).

Nivolumab® (anti-PD-1) mAb has been approved for the treatment of unrespectable melanoma in 2014 in Japan. Pembrolizumab® (anti-PD-1) was approved by the FDA for the treatment of metastatic or unresectable melanoma also in 2014. Treating metastatic melanoma patients in phase III clinical trial with Nivolumab® has improved the survival when compared with Dacarbazine "Imidazole Carboxamide a chemotherapeutic medication used for treating melanoma", 73% and 42% respectively (Robert, Long, et al., 2015). Nivolumab® has shown 31% objective response rate (ORR) and a duration period of 18 to 117 weeks in a study in melanoma patients (Sznol et al., 2013)

compared to Pembrolizumab® which had an ORR of 38% for 2 to 11 months (Hamid, Robert, et al., 2013).

Anti-PD-L1 mAb Durvalumab® as a single therapy has shown limited clinical activity in advanced melanoma in several studies (Lutzky, 2014; Redman, Gibney, & Atkins, 2016). However, Atezolizumab® anti-PD-L1 mAb has shown 26% ORR in patients with advanced or metastatic melanoma (Hamid, Sosman, et al., 2013).

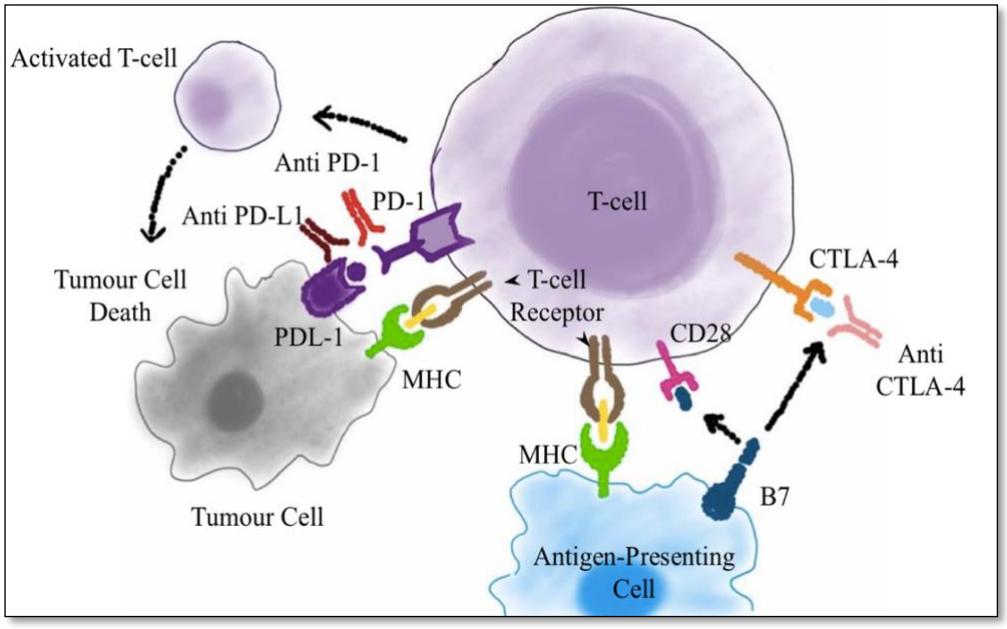

Figure 1. 3 Mechanism of action of check-point inhibitors (anti-PD-1, anti-PD-L1 and anti-CTLA-4)

PD-1 receptor is expressed on activated T-cells, PD-1 binds to its ligand PD-L1 on tumour cells causing exhaustion of the activated T-cells. CD28 receptor on T-cell surface binds the costimulatory molecule B7 on APCs resulting in activation of T-cells. CTLA-4 is a high affinity receptor to B7, therefore CTLA-4 is mainly engaged when B7 levels are low on APCs, while CD28 has 20-50-fold lower affinity to B7 receptors and therefore CD28 is mainly engaged when B7 levels are relatively high such as in case on infection. Blockade of PD-1 or PD-L1 or CTLA-4 by mAbs result in effective stimulation of T-cells and enhance the anti-tumour activity (Raman & Vaena, 2015).

In general, immunotherapy using anti-CTLA4 (Ipilimumab®), anti-PD-1 (Nivolumab®) or anti-PD-L1 (Atezolizumab®) has delivered new therapeutic options for oncologists and cancer patients and enhanced the survival. They have also revealed better safety measures when compared to the conventional chemotherapy treatment in lung cancer, renal cancer and metastatic melanoma (Miranda Poma, Ostios Garcia, Villamayor Sanchez, & D'Errico, 2018). Overall, antagonizing the inhibitory signals utilizing checkpoint inhibitors still shows < 50% response in melanoma, and < 25% in all other cancer types (D. S. Chen & Mellman, 2013; Johnston et al., 2014). While conventional cancer treatment such as chemotherapy could weaken the patient's immune system, checkpoint inhibitors could result in hyper-activation. Increasing number of reports indicate that such immunotherapy result in distinct and unique adverse side effects called immune-related adverse events (irAEs). The mild side effects in melanoma patients treated with anti-PD-1 or anti-PD-L1 include rash, fatigue, GI disorders, skin problems and diarrhea. The moderate side effects included colitis, encephalitis, pneumonitis, hepatitis, renal dysfunction, nephritis, hyperglycemia, pleural effusion and acute kidney failure (Alsaab et al., 2017; Naidoo et al., 2015).

Anti-PD-1 and anti-PD-L1 mAbs have shown less toxicity and irAEs when compared to anti-CTLA4 (Ribas et al., 2013; Weber, Yang, Atkins, & Disis, 2015). Increased grades of irAEs have been reported in 7-12% patients receiving single agent anti-PD-1 or PD-L1 (Robert, Schachter, et al., 2015; Weber, D'Angelo, et al., 2015) in contrast to 10-18% patients receiving anti-CTLA4 in phase III clinical trial (Hodi et al., 2010; Ribas et al., 2013). Furthermore, combining different check-point inhibitors could increase the

toxicity and the severity of the side effects (Larkin, Hodi, & Wolchok, 2015; Postow et al., 2015).

1.1.4.2.2 Therapeutic cancer vaccines

Therapeutic cancer vaccines aim to strengthen the immune response by reactivating anergic or dormant T-cells or by triggering the naive T-cell repertoire and thus can be utilized to hinder the growth of malignant or relapsing tumours (S. H. van der Burg, R. Arens, F. Ossendorp, T. van Hall, & C. J. Melief, 2016). The idea of a therapeutic cancer vaccine is not new, William Coley made the first attempt in 1891 to locally immunize cancer patients with inactivated bacteria (Streptococcus pyogenes and Serratia marcescens) known as Coley's Toxin (McCarthy, 2006). His work showed effective responses in patients but was viewed with some doubt by the medical community. However, recently modern immunologists have shown that Coley's work was indeed correct (Guo et al., 2013). Similar to Coley's toxin, Bacillus Camette-Guerin (BCG) is used nowadays for the treatment of superficial bladder cancer (Lamm et al., 1991; Morton et al., 1992; van der Meijden et al., 2003). Chapter (1.1.4.2.4) lists some examples of therapeutic cancer vaccines that have also been used in melanoma treatment.

1.1.4.2.3 Building an effective cancer vaccine

Recent knowledge in tumour-antigen discovery and of immunomodulatory agents has led to the advancement in our understanding of the key components of effective vaccination (Hu, Ott, & Wu, 2018). A fundamental step to mount an effective anti-tumour response from naïve T-cells is the activation of APCs,

especially DCs (Figure 1.4) at the injection site and in secondary lymphoid organs (Hu et al., 2018). DCs capture viruses, proteins, bacteria, immune complexes and dying tumour cells via endocytosis, macro-pinocytosis or phagocytosis through different arrays of receptors that also function in cell-cell interaction and signaling pathways (O'Neill, Adams, & Bhardwaj, 2004). The captured antigen will then be processed into peptides for effective loading onto major histocompatibility classes I and II (MHC-I and MHC-II). Peptide-loaded MHC I and II (pMHC I/II) complexes will be translocated to the cell surface for recognition by $CD8^+$ and $CD4^+$ T cells, *respectively* (Guermonprez, Valladeau, Zitvogel, Thery, & Amigorena, 2002).

Endogenous antigens present in the cytosol –usually synthesized within cells- are typically loaded onto MHC-I molecules. This cytosolic pathway involves ubiquitination and proteosomal degradation of proteins and peptide transportation to the endoplasmic reticulum (ER) by transporters for antigen presentation (TAP) resulting finally in peptide-binding to MHC-I molecule. Exogenous, extracellular antigens are endocytosed into vesicles where they will be processed and loaded on MHC-II molecules (Neefjes, Jongsma, Paul, & Bakke, 2011). Tumour-specific antigens will be loaded on MHC-I and MHC-II molecules for effective naïve and memory $CD8^+$ and $CD4^+$ response, *respectively*. DCs would also permit exogenous or extracellular antigen to traffic from endosomal vesicles to the cytosol in a unique process called cross-presentation resulting in cross-priming. An alternative pathway consists of endosomal loading of MHC class I molecules before they return to the cell surface (Bachmann et al., 1995). Such process indicates that one cell type (DCs) is capable of presenting antigens from other cells (such as tumour cells) and

prime T-cells (Joffre, Segura, Savina, & Amigorena, 2012). In the case of DC based cancer vaccines, the antigen would be exogenously loaded *in vitro* before injection (Palucka & Banchereau, 2013). The loaded APCs will traffic to the secondary lymphoid organs, the site of T-cells initial activation and priming. T-cell priming is a process that refers to the first contact of naïve T-cell with its specific antigen loaded on MHC-I/II molecules on APCs "mainly DCs". Priming of T-cells causes their activation and differentiation to effector cells. Naïve $CD8^+$ T-cells differentiate into cytotoxic cells capable of killing tumour cells while $CD4^+$ generate a diverse array of different effector cells. The effector activity of $CD4^+$ T-cells may include cytotoxicity, but mostly it induces the secretion of cytokine sets that target $CD8^+$ cells for more efficient killing response (Murphy M. K., 2016).

The effective proliferation and differentiation of naïve T-cells into effector and memory cells requires mainly three signals: antigen recognition as a 1^{st} signal, co-stimulation as a 2^{nd} signal and cytokine production as a 3^{rd} signal. As discussed earlier, antigen recognition by $CD8^+$ and $CD4^+$ T-cells involves recognition of pMHC-I/II molecules, *respectively*. Such a process ensures that the resultant immune response is specific for the antigen presented by MHC molecules. The costimulatory molecules highly expressed by DCs are essential for T-cell activation as a 2^{nd} signal. CD28 T-cell surface receptor is the best characterized costimulatory pathway that binds the costimulatory molecules B7-1 and B7-2 (CD80 and CD86 *respectively*) expressed by DCs and other APCs (L. Chen & Flies, 2013). CD40L is a TNF membrane protein expressed on activated T-cells that engages the TNFR family member CD40 on DCs. This interaction results in further activation of DCs by enhancing the expression of

B7 molecules and the secretion of IL-12 and type-I IFN production which will finally promote the expansion of specific T-cells followed by trafficking of tumour-specific T-cells to the tumour sites (Greenwald, Freeman, & Sharpe, 2005).

Cytokines play a critical role in the activation of T-cells. $CD4^+$ helper T-cells generate the largest amounts of T-cell cytokines followed by $CD8^+$ T-cells. The cytokines produced by DCs also serve an important role in the activation and the development of potent T-cell response. The cytokines produced during the adaptive immune response phase are highly involved in the proliferation and generation of antigen specific effector T-cell response. IL-2 is an essential cytokine that plays a role in T-cell survival and differentiation, it is mainly produced by $CD4^+$ but also by $CD8^+$ T-cells following antigen recognition and co-stimulation (W. Liao, Lin, & Leonard, 2013). Different cytokines such as IL12, IL18 and type-I IFN are essential for the differentiation and development of $CD4^+$ T-cells to T_H1 effector cells upon encountering intracellular antigens (Yoshimoto et al., 1998). IFN-γ is an essential macrophage-activating cytokine, belongs to type-II interferon and is a potent activator of effector T-cells. T-cells ($CD4^+$ and $CD8^+$) secrete IFN-γ in response to antigen recognition which can be further enhanced by IL-12 and IL-18 secretion. IFN-γ increases $CD4^+$ T-cells differentiation into T_H1 subset and enhances antigen presentation by APCs and other cell types which results in amplification of T-cell response (Martinez-Lostao, Anel, & Pardo, 2015).

Upon encountering the cognate antigen in the tumour, CTLs will initiate the killing process by the release of granzymes, perforin and granulysin molecules. These cytotoxins will activate a series of cysteine proteases leading

to programmed cell death (apoptosis) of the tumour cells. Tumour antigens will also be released from lysed cells and get captured by APC, resulting in the induction of a polyclonal T-cell response. Such processes will enhance tumour-epitope spreading activity (Hu et al., 2018).

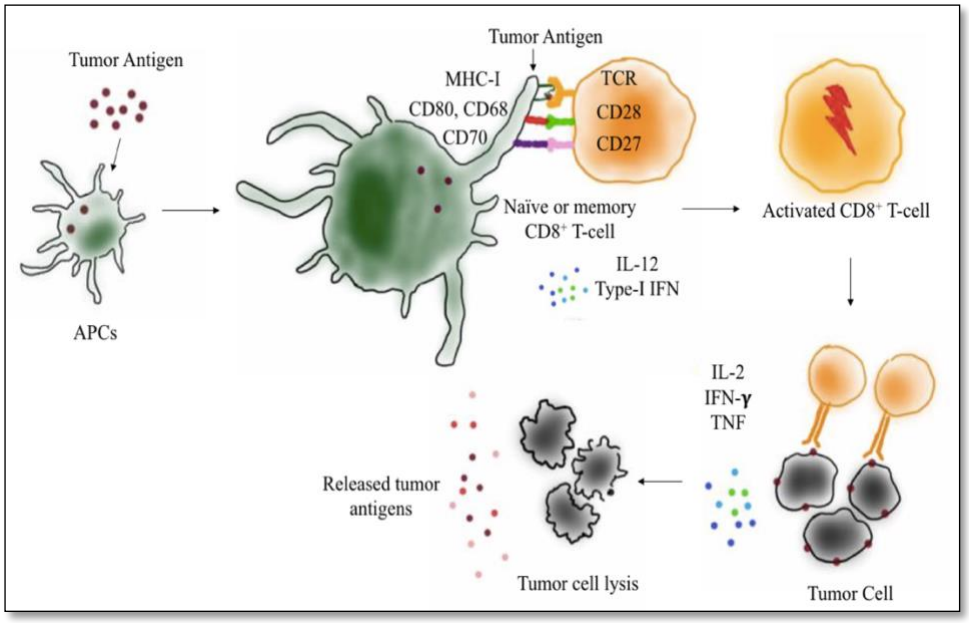

Figure 1. 4 A schematic diagram illustrating the fundamental steps to mount an effective anti-tumour response from naïve T-cells

APCs mainly DCs capture tumour antigens and present them on MHC-I and II molecules to prime $CD8^+$ and $CD4^+$ T-cells, respectively in the secondary lymphoid organs. The 3 signals -discussed earlier- are essential for effective priming of T-cells, 1^{st} signal is antigen-recognition, 2^{nd} signal is cos-stimulation and the 3^{rd} signal is cytokine production such as IL12, IL18, IFN- γ. Upon successful activation, tumour-specific T-cells expand and migrate to tumour sites to initiate tumour killing process by the release of granzymes and perforin. In general, effective cancer vaccines contain four main components: tumour-antigen, delivery vehicle, adjuvants and finally formulation. Table 1.4 lists some examples of these components.

Table 1. 4 Components of cancer vaccine candidates, examples of tumour-antigen, delivery vehicles, adjuvants and formulation

Tumour-Antigen	Delivery Vehicle	Adjuvants	Formulation
- **Tumour-associated Ag** ▪ Oncofetal Ag ▪ Cancer-testis Ag ▪ Tissue-differentiation Ag ▪ Overexpressed Ag - **Tumour-specific Ag** ▪ Neoantigens ▪ Oncogenic viral Ag	▪ **Nanoparticles** ▪ **Liposomes** ▪ **Virosomes** ▪ **Emulsions** (ex. Montanide)	- **TLR agonists:** ▪ CpG ODN ▪ Poly-IC ▪ MPL ▪ Imiquimod - **GM-CSF** - **STING-ligands** - **DC-targeted mAb** ▪ CD40 Agonist ▪ DEC205 - **Tetanus or diphtheria toxoid**	- Tumour-based - DC-based - Genetic-based - Peptide/protein-based

1.1.4.2.4 Types of therapeutic cancer vaccine

- **Tumour cell vaccine**

Tumour cell vaccines can be divided into autologous and allogeneic vaccines. The autologous vaccine is considered one of the first therapeutic cancer vaccines to be tested (Hanna & Peters, 1978) in various cancers including melanoma (Berger, Kreutz, Horst, Baldi, & Koff, 2007; Mendez et al., 2007; Ruttinger et al., 2007). It is prepared from the cancer patient's tumour cells (autologous). A major advantage of this type of vaccination is the potential of presenting the whole range of TAAs to the patients' immune system combined with adjuvants. This mixture would increase and augment the individual' immune response. However, a major limitation of this vaccine is the need for

sufficient tumour cells which would not always be feasible in the clinical settings (Guo et al., 2013).

The allogeneic tumour cell vaccine has the advantage over the autologous vaccine as it contains two or more human cell lines and therefore can overcome the limited availability issue. On the other hand, the process fully relies on cross-presentation and shared tumor-associated antigens. Some allogeneic vaccines have made it to clinical trials such as Canvaxin™ for the treatment of metastatic melanoma. Canvaxin™ is a polyvalent melanoma vaccine developed in 1984 from three different melanoma cell lines in combination with BCG as an adjuvant (Morton et al., 1992). Canvaxin™ has shown an increase in overall survival (OS) in phase II trials for stage III/IV melanoma patients (Morton et al., 2002). However, the outcome of phase II multi-institutional randomized trials failed to achieve significant results and was discontinued (Sondak, Sabel, & Mule, 2006). Given the above-mentioned limitations, this may not be a major surprise.

- **DC-based cancer vaccine**

The origin of dendritic cell (DC) vaccine development is based on initial findings by Inaba and Steinman who have shown more than 25 years ago that mouse DCs can be cultured *ex vivo* from bone marrow precursors (Inaba et al., 1992). Human DCs can also be generated from $CD34^+$ hematopoietic progenitors cultures from Peripheral Blood Mononuclear Cells (PBMCs) (Banchereau & Palucka, 2005). Cancer DC vaccines are mainly developed by loading the patient's harvested autologous DCs with tumour-associated antigens, tumour derived antigens or peptides (Banchereau et al., 2001; Schuler-

Thurner et al., 2002), whole tumour cells (Saito, Frleta, Dubsky, & Palucka, 2006), DCs and tumour cells fusion (Rosenblatt et al., 2011) or virus/DNA or RNA (Nair et al., 2002; Steele et al., 2011) delivered with potent adjuvants have also been evaluated. A study conducted in 2011 demonstrated the efficacy of both monocyte-derived DCs and human Langerhans cells in mounting good specific T-cell response in stage III/IV melanoma patients (Romano et al., 2011). Several other studies have also tested the immunogenicity and effectiveness of DC vaccine in melanoma (Lesterhuis et al., 2011; Nestle et al., 1998).

However, there are some challenges with DC-based vaccines including; the vaccine preparation requires leukophoresis to isolate PBMCs from the patient in addition to cell culture processing, this may limit the number of vaccinations achievable by this method. Additionally, DCs characteristics should be better identified for successful modulation of the immune system. DC-based vaccine is emerging as an attractive approach in cancer, however there is no consensus in the field on the preferred cell type and molecules to be targeted. Further studies are needed to compare the immunogenicity of targeting multiple DC subsets to the currently well-formulated protein/peptide-based vaccines in inducing durable T-cell responses (P. Chen et al., 2016).

- **Genetic cancer vaccines (DNA/mRNA/Viral Vectors)**

Genetic cancer vaccines are based on delivering antigen *in vivo* by utilizing RNA, plasmid DNA or viral vectors that carry the required expression cassettes. Upon vaccination, they will transfect somatic cells including DCs and monocytes residing in the skin. This would result in immediate antigen

presentation which leads to successful priming. Alternatively, non-bone marrow derived tissue cells are transfected and their antigens cross-presented subsequent to their lysis. Genetic vaccines can be used to deliver multiple antigens in one plasmid or vector (Aurisicchio & Ciliberto, 2012). Modest to strong anti-tumour CTL responses have been elicited in preclinical studies using plasmid DNA vaccine. This encouraged a study that used an electroporation system to vaccinate melanoma patients (stage IIb-IV) with murine Tyrosinase DNA vaccine, aiming at inducing a specific CTL response. The results indicated that patients who received 1.5mg of the vaccine generated Tyr-reactive $CD8^+$ cells but not the ones that received 0.2 or 0.5mg vaccine. Overall, six out of 15 patients showed response in this study (Yuan et al., 2013). Furthermore, it has been shown that xenogeneic human cDNA encoding melanoma antigens such as (tyrosinase – gp100- TRP2 and TRP1) are effective at inducing specific T-cell responses and protect mice against tumour challenge. However, this was not the case when using plasmid DNA that encodes mouse antigens (Bowne et al., 1999; Gold et al., 2003; J. C. Liao et al., 2006; Naftzger et al., 1996; Wolchok et al., 2007).

DNA vaccines in general have shown some promise in preclinical trials (Xiang, Luo, Niethammer, & Reisfeld, 2008) but failed to translate this success to non-human primates or to human subjects (M. A. Liu & Ulmer, 2005; Rice et al., 2006). In addition, there have been several concerns about DNA vaccine. The major safety concern is the integration of DNA plasmid into the host genome, the formation of anti-DNA antibodies (Abs) that could result in autoimmunity/immune complex diseases and other adverse immunological events (Medjitna, Stadler, Bruckner, Griot, & Ottiger, 2006). Chinese scientists

have observed vitiligo (loss of skin pigment) in mice after a third immunization with pcDNA3-b vaccine indicating an autoimmune response, that may, however, be indicative of protection (Zhou et al., 2011).

mRNA can also be used to induce specific CTL response (Carralot et al., 2005; Scheel et al., 2005). RNA vaccines are safer than DNA vaccines as they are rapidly degraded *in vivo* and thus are unlikely to cause autoimmunity and cannot integrate into the genome. RNA is usually formulated in other agents for stabilization, facilitation o transfection and/or adjuvants activity (Espuelas, Roth, Thumann, Frisch, & Schuber, 2005; Fotin-Mleczek et al., 2012; Scheel et al., 2005). RNA vaccines can also be modified by chemical alteration of the backbone (Scheel et al., 2004) or by integrating an RNA replicase polyprotein which has been derived from a virus aiming to generate a "self-replicating" RNA vaccine (also called RNA replicon) (Ying et al., 1999).

Generally, RNA cancer vaccines have shown exciting immunogenecity and power to induce at least partially protective T-cell responses when applying multiple epitopes simultaneously. Nevertheless, RNA vaccines have so far by and large failed to induce cytotoxic T-cells in humans and it remains unclear how protection was brought about. In addition, RNA is inherently unstable, rendering it's use in normal clinical settings difficult. Hence, it will be interesting to see direct comparisons of the RNA and other platforms in a clinical study using the same epitopes.

Viral-vector cancer vaccines are based on using low disease-causing and low intrinsic immunogenicity potential viruses engineered to encode tumour-associated antigens (TAAs), usually combined with other immune-modulators (Guo et al., 2013). A number of different viruses have been used as cancer

vaccine, however most oncolytic viruses have been developed based on adenovirus or HSV (Chiocca & Rabkin, 2014; Kirn, Martuza, & Zwiebel, 2001). The adenovirus vector is considered the most immunogenic of vectors amongst the group, and overcoming its immunogenicity was one of the main challenges to scientists. The adenovirus vector is known to induce a strong CTL response as well as a potent inflammatory cytokine response (Kafri et al., 1998). However, humoral antibody responses, mainly against the viral capsid, have also been induced rendering multiple use of the same strain difficult (Thomas, Schiedner, Kochanek, Castro, & Lowenstein, 2001; Yu et al., 2013).

Modified-vaccinia ankara (MVA) and ALVAC (canarypox virus vector) were the first viral-vectored cancer vaccines to be tested in clinical trials (Marshall et al., 1999; Marshall et al., 2000; Walsh & Dolin, 2011). A promising viral-vector cancer vaccine is PROSTVAC, an "off-the-shelf" vaccine containing the prostate-specific antigen PSA in addition to the TRICOM costimulatory molecules (CD58, CD54 and CD80) (Hodge, Chakraborty, Kudo-Saito, Garnett, & Schlom, 2005). PROSTVAC improved the median survival of metastatic prostate cancer patients (Kantoff et al., 2010). A phase III 3-arm trial tested whether PROSTVAC alone or in combination with granulocyte macrophage colony-stimulating factor (GM-CSF) is more effective in enhancing the survival in patients with prostate cancer (NCT01322490). However, no results have been published yet. Oncovex$^{GM\text{-}CSF}$ is an oncolytic enveloped dsDNA (HSV-1) which also encodes GM-CSF but does not carry a tumor specific antigen. Oncovex$^{GM\text{-}CSF}$ was tested in phase II clinical trial by direct injection into accessible melanoma tumours. The results showed 28% positive response, characterized by tumour regression of the accessible and

inaccessible lesions highlighting a localized and systemic anti-tumour activity (Senzer et al., 2009). A third phase clinical trial has also been initiated to evaluate the effectiveness and safety of the vaccine in unresectable metastatic melanoma patients (Kaufman & Bines, 2010). The study's endpoint aimed to demonstrate the overall clinical benefit for the enrolled patients treated with Oncovex^{GM-CSF} vs GM-CSF alone, the the final results are not yet published. Nevertheless, based on the observed clinical endpoints, Oncovex^{GM-CSF} has been approved (https://opentherapeutics.org/fda-joint-committee-meeting-votes-to-approve-the-biologics-license-application-for-talimogene-laherparepvec-for-patients-with-metastatic-melanoma/) and is now routinely used in the clinic.

Developments to overcome viral-vector immunogenicity by using engineered vectors has led to considerable reduction in their overall immunogenicity (Ahi, Bangari, & Mittal, 2011; Mingozzi & High, 2013). Inappropriate activation of cytokines and inflammatory genes induced by adenoviruses vectors can be highly dangerous leading to multi-organ failure, disseminated intravascular coagulation and even death (Wilson, 2009). Generally, viral-vector vaccines can induce toxicity leading to harmful cytokine responses and other complications based on the vector dose ("Assessment of adenoviral vector safety and toxicity: report of the National Institutes of Health Recombinant DNA Advisory Committee," 2002).

- **Peptide/ protein-based cancer vaccine**

Several limitations in whole tumour cell vaccines and DC vaccines have affected their broad use in clinical trials, predominantly due to the complex preparation process and the often limited availability of patients' samples, as

diagnostics remains the primary goal and often uses up large fractions of the available tumour tissue (Guo et al., 2013). Peptide or protein-based vaccines identified from tumour-associated antigens (TAAs) have shown advantages over whole tumour cell vaccines or DC vaccines and provided new opportunities to design therapeutic cancer vaccines.

In a recent study, synthetic pentatope RNA of 27 mers encoding neoantigens has shown considerable success. The RNA vaccine contained non-immunogenic linkers as well as signal peptide (SP) and MHC class-I trafficking (MITD) domains to enhance routeing to HLA-I and II molecules. The backbone element of the vaccine was also modified to increase the vaccine stability and translational efficiency (Sahin et al., 2017).

Surprisingly, the majority of the resultant induced T-cell response consisted of $CD4^+$ T-cells and a smaller fraction only was made up by $CD8^+$ CTL. Two out of the five immunized patients had a late relapse while a third patient required additional combinatorial therapy with anti-PD-1 (Sahin et al., 2017). A long synthetic RNA vaccine has also been used in another study to immunize melanoma patients (Ott et al., 2017). The results showed that a long synthetic RNA vaccine encoding neoantigens can induce $CD4^+$ and $CD8^+$ T-cell response in melanoma-resected patients. Four out of six immunized patients had no recurrence in over 25 months surveillance, while the remaining two patients also needed anti-PD-1 treatment (Ott et al., 2017).

Melanoma specific antigens can be divided into different categories including cancer testes antigens (MAGE, NY-ESO-1) (Desmet et al., 1994; O. Hofmann et al., 2008) and tissue differentiation antigens which are shared by normal and cancerous tissue (Tyrosinase, gp100, Mart-1/Melan-A) (Bakker et

al., 1994; Kawakami et al., 1994; Parkhurst et al., 1998). Peptide/ protein-based cancer vaccines are considered an attractive treatment, however the use of only one or few tumour antigens is insufficient to generate and maintain therapeutic immune responses in cancer patients (D. S. Chen & Mellman, 2013; Kruit et al., 2013).

Generally, peptide/protein-based vaccines have several advantages over other discussed cancer vaccines such as being safe, economical, inexpensive and would avoid any inclusion that might cause high reactogenecity to the host such as lipid and toxins. Despite their advantages, such vaccine is poorly immunogenic if used alone and would require a potent adjuvant. The right adjuvant and vaccine formulation strategies are needed to enhance the vaccine's immunogenicity and to facilitate its up-take by APCs without causing extra toxicity for the patients (W. Li, Joshi, Singhania, Ramsey, & Murthy, 2014).

1.2 Combinatorial melanoma vaccine therapy

Combinatorial cancer vaccine therapy is an attractive and feasible method to enhance the final treatment outcome for cancer patients. A wide variety of combinational immunotherapeutic drugs and modalities have been approved by the FDA or are currently undergoing assessment, such as therapeutic mAbs, checkpoint inhibitors or other immune modulating mAbs. Therefore, a rational combination therapy is highly recommended (if one ignores the costs) to achieve durable anti-tumour effect and to enhance the therapeutic outcome for patients. An attractive possibility is the combination of vaccines with other therapies. A randomized phase III clinical trial in 2011 produced encouraging results for stage IV/III melanoma patients as the group treated with gp100,

Montanide ISA-51 “a mixture of water and oil combined with the antigen” and IL-2 showed the best overall clinical response and progression free survival (Schwartzentruber et al., 2011).

FDA approval of ipilimumab (anti-CTLA4) for the treatment of metastatic melanoma has undoubtedly supported the combination of this therapy with other vaccines (Hodi et al., 2010; Lipson & Drake, 2011; X. Y. Wang, Zuo, Sarkar, & Fisher, 2011). Additionally, combining GVAX “The whole tumour cancer vaccine” that is genetically modified to secrete GM-CSF with ipilimumab has shown meaningful anti-tumour effects in a large number of patients with metastatic melanoma (Hodi et al., 2008). Several clinical trials testing rational combinatorial immunotherapies for melanoma are ongoing (Table 1.5).

Table 1. 5 Example of some ongoing clinical trials combining immunotherapies for patients with melanoma

Study Title	Intervention	Phase	Clinical Trial No. *Clinicaltrials.gov*
Vaccine combining multiple class-I peptides and Montanide ISA 51VG with escalating doses of anti-PD-1 mAb “Nivolumab” for patients with resected stage IIIC/IV melanoma	NY-ESO-1 Nivolumab gp100 Montanide Ipilimumab	I	NCT01176474 *https://clinicaltrials.gov/ct2/show/NCT01176474?term=vaccine+melanoma&cond=anti+PD1&rank=1*
Multiple class-I peptides & Montanide, multiple class-I peptides & Montanide ISA 51VG with escalating doses of anti-PD-1 mAb BMS93655	- MART - NY-ESO - gp100 - gp100 - Montanide ISA 51 VG	I	NCT01176461 *https://clinicaltrials.gov/ct2/show/NCT01176461?term=vaccine+melanoma&cond=anti+PD1&rank=2*

Trial for the evaluation of the effect of systemic low dose IL-2 on the immunogenicity of a vaccine comprising GM-CSF-In adjuvant, in patients with high risk melanoma (MEL36)	- Low dose IL-2 - Melanoma vaccine		II	NCT00928902 *https://clinicaltrials.gov/ct2/show/NCT00928902?term=vaccine+melanoma&cond=IL2&rank=1*
Vaccine plus IL-2 in treating patients with advanced melanoma stage IV	- IL-2 - gp100		II	NCT00005949 *https://clinicaltrials.gov/ct2/show/NCT00005949?term=vaccine+melanoma&cond=IL2&rank=2*
Augmentation of DC-based vaccine in melanoma patients by depletion of regulatory T-cells in stage IV melanoma patients	- Daclizumab - DC vaccine		I II	NCT00847106 *https://clinicaltrials.gov/ct2/show/NCT00847106?term=melanoma&cond=daclizumab&rank=2*

Daclizumab is an approved drug by FDA acts by blocking CD25, the high affinity receptor for IL-2 in humans. IL-2 is important for proliferation of specific T-cells but is also key for induction/maintenance of Tregs. A study has evaluated the function and survival of Tregs when administering Daclizumab in combination with peptide-based cancer vaccine for metastatic breast cancer patients. It showed that targeting CD25 did not mediate antibody-dependent cellular cytotoxicity (ADCC) or cause autoimmunity. On the contrary, the results indicated that treatment with Daclizumab can cause Tregs to lose their ability for suppression and restored the production of IFN-γ (Rech et al., 2012). Six out of 10 patients exhibited the best clinical response (as determined by

RECIST), with a progression-free survival of 4.8 months and a median overall survival of 27.8 months (Rech et al., 2012).

^{90}Y-daclizumab has been used in a radioimmunotherapy study targeting CD25 on localized tumours in relapsed Hodgkin lymphoma patients. The results showed ORR in 23 out of 46 treated patients and 30% reached complete response while 20% reached partial-response (Janik et al., 2015; Neelapu & Sharma, 2015). There is an important difference between daclizumab and anti-CD25 antibodies used in mice. In contrast to the human antibodies, which do not deplete Tregs, the murine antibodies usually do, enhancing their anti-tumor activity.

1.3 Virus-Like Particles (VLPs) & VLP-based vaccines

1.3.1. General overview of VLPs

Virus-like particles (VLPs) are multi-protein supra molecular structures that form icosahedral or rod-shape structures and carry several characteristics of viruses, which can be harnessed for effective vaccine development (Crick & Watson, 1956; Roldao, Mellado, Castilho, Carrondo, & Alves, 2010). VLPs usually mimic the parental native viruses in their final conformation and organization as they form "autologous" shapes consisting uniquely of structural proteins similar to the target virus (Pumpens, 2008). The symmetrical structure of VLPs is one of their main key features, which often resembles symmetric patterns found in classical art (Figure 1.5). Nevertheless, they constitute a safe vaccine template as they lack the viral genome making them non-infectious (Bachmann & Jennings, 2010; Zeltins, 2013).

Figure 1. 5 The unique symmetrical structure of icosahedral virus-like particles (VLPs) resembling the symmetrical patterns found in classical art.

More than 170 different host systems can be utilized for VLP production including bacteria, yeast, mammalian and insect cells. The different hosts for VLP production reflect in part the broad host-spectrum of viruses from which VLPs are derived (Pumpens, 2016). ~30% of VLPs are produced in bacteria "mainly using *E.* coli", the viral-structural protein genes are codon-optimized and cloned into *E.* coli plasmids and expressed using strong promotors (S. D. Brown, Fiedler, & Finn, 2009; Hwang, Roberts, & Wilson, 1994). Such processes ensure high yield production of the desired viral-structural proteins. Beside *E.* coli, Lactobacillus and Pseudomonas were used for the production of human papilloma virus (HPV L1-VLPs) (Cortes-Perez, Kharrat, Langella, & Bermudez-Humaran, 2009; Phelps, Dao, Jin, & Rasochova, 2007) and cowpea chlorotic mosaic virus (CCMV-VLPs), *respectively* for vaccine development (Phelps, Dao, et al., 2007).

There are some drawbacks associated with the bacterial host system including endotoxin contamination and difficulty in introducing post-

translational glycosylation modification in the eukaryotic protein (Zhao et al., 2012). Endotoxin contamination can be solved by simple polishing techniques (Q. Chen & Lai, 2013). The commercially available VLP-based vaccines against hepatitis B-virus (HBV) and HPV have been produced utilizing yeast host expression systems (K. J. Hofmann et al., 1995; Valenzuela, Medina, Rutter, Ammerer, & Hall, 1982). Production of VLPs using insect cell expression-systems have been employed since 1980s and are also used to produce HPV vaccines. Mammalian and plant cells have also been utilized in a number of cases (Pumpens, 2016). Generally, VLPs can be efficiently and rapidly produced in massive quantities when using optimized cultural conditions. Upon successful production in the host system, VLPs self-assemble into a final shape that usually imitates the original virus symmetry (Bachmann & Jennings, 2010).

1.3.2 VLPs trafficking to and in the draining lymph nodes

In general, VLPs ranging between 20-200nm –with the optimal size being 30-40nm- can diffuse freely through the 200nm pores of the lymphatic vessels (Manolova et al., 2008) upon subcutaneous injection. VLPs can also be actively transported with specialized cells such as DCs (dermal DCs and Langerhans cells) and skin-derived macrophages (Figure 1.6) (Ruedl, Storni, Lechner, Bachi, & Bachmann, 2002). Previous studies have shown that DCs characterized with $CD11c^{hi}CD40^{hi}CD8^{-}$ as well as $CDc^{int}CD40^{hi}CD8^{-}$ can efficiently uptake VLPs and cross-prime CTLs upon intradermal injection (Ruedl et al., 2002). However, $CD8^{+}$ DCs are more potent in cross-presenting antigens presented by VLPs (Keller et al., 2010). VLPs will be distributed in

the draining LN upon arrival. It has been shown previously that VLPs ranging from 20-200nm colonize the sub-capsular, medullar as well as the cortical regions of the draining LNs 2h post subcutaneous injection (Manolova et al., 2008). DCs also participate in capturing VLPs and present VLP-derived peptides in the T-cell zone causing T and subsequent T_H cell dependent B-cell activation (Wykes, Pombo, Jenkins, & MacPherson, 1998). dDCs preferentially migrate to the paracortex areas in the draining LNs underneath B-cell zone while LCs colonize the inner-paracortex region (Kissenpfennig et al., 2005).

It has been shown earlier that skin-derived DCs are the initial transporters of herpes-simplex virus (HSV) to $CD8^+$ DCs for effective CTL response (Allan et al., 2006). Accordingly, it is assumed that actively transported VLPs via (dDCs or LCs) would follow the same migration pattern to T-cell zone and act as key activator of the immune response (Figure 1.6) (Mohsen, Gomes, Vogel, & Bachmann, 2018).

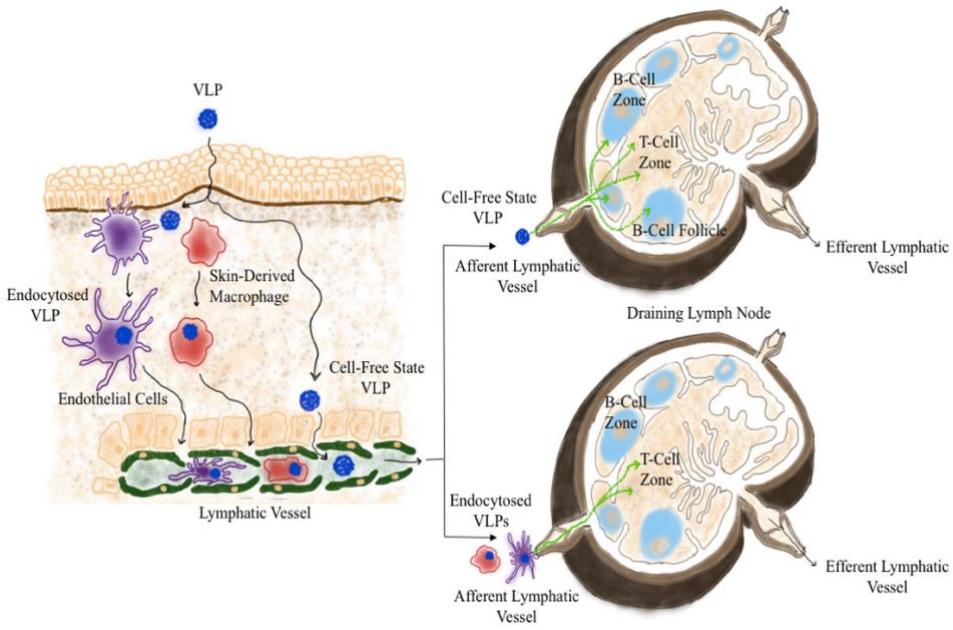

Figure 1. 6 VLPs trafficking to and in the draining lymph nodes

VLPs ranging from 20-200nm can freely drain to the lymphatic vessels or actively transported by dDCs and LCs to the draining LNs. When VLPs reach the sub-capsular region of the draining LNs they will be phagocytosed or bound by different APCs and preferentially colonize B or T-cell zones. VLPs actively transported by dDCs or LCs mostly reach T-cell zone for T-cell activation and priming. Adapted from: (Mohsen et al., 2018).

1.3.3 VLP-derived antigen presentation by major-histocompatibility molecules (MHC)

The up-taken VLPs will be next presented on MHC molecules of APCs. VLPs can be efficiently presented on MHC-I and II (Bachmann & Jennings, 2010) and the efficiency of both pathways have been quantified *in vivo* in a previous study (Storni & Bachmann, 2004). This was carried out by using MHC-I or II LCMV-derived antigen linked to VLPs and the results indicated that cross-presentation of VLP displaying the antigen on MHC-I molecules were only 1 to 10-fold less efficient than the classical presentation of MHC-II molecules. Such

data indicates that exogenous VLP can be loaded efficiently on MHC-I molecules (Storni & Bachmann, 2004).

1.3.4 VLPs as a vaccine template

VLPs possess powerful pathogen-associated structural pattern (PASP) that enhances and facilitates their interaction with the innate and adaptive immune system. VLPs have been used as effective vaccines. The advantages of using VLPs as a vaccine template (Figure 1.7) are mainly based on; their favorable size; the ability to modify their exterior surface; and the ability to package them with different immune-stimulators (Bachmann & Jennings, 2010; Gomes, Mohsen, & Bachmann, 2017; Mohsen, Zha, Cabral-Miranda, & Bachmann, 2017).

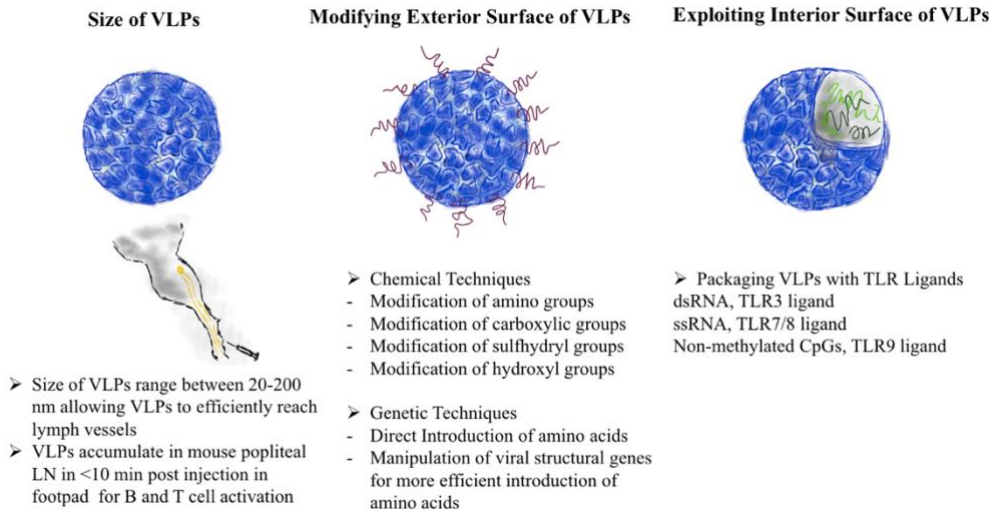

Figure 1. 7 General characteristics of virus-like particles which render them an attractive vaccine platform

The characteristics include the size of VLPs, the ability to modify the exterior surface of VLPs and the ability to exploit the interior surface to package different nucleic acids. Modified from: (Mohsen, Zha, et al., 2017).

1.3.4.1 VLPs' size influence their draining kinetics and immunogenicity

The lymphatic vessels regulate the fluid balance in the body as well as immune cell trafficking to different lymphoid organs, in (Mohsen, Zha, et al., 2017) particularly to the LNs (Randolph, Angeli, & Swartz, 2005). The initial lymphatic vessels are very permeable due to the presence of gaps or button-like junctions between the endothelial cells lining the vessels (Baluk et al., 2007). Therefore, particulate substances such as VLPs with 20-200nm in diameter (optimal size 30-40nm) can directly drain into the lymphatic vessels (Figure 1.8), and thus facilitate fast and immediate encounters with immune cells (Manolova et al., 2008). It has been shown that the drainage properties of antigens influence their overall immunogenicity (Fifis et al., 2004; Jia, Guo, & Fan, 2012).

VLPs can also be actively transported to the draining LNs by skin-resident macrophages and dendritic cells (DCs), especially Langerhans cells (LCs) and dermal DCs (dDCs) (Gomes, Flace, et al., 2017; Niikura et al., 2013; Yue et al., 2010). These cells will squeeze through the gaps in the lymphatic vessels along CCL19/ CCL21 gradient to the draining LN. VLPs can actively been taken and cross-presented for CTL response by dermal DCs characterized by $CD40^{hi}CD11^{+}CD8^{-}$ and $CD40CD11^{int}CD8^{+}$ following an intradermal injection (Ruedl et al., 2002). However, $CD8^{+}$ DCs are more powerful in cross-presenting VLPs (Keller et al., 2010).

In summary, the size of VLPs influence their immunogenicity in two ways; by allowing fast kinetics to the secondary lymphoid organs, and secondly by enhancing and facilitating their immediate and efficient interaction with APCs.

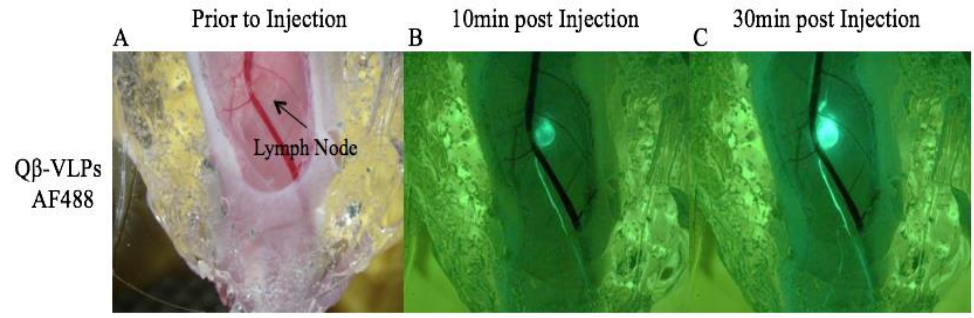

Figure 1. 8 VLPs' size influence their draining kinetics and immunogenicity

The draining kinetics of labeled Qβ-VLPs bearing the size of ~ 20nm at the popliteal LNs after subcutaneous injection into mice footpad. Adapted from (Mohsen, Gomes, et al., 2017).

1.3.4.2 Modifying the exterior surface of VLPs

VLPs outer surface can be modified, principally by chemical techniques or genetic modification (Brune et al., 2016; Schwarz et al., 2005). The most commonly used chemical method for covalent attachment are via Lys or Cys modifications. In the cysteine modification method, a cysteine may be naturally presented on the surface of VLPs or added by mutation. This method has been used to couple antigens to some VLPs such as P22, MS, CPMV and CCMV (Chatterji et al., 2004; Pan et al., 2012; Servid, Jordan, O'Neil, Prevelige, & Douglas, 2013; Yildiz, Shukla, & Steinmetz, 2011). Lysine modification is based on modifying the primary amino group on VLPs surface. This is an efficient and simple method for displaying proteins, peptides or fluorescent probes on the surface of VLPs (Comellas-Aragones et al., 2009; Phelps, Dang, & Rasochova, 2007; Wu et al., 2012). The advantage of genetic techniques is that they facilitate better introduction of specific attachment sites for complete modification of the VLP protein coat. For example, Asp and Glu can be changed

to Gln and Asn in TMV-VLPs (A. D. Brown, Naves, Wang, Ghodssi, & Culver, 2013).

1.3.4.3 Packaging VLPs with immuno-stimulators

Viruses naturally evolved to package their own viral genome. However, VLPs are expressed and produced in the absence of any viral genes, therefore they form a safe template for vaccine development as they do not package any viral genome (Gomes, Mohsen, et al., 2017). However, during expression in host system VLPs assemble around the host RNA. Several RNA phage-derived VLPs, package bacterial RNA upon expression in *E*. coli (Fang et al., 2017; Storni et al., 2004). Furthermore, VLPs can be disassembled and reassembled around different nucleic acids or other polyanions to modulate the innate immune response by engaging pathogen-recognition receptor (PRRs) (Gomes, Mohsen, et al., 2017; Janeway & Medzhitov, 2002; Storni et al., 2004).

VLPs are generally inefficient at inducing strong CTL response, however the addition of TLR ligands such as TLR-9 ligands can enhance T_H1 and CTL responses (Storni et al., 2004). Nonmethylated CpGs are TLR9-ligands and classified into three main categories based on their structure and the immune response they generate. Generally, CpGs can activate type-I IFN and several inflammatory cytokines in plasmacytoid DCs (Tabeta et al., 2004). Type-A CpGs consist of a phosphodiester poly-G and an internal palindrome sequence. Type-A CpGs can considerably induce type-I IFN specially by pDCs (Akira, Uematsu, & Takeuchi, 2006). On the other hand, type-B CpGs consist of phosphorothioate backbone which is capable of inducing less type-I IFN but higher levels of pro-inflammatory cytokine such as IL-12 (Utaisincharoen et al.,

2003). TLR7/8 within the endosomes of APCs can effectively recognize uridine/guanosine ssRNA as well as guanine nucleotides such as R848 (Hemmi et al., 2000). RNase enzymes in the extra-cellular matrix are usually responsible for degradation of free RNA. Accordingly, the possibilities that free RNA will effectively reach the endosomes of APCs are quite low. Therefore, packaging ssRNA (TLR7/8 ligands) in VLPs can protect it from degradation and enables the RNA to reach the endosomal compartments.

TLR3 can recognize dsRNA and is primarily expressed in cDCs such as poly I:C adjuvant which causes effective production of type-I IFN as well as pro-inflammatory cytokines (Figure 1.9) (Lopez & Peppas, 2004). Furthermore, formulating VLPs with Poly I:C adjuvant can enhance and improve CTL response (Schwarz et al., 2003).

Generally, VLP protein shells will be degraded in the endosomal compartment of APC upon internalization. The release of the packaged nucleic acids in the endosomes will result in TLR-dimerization which will initiate the signalling pathways of different transcription factors such as interferon-regulatory factors 3&7 (IRF3 and IRF7), activator protein-1 (AP-1) and nuclear factor kappa-light chain enhancer of activated B cells (NF-κB). AP-1 and NF-κB enhance the expression of several pro-inflammatory proteins including chemokines (CCL2 and CXCL8), cytokines (IL-6 and TNF) as well as other co-stimulatory molecules (CD80 and CD86). IRF3 and 7 are responsible for the expression of genes related to Type-I IFNs (Lester & Li, 2014; Takeda & Akira, 2005; Xagorari & Chlichlia, 2008).

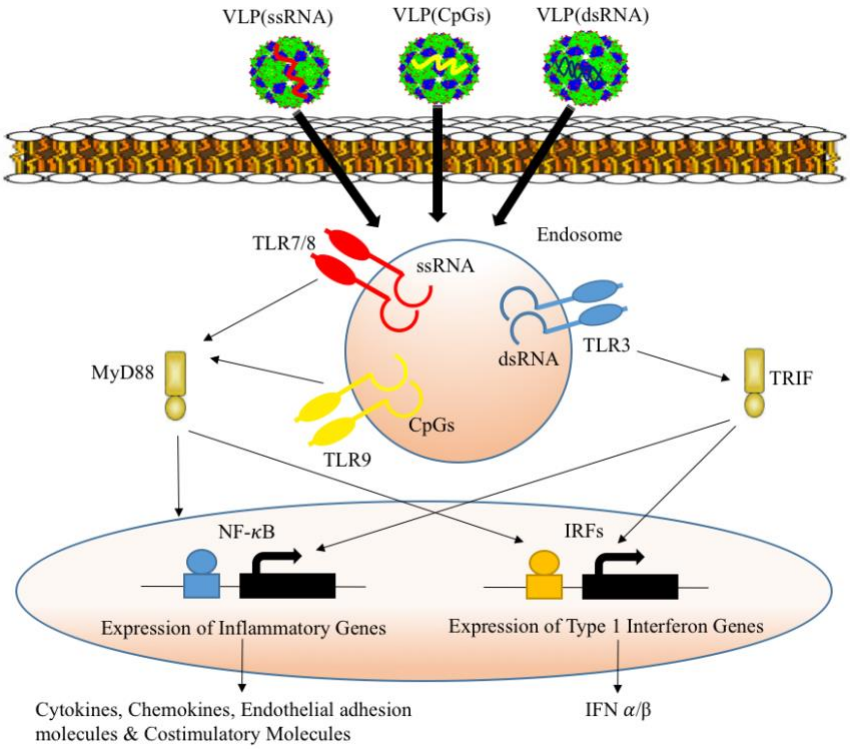

Figure 1. 9 Packaging VLPs with immuno-stimulators

The interior surface of VLPs can efficiently be packaged with different nucleic acids such as ssRNA –TLR7/8 ligand-, dsRNA –TLR3 ligand- or CpGs –TLR-9 ligand-. The packaged VLPs will be internalized by APCs and the nucleic acids will be released in the endosomes following the degradation of the VLP outer protein shell. The release of the nucleic acid causes TLR-dimerization which result in the activation of several transcription factors such as AP-1, NF-κB and IRFs. The activation of these transcription factors will induce the expression of type-I IFN and inflammatory genes. Adapted from (Mohsen et al., 2018).

Based on the above, VLPs represent an attractive, robust, effective, safe and affordable template for vaccine development. VLP-based vaccines have made remarkable steps in vaccinology and the field is rapidly growing. Several prophylactic VLP-based vaccines have been commercialized nowadays including vaccines against human papilloma virus (HPV) such as Cervarix®, Gardasil® and Gardasil9®. Also, a third-generation vaccine against hepatitis-B

virus (HBV) Sci-B-Vac™ has been developed to overcome some of the drawbacks of the first and second hepatitis B vaccine. The VLP-based vaccine Sci-B-Vac™ has been approved and licensed for use in several east Asian countries as well as in Israel (Zuckerman et al., 2001).

Recently a VLP-based vaccine against malaria Mosquirix™ has been approved by the European authorities (Moorthy & Ballou, 2009; Olotu et al., 2011; Regules, Cummings, & Ockenhouse, 2011). Plenteous other VLP-based vaccines are undergoing preclinical and clinical testing targeting different infectious diseases such as HIV, malaria, influenza and chikungunya and chronic diseases such as allergy, smoking, Alzheimer`s and hypertension. VLP-based vaccines against cancer have also been extensively developed and tested in preclinical and clinical trials as discussed next.

1.3.5 VLPs as a therapeutic cancer vaccine

The ultimate aim and objective of a therapeutic cancer vaccine is to generate protective cell-mediated immune responses. This is achieved by efficient priming of T_H1 cells, which will help activation of protective CTL effector responses and thus enable the clearance and destruction of cancerous cells (Maecker, Umetsu, DeKruyff, & Levy, 1998). VLPs displaying tumour specific antigens have shown to selectively generate a strong CTL response against tumours while reducing the risk of autoimmunity (Speiser et al., 2010). VLPs have been utilized as a therapeutic cancer vaccine platform in several types of cancers including: hepatocellular carcinoma, breast cancer, melanoma, pancreatic cancer and cervical cancer (Ong, Tan, & Ho, 2017). Table 1.6 lists some of the studies presenting effective CTL response using VLP-based

vaccines in different types of cancers. Additionally, there is evidence that VLP-based vaccines can overcome the inhibitory effect of the tumour microenvironment (Cubas, Zhang, Li, Chen, & Yao, 2011; M. Li et al., 2008).

Table 1. 6 List of some preclinical studies of VLPs in different types of cancers

Virus-Like Particle	Cancer Type	Cancer Antigen Targeted	Reference
Hamster polyomavirus	Hepatocellular Carcinoma	-	(Pleckaityte et al., 2015)
HBc	Hepatocellular Carcinoma	MAGE-1, MAGE-3, AFP-1	(H. G. Zhang et al., 2007)
HBc	Hepatocellular Carcinoma	HBx	(Ding et al., 2009)
IBDV	Cervical Cancer	E7	(Martin Caballero et al., 2012)
RHDV	Cervical Cancer	E6	(Jemon et al., 2013)
SIV	Pancreatic Cancer	Trop2	(Cubas et al., 2011)
SHIV	Pancreatic Cancer	hMSLN	(M. Li et al., 2008)
SHIV	Pancreatic Cancer	mMSLN	(S. Zhang et al., 2013)
Murine polyomavirus	Breast Cancer	Her2	(Tegerstedt, Franzen, Ramqvist, & Dalianis, 2007; Tegerstedt et al., 2005)
HBc	Melanoma	MAGE-3	(Kazaks, Balmaks, Voronkova, Ose, & Pumpens,

			2008)
Murine polyomavirus	Melanoma	OVA (model antigen), TRP2	(Brinkman et al., 2005)

Previous studies have provided good evidence that VLPs constitute a good template for melanoma vaccine development. It has been shown that peptides coupled to VLPs loaded with CpGs induce a powerful $CD8^+$ T-cell response in mice, which protect against viral infections as well as fibrosarcoma tumour cell lines transfected with the relevant epitope used for vaccination (Storni & Bachmann, 2004). More recently, these findings have been extended to an industry standard model of chronic HPV infection, where it has demonstrated almost complete protection against transplanted tumour cells in a therapeutic setting upon VLP-based vaccination against E7 (Gomes, Flace, et al., 2017).

Furthermore, VLP-based cancer vaccine approach has been translated from mouse to patients in several clinical trials in different chronic diseases including cancer (specifically melanoma). Indeed, a therapeutic VLP-based vaccine [Qβ(G10)-Melan-A] for melanoma has been successfully developed and tested in phase I/II for stage II/IV melanoma patients. The VLP-based vaccine was designed by linking melanoma differentiation specific antigen Melan-A/Mart1 to Qβ-VLPs which were packaged with TLR-9 ligand (type-A CpGs) as an adjuvant for effective stimulation of dendritic cells (DCs) and $CD8^+$ T-cells. Type A CpGs were used as in humans, only pDCs express TLR9 that respond best to A-type CpGs (Pashine, Valiante, & Ulmer, 2005). The results of the study were promising as 14 out of 22 patients generated specific T-cell responses capable of producing high levels of IL-2, IFN-γ and TNF-α and exhibiting mostly a central memory phenotype. The route of administration

(subcutaneous or intradermal) did not reveal important difference (Speiser et al., 2010). In addition to strong $CD8^+$ T-cell responses, Melan-A specific $CD4^+$ T-cell responses were also induced upon vaccination (Braun et al., 2012). Consequently, a phase IIa study for stage II/IV melanoma patients was conducted using the same vaccine, Qβ(G10)-Melan-A, in addition to different adjuvants such as Montanide or topical Imiquimod comparing different routes of administration. The results have shown that 76% of the patients generated specific T-cell responses. Using Imiquimod as adjuvants was most effective and resulted in higher levels of central memory T-cells. This study concluded that combining CpGs with Imiquimod would enhance $CD8^+$ central memory T-cell responses in melanoma patients (Goldinger et al., 2012).

Furthermore, and most remarkably, the study demonstrated by PET an ongoing immune response for more than a year in draining LNs of vaccinated individuals. This reveals a sustained immune response induced by the VLP-based vaccine. In addition to the strong and sustained immune responses, a reasonable number of biopsies ~50% exhibited elimination of Melan-A, demonstrating that strong T-cell responses were induced, but targeting a single epitope may not be sufficient to eliminate tumours (Goldinger et al., 2012). Furthermore, ongoing clinical trials for (CMP-001) have shown promising results. CMP-001 is a Qβ-VLPs loaded with A-type CpGs which has shown great promise as a cancer therapeutic even without tumour-specific antigen(s). Table 1.7 summarized CMP-001 ongoing clinical trials for patients with melanoma.

Table 1. 7 Ongoing clinical trials of CMP-001 vaccine for Melanoma patients

Study Title	Intervention	Phase	Clinical Trial No. *Clinicaltrials.gov*
Clinical study of CMP-001 in combination with Pembrolizumab or as a monotherapy for stage IV skin melanoma	CMP-001 Pembrolizumab (anti-PD-1)	I	NCT02680184 https://www.clinicaltrials.gov/ct2/show/NCT03596476?rank=1
Phase 1b study evaluating alternative routes of administration of CMP-001 in combination with Pembrolizumab in subjects with advanced melanoma	• CMP-001 • Pembrolizumab (anti-PD-1)	I II	NCT03084640 https://www.clinicaltrials.gov/ct2/show/NCT03084640?cond=CMP-001&rank=3

1.4 Challenges in cancer vaccine development

Over the last three decades therapeutic cancer vaccines have achieved only modest immune responses mainly due to several challenges. Briefly these challenges include, inappropriate or suboptimal vaccine platforms and formulation, insufficient delivery of target antigens, insufficient or ineffective adjuvants, difficulties in identifying immunogenic tumour antigens, and immunosuppressive mechanisms of tumour microenvironment (S. H. van der Burg, R. Arens, F. Ossendorp, T. van Hall, & A. J. M. Melief, 2016).

Furthermore, it is likely that use of only one or two tumour antigens is insufficient to generate and maintain therapeutic immune responses in cancer patients (D. S. Chen & Mellman, 2013; Kruit et al., 2013).

Taken together, it is proposed that the development of a VLP-based vaccine for melanoma may solve a number of these challenges and constitutes a promising approach for developing an affordable therapeutic cancer vaccine which can be translated into clinics.

2. Targeting germline and mutated epitopes enhances the immunogenicity of a preclinical model of personalized VLP-based vaccine

2.1. Introduction

2.1.1. Towards personalized cancer vaccine

Recently, several methods aimed to harness the exquisite uniqueness of the immune system have been developed (Hu et al., 2018). Immunotherapy is considered nowadays an important arm in the treatment of individuals with cancer. Approaches such as adoptive T-cell transfer therapy and CAR-T cell therapy against CD19 have been approved by the FDA in 2017 for the treatment of childhood acute lymophoblastic leukemia (Naddafi & Davami, 2015). Another effective approach that has been discussed earlier is the use of mAbs directed against CTLA4, PD-1 or PD-L1. These checkpoint inhibitors have shown good outcome in clinical trials and therefore have been approved by the FDA for the treatment of several solid tumours (Sharma & Allison, 2015; Whiteside, Demaria, Rodriguez-Ruiz, Zarour, & Melero, 2016). Despite the promising results, both adoptive T-cell therapy and check-point inhibitors have some limitations, reflected mainly by the restricted number of patients who could benefit from these therapies. CAR-T cell therapy is targeting mainly a single antigen, and has shown impressive results in patients with B-cell lymphoma expressing CD19 surface antigen (Park, Geyer, & Brentjens, 2016). Solid tumours in general lack a single common surface antigen and therefore pose a challenge for effective CAR-T cell therapy. Besides, CAR-T cells fail to survive in the solid tumour microenvironment as the intricate net of tumour components, immune cells and stromal cells leads to CAR-T cell exhaustion

and anergy (D'Aloia, Zizzari, Sacchetti, Pierelli, & Alimandi, 2018). Similarly, the ORR of using single checkpoint inhibitor was only 30% in several solid tumours (D. F. McDermott et al., 2015; Topalian et al., 2012; Topalian et al., 2014). Furthermore, it has been shown that checkpoint inhibitor activity is negligible to absent in some malignancies including pancreatic cancer (Brahmer et al., 2012) and microsatellite-stable colorectal cancer (Le et al., 2015). Therefore, there is an increasing focus to better understand the biological basis of variable response among cancer patients.

With the advancement in identifying and predicting candidate tumour epitopes by computational pipelines in real-time, personalized cancer vaccine theory becomes real. Melanoma was selected for this mission due to its high mutational burden and heterogeneity. Few successful clinical trials have been done recently based on neoantigen pipeline discovery in patients with advanced melanoma – some have been discussed earlier in *therapeutic cancer vaccine chapter* under *DC-based vaccine* (Fritsch, Hacohen, & Wu, 2014) and *RNA-based vaccine* (Ott et al., 2017; Sahin et al., 2017). A summary of these trials are listed hereunder in Table 2.1 (Vasquez, Tenesaca, & Berraondo, 2017).

Table 2. 1 Summary of most successful personalized cancer vaccines

Research center/company	Title	Phase	Clinical trial
Dana-Farber Cancer Institute A phase I study with a personalized NeoAntigen cancer vaccine for stage IIIB, IIIC, and IVM1a and b cutaneous melanoma	▪ (NeoVax) Peptide ▪ Poly-IC	I Active, not recruiting	NCT01970358 https://clinicaltrials.gov/ct2/show/NCT01970358 (Ott et al., 2017)

BioNTech IVAC Mutanome phase-I clinical trial in advanced melanoma patients using intra-nodal administration	▪ RBL001/RBL002 ▪ IVAC MUTANOME Both are naked (RNA) based recombinant vaccines	I Active, not recruiting	NCT02035956 https://clinicaltrials.gov/ct2/show/NCT02035956
Neon Therapeutics For patients with: Urinary Bladder Cancer, Carcinoma of the Bladder, Malignant Melanoma Non-Small-Cell Lung Cancer	▪ (NEO-PV-01) Peptide ▪ Anti-CTLA4	I Recruiting	NCT02897765 https://clinicaltrials.gov/ct2/show/NCT02897765
University of Pennsylvania Dendritic cells (White Blood Cells) vaccination for advanced melanoma	▪ Mature DC vaccine against gp100 ▪ Cyclophosphamide	I Completed	NCT00683670 https://clinicaltrials.gov/ct2/show/NCT00683670 No results published yet

2.1.2. Intra-tumour heterogeneity of melanoma

Intra-tumour heterogeneity (ITH) is found in almost all human solid tumours and is considered a major challenge in the development of therapeutic cancer vaccines (J. Zhang et al., 2014). It has been observed that malignant cells consist of morphologically distinct cells differ in their genomics, proteomics, epigenomics and transcriptomes as well as their metastatic potentials (Dick, 2008; Marusyk & Polyak, 2010).

A crucial issue is the clonal evolution of tumours that arises mainly from selective pressure, causes some mutants to expand (Meacham & Morrison, 2013; Sharma, Hu-Lieskovan, Wargo, & Ribas, 2017). Melanoma is an aggressive, heterogeneous, and complex class of cancer with high propensity to metastasize (Andor et al., 2016; Gupta et al., 2005). According to the Cancer Genome Atlas, melanoma has the highest rate of mutations amongst all types of cancers (Lawrence et al., 2013). The average number of mutational rate in melanoma is about 16.8 mutations per megabase (Mb) (Cancer Genome Atlas, 2015). The complexity of the melanoma phenotype affects its responsiveness to various therapies. Therefore, scientists emphasize the need for personalized treatments, including vaccinations that target neoantigens representing the uniqueness of each patient's tumour. Neoantigens are considered an attractive hit because T-cells specific for these altered-self antigens are not (or less) attenuated by immune tolerance mechanisms when compared to T-cells specific for conserved self (germline) antigens (Hacohen, Fritsch, Carter, Lander, & Wu, 2013).

2.1.3. Tumour-antigen identification

Identifying the tumour antigen is another main challenge in therapeutic vaccine development. Previous vaccination attempts have mainly targeted overexpressed antigens, tumour associated antigens, differentiation antigens or oncofetal antigens. However, it has remained difficult to identify tumour-specific T-cell epitopes that are actually displayed on tumour-MHC molecules and that are able to induce/ re-ignite tumour-specific T-cell responses. It may be possible to select tumour-specific T-cell epitopes based on RNA-expression

and/ or whole exome sequencing data. The methodology is straightforward, but results may be confounded by false positive and false negative hits, in particular for less well described HLA-molecules. This is mainly due to the hyperpolymorphism among HLA genes which poses a real challenge for accurate HLA-binding prediction based on whole exome sequencing data (Dilthey et al., 2016).

An alternative approach is based on identification of peptides bound to MHC molecules using mass-spectroscopy (MS), also known as immunopeptidomics (Bassani-Sternberg & Coukos, 2016). Immunopeptidomics is based on identifying and quantifying MHC-bound peptides by mass spectroscopy. Identifying this peptide repertoire, has advanced our understanding of immunology, cancer immunology and will pave the way for novel vaccine designs (Faridi, 2018; Neefjes et al., 2011). However, leading scientists have recently gathered to discuss the goals and challenges of the Human Immuno-peptidome project (HIPP) which is focused on mapping HLA-bound peptide repertoire presented to T-cells. The challenges are mainly due to the tremendous HLA allelic polymorphism among individuals and the difficulties in the detection of rare but perhaps important peptides which may result in false negative results (Caron, Aebersold, Banaei-Esfahani, Chong, & Bassani-Sternberg, 2017). Basically, immunopeptidomics approach is using the same sequence identification workflow as the field of proteomics. Therefore, immunopeptidomics shars the same drawback, including considerable differences in sample preparation and stability (Faridi, 2018). Previous attempts to identify personalized neoantigens have mainly been based on whole exome sequencing combined and validated by RNA-sequencing (Ott et al.,

2017; Sahin et al., 2017). In the future, combining whole exome sequencing with MS approaches may be able to overcome these limitations.

Furthermore, using tumour-infiltrating cells to probe recognition of identified peptides by pre-existing T-cells is a promising way to prioritize the peptides identified in silico or by peptidomics. However, there is no consensus in the field as to which approach is optimal both in terms of potential immunogenecity, as well as clinical feasibility, and it may vary between tumour types and vaccination approaches. Most efforts have attempted to identify MHC class I restricted epitopes recognized by $CD8^+$ T-cells. Recently, it has become evident that additional induction of $CD4^+$ T-cells is clinically very important as well and may be easily achieved using long peptides (Kreiter et al., 2015; Ott et al., 2017; Sahin et al., 2017).

Given the facts that powerful tumour infiltrating T-cells (TILs) recognize multiple tumour antigens, and that the targeting of single antigens allows tumours to relapse as antigen- or MHC-loss escape variants, it is desirable to target multiple antigens (D. S. Chen & Mellman, 2013; Hu et al., 2018; Kruit et al., 2013). However, identifying sufficient numbers of neoantigens may be challenging for many types of human tumours as some have only relatively low mutational burden in the repertoire of peptides bound to MHC (Yarchoan, Hopkins, & Jaffee, 2017). Additionally, a cancer cell usually expresses only a fraction of the proteins encoded by its genome and most of the mutated proteins may not generate mutated peptides binding to MHC class I proteins. It has been shown that a typical colorectal or breast cancer would contain an average of 7 to 10 mutated peptides that can bind HLA protein (Segal et al., 2008; Vogelstein et al., 2013). Targeting neoantigens by vaccination has

therefore so far only been done in patients with tumours of high mutational burden, essentially melanoma (Carreno et al., Science 2015; Ott et al., 2017; Sahin et al., 2017). Hence, it remains important to investigate the relative importance and therapeutic potential of mutated versus germ-line epitopes.

2.1.4. Tumour-microenvironment immunosuppression

Immunotherapy has revolutionized the landscape of melanoma treatment. Yet, clinical trials have mostly produced modest results and primary and acquired resistant cases have been reported among treated patients (Gide, Wilmott, Scolyer, & Long, 2018). Such treatment barriers could be due to several factors playing an essential role in augmenting the immunosuppressive effect of the tumour microenvironment (Rivoltini et al., 2005; Zigrino, Loffek, & Mauch, 2005). Stromal cells of tumour microenvironment participate in immune escape by recruitment of different immunosuppressive cells such as: regulatory T-cells (Tregs) (Gajewski, 2007), regulatory DCs (McCarter et al., 2007; Shurin, Naiditch, Zhong, & Shurin, 2011), tumour-associated macrophages (M2) (P. Chen et al., 2011; Qian et al., 2017) and myeloid-derived suppressor cells (MDSCs) (Gabrilovich, Ostrand-Rosenberg, & Bronte, 2012; Umansky & Sevko, 2012; Umansky, Sevko, Gebhardt, & Utikal, 2014). MDSCs are immature population of myeloid cells, and represent precursors for DCs, macrophages and granulocytes that failed to terminally differentiate due to different pathological conditions such as chronic inflammation, stress or cancer (Gabrilovich, 2017). Ample studies support that MDSCs play an important role in tumour progression, immunotherapy resistance, angiogenesis and metastasis (Ostrand-Rosenberg, 2010; Tartour et al., 2011). MDSCs consist of two main

categories, granulocytic MDSCs (PMN-MDSCs) and monocytic MDSCs (M-MDSCs) (Bronte et al., 2016). In murine models, MDSCs express CD11b and Gr1 markers and can be further divided into two main subsets: granulocytic MDSCs $CD11b^{+}Ly6G^{+}Ly6C^{low}$ and monocytic MDSCs $CD11b^{+}Ly6G^{low}Ly6C^{hi}$ (Umansky et al., 2014). Human MDSCs are also divided into two main subsets: PMN-MDSCs HLA-$DR^{-/low}CD11b^{+}CD15^{+}CD14^{-}$ or HLA-$DR^{-/low}CD11b^{+}CD66b^{+}CD14^{-}$, and secondly, M-MDSCs HLA-$DR^{-/low}CD11b^{+}CD15^{-}CD14^{+}$.

2.1.5. Experimental approach

In this study, the Qb VLP/CpG has been adapted to develop a platform for the generation of "personalized" cancer vaccines in mice. Using immunopeptidomics and whole exome sequencing, tumour-specific germ-line as well as mutated CTL epitopes of the B16F10 melanoma cell line were identified. B16F10 melanoma cell line was transfected with p33 peptide derived from Lymphocytic Choriomeningitis virus (LCMV) as an internal control. Peptide p33 is a strong H-2Db restricted epitope that has been used as model epitope for many years (Lacasse, Denis, Lapointe, Leclerc, & Lamarre, 2008; Oehen & Brduscha-Riem, 1998; Ruedl et al., 2005).

The identified epitopes were then prioritized and validated by bioinformatics and *in vitro* experiments. The selected peptides were coupled to Qβ-VLPs using bio-orthogonal Cu-free click chemistry forming multi-target vaccine cocktails (MTV), Qβ-VLPs were also loaded with B-type CpGs as a potent immune-stimulator. The vaccines were produced with germline epitopes (GL-MTV) or mutated epitopes (Mutated-MTV) or a mixture of both (Mix-

MTV) and tested in mice harboring the aggressive B16F10p33 melanoma tumours in combination with anti-CD25 mAb.

The developed platform provides a proof of concept for a personalized cancer vaccine based on both immunopeptidomics and whole exome sequencing methods and by using the bio-orthogonal Cu-free click chemistry that would potentially allow peptide-VLP linking at the patients' bedside, paving the way for rapid translation to clinical application.

2.2. Research questions and objectives

2.2.1. Research questions

1. Can we build an algorithm for the development of a personalized melanoma vaccine based on VLPs?
2. Can we develop a better, safer and less toxic chemistry for coupling antigens of interests to VLPs? Is using Cu-free click chemistry as efficient and effective as SMPH chemistry when developing VLP-based vaccine?
3. Can immunopeptidomics be used to identify tumour-specific T-cell epitopes?
4. Can we use TILs to validate the immunogenicity of T-cell epitopes identified by immunopeptidomics or whole exome sequencing?
5. Which group of multi-target VLP-based vaccine confers the best protection against B16F10p33 melanoma tumour model?
6. Which group of the multi-target VLP-based vaccine can alter the myeloid cell composition of the tumour?

2.2.2. Research objectives

1. To develop an algorithm for generation of personalized melanoma vaccine platform based on VLPs.
2. To test whether Cu-free click chemistry is more efficient than SMPH chemistry in coupling antigen of interest to VLPs, and whether it enhances the production of specific CTL response.
3. To test if immunopeptidomics in combination with whole exome sequencing can be an efficient method to identify and predict T-cell epitopes.
4. To test whether TILs can be used to prioritize epitopes identified by immunopeptidomics or predicted by whole exome sequencing.
5. To test the immunogenecity of the developed multi-target VLP-based vaccines, germline epitopes, mutated epitopes or a mixture of both in terms of tumour regression and CTL response.
6. To test whether the developed vaccines can alter the myeloid composition of the tumour.

2.3. Reagents and materials

Table 2. 2 Name, supplier and catalogue number of peptides, reagents and materials

Reagent	Supplier	Catalogue Number
SMPH (succinimidyl-6-(X-maleimidopropionamido) hexanoate NHS ester)	Thermo Fisher SCIENTIFIC	22363
DBCO (Dibenzocyclooctyne NHS ester)	Sigma-Aldrich	761524
DMSO	Sigma-Aldrich	M81802

DMEM Medium	Sigma-Aldrich	D6046
Fc Block antibody	eBioscience	553142
CD8α mAb/anti-mouse/PerCP-Cyanine 5.5	eBioscience	45-0081-80
CD45.2 mAb (104), PE-Cyanine7	eBioscience	25-0454-80
F4/80 mAb (BM8), PE	eBioscience	12-4801-80
CD11b mAb (M1/70), PE-Cyanine7	eBioscience	25-0112-81
Ly-6G mAb (1A8-Ly6g), APC	eBioscience	17-9668-80
FITC anti-mouse Ly-6C mAb	Biolegend	128005
MHC Class II (I-A/I-E) mAb (M5/114.15.2), PerCP-eFluor 710	eBioscience	46-5321-80
IFN-γ mAb/anti-mouse/APC	eBioscience	554413
TNF-α mAb/anti-mouse/PE	eBioscience	12-7321-81
Tetramers H2-Db (KAVYNFATM) PE	TCMetrix	Custom made
anti-mouse mAb PD-1 (CD279)	BioXCell	BE0146
Purified anti-mouse CD25 mAb	Biolegend	1020021
Monensin	BD Bioscience	554724
BrefeldinA	BD Bioscience	555029
IC Fixation Buffer	Fisher-Scientific SCIENTIFIC	00-8222-49
Permeabilization Buffer 10x	Fisher-Scientific SCIENTIFIC	00-8333-56
Collagenase D	Roche	11 088 858 001
DNase I	Sigma-Aldrich	000000004716 728001
p33 (NH2-KAVYNFATMGCC-H2)	Pepscan PRESTO	Custom made
p33 (NH2-KAVYNFATMGCCN3-H2)	Pepscan PRESTO	Custom made

B-type CpGs 5″-TCC ATG ACG TTC CTG ATG CT-3″	Iba	Tlrl-1668c
SYBR Safe DNA gel stain	Thermo Fisher Scientific	S33102
Brilliant Blue R Staining Solution	Sigma-Aldrich	6104-59-2
Materials	**Supplier**	**Catalogue Number**
Amicon centrifuge tubes 100 kDa MWCU	Thermo Fischer Scientific	UFC501008
Any kD mini-protein TGX precast protein gel	Bio-RAD	4569033
70 μM cell strainer	BD Bioscience	352350

2.4. Methods

2.4.1. Production & purification of Qβ-VLPs

Qβ-VLPs expression and production was performed and provided by the core lab facility at University of Bern.

Qβ-VLPs expression and production was performed as previously described in detail in (Cielens et al., 2000; Kozlovska et al., 1996; Storni et al., 2002).

2.4.2. Packaging Qβ-VLPs with type-B CpGs

The 20mer B-type CpGs (5″-TCC ATG ACG TTC CTG ATG CT-3″) (20 mer) with phosphorothiate backbone was synthesized by (IBA). 20 mM HEPES was used to solubilize Qβ-VLPs. The natural RNA was digested as explained earlier by RNaseA. Qβ-VLPs was then repackaged with B-type CpGs (1.125 μg/ 20μg Qβ-VLPs) and packaging was confirmed using 1% agarose gel stained by SYBRsafe stain, while Qβ-VLPs protein was detected by subsequent Coomassie Blue stain.

2.4.3. Generation of Qβ(CpGs)-p33 vaccines using SMPH chemistry

B-type CpGs were packaged in Qβ-VLPs as described above. Qβ(CpGs)-VLPs were derivatized using SMPH heterobifunctional for 1 h at RT. Excess SMPH cross-linker was removed using Amicon centrifuge tubes of 100kDa MWCO. Modified version of p33 model peptide (H-KAVYNFATMGGC-NH2) was purchased from (Pepscan PRESTO) which has been synthesized by adding GCC amino acids to the C terminus of the peptide to facilitate its coupling to SMPH cross-linker. The modified peptide was reconstituted in DMSO. 10-fold molar excess of the modified peptide was added over Qβ(CpGs)-VLPs monomer. The mixture was incubated at RT for 2 h and excess peptide was removed using Amicon centrifuge tubes. The efficiency of the coupling was tested by using SDS-PAGE (Any kD mini-protein TGX precast protein gel, Bio-Rad). The gel was run at 200V for 35 min and stained with Coomassie Blue and destained as previously described. The coupling efficiency was assessed by densitometric analysis of SDS-PAGE of Qβ-VLP monomer bands compared to Qβ-VLP monomer plus p33 after coupling.

2.4.4. Generation of Qβ(CpGs)-p33 vaccines using DBCO (Cu-free click chemistry)

B-type CpGs were packaged in Qβ-VLPs as described above. After packaging. Qβ(CpGs)-VLPs were derivatized for 30 min, 24°C on shaker (400 rpm) using DBCO cross-linker (dibenzocyclooctyne NHS ester) purchased from (Sigma-Aldrich). Excess uncoupled DBCO was dialyzed by 100kDa MWCO amicon centrifuge tubes. Modified P33 peptide H-KAVYNFATMGGCK(N3)-NH2 was purchased from (Pepscan PRESTO) and added to Qβ(CpGs)-VLPs in a 5-fold molar excess over the VLPs monomers. The coupling was performed for 1

h, 24°C on shaker (400 rpm) and excess peptide was removed. The efficiency of the coupling was tested by SDS-PAGE stained with Coomassie stain.

2.4.5. Measuring p33 specific T-cell response with tetramers

P33 (H-KAVYNFATM-NH2) tetramers designed with H2-Db allele and APC or PE fluorochrome (TCMetrix) were used to measure p33 specific T-cell response in C57BL/6 mice (6-8 weeks old; Harlan) seven days after a single s.c. injection of 50μg Qβ(CpGs)-p33 vaccine coupled with SMPH cross-linker or DBCO cross-linker. The spleens were collected and smashed using 70 μM cell strainer. The collected cells were washed 1x with sterile PBS and RBCs were lysed using ACK lysis buffer. 1 x 10^6 cells were collected in 96-well V-bottom plate and stained with live/dead, Fc block, anti-CD8α mAb purchased from (eBioscince). The cells were washed 1x with sterile PBS and then stained with p33 specific tetramers (H-KAVYNFATM-NH2) designed with H-2Db allele APC or PE fluorochrome purchased from (TCMetrix). Analysis was carried out by flow cytometry by gating on singlets, lymphocytes, $CD8^+$ cells and then $Tetramer^+$ cells.

2.4.6. Intra-cellular cytokine (ICS) staining for IFN-γ and TNF-α

Intra-cellular cytokine staining was performed on spleens and TILs of immunized mice to measure IFN-γ and TNF-α cytokines. In general, 2 x 10^6 cells were collected from spleen (as explained in methods 2.4.5) or TIL (as explained in methods 2.4.11) (and pulsed with 2 μg of p33 peptide (H-KAVYNFATM-NH2) for 6 h at 37°C with a mixture of Brefeldin A (1:1000) (Sigma-Aldrich) and Monensin (1:1000) (Sigma-Aldrich) (as per the manufacturer's instructions). Cells were collected and washed 3x with sterile PBS, 0.1% BSA. 1 x 10^6 cells were collected in 96-well V-bottom plate and

stained with live/dead, Fc block, anti-CD8α mAb purchased from (eBioscince). Cells were then fixed using 100µl of fixation buffer (Invitrogen) and permeabilization was done using 1x permeabilization buffer (Invitrogen) as per the manufacturer's instructions. Cells were then stained for intra-cellular cytokines anti- IFN-γ and TNF-α mAb (eBioscience). Analysis was carried out by flow cytometry by gating on singlets, lymphocytes, $CD8^+$ cells and then IFN or TNF. Full ICS staining protocol was adapted from: *http://www.biolegend.com/media_assets/support_protocol/BioLegend_Intracellular_Cytokine_Staining_protocol.pdf.*

2.4.7. CFSE *in vivo* cytotoxic assay

C57BL/6 mice (6-8 weeks old; Harlan) were immunized with a single s.c. injection of 50 µg Qβ(CpGs)-p33 vaccine coupled with SMPH cross-linker or DBCO cross-linker. Seven days later, target splenocytes from naïve mice were collected and RBCs were lysed and divided into 2 groups for each mouse. The 1st naïve splenocyte group was labelled with 2 µM CFSE (Thermo Fisher Scientific) and kept unpulsed while the 2nd naïve splenocytes group was first pulsed with 1 µM p33 and then labelled with 10 µM CFSE. The prepared target groups were then mixed in 1:1 ratio and each previously vaccinated mouse received $1 \times 10^7$of unpulsed $CFSE^{low}$ cells and $1 \times 10^7$of unpulsed $CFSE^{high}$ cells i.v. Four h later the spleens of vaccinated mice were collected and analysed by flow cytometry for frequency of $CFSE^{low}$ and ^{high}. Specific lysis for each group was measured using the formula "Ratio = ($CFSE^{high}$ / $CSFE^{low}$)".

2.4.8. Immunopeptidomics for B16F10p33 melanoma cell line

Immunopeptidomics was performed by Dr. Nicola Ternette at the Target Discovery, University of Oxford.

B16F10p33 melanoma cell line "transfected with p33 peptide derived from LCMV" was kindly been given by (Adrian Ochsenbein lab) and cultured in T-150cm flask using Dulbecco's modified Eagle's medium (DMEM) with 10%FBS and 1% Streptomycin/Penicillin. When cells reached 80% confluency, they were washed 2x with sterile PBS to remove excess medium. Cells were collected with scrapers, centrifuged and freezed at -80°C in Eppendorf tubes. Cell pellets were stored frozen at -80ºC. Cells were lysed using 5 ml lysis buffer (1% Igepal, 300 mM sodium chloride, 100 mM Tris, pH 8.0) supplemented with protease inhibitor cocktail (Roche) for 30 min on ice. Lysates were cleared by two centrifugation steps at 500 g for 10 min and then 20,000 g for 60 min. One mg of anti-mouse MHC class I antibody (ATCC HB-51) was bound and cross-linked to 1 ml Protein G beads (GE healthcare). Lysates were incubated with the antibody beads over night at 4ºC and washed subsequently with 50 mM Tris, pH 8.0 containing either 150 mM, 450 mM and no salt. Peptides were eluted with 5 ml 10% acetic acid and concentrated in a vacuum concentrator (Eppendorf). Peptides were then injected onto a 4.6 x 50 mm ProSwift RP-1S column on an Ultimate 3000 system (Thermo Scientific). Peptides were separated from larger complex components by elution using a 500 µl/ min flow rate over 10 min from 2-30% ACN in 0.1% TFA. Alternate fractions that did not contain the beta-2-microglobulin were pooled and two final fractions were analysed by nano-ultra performance liquid chromatography tandem mass spectrometry (nUPLC-MS^2) on a Fusion Lumos (Thermo Scientific). Peptides

were separated on a Ultimate 3000 RSLCnano system (Thermo Scientific) using a PepMap C18 column, 2 µm particle size, 75 µm x 50 cm (Thermo Scienific) with a 1 h linear gradient of 3-25% buffer B (0.1% formic acid, 5% DMSO in acetonitrile) in buffer A (0.1% formic acid, 5% DMSO in water) at a flow rate of 250 µl/ min. Peptides were introduced using an Easy-Spray source at 2000 V to a Fusion Lumos (Thermo Scientific) at 305ºC. Full MS spectra were recorded from 300-1500 m/z in the Orbitrap at 120,000 resolution with an AGC target of 400,000. Precursor selection was performed using TopSpeed mode at a cycle time of 2 s. Peptide ions were isolated using an isolation width of 1.2 amu and trapped at a maximal injection time of 120 ms with an AGC target of 300,000. Higher-energy collisional dissociation (HCD) fragmentation was induced at an energy setting of 28 for peptides with a charge state of 2-4, while singly charged peptides were fragmented at an energy setting of 32 at lower priority. Fragments were analysed in the Orbitrap at 30,000 resolution. Analysis of raw data was performed using Peaks 7.5 software (Bioinformatics Solutions). Sequence interpretation of MS^2 spectra was carried out using databases containing all mus musculus UniProt database entries at a FDR of 1.4. Motif analysis of common amino acids in peptide sequences was performed using WebLogo 3.5 (weblogo.threeplusone.com). Peptide binding predictions were performed using NetMHCpan 4.0 [http://www.cbs.dtu.dk/services/NetMHCpan/].

2.4.9. Whole exome sequencing for B16F10p33 melanoma cell line

Sequencing was performed by the service company FASTERIS, Switzerland. B16F10p33 melanoma cell line was cultured and collected as described earlier. DNA was isolated using Purelink genomic DNA mini kit according to

manufacturer's instructions (K1820-01, Thermo Fisher Scientific), which gives a yield of 394 ng/ul. The quality of the DNA yield was assessed by loading an aliquot on 2% agarose gel. A library was prepared by using Agilent SureSelect XT, based on the cRNA-baits targeted capture. The Mouse All Exon kit captures 49.6 Mb region that covers 221,784 exons within 24,306. Sequencing was performed using HiSeq 2500 machine with paired end 2 x 125 run, aiming x 100 (raw data) exome coverage by (FASTERIS).

2.4.10. Bioinformatics analysis for whole exome sequencing

Bioinformatics was performed by Dr. Julius Muller and Dr. Silvia Salatino at the Wellcome Centre for Human Genetics, University of Oxford.

Sequenced reads from the B16F10p33 melanoma cell line sample were mapped to the Mus musculus reference genome assembly GRCm38 from NCBI using the software BWA-MEM arXiv:1303.3997 (Heng Li, 2013) with default parameters. Supplementary alignments were removed and the resulting BAM file was sorted with SAMtools (H. Li et al., 2009). Mapped reads were subsequently used as input for the variant calling software Platypus (version 0.8.1, specifying the option "--minFlank=0") (Rimmer et al., 2014) to identify SNPs and short indels (<50 bp). The 74138 identified variants were annotated with standard R packages using GENCODE and further investigated with the Variant Effect Predictor Ensembl frame-work (VEP, release 90) (McLaren et al., 2016). Peptides were extracted using a sliding window from +/-8AA to +/-14AA around the mutation. HLA type prediction for H2-Db and H2-Kb alleles was performed using NetMHC4.0.

2.4.11. Prioritization assay (T-cell assays)

1 x 10^6 B16F10p33 melanoma cells were injected into 1 flank in $RAG^{-/-}$ (6-8 weeks old; Harlan). Twelve days later the growing tumours were collected and processed for transplantation into C57BL/6 mice (6-8 weeks old; Harlan) into one flank under anesthesia. The transplanted mice received a dose of anti-dot as per the regulations of (University of Oxford and University of Bern). The tumours were allowed to grow (without any treatment) for 14 days (set as the humane end point) and then were collected and kept on ice for further processing. Tumours were digested by DNaseI (Boehringer) and collagenase D (Roche) in 5% FSC containing DMEM for 1 h at 37°C. Tumours were then smashed in 100µm cell strainer (Sigma-Aldrich) and washed 2x with PBS. Tumour-infiltrating lymphocytes (TILs) were collected by Ficoll-paque premium (GE Healthcare) and centrifuged for 30 min at RT at 1800 rpm. TILs were collected and kept on ice for ICS experiment. At the same time bone marrow derived DCs (BMDCs) were prepared from naïve C57BL/6 mice (6-8 weeks old; Harlan) and pulsed with the selected peptides separately or as a mixture for 1 h at 37°C. The pulsed BMDCs were then washed 3x with DMEM medium and co-cultured with the collected TILs for 6 h at 37°C in addition to Brefeldin A (1:1000) (Sigma-Aldrich) and Monensin (1:1000) (Sigma-Aldrich). Surface staining was done by live/dead, Fc block and anti-CD8α mAb (eBioscience). Cells were then fixed and permeabilized for intra-cellular staining with anti- IFN-γ antibodies (eBioscience) as explained in (method 2.4.6). Analyses were carried out by flow cytometry.

2.4.12. Generation of multi-target vaccine based on Qβ(CpGs) using DBCO (Cu-free click chemistry)

The selected peptides were modified by extending them by 4-5 amino-acids at the C-terminus and by the addition of an azide (N3) group. Qβ-VLPs were first packaged with B-type CpGs as described in (Mohsen, Gomes, et al., 2017). After packaging, Qβ(CpGs)-VLPs were derivatized for 30 min 24°C on shaker 400 rpm using DBCO cross-linker (Sigma-Aldrich). Excess uncoupled DBCO was dialyzed by 100 kDa MWCO amicon centrifuge tubes. Modified peptides were added to Qβ(CpGs)-VLPs in a 5-fold molar excess over the VLP monomers. The coupling was performed for 1 h 24°C, shaking at 400 rpm, and excess peptide was removed as described above. The efficiency of the coupling was tested by SDS-PAGE stained with Coomassie stain.

2.4.13. Measuring Treg response

Peripheral blood from C57BL/6 mice immunized with the different multi-target vaccines was collected in heparin. RBCs were lysed with ACK lysing buffer (Thermo Fisher Scientific). Cells were stained with live/dead, Fc block and then with anti CD4 and anti-CD25 mAb (eBioscience), analyses were carried out by flow cytometry and gating strategy was done by gating on lymphocytes population followed by gating on $CD4^{+}$ $CD25^{hi}$ (Figure 2. S4).

2.4.14. Tumour experiments and survival rate

$1x10^{6}$ B16F10p33 melanoma cells were injected into 1 flanks in $RAG^{-/-}$ C57BL/6 mice (6-8 weeks old; Harlan). Twelve days later the growing tumours were collected and processed into ~1-2mm^{2} for transplantation into wild-type C57BL/6 mice (6-8 weeks old; Harlan) into 1 flank. The transplanted C57BL/6 mice were divided into 5 groups and treated 3 times over 14 days as described

hereunder (Table 2.4).

Table 2. 4 The prepared groups, treatment and route of injection

Groups	Treatment	Route of Injection
1	120 µg Qβ(CpGs)-VLPs (control group)	s.c.
2	10 µg anti-CD25 (control group)	i.v.
3	Germline multi-target vaccine (GL-MTV) 120 µg containing: 20 µg Qβ(CpGs)-PMEL17 20 µg Qβ(CpGs)-MTC-1 20 µg Qβ(CpGs)-Calpastatin 20 µg Qβ(CpGs)-ZFP518 20 µg Qβ(CpGs)-TRP-2 20 µg Qβ(CpGs)-Caveolin2	s.c
	10 µg anti-CD25	i.v.
4	Mutated multi-target vaccine (Mutated-MTV) 120 µg containing: 60 µg Qβ(CpGs)-Cpsf3l 60 µg Qβ(CpGs)-Kifl8b	s.c.
	10 µg anti-CD25	i.v.
5	Mix multi-target vaccine (Mix-MTV) 120 µg containing: 15 µg Qβ(CpGs)PMEL17 15 µg Qβ(CpGs) MTC-1 15 µg Qβ(CpGs)-Calpastatin 15 µg Qβ(CpGs)-ZFP518 15 µg Qβ(CpGs)-TRP-2 15 µg Qβ(CpGs)-Caveolin2 15 µg Qβ(CpGs)-Cpsf3l 15 µg Qβ(CpGs)-Kifl8b	s.c.
	10 µg anti-CD25	i.v.

Tumours were collected and tumour volume was measured using a caliper according to the formula V=(W x W x L)/2, where V is tumour volume, L is

tumor length and W is tumour width. TILs were isolated as explained in (method 2.4.11). TILs were stained with live/dead, Fc block and then anti-CD8α, IFN-γ, CD11b, Ly6C, MHC-II, CD45 mAb (eBioscience), and analyses were carried out by flow cytometry. Survival rates were evaluated and compared using the same designated groups. Transplanted C57BL/6 mice (6-8 weeks old; Harlan) were immunized twice a week and tumour volumes were monitored daily and measured using a caliper as explained earlier. Mice were sacrificed according to the humane end-point as per the score-sheet as per the regulations of (University of Oxford and University of Bern).

2.4.15. Statistics

Tumour growth curves were compared by calculating the area-under curve (AUC) and analysed by One-Way ANOVA (Turkey's Multiple Comparison Test). Other data in this chapter has been presented as mean ± SEM. Comparison between the groups was performed by One-Way ANOVA (Turkey's Multiple Comparison Test). Comparison between the different germline or mutated peptides vs Actin was performed by Student's *t* test. Survival rate was analysed by Log-rank (Mantel-Cox) test. GraphPad Prism7 software was used for the analysis. ns = not significant, ***=P value < 0.0001; **=P value < 0.001; *=P value < 0.01.

2.5. Results

2.5.1. Novel precision vaccine platform based on VLPs for personalized preparation at the bedside

Figure 2.1 illustrates the algorithm of developing a personalized VLP-based vaccine. First, patient-specific tumour epitopes need to be identified in a

systematic way. Previously performed clinical trials aiming at developing a personalized cancer vaccine have mainly used whole exome sequencing validated by RNA-sequencing to predict patient's specific neoantigens. Here, immunopeptidomics approach has been used to identify potential tumor-specific germ-line epitopes and whole exome sequencing to predict the mutated epitopes. To our knowledge, combining both approaches for the development of a personalized cancer vaccine has not been done before. In a second step, the identified and predicted epitopes should be prioritized and this was basically achieved by bioinformatics and stimulation of tumour-infiltrating cells using *in vitro* T-cell assays. Next, these epitopes need to be rendered immunogenic therefore, they have been extended slightly to 14 aa long peptides using their flanking protein sequence for the goal of targeting $CD8^+$ CTL. The extended peptides are then synthesized and coupled to CpG-loaded VLPs using Cu-free click chemistry. The bio-orthogonal chemistry employed in this study is a key step, as the compounds are completely non-toxic and will allow the formulation of peptides with VLPs at bedside. The process will result in VLPs displaying tumour-specific T-cell epitopes ready for vaccination.

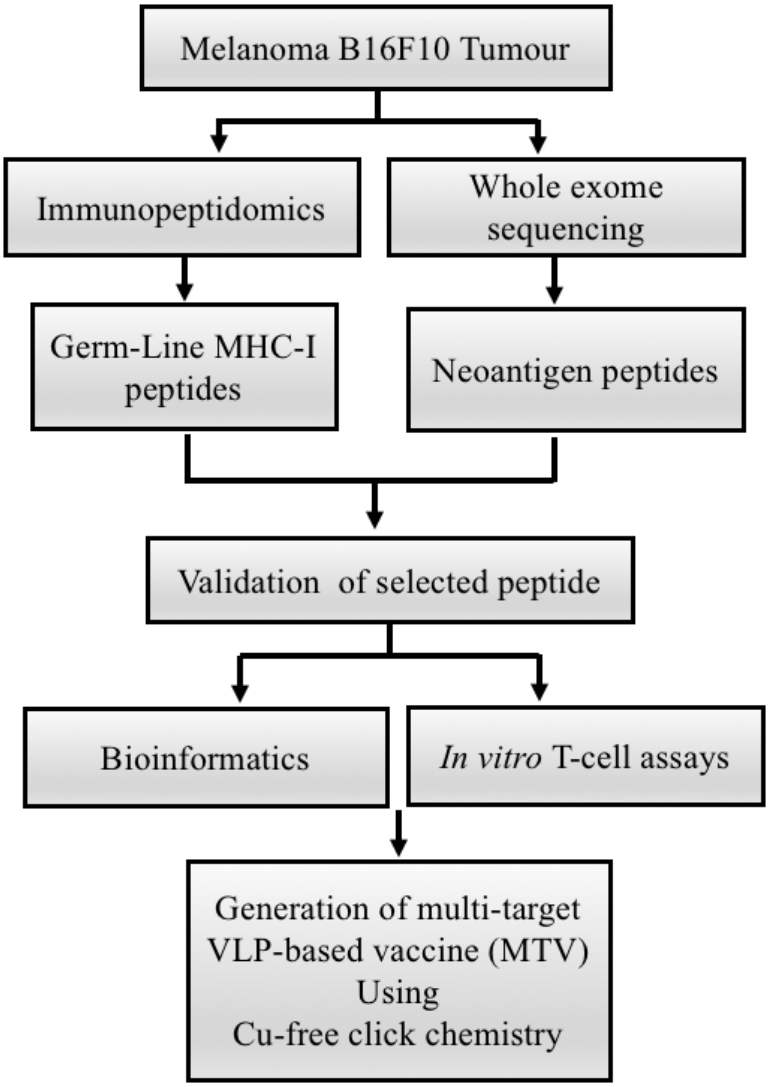

Figure 2. 1 Algorithm for generation of personalized melanoma vaccine platform based on VLPs

First, patient-specific tumour epitopes need to be identified in a systematic way. Here, immunopeptidomics approach has been used to identify potential tumour-specific germline epitopes and whole exome sequencing to predict the mutated ones. In a second step, the identified and predicted epitopes should be prioritized and this was basically achieved by bioinformatics and stimulation of tumour-infiltrating cells using *in vitro* T-cell assays. Next, the selected epitopes need to be extended to ~12-13 amino acids long peptides using their flanking protein sequence for the goal of targeting $CD8^+$ CTL. The extended peptides are then synthesized and coupled to CpG-loaded VLPs using Cu-free click chemistry. A mix-multi target VLP-based vaccine is proposed.

2.5.2. Bio-orthogonal Cu-free click chemistry is an efficient method for coupling peptide of interest to VLPs

For the development of VLP-based vaccines, SMPH cross-linker has been mostly used to couple the peptide of interest to VLPs (Fig. 2.S1) (Gomes, Flace, et al., 2017; Mohsen, Gomes, et al., 2017; Storni & Bachmann, 2004; Storni et al., 2002). Linking of cysteine on peptides to lysine on VLPs by SMPH has indeed proven reliable for development of VLP-based vaccines. However, for the generation of a personalized cancer vaccine, the method may have several disadvantages, namely that epitope internal cysteine will also react with SMPH on VLPs, causing their inactivation and non-reacted SMPH on VLPs is potentially toxic, requiring complex inactivation and purification procedures after coupling. Therefore, this technique is not well suited for rapid personalized vaccine production.

For these reasons, coupling method based on bio-orthogonal Cu-free click chemistry using DBCO cross-linker is proposed (Fig. 2.S2). This method is non-toxic and thus enables rapid and efficient coupling of regulatory compliant GMP produced VLPs and peptides that can potentially be done at patients' bedside. The effectiveness of DBCO based Cu-free click chemistry has been compared to the standard SMPH-based method by coupling p33 peptide –as a model antigen- derived from LCMV to Qβ-VLPs loaded with B-type CpGs. Cu-free click chemistry enhanced coupling efficiency in comparison to SMPH when assessed by SDS page (Figure 2.2A).

Immunization of C57BL/6 mice with Qβ(CpGs)-p33 vaccine based on Cu-free click chemistry resulted in increased frequencies of p33 specific $CD8^+$ T-cells as assessed by tetramer staining (Figure 2.2 B and E) and production of

IFN-γ seven days after a single subcutaneous injection (Figure 2.2 C). Lytic activity was also increased if assayed *in vivo* by performing CFSE cytotoxicity assays (Fig. 2.2 D and E). Thus, Cu-free click chemistry improves coupling-efficiency and vaccine immunogenicity compared to the standard SMPH chemistry.

A.

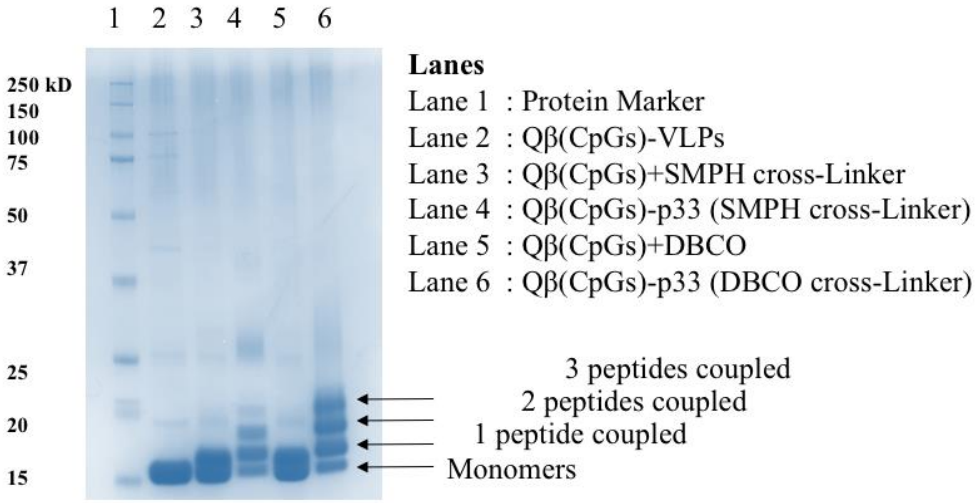

B.

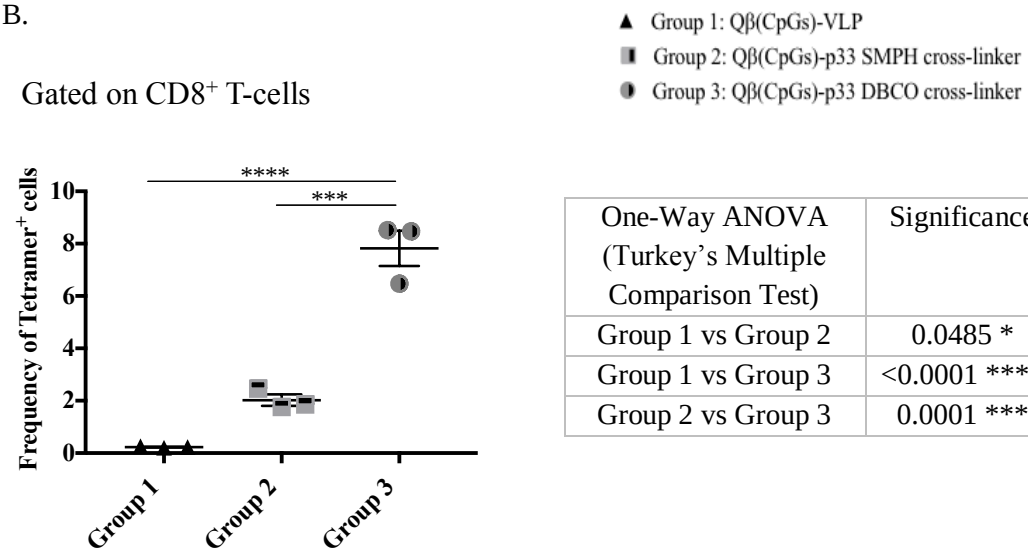

One-Way ANOVA (Turkey's Multiple Comparison Test)	Significance
Group 1 vs Group 2	0.0485 *
Group 1 vs Group 3	<0.0001 ****
Group 2 vs Group 3	0.0001 ***

C. Gated on $CD8^+$ T-cells

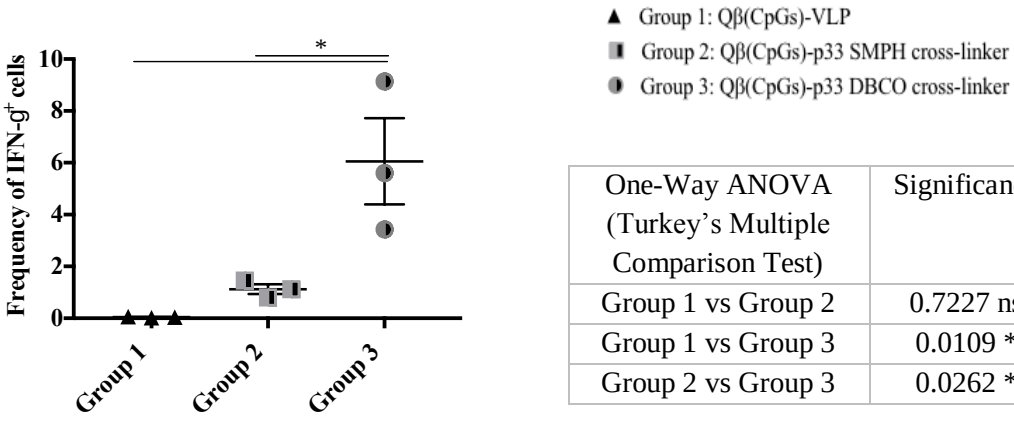

One-Way ANOVA (Turkey's Multiple Comparison Test)	Significance
Group 1 vs Group 2	0.7227 ns
Group 1 vs Group 3	0.0109 *
Group 2 vs Group 3	0.0262 *

D.

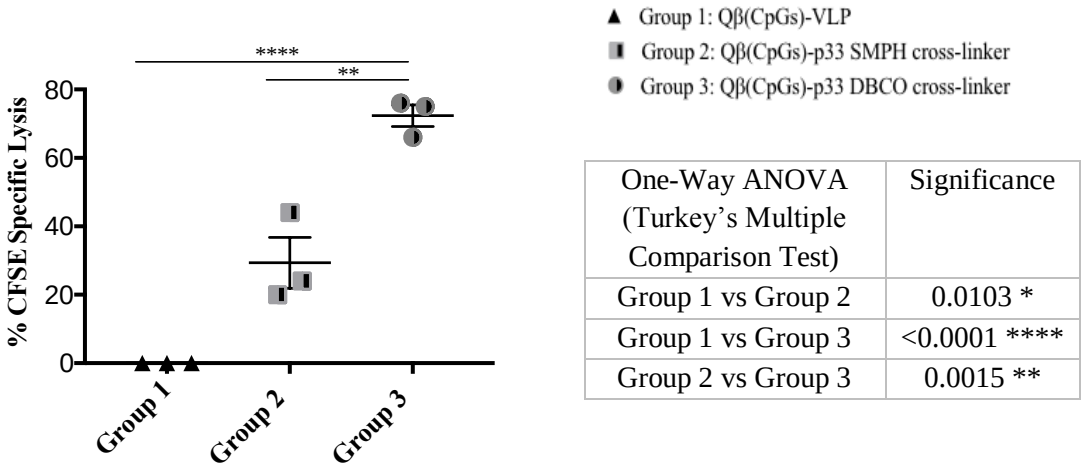

One-Way ANOVA (Turkey's Multiple Comparison Test)	Significance
Group 1 vs Group 2	0.0103 *
Group 1 vs Group 3	<0.0001 ****
Group 2 vs Group 3	0.0015 **

E.

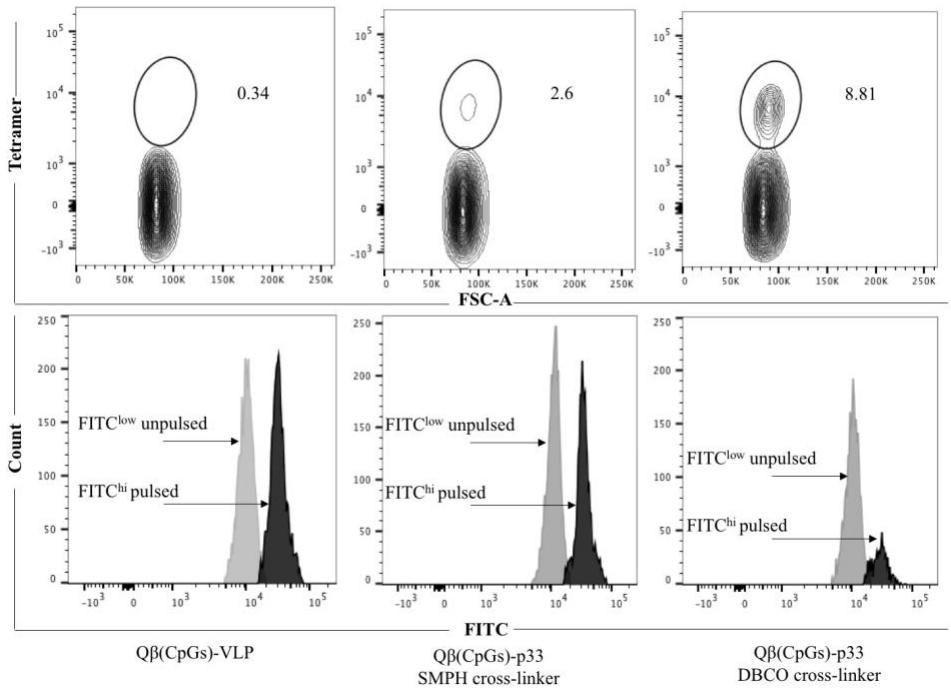

Figure 2. 2 Bio-orthogonal Cu-free click chemistry: An efficient method for coupling antigens to VLPs

A, SDS PAGE stained with Coomassie Blue Stain showing the coupling efficiency of p33 p to Qβ(CpGs)-VLPs using SMPH cross-linker or DBCO cross-linker (Lane 1, protein ladder, Lane 2: Qβ(CpGs)-VLPs, Lane 3: Qβ(CpGs)-VLPs derivatized with SMPH cross-linker, Lane 4: Qβ(CpGs)-VLPs derivatized with SMPH cross-linker and coupled to p33 peptide, Lane 5: Qβ(CpGs)-VLPs derivatized with DBCO cross-linker and Lane 6: Qβ(CpGs)-VLPs derivatized with DBCO cross-linker and coupled to p33 antigen) each extra band in Lanes 4 and 6 indicates a peptide binds to a Qβ monomer. *B*, Comparing the frequency of $CD8^+$ $Tetramer^+$ cells (means ± SEM) in the spleen when coupling p33 to Qβ(CpGs)-VLP using SMPH or DBCO cross-linker. Statistical analysis by One-Way ANOVA (Turkey's Multiple Comparison Test). *C*, Comparing the frequency of $CD8^+$ IFN-γ^+ cells (means ± SEM) in the spleen when coupling p33 to Qβ(CpGs)-VLP using SMPH or DBCO cross-linker. Statistical analysis by One-Way ANOVA (Turkey's Multiple Comparison Test). *D*, Comparing CFSE in vivo lytic activity in the spleen when coupling p33 to Qβ(CpGs)-VLP using SMPH or DBCO cross-linker, calculated % of specific lysis in each group 100X(1–CFSE high pulsed/CSFE low un-pulsed). Statistical analysis by One-Way ANOVA (Turkey's Multiple Comparison Test). *E*, top: Representative flow cytometry dot plots of tetramer frequency, bottom: representative flow cytometry histograms of CFSE. (n=3) mice per group, one representative of 3 similar experiments is shown.

2.5.3. Identification of $CD8^+$ T-cell epitopes of B16F10p33 melanoma by immunopeptidomics and whole exome sequencing

2.5.3.1. Immunopeptidomics

Immunopeptidomics for B16F10p33 murine melanoma cell line has been performed to identify peptides naturally presented on MHC-I molecules. As expected, a large number of MHC-I-associated peptides was identified (Figure 2.3A). I have evaluated the identified peptides for a number of essential physical parameters including the length (peptides of 8 or 9 aa "mers") (Figure 2.3B), MHC haplotype (H2-Db and/or H2-Kb) and affinity to MHC-I (high ranking

affinity peptides) as summarized in (Table 2.4). Using literature-based assessment, key characteristics such as being melanocyte-specific (*e.g.* Melanocyte protein PMEL17) or a candidate oncogene (*e.g.* Malignant T cell-amplified sequence 1) were also considered (Table 2.S1).

Table 2. 4 Selected Peptides from immunopeptidomics for the development of Multi-Target VLP-based vaccine

Selected Peptide	Sequence	# of AA	MHC haplotype	MHC-I affinity
Melanocyte protein PMEL (Melanocyte protein Pmel 17) (Premelanosome protein) (Silver locus protein) [Cleaved into: M-alpha; M-beta]	VLYRYGSF	8	H2-Kb	0.08
MTC-1 Malignant T- cell-amplified sequence 1 (MCT-1) (Multiple copies T- cell malignancies 1)	IGIENIHYL	9	H2-Db	0.01
Calpastatin (Calpain inhibitor)	SSPANISSL	9	H2-Db, H2-Kb	0.01
Zinc finger protein 518B	SSVQNKEYL	9	H2-Db	0.01
L-dopachrome tautomerase (DCT) (DT) (EC 5.3.3.12) (L-dopachrome Delta-isomerase) (SLATY locus protein) (Tyrosinase-related protein 2) (TRP-2) (TRP2)	SQVMNLHNL	9	H2-Db	0.015
Caveolin2	VMYKFLTV	8	H2-Kb, H2-Db	0.015

2.5.3.2. Whole exome sequencing

Castle et al, have exploited the mutanome of B16F10 melanoma cell line and identified 962 somatic non-synonymous point mutations. A total of 563 of the identified mutations occur in expressed genes (Castle et al., 2012). The authors performed systematic screening to test the immunogenicity of the identified mutanomes. Peptides with mutations in Kif18b and Cpsf31 (also known as Inst11) genes were tested separately for their anti-tumour effect, as long synthetic peptides in B16F10 murine models with Poly (I:C) adjuvant and have shown the best protection.

Based on these findings whole exome sequencing was carried out to confirm somatic point mutations in these specific two genes in B16F10 cell line. Several nonsynonymous single nucleotide variants (SNVs) have been identified, including a point-mutation in the 13th exon of the Kif18b gene affecting the transcript ENSMUST00000021311 (Chr11:102,908,157; c.2367T>G; p.Lys739Asn), and in the 9th exon of the Cpsf3l gene affecting both ENSMUST00000120794 (Chr4:155,886,970; c.1021G>A; p.Asp292Asn) and ENSMUST00000030901 (Chr4:155,886,970; c.1087G>A; p.Asp314Asn) isoforms (Figure 2.5.3C). As the sequences around the last couple of mutations were identical, one isoform/ protein was used. The extracted peptides were then tested *in silico* for MHC-I affinity H2-Db and H2-Kb as shown in Table 2.5. The affinity of MHC-I to the predicted mutated peptides from whole exome sequencing was much lower than those identified from immunopeptidomics. However, it has been suggested by *Fritch et al.,* that the immunogenic potency of the neoantigens do not always depend on the binding intensity to MHC molecule (Fritsch, Rajasagi, et al., 2014).

Table 2. 5 Selected peptides from whole exome sequencing for the development of multi-target VLP based vaccine

Mutated Epitope	AA Sequence	# of AA	MHC haplotypes	MHC-I affinity
Cpsf3l	TFANNPGPM p.D314N	9	H2-Db H2-Kb	0.7616 7.83 NetMHCpan4.0
Kif18b	FQEFVDWENV p.K739N	10	H2-Db H2-Kb	1.7 26 NetMHC4.0

A. B.

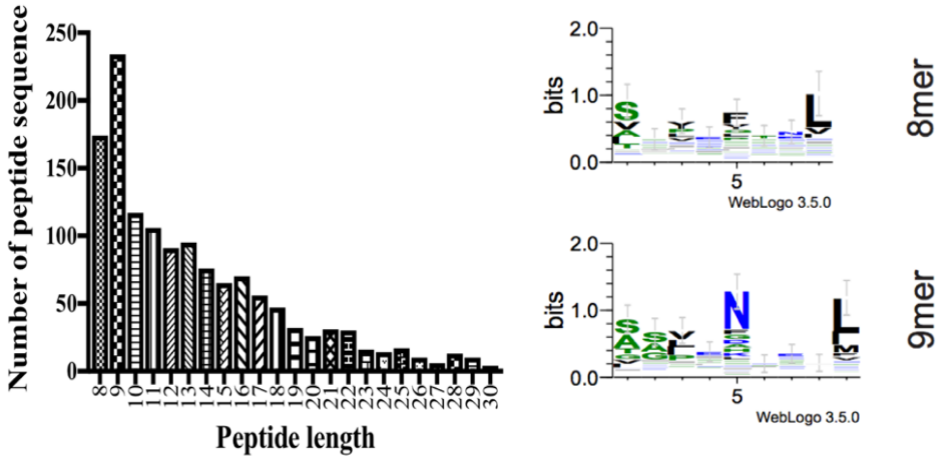

C.

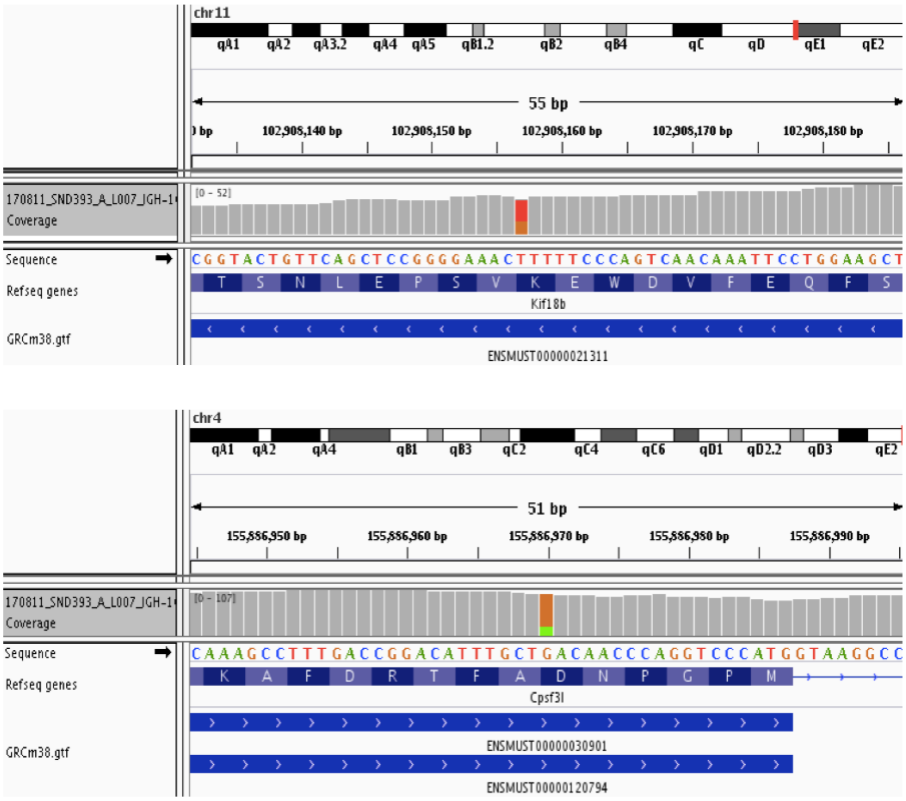

Figure 2. 3 Identification of CD8$^+$ T-cell epitopes of B16F10p33 melanoma cells by immunopeptidomics and whole exome sequencing

A, Length distribution of peptides identified by immunopeptidomics. *B*, 8 and 9 mers motifs identified by immunopeptidomics. *C*, Top: whole exome sequencing results showing a heterozygous SNV (marked in red and orange) in the 13th exon of gene Kif18b at position Chr11:102,908,157 (ENSMUST00000021311: c.2367T>G, p.Lys739Asn), causing a K>N missense mutation. Bottom: whole exome sequencing results showing a heterozygous SNV (marked in orange and green) in the 9th exon of gene Cpsf3l at position Chr4:155,886,970 (ENSMUST00000120794: c.1021G>A, p.Asp292Asn and ENSMUST00000030901: c.1087G>A; p.Asp314Asn), causing a D>N missense mutation.

2.5.4. Validation of germline and mutated epitopes identified by immunopeptidomics and whole exome sequencing

Next, the natural immunogenicity of the selected epitopes from immunopeptidomics and whole exome sequencing was validated. Tumour-infiltrating lymphocytes (TILs) are highly enriched with tumour specific T-cells and thus are the most relevant T-cell population in this regard. Therefore, selected peptides (Tables 2.3 and 2.4) were synthesized and assessed for recognition by TILs. To this end, TILs were isolated from C57BL/6 bearing the B16F10 melanoma cell line and activated them *ex vivo* with IL2 for 2 days. The activated TILs were then co-cultured with bone marrow derived DCs (BMDCs) pulsed separately with the selected peptides. The used B16F10 melanoma cell line is also tranfected with H2-Db restricted p33 epitope derived from LCMV. Therefore, p33 peptide was used as a positive control while actin peptide was used as a negative control. IFN-γ^+ production was then assessed by performing intra-cellular cytokine staining and analysed by flow cytometry as shown in (Figure 2.4). The results indicated that the selected peptides from immunopeptidomics and whole exome sequencing were effective at inducing significant IFN-γ^+ production (for example PMEL17 p 0.0005) when compared to actin as a negative control.

A.

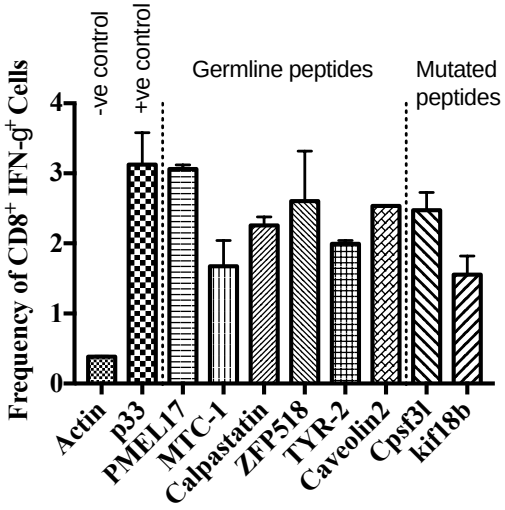

B.

Peptide	*P* value
PMEL17 vs Actin	0.0005 ***
MTC-1 vs Actin	0.0716 ns
Calpastatin vs Actin	0.0041**
ZFP518 vs Actin	0.09 ns
TRP-2 vs Actin	0.0008 ***
Caveolin2 vs Actin	0.0001 ****
Cpsf3l vs Actin	0.0146*
Kif18b vs Actin	0.0477 *

C.

PEPTIDE	$CD8^+$ IFN-γ^+ CELLS
Actin	0.385
p33	3.125
PMEL17	3.06
MTC-1	1.675
Calpastatin	2.26
ZFP518	2.605
TRP-2	1.995
Caveolin2	3.805
Cpsf3l	2.475
Kif18b	1.55

D.

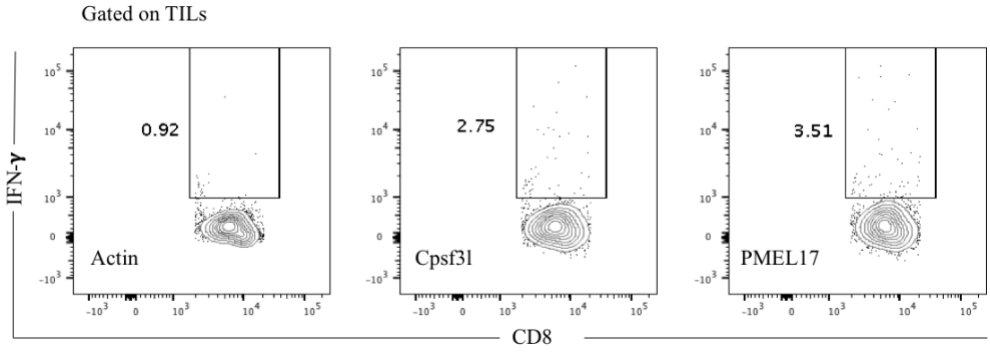

Figure 2. 4 Validation of germline and mutated epitopes identified by immunopeptidomics and ewhole xome sequencing

A, Frequency of $CD8^+$ IFN-γ^+ cells in TILs in naive C57BL/6 mice bearing B16F10p33 melanoma cell line using ICS on graph. *B*, Comparison between Actin and selected peptides (germline and mutated), statistical analysis by Student's *t* test. *C*, Average of two readings of frequency of $CD8^+$ IFN-γ^+ cells in TILs. *D*, Representative flow cytometry dot plots for Actin, Cpsf3l and PMEL17 peptides. One representative of 3 similar experiments is shown.

2.5.5. Multi-target VLP-based vaccine displaying B16F10p33 specific T-cell epitopes can be efficiently developed using Cu-free click chemistry

Displaying peptides on CpG-loaded VLPs renders them highly immunogenic for T-cells and represents a unique possibility to increase their immunogenicity. Hence, Qβ-VLPs were used and packaged with B-type CpGs as a scaffold. The efficiency of the packaging was confirmed using 1% agarose gel stained with SYBRsafe and Coomassie Blue Stain to assess the integrity of VLPs following the packaging process (Figure 2.5A). Three groups of multi-target vaccines (MTVs) were prepared as described in (Table 2.6).

The aim of testing the three groups separately was to compare the immunogenicity of germ-line T-cell epitopes identified by immunopeptidomics versus mutated peptides predicted by whole exome sequencing, and also versus the combination of both T-cell epitopes in one vaccine.

Table 2. 6 The three multi-target vaccines (MTV)

VLP Multi-Target Vaccine	Peptides
Germ-line epitope vaccine (GL-MTV) **Based on Immunopeptidomics**	▪ Melanocyte protein **(PMEL17)** ▪ Malignant T- cell- amplified sequence 1 (**MTC-1)** ▪ (Calpain inhibitor) **Calpastatin**

	▪ Zinc finger protein 518B **(ZFP518)** ▪ Tyrosinase-related protein 2 **(TRP-2)** ▪ **Caveolin2**
Mutated epitope vaccine (Mutated-MTV) **Based on whole exome sequencing/prediction**	▪ **Cpsf3l** ▪ **Kif18b**
Mix multi-target vaccine (Mix-MTV) **Based on both immunopeptidomics and whole exome sequencing/prediction**	▪ Melanocyte protein **(PMEL17)** ▪ Malignant T- cell- amplified sequence 1 (**MTC-1)** ▪ (Calpain inhibitor) **Calpastatin** ▪ Zinc finger protein 518B **(ZFP518)** ▪ Tyrosinase-related protein 2 **(TRP-2)** ▪ **Caveolin2** ▪ **Cpsf3l** ▪ **Kif18b**

In order to facilitate the proteasomal and endosomal processing of the selected peptides, the peptides were extended by 4-5 a.a. at the C-terminus, and also incorporated the coupling moiety. It has previously seen that C-terminal extensions allow efficient processing and efficient cross-presentation (Storni & Bachmann, 2004). Coupling of the selected peptides to Qβ(CpGs)-VLPs was carried out using the Cu-free click chemistry (DBCO cross-linker). Coupling efficiency was assessed by SDS-PAGE stained with Coomassie Blue Stain as shown in (Figure 2.5 B).

A.

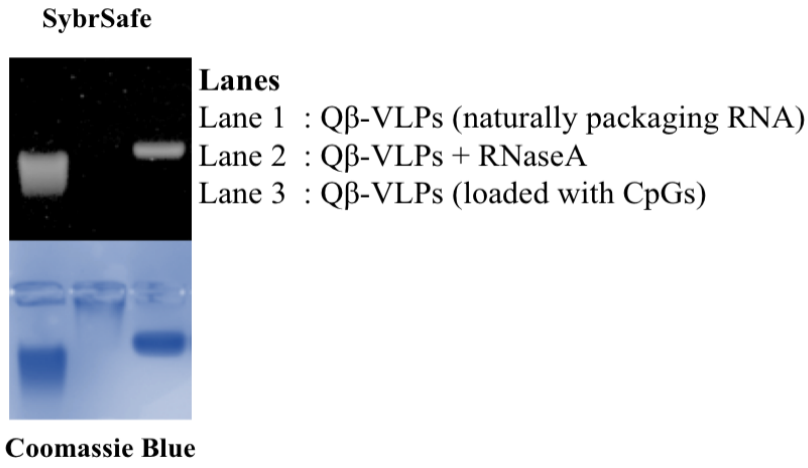

B.

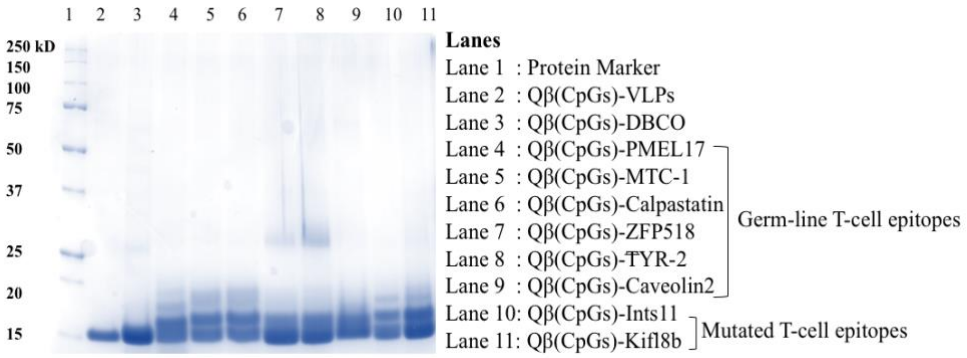

Figure 2. 5 Multi-target VLP-based vaccine displaying B16F10p33 specific T-cell epitopes can be efficiently developed using Cu-free click chemistry

A. Packaging of Qβ-VLPs was achieved by digesting the naturally packaged RNA and diffusing B-type CpGs into the empty capsid using 1.125µg CpGs/20µg Qβ for each single vaccine separately. The efficiency of the packaging was assessed using 1% agarose gel stained with SYBR safe (top: staining DNA and RNA) and Coomassie Brilliant Blue (bottom: staining protein) to confirm the stability of the packaged Qβ(CpGs)-VLPs. *B.* Packaged Qβ(CpGs)-VLPs were derivatized by DBCO cross-linker for coupling of the selected peptides (Table 2.5), SDS-PAGE shows the coupling efficiency of each peptide to Qβ(CpGs)-VLPs.

2.5.6. Mix multi-target VLP-based vaccine (Mix-MTV) in combination with anti-CD25 hindered B16F10p33 tumour progression

The developed multi-target VLP-based vaccine was then tested in C57BL/6 mice bearing B16F10 melanoma tumour. The aim of this project is to develop a therapeutic cancer vaccine. Therefore, a challenging experimental method was adapted by transplanting a $2mm^3$ sized B16F10p33 melanoma tumour into the flank of C57BL/6 mice and let the tumour grow for 5 more days *in vivo* before initiating vaccination (Figure 2.6A). C57BL/6 mice were vaccinated s.c. with the developed multi-target VLP-based vaccine in combination with low dose of anti-CD25 (10 μg/ injection) 3 times over 14 days as illustrated in Figure 2.6 B. Anti-CD25 was chosen based on the preliminary data that had shown that anti PD-1 mAb did not enhance the immunogenecity of various forms of the multi-target VLP-based vaccines, while anti-CD25 enhanced tumour regression in combination with the vaccines (Fig. 2S.3). Therefore, in order to increase the immunogenecity of the developed multi-target VLP-based vaccines and enhance CTL infiltration, they were combined with anti-CD25 mAb to deplete Tregs. The depletion of Tregs ($CD4^+$, $CD25^{hi+}$) was assessed in the periphery of vaccinated mice on day 6 (Fig. 2S.4), the results show significant depletion of ~80% (p 0.0001). All three multi-target VLP-based vaccines [GL-MTV+anti-CD25 mAb] (p <0.0001), [Mutated-MTV+ anti-CD25 mAb] (p 0.0001) and [Mix-MTV+ anti-CD25 mAb] (p <0.0001) could significantly hinder B16F10p33 melanoma tumour progression (Figure 2.6 C-D). However, the Mix-MTV group or GL-MTV group were more potent in causing melanoma regression when compared to the Mutated-MTV group. Treatment with anti-CD25 mAb alone did not show any protective results when used separately.

A.

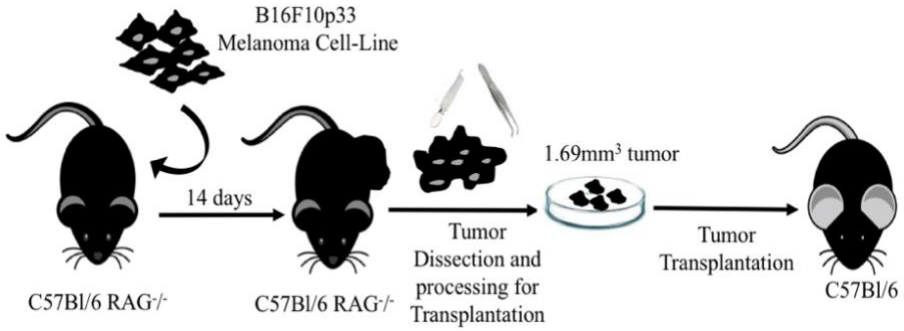

B.

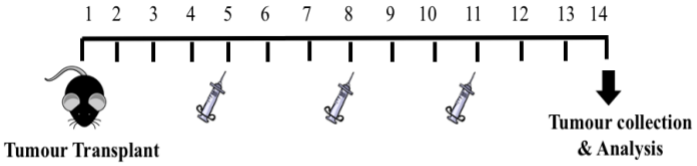

Qβ(CpGs)-VLPs 120 µg/ dose s.c.

anti-CD25 mAb 10 µg/ dose i.v.

GL-MTV 120 µg/ dose s.c. (containing 20 µg of each GL peptide)+ anti-CD25 mAb 10 µg/ dose i.v.

Mutated-MTV 120 µg/ dose s.c. (containing 60 µg of each mutated peptide)+ anti-CD25 mAb 10 µg/ dose i.v.

Mix-MTV 120 µg/ dose s.c. (containing 15 µg of each GL and mutated peptides)+ anti-CD25 mAb 10 µg/ dose i.v.

C.

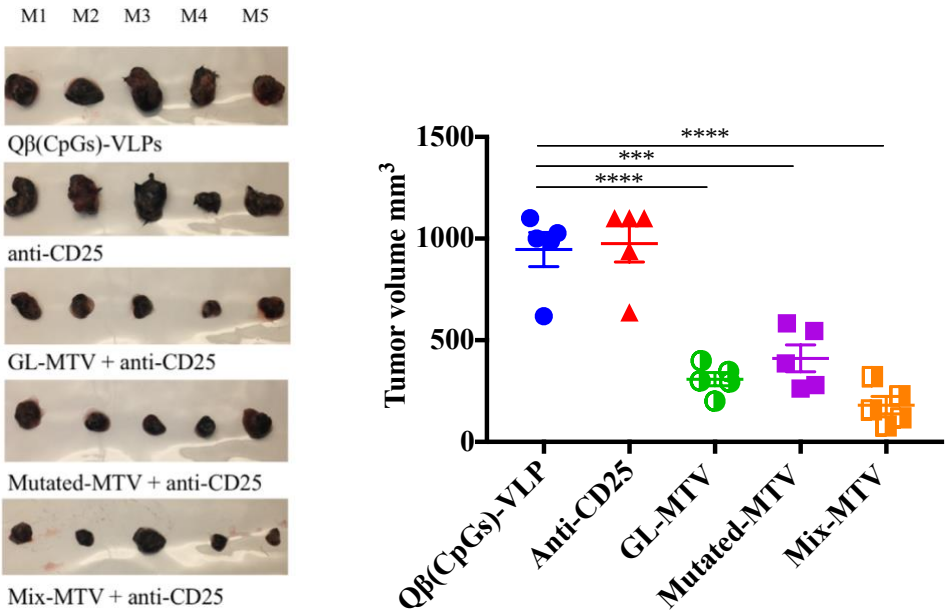

One-Way ANOVA (Turkey's Multiple Comparison Test)	Significance
Qβ(CpGs)-VLPs vs anti-CD25	0.998 ns
Qβ(CpGs)-VLPs vs GL-MTV	<0.0001 ****
Qβ(CpGs)-VLPs vs Mutated-MTV	0.0001 ***
Qβ(CpGs)-VLPs vs Mix-MTV	<0.0001 ****
anti-CD25 vs GL-MTV	<0.0001 ****
anti-CD25 vs Mutated-MTV	<0.0001 ****
anti-CD25 vs Mix-MTV	<0.0001 ****
GL-MTV vs Mutated-MTV	0.817 ns
GL-MTV vs Mix-MTV	0.6661 ns
Mutated-MTV vs Mix-MTV	0.1467 ns

D.

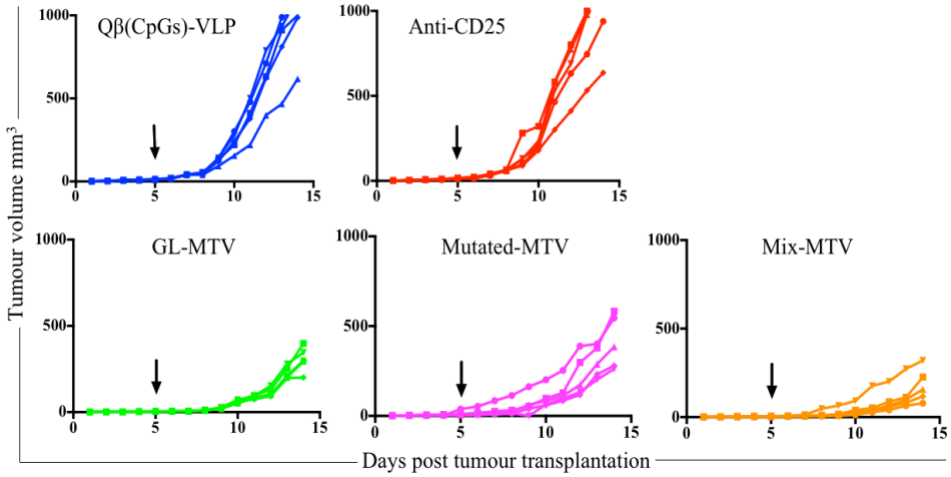

E.

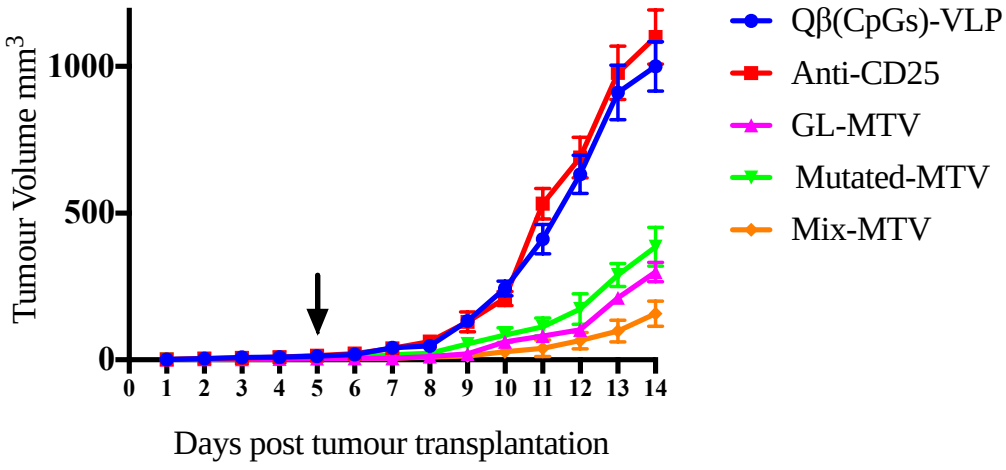

One-Way ANOVA (Turkey's Multiple Comparison test)	Significance
Qβ(CpGs)-VLPs vs anti-CD25	0.605 ns
Qβ(CpGs)-VLPs vs GL-MTV	<0.0001 ****
Qβ(CpGs)-VLPs vs Mutated-MTV	0.0004 ***
Qβ(CpGs)-VLPs vs Mix-MTV	<0.0001 ****
anti-CD25 vs GL-MTV	<0.0001 ****
anti-CD25 vs Mutated-MTV	<0.0001 ****
anti-CD25 vs Mix-MTV	<0.0001 ****
GL-MTV vs Mutated-MTV	0.7719 ns
GL-MTV vs Mix-MTV	0.8815 ns
Mutated-MTV vs Mix-MTV	0.2613

Figure 2. 6 Mix multi-target VLP-based vaccine [Mix-MTV] hindered B16F10 tumour progression

A, B16F10 tumour volume mm^3 (means ± SEM) measured at day 14 post tumour transplantation in mice treated with Qβ(CpGs)-VLP, Anti-CD25, [GL-MTV + anti-CD25], [Mutated-MTV+anti-CD25] and [Mix-MTV+anti-CD25], each dot represents a tumour. Statistical analysis by One-Way ANOVA (Turkey's Multiple Comparison Test). *B*, Individual tumour growth curve of s.c. B16F10 melanoma treated with the designated groups, arrows indicate start of treatment. *C*, Combined tumour growth curves of the five designated groups. arrows indicate start of treatment. Statistical analysis by measuring AUC analyzed by One-Way ANOVA (Turkey's Multiple Comparison Test). (*n=5*) mice per group, one representative of 3 similar experiments is shown.

2.5.7. Mix multi-target VLP-based vaccine (Mix-MTV) increased $CD8^+$ T-cell infiltration into the tumour

The groups vaccinated with [Mix-MTV + anti-CD25 mAb] and [GL-MTV + anti-CD25 mAb] have shown a sizeable frequency of $CD8^+$ T-cells when compared with the control group. Howver, such frequency was not statistically significant (*p* 0.1057 and 0.2364 respectively). Furthermore, [Mix-MTV + anti-CD25 mAb] did not show significant different results when compared to the

groups vaccinated with [Mutated-MTV+anti-CD25 mAb] or anti-CD25 (Figure 2.7 A and C).

When calculating the density of $CD8^+$ T-cells infiltrated in each tumour (number of $CD8^+$ T-cells divided by the tumour volume mm^3), there was a significant difference between the groups vaccinated with [Mix-MTV+anti-CD25 mAb] and the groups immunized with Qβ(CpGs)-VLPs (*p* 0.0028), anti-CD25 alone (*p* 0.0076) or [Mutated-MTV+anti-CD25 mAb] (*p* 0.0101). However, there was no significant difference between both groups [Mix-MTV+anti-CD25 mAb] and [GL-MTV + anti-CD25 mAb] (*p* 0.0611) (Figure 2.7 B). For IFN-γ^+ production by TILs, [Mix-MTV + anti-CD25 mAb] induced the strongest cytokine production when compared to the groups vaccinated with Qβ(CpGs)-VLPs (*p* 0.0044), anti-CD25 alone (*p* 0.0134). Interestingly, there was no significant difference (*p* 0.3500) between the [Mix-MTV+anti-CD25mAb] and [Mutated-MTV+anti-CD25] or [GL-MTV+anti-CD25] mAb groups in cytokine production (Figure 2.7D).

A.

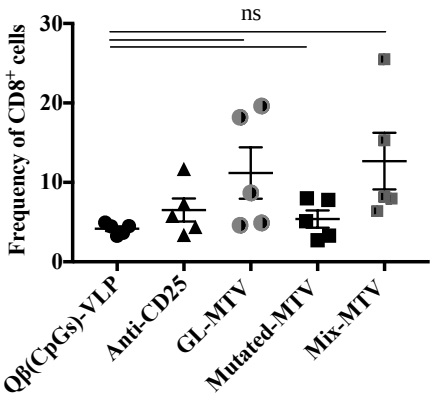

Unpaired *t* test	*P* value
Qβ(CpGs)-VLP vs anti-CD25	0.9493 ns
Qβ(CpGs)-VLP vs GL-MTV	0.2364 ns
Qβ(CpGs)-VLP vs Mutated-MTV	0.9955 ns
Qβ(CpGs)-VLP vs Mix-MTV	0.1057 ns
anti-CD25 vs GL-MTV	0.6132 ns
anti-CD25 vs Mutated-MTV	0.9966 ns
anti-CD25 vs Mix-MTV	0.3531 ns
GL-MTV vs Mutated-MTV	0.4104 ns
GL-MTV vs Mix-MTV	0.9903 ns
Mutated-MTV vs Mix-MTV	0.2063 ns

B.

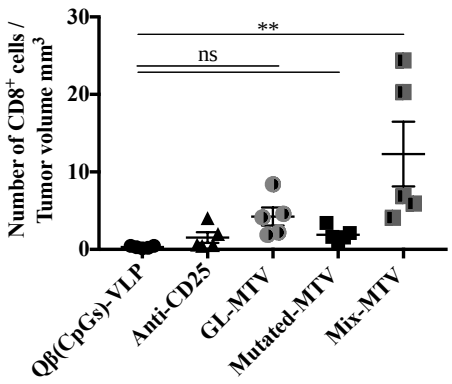

Student's *t* Test	*P* value
Qβ(CpGs)-VLP vs anti-CD25	0.9917 ns
Qβ(CpGs)-VLP vs GL-MTV	0.6273 ns
Qβ(CpGs)-VLP vs Mutated-MTV	0.9784 ns
Qβ(CpGs)-VLP vs Mix-MTV	0.0028 **
anti-CD25 vs GL-MTV	0.8639 ns
anti-CD25 vs Mutated-MTV	>0.99 ns
anti-CD25 vs Mix-MTV	0.0076 **
GL-MTV vs Mutated-MTV	0.913 ns
GL-MTV vs Mix-MTV	0.0611 ns
Mutated-MTV vs Mix-MTV	0.0101 *

C.

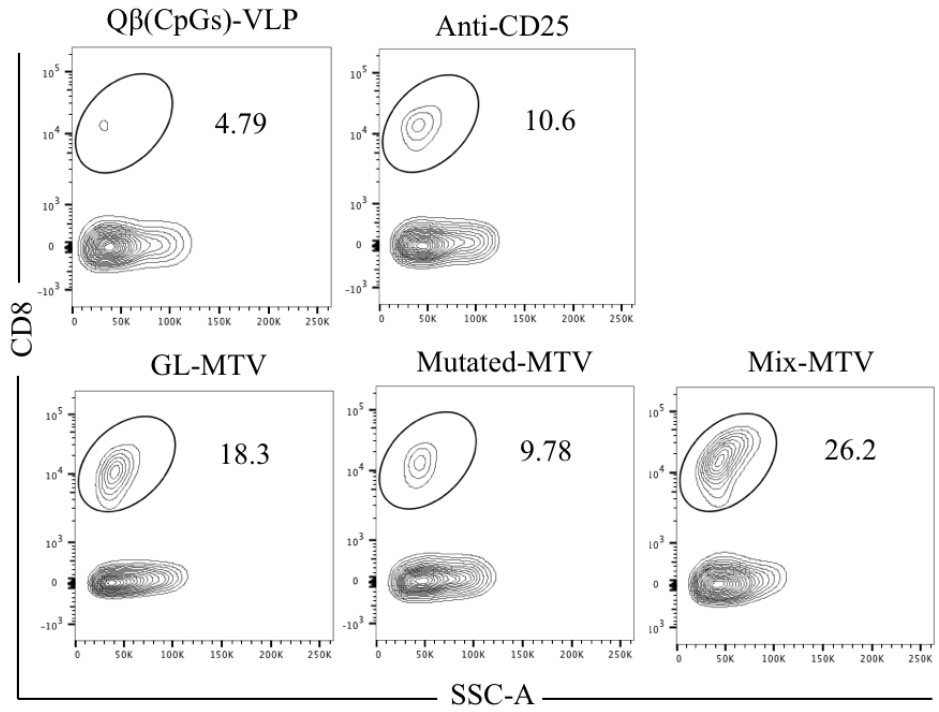

D.

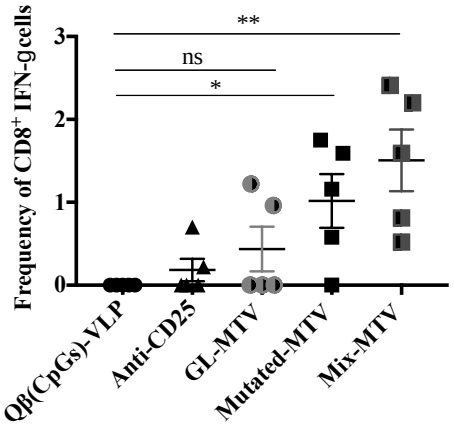

One-Way ANOVA (Turkey's Multiple Comparison Test)	*P* value
Qβ(CpGs)-VLP vs anti-CD25	0.9862 ns
Qβ(CpGs)-VLP vs GL-MTV	0.7564 ns
Qβ(CpGs)-VLP vs Mutated-MTV	0.9773 ns
Qβ(CpGs)-VLP vs Mix-MTV	0.0044 **
anti-CD25 vs GL-MTV	0.9567 ns
anti-CD25 vs Mutated-MTV	0.1949 ns
anti-CD25 vs Mix-MTV	0.0134 *
GL-MTV vs Mutated-MTV	0.5237 ns
GL-MTV vs Mix-MTV	0.0576 ns
Mutated-MTV vs Mix-MTV	0.6716 ns

Figure 2.7 Mix multi-target VLP-based vaccine [Mix-MTV] increased $CD8^+$ T-cells infiltration into the tumour

A, Frequency of $CD8^+$ T-cells (means ± SEM) in TILs from s.c. B16F10 tumours in C57Bl/6 mice treated with Qβ(CpGs)-VLP, Anti-CD25, [GL-MTV + Anti-CD25], [Mutated-MTV+Anti-CD25] and [Mix-MTV+Anti-CD25], measured at day 14 post tumour transplantation, each dot represents a tumour. Statistical analysis One-Way ANOVA (Turkey's Multiple Comparison Test). *B*, Density of $CD8^+$ T-cells in TILs in mice treated with the designated groups, each dot represents a tumour. Measured by dividing frequency of $CD8^+$ T-cells number by the tumour volume mm^3 in each mouse. Statistical analysis One-Way ANOVA (Turkey's Multiple Comparison Test). *C*, Representative flow cytometry dot plots showing the frequency of $CD8^+$ T-cells in TILs treated with the designated groups. *D*, Frequency of $CD8^+$ IFN-γ^+ (means ± SEM) in TILs in mice treated with the designated groups. Statistical analysis One-Way ANOVA (Turkey's Multiple Comparison Test). (*n=5*) mice per group, one representative of 3 similar experiments is shown.

2.5.8. Mix multi-target vaccine Mix-MTV altered the myeloid composition of B16F10 tumour and enhanced the survival time

The effect of vaccination with multi-target vaccines GL-MTV, Mutated-MT and Mix-MT on tumour immune cell composition have been investigated next. Specifically, I have looked at both granulocytic and monocytic myeloid

populations in TILs. The results show a significant increase in the granulocytic population ($CD11b^{+}Ly6G^{+}$) in the groups vaccinated with [Mix-MTV+Anti-CD25] (p <0.0001) and [GL-MTV+Anti-CD25] (p 0.0345) accompanied by significant decreased in infiltration of the monocytic population ($CD11b^{+}Ly6C^{+}$) only in the group vaccinated with [Mix-MTV+Anti-CD25] (p <0.0001) "Figure 2.8 A, B and C". The observed increase in granulocytic population and the decrease in monocytic one was significantly correlated with the tumour volume (p 0.0001 & 0.0011) as shown in "Figure 2.8D and E" and is compatible with induction of a more protective environment (Moynihan et al., 2016; Murray, Wang, Fiering, & Steinmetz, 2018).

Whether the different multi-target VLP-based vaccines can extend the life-span of tumour-bearing mice was tested next. Mice were transplanted with tumours and vaccination was initiated 5 days later and repeated twice weekly. Tumours in control mice or mice treated with anti-CD25 mAb alone reached their ethically allowed maximal size of ~1000mm^3 within 13-16 days, underscoring the aggressiveness of the model used. Vaccination with the GL-MTV or Mutated-MTV in combination with anti-CD25 mAb extended the mouse life-span by about 8 days while the Mix-MTV did so by about 16 days "Figure 2.8 F". In fact, vaccination with the Mix-MTV reached protective levels of the vaccine based on p33 peptide, one of the strongest T-cell epitopes known in mice.

A.

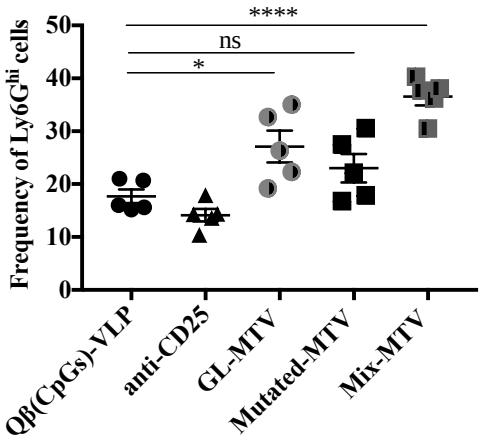

One-Way ANOVA (Turkey's Multiple Comparison Test)	*P* value
Qβ(CpGs)-VLP vs anti-CD25	0.747 ns
Qβ(CpGs)-VLP vs GL-MTV	0.0345 *
Qβ(CpGs)-VLP vs Mutated-MTV	0.407 ns
Qβ(CpGs)-VLP vs Mix-MTV	<0.0001 ****
anti-CD25 vs GL-MTV	0.0024 **
anti-CD25 vs Mutated-MTV	0.0497 *
anti-CD25 vs Mix-MTV	0.0001 ****
GL-MTV vs Mutated-MTV	0.644 ns
GL-MTV vs Mix-MTV	0.0331 *
Mutated-MTV vs Mix-MTV	0.0015 **

B.

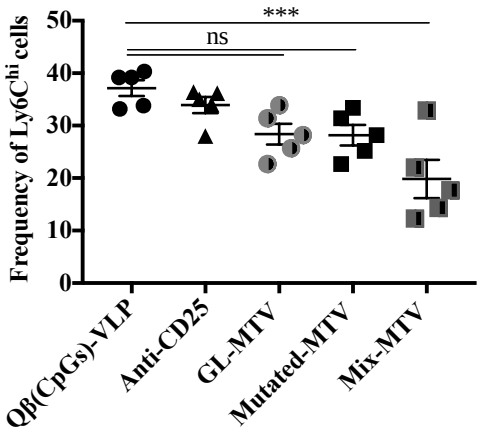

One-Way ANOVA (Turkey's Multiple Comparison Test)	*P* value
Qβ(CpGs)-VLP vs anti-CD25	0.851 ns
Qβ(CpGs)-VLP vs GL-MTV	0.0848 ns
Qβ(CpGs)-VLP vs Mutated-MTV	0.0751 ns
Qβ(CpGs)-VLP vs Mix-MTV	0.0002 ***
anti-CD25 vs GL-MTV	0.4419 ns
anti-CD25 vs Mutated-MTV	0.4076 ns
anti-CD25 vs Mix-MTV	0.0024 **
GL-MTV vs Mutated-MTV	>0.999 ns
GL-MTV vs Mix-MTV	0.0968 ns
Mutated-MTV vs Mix-MTV	0.1089 ns

C.

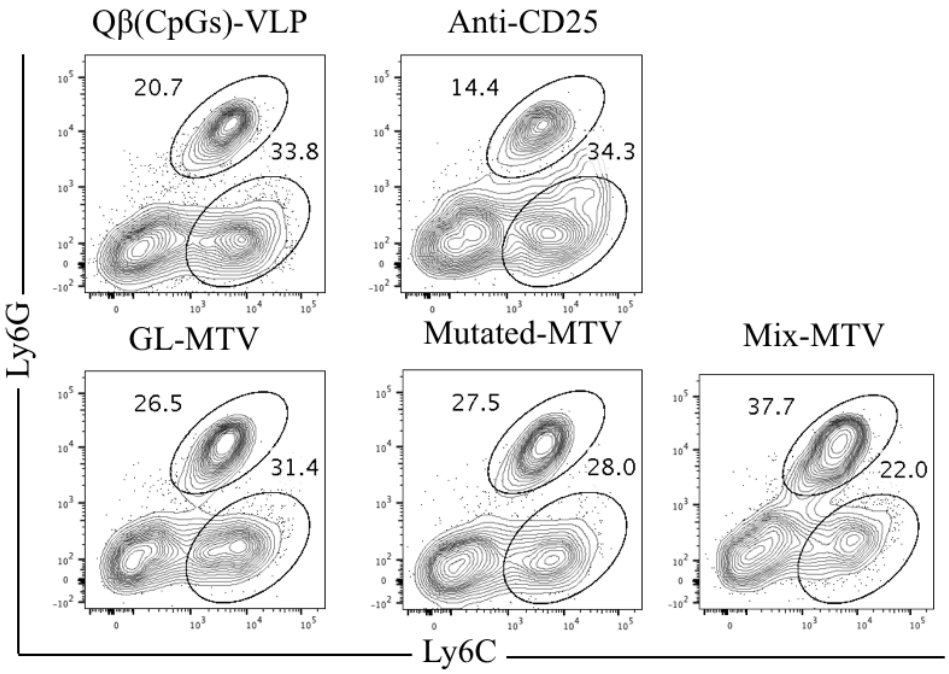
Qβ(CpGs)-VLP
Anti-CD25
GL-MTV
Mutated-MTV
Mix-MTV
20.7
33.8
14.4
34.3
26.5
31.4
27.5
28.0
37.7
22.0
Ly6G
Ly6C

D.

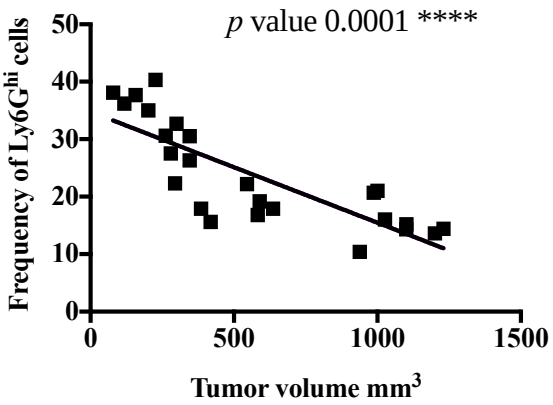
p value 0.0001 ****
Frequency of Ly6G^hi cells
Tumor volume mm3
0
10
20
30
40
50
0
500
1000
1500

E.

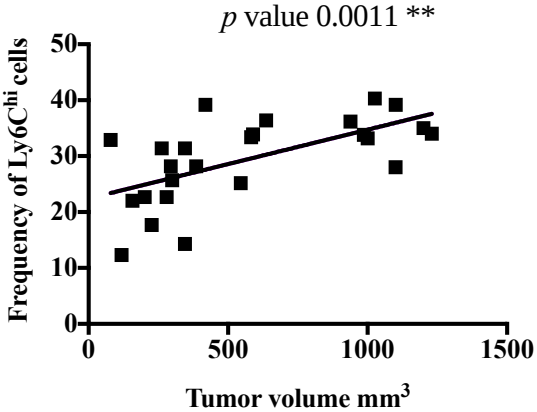
p value 0.0011 **
Frequency of Ly6C^hi cells
Tumor volume mm3
0
10
20
30
40
50
0
500
1000
1500

F.

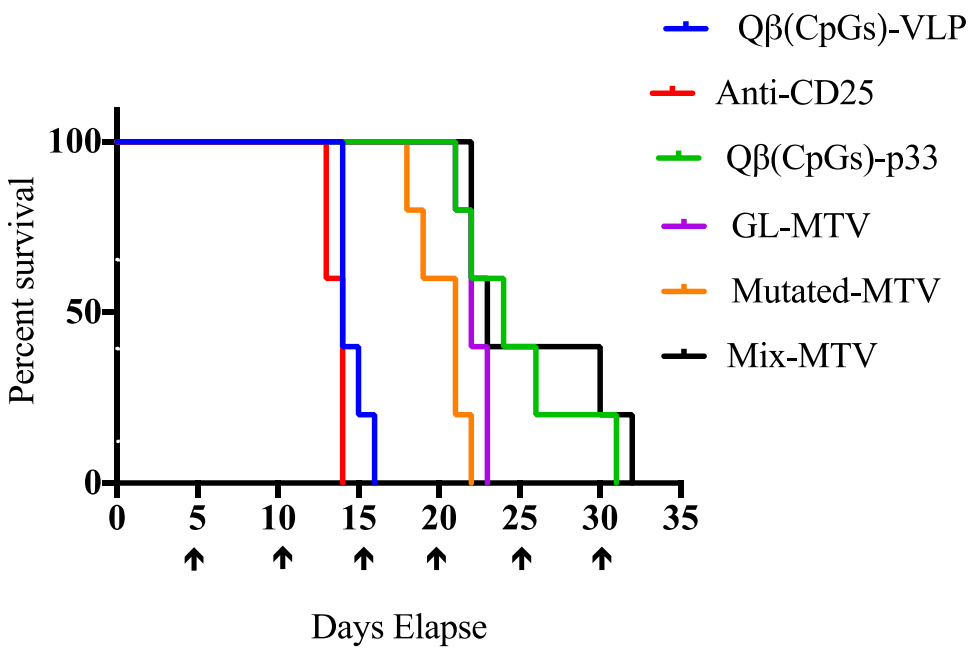

Log-Rank Test	*P* value
Qβ(CpGs)-VLP vs anti-CD25	0.0571 ns
Qβ(CpGs)-VLP vs GL-MTV	0.0015 **
Qβ(CpGs)-VLP vs Mutated-MTV	0.0015 **
Qβ(CpGs)-VLP vs Mix-MTV	0.0015 **
anti-CD25 vs GL-MTV	0.0031 **
anti-CD25 vs Mutated-MTV	0.0031 **
anti-CD25 vs Mix-MTV	0.0001 ****
GL-MTV vs Mutated-MTV	0.0363 *
GL-MTV vs Mix-MTV	0.1694 ns
Mutated-MTV vs Mix-MTV	0.0089 **
Qβ(CpGs)-p33 vs GL-MTV	0.1420 ns
Qβ(CpGs)-p33 vs Mutated-MTV	0.023 *
Qβ(CpGs)-p33 vs Mix-MTV	0.607 ns

Figure 2.8 Mix multi-target VLP-based vaccine [Mix-MTV] altered the myeloid composition of B16F10 tumour and enhanced the survival time

A, Frequency of $CD11b^{+}Ly6G^{+}$ cells (means ± SEM) in TILs from s.c. B16F10 tumours in C57Bl/6 mice treated with Qβ(CpGs)-VLP, Anti-CD25, [GL-MTV + Anti-CD25], [Mutated-MTV+Anti-CD25] and [Mix-MTV+Anti-CD25], measured at day 14 post tumour transplantation, each dot represents a tumour. Statistical analysis by Oneway ANOVA (Turkey's Multiple Comparison Test). *B*, Frequency of $CD11b^{+}Ly6C^{+}$ cells (means ± SEM) in TILs from s.c. B16F10 tumours in C57Bl/6

mice treated with the designated groups, measured at day 14 post tumour transplantation, each dot represents a tumour. Statistical analysis by Statistical analysis by Oneway ANOVA (Turkey's Multiple Comparison Test). *C,* Representative flow cytometry dot plots showing the frequency of $CD11b^{+}Ly6G^{+}$ and $CD11b^{+}Ly6C^{+}$ in TILs of mice treated with the designated groups. *D,* Correlation between the frequency of $CD11b^{+}Ly6G^{+}$ population with tumour volume mm^3 in mice treated with the designated groups. Statistical analysis by linear regression. *E,* Correlation between the frequency of $CD11b^{+}Ly6C^{+}$ population with tumour volume mm^3 in mice treated with the designated groups. Statistical analysis by linear regression. *F,* Survival of mice bearing B16F10 melanoma, mice were euthanized when the tumour reached $1000mm^3$. The arrows indicate vaccination time. Statistical analysis by log-rank test. (*n=5)* mice per group, one representative of 3 similar experiments is shown.

2.6. Discussion

VLPs have shown to be a promising platform for the development of effective vaccines. Such platforms have shown to enhance the immunogenicity of tumour epitopes and help overcoming tolerance and anti-inflammatory milieus (Bachmann & Jennings, 2010; Makkouk & Weiner, 2015). Indeed, it has been shown previously that a VLP-based melanoma vaccine can be utilized for active immunization against melanoma and vaccination against a single epitope resulted in strong CTL responses and exerted therapeutic pressure to the extent of provoking outgrowth of antigen escape variants (Goldinger et al., 2012; Schwarz et al., 2005; Speiser et al., 2010).

Personalized cancer vaccines targeting the patient's tumour specific mutanome may have the potential to generate clinically effective T-cell responses (Ott et al., 2017; Sahin et al., 2017). In previous studies, multi-target long peptides or RNA-based vaccine have been used to induce $CD8^{+}$ (and $CD4^{+}$) T-cell responses in melanoma patients. Interestingly, even though the vaccines were designed to induce CTL responses, they preferentially stimulated

$CD4^+$ T-cells, reminiscent of the generally acknowledged difficulties in mobilizing strong and broad $CD8^+$ T-cell responses by vaccination (Donaldson et al., 2017; Okuyama, Aruga, Hatori, Takeda, & Yamamoto, 2013; Ott et al., 2017; Sahin et al., 2017). Nevertheless, these findings support the concept that a multi-target vaccine covering a broader range of cancer antigens can control tumour progression and avoid outgrowth of antigen-escape variants.

In this study, a novel platform for the generation of a personalized VLP-based vaccine has been developed by utilizing both immunopeptidomics and whole exome sequencing techniques. Earlier versions of VLP-based vaccines used SMPH chemistry to couple antigens of interest to VLPs which showed good efficiency. SMPH reacts with free Lysine on the VLP and free cysteine on the peptides. However, not only cysteines of the linker but also cysteines within the target epitope may react with SMPH, resulting in the inactivation of cysteine-containing epitopes. In addition, non-reacted SMPH on VLPs may be toxic as it can react with cysteines in the body after injection of the vaccine. To overcome this problem and enable mixing and coupling of peptides with VLPs at bedside, a new coupling chemistry should be employed that leaves cysteines untouched and that will not react with anything in the host. To this end, biorthogonal Cu-free click chemistry has been implemented for GMP-compatible production. The results show that DBCO is superior to SMPH cross-linker in terms of 1) coupling efficiency to Qβ-VLPs and 2) in inducing significant CTL (p 0.0001) and IFN-γ (p 0.0262) response *in-vivo*. Bio-orthogonal in general, refers to any chemical reaction that can occur in the living organism without causing cellular toxicity or interfering with natural biological reactions (Chang et al., 2010). Furthermore, the azide groups attached to the

peptides are metabolically stable and lack any reactivity with any natural biological functionalities in the cells as it only reacts with the alkyne groups (Baskin et al., 2007; Mohsen, Zha, et al., 2017). This new coupling method has shown high selectivity and paved the way for new innovations for *in vivo* studies (Jewett & Bertozzi, 2010) such as for labelling, imaging and tracking cells (Baskin et al., 2007; Yoon et al., 2016). Cu-free click chemistry has been recently applied for the synthesis of glucoconjugate O-antigen vaccine and CRM_{197} carrier protein against Salmonella Typhimurium (Stefanetti, Saul, MacLennan, & Micoli, 2015).

Identification of optimal cancer-specific antigens remains a priority in the field of cancer immunotherapy. Some scientists favour peptides that are actually presented on the tumour using immunopeptidomics and others are focused on epitope prediction based on whole exome sequencing. The successful clinical trials conducted so far to test a personalized cancer vaccine have mainly used whole exome sequencing validated by RNA-seq to predict tumor-specific neoantigens. Immunopeptidomics identifies peptides that are actually presented and requires relatively large amounts of tumour-tissue. By comparison, whole exome sequencing can be performed with minimal cell numbers, but epitopes are only predicted and their presence is not actually physically assessed. In addition, the relative merits of germline vs mutated epitopes for vaccine design is also disputed. While the former may be conserved from tumour to tumour in many patients, the latter most likely induces less or even no immune tolerance, as they are not expressed in the thymus during early development nor in the periphery other than in tumour cells (Kroemer & Zitvogel, 2012; Ott et al., 2017; Sahin et al., 2017). To directly compare the

different approaches, both immunopeptidomics and whole exome sequencing were performed to identify and predict both types of T-cell epitopes. Several T-cell epitopes have been identified and prioritized by bioinformatics, as well as by their ability to stimulate TILs from tumour-bearing mice. TILs are highly enriched with specific T-cells and thus the most relevant T-cell population for anti-tumour T-cell response. Using these approaches, two sets of peptides (germline and mutated epitopes) were identified and displayed on VLPs loaded with CpGs.

In recent years, it has become evident that anti-tumour response may be enhanced in the presence of checkpoint inhibitors. Blocking PD-1 vs depleting Tregs using anti-CD25 mAb was compared. While blocking PD-1 had minimal impact on B16F10 tumour growth, anti-CD25 mAb substantially enhanced protection. Therefore, the developed multi-target VLP-based vaccines were combined with anti-CD25 mAb treatment.

The results showed that using germline peptides or mutated or a mixture of both can confer protection against tumour growth in B16F10 melanoma model, however the groups vaccinated with germline or mix peptides were more efficient than the group vaccinated with mutated peptides only. This effect may be due to the fact that using 6 different germline epitopes is more efficient than using only two mutated ones. However, calculating the density of $CD8^+$ T-cells in the tumour shows that combining both germline and mutated peptides (Mix-MTV) has the best effect (p 0.0028). Furthermore, the effect of the vaccine on the myeloid composition of the tumour was with high statistical significance in the group vaccinated with the combined peptides (Mix-MTV). The notable reduction in $Ly6C^{hi}$ population was not statistically significant after vaccination

with GL-MTV (p 0.0848) or Mutated-MTV (p 0.0751). Indeed, protection using the Mix-MTV was as potent as observed with the artificial model antigen, peptide p33, one of the strongest T-cell epitopes known in mice.

The approach of vaccinating with only 2 neoantigens and combining them with germ-line antigens avoids the need for identifying large numbers of neoantigens that may represent a particular problem in tumours of low mutational burden. Keeping the numbers of neoantigens low may also simplify the production of this type of personalized vaccines to some extent. Also, the final vaccine formulations would vary less from one patient to the next one, easing the regulatory challenges for producing and releasing these pharmaceutical products for clinical use.

In conclusion, this study demonstrates the development of a novel platform for an immunogenic personalized melanoma vaccine based on VLPs. This vaccine utilizes CTL epitopes predicted and validated by both immunopeptidomics and whole exome sequencing techniques. The peptides were coupled to the highly immunogenic VLPs by Cu-free click chemistry, representing a fast, safe and efficient method of coupling, enabling GMP compliant production for future use in clinical settings. The platform developed here can be used to target potentially any malignant solid tumour and thus can be applied broadly in cancer medicine.

Future Directions:

- The developed platform can be further tested in less aggressive melanoma model which would imitate the human's melanoma tumours.
- Furthermore, the developed platform can be tested in other types of cancer such as breast cancer or colorectal cancer that show less mutation burden than melanoma.
- The identified tumor epitopes from immunopeptidomics and the predicted mutated epitopes can be synthesized as longer peptides targeting both $CD8^+$ and $CD4^+$ T-cells.
- Different vaccine formulations and adjuvants can be tested to enhance the immunogenicity of the VLPs-based vaccine.

Challenges in personalized cancer vaccine

- One of the conceptual challenges of whole exome sequencing and immunopeptidomics is the limited amount of patient's tumour sample.
- In some cases, repetitive biopsies or biopsies from multiple tumour sites or lesions are not possible due to technical or ethical reasons. Such biopsies may be needed during the course of the tumour progression due to increased tumour heterogeneity to detect robust epitopes for effective cancer vaccine.
- Only few epitope prediction algorithms for predicting peptide-MHC complex binding are accurate such as NetMHC algorithm (Ito, 2015; Snyder & Chan, 2015). Additionally, these algorithms still suffer from unavoidable limitations mainly due to HLA-allele low frequency and the scarce binding data.

- *In vitro* T-cell assays by (ICS or ELISPOT) used to validate the immunogenicity of T-cell epitopes identified by immunopeptidomics or predicted by whole exome sequencing may also have some limitations including: low sensitivity specially when the T-cell clone recognizing the epitope is represented in patient's T-cell repertoire. Studies have shown that the proportion of validated neoantigens from *in silico* prediction is only 0.5-1% (Castle et al., 2012). In addition, the patient's pre-existing T-cell response may influence the spectrum of candidate epitopes (Ito, 2015).

3. Vaccination with nanoparticles combined with micro-adjuvants protects against cancer

3.1. Introduction

3.1.1. Components of effective cancer vaccine

As discussed formerly, cancer vaccines are constantly improved by optimizing vaccine delivery platforms, cancer antigens, adjuvants and formulations. Large number of approaches have been studied extensively in the past years. However, comparative data are still rare in humans (Hu et al., 2017).

3.1.1. Cucumber-mosaic virus (CMV) as VLP-based vaccine platform

Cucumber-mosaic virus (CMV) coat protein can be expressed as a recombinant plant virus-like particle (VLP) and has been proposed as a promising candidate vaccine platform by displaying relevant epitopes for induction of immune responses (Lebel, Chartrand, Leclerc, & Lamarre, 2015). It is an icosahedral particle capable of inducing both humoral and cellular immune responses by generating neutralizing mAb and $CD8^+$ T-cells, *respectively* (Nuzzaci et al., 2007; Piazzolla et al., 2005). Expressing hepatitis C virus R9 epitope on the surface of the VLP demonstrated that potent CTL responses may be induced by vaccination which was mainly due to efficient processing and presentation of the fused epitope on CMV-VLPs (Nuzzaci et al., 2007). Previously, an engineered CMV-derived VLP that incorporated a universal Tetanus toxoid epitope tt830-843 was developed, and termed $CuMV_{TT}$-VLP (Zeltins et al., 2017). The incorporation of the tt830-843 T-cell epitope has been shown to be a powerful enhancer of immune responses in Tetanus toxoid immunized mice. Similarly, use of the engineered $CuMV_{TT}$-VLPs as a vaccine platform in

humans is also expected to enhance immune responses, since this epitope is universally recognized in humans who have memory T_H cells specific for the epitope due to ubiquitous prior vaccination against tetanus (Zeltins et al., 2017).

The evidence for inherent immunogenicity is mounting, as $CuMV_{TT}$-VLP-based vaccines have been shown to induce protective and therapeutic antibody responses in mice, horses and dogs (Bachmann et al., 2018; Fettelschoss-Gabriel et al., 2018; Zeltins et al., 2017).

3.1.2. Role of depot-forming adjuvants in cancer vaccine development

Adjuvants enhance vaccine immunogenicity by different means. Firstly, depot-forming adjuvants extend antigen presentation time and may protect it from degradation by different cell-associated or serum peptidases and proteases (Cox & Coulter, 1997). Secondly, adjuvants in general would increase antigen uptake by antigen-presenting cells (APC) by forming them into comparable size particles of pathogens (O'Hagan & Valiante, 2003). Thirdly, some studies suggest that depot adjuvants enhance antigen transport to peripheral LNs and thus increase the chances of encountering APCs and increase antigen presentation (Johansen, Mohanan, Martinez-Gomez, Kundig, & Gander, 2010). Overall, depot adjuvants may drastically enhance T-cell responses by prolonging the antigen presentation optimal for T-cell clonal expansion, effector and memory function (Blair et al., 2011).

3.1.3. Microcrystalline Tyrosine as a depot-forming adjuvant

Microcrystalline Tyrosinse (MCT®) is a proprietary depot adjuvant that has been approved and licensed decades ago in allergen-specific immunotherapy

products. MCT's building blocks consist of the naturally occurring tyrosine amino acid. MCT forms crystals that act as a depot adjuvant facilitating the slow and prolonged release of antigens at injection site. Due to the micron-size of the particles, they cannot readily enter the lymphatics but remain at the injection site, causing local inflammation. MCT is biodegradable and will be efficiently catabolized in the body. A 48h half-life at the injection site has been previously reported (Cabral-Miranda, Heath, Mohsen, et al., 2017; Heath et al., 2017; Leuthard et al., 2018; Wheeler, Moran, Robins, & Driscoll, 1982).

In addition to its depot function, MCT also activates the inflammasome *in vitro* and has facilitates a sustained and robust innate responses, including, more recently, specific adaptive T-cell responses in a variety of immunotherapy applications (Cabral-Miranda, Heath, Mohsen, et al., 2017; Heath et al., 2017; Leuthard et al., 2018). Moreover, MCT's physicochemical compatibility and immunological synergy with other immunomodulatory compounds (notably TLR ligands) and delivery systems (such as virus-like particles) have been demonstrated (Bell et al, Cabral-Miranda et al 2017, (Wheeler, Marshall, & Ulrich, 2001). Overall, MCT represents a rather distinct biodegradable alternative depot adjuvant compared with the classical use of Alum, that already has had been administered in humans for many years in a niche area of allergy immunotherapy, thus constituting a comprehensive safety profile (Klimek et al, 2017).

3.1.4. Experimental approach

In the current study, the draining kinetics of CuMV$_{TT}$-VLPs have been studied with/without formulation with MCT adjuvant. Furthermore, the depot effect of

MCT adjuvant has been also assessed using different imaging techniques. Next, the immunogenecity of the vaccine platform CuMV$_{TT}$-VLPs in inducing specific T-cell response when formulated with MCT adjuvant has been studied using the aggressive B16F10p33 murine melanoma model. MCT adjuvant has also been compared to some commonly used adjuvants such as the well-established Alum and the potent immune-stimulatory oligonucleotide, B-type CpGs.

3.2. Research questions and objectives

3.2.1. Research questions

1. What is the drainage kinetics of CuMV$_{TT}$-VLP *in vivo*?
2. Can CuMV$_{TT}$-VLP be used as an efficient vaccine platform to display antigen of interest? Which chemistry is more efficient in coupling the antigen of interest to CuMV$_{TT}$-VLP?
3. Does MCT have a depot-forming adjuvant when formulation with CuMV$_{TT}$-VLP?
4. Can CuMV$_{TT}$-p33 formulated with MCT induce p33 specific T-cell response in the aggressive B16F10p33 melanoma murine model?
5. Can CuMV$_{TT}$-p33 formulated with MCT induce significant production of IFN-γ and TNF-α n the aggressive B16F10p33 melanoma murine model?
6. Is MCT adjuvant activity is comparable to the potent B type-CpGs or the widely Alum?

3.2.2. Research objectives

1. To test the drainage kinetics of CuMV$_{TT}$-VLP *in vivo*.

2. To test the immunogenecity of CuMV$_{TT}$-VLP in forming a vaccine platform for epitope display.
3. To test the hypothesis whether MCT constitute a depot-forming adjuvant when formulation with CuMV$_{TT}$-VLP.
4. To answer the question whether CuMV$_{TT}$-p33 formulated with MCT can induce specific T-cell response in murine model harbouring B16F10p33 tumours.
5. To answer the question whether CuMV$_{TT}$-p33 formulated with MCT can induce IFN-γ and TNF-α response in murine model harbouring B16F10p33 tumours.
6. To compare the adjuvant activity of MCT with the potent B type CpGs and the widely used Alum.

3.3. Reagents and materials

Table 3. 1 Name, supplier and catalogue number of peptides, reagents and materials

Reagent	Supplier	Catalogue Number
SMPH (succinimidyl-6-(X-maleimidopropionamido) hexanoate NHS ester)	Thermo Fisher SCIENTIFIC	22363
DBCO (Dibenzocyclooctyne NHS ester)	Sigma-Aldrich	761524
DMSO	Sigma-Aldrich	M81802
DMEM Medium	Sigma-Aldrich	D6046
Fc Block antibody	eBioscience	553142
CD8α mAb/anti-mouse/PerCP-Cyanine 5.5	eBioscience	45-0081-80
IFN-γ mAb/anti-mouse/APC	eBioscience	554413
TNF-α mAb/anti-mouse/PE	eBioscience	12-7321-81

Tetramers H2-Db (KAVYNFATM) PE	TCMetrix	Custom made
Monensin	BD Bioscience	554724
BrefeldinA	BD Bioscience	555029
IC Fixation Buffer	Fisher-Scientific SCIENTIFIC	00-8222-49
Permeabilization Buffer 10x	Fisher-Scientific SCIENTIFIC	00-8333-56
Alexa Fluor 488 NHS ester dye	Thermo Fisher SCIENTIFIC	A20000
Collagenase D	Roche	11 088 858 001
DNase I	Sigma-Aldrich	000000004716728001
p33 (NH2-KAVYNFATMGCC-H2)	Pepscan PRESTO	Custom made
B-type CpGs 5″-TCC ATG ACG TTC CTG ATG CT-3″	Iba	Tlrl-1668c
SYBR Safe DNA gel stain	Thermo Fisher Scientific	S33102
Brilliant Blue R Staining Solution	Sigma-Aldrich	6104-59-2
Materials	**Supplier**	**Catalogue Number**
Amicon centrifuge tubes 100 kDa MWCU	Thermo Fischer Scientific	UFC501008
Tissue-Tek O.C.T. compound	Sakura	25608-930
Fluoromount G solution	Thermo Fisher SCIENTIFIC	00-4958-02
Any kD mini-protein TGX precast protein gel	Bio-RAD	4569033
70 μM filters	BD Bioscience	352350

3.4. Methods

3.4.1. Expression and production of $CuMV_{TT}$-VLPs

$CuMV_{TT}$-VLPs expression and production was performed and provided by the core lab facility at University of Bern.

Cucumber mosaic virus expression and production was performed as described in detail in (Zeltins et al., 2017).

3.4.2. Electron Microscopy

Electron microscopy imaging was performed by Cyrill Lipp at the core facility lab, University of Bern.

Physical stability and integrity of $CuMV_{TT}$-VLPs were visualized by transmission electron microscopy using the Philips CM12 EM. For imaging, sample-grids were glow discharged and 5µl of VLP solution was added for 30 seconds. The grids were then washed 3x with ddH_2O and negative stained with 5µl of 5% uranyl acetate for 30 seconds. Finally, excess uranyl acetate was removed by pipetting and the grids were air dried for 10 minutes. Images were taken with 84,000x and 110,000x magnification.

3.4.3. Stereomicroscopic imaging

The stereomicroscopic imaging was performed by Prof. Jens V. Stein at the Theodor Kocher Institute, University of Bern.

C57BL/6 mice (8-12 weeks; Harlan) were anesthetized and prepared for imaging by shaving their right leg. Skin and adipose tissues were removed to expose the popliteal LNs as described in detail in (Mempel, Henrickson, & Von Andrian, 2004). The anesthetized mice were then stabilized on a customized platform for imaging. The popliteal LN was located by bright field illumination imaging. A dose of 25µg of $CuMV_{TT}$-VLPs vaccine was labelled with Alexa

Fluor 488 and injected subcutaneously in to a mouse footpad to study the biodistribution kinetics. Fluorescent light illumination with a CCD Nikon camera was used for imaging.

3.4.4. Coupling p33 peptide to CuMV$_{TT}$-p33 using SMPH chemistry

CuMV$_{TT}$-VLPs were derivatized for 1 h at RT on a shaker at 400rpm using SMPH cross-linker (Sigma-Aldrich) in 2 mM EDTA and 20 mM NaP, pH 7.5. Excess uncoupled DBCO was removed by several diafilitration steps using 100kDa MWCO amicon centrifuge tubes (Millipore). Modified p33 peptide H-KAVYNFATMGGC-NH2 was purchased from (Pepscan PRESTO) and reconstituted using DMSO. The modified peptide was then mixed with the derivatized CuMV$_{TT}$-VLPs at a molar ratio of CuMV$_{TT}$-VLP monomer to the modified peptide monomer of 1:5 or 1:10 and incubated at RT in a shaker at 400rpm for 1 h for coupling. TCEP was added in a 5-molar excess to liberate cysteine residues at the C-terminus on the VLPs. The coupling was performed for 1 h at RT on shaker at 400rpm. Excess peptide was removed using 100kDa MWCO amicon centrifuge tubes as before. The efficiency of the coupling was tested by using SDS-PAGE (Any kD mini-protein TGX precast protein gel, Bio-RAD). The gel was run at 200V for 35 min and stained with Coomassie Blue and then destained using a destainer solution containing (10% acetic acid and 40% methanol). The coupling efficiency was assessed by densitometric analysis of SDS-PAGE of CuMV$_{TT}$-VLP monomer bands compared to CuMV$_{TT}$-VLP monomer plus p33 after coupling.

3.4.5. Coupling p33 peptide to CuMV$_{TT}$-p33 using DBCO (Cu-free click chemistry)

CuMV$_{TT}$-VLPs were derivatized for 30 min at RT on a shaker at 400rpm using DBCO cross-linker (Dibenzocyclooctyne-*N*-hydroxysuccinimidyl ester)

(Sigma-Aldrich) in 2mM EDTA and 20 mM NaP, pH 7.5. Excess uncoupled DBCO was removed by diafilitration steps as described above. Modified p33 peptide H-KAVYNFATMGGCK(N3)-NH2 was purchased from (Pepscan PRESTO) and reconstituted using DMSO. The modified peptide was then mixed with the derivatized CuMV$_{TT}$-VLPs at a molar ratio of CuMV$_{TT}$-VLP monomer to the modified peptide monomer of 1:5, 1:10 or 1:20 and incubated at RT in shaker at 400rpm for 1 h for coupling. 5, 10 and 20 peptide molar excess showed efficient results. TCEP was added in a 5-molar excess to liberate cysteine residues at the C-terminus on the VLPs. Peptide at 10 x molar excess was used in the study for all experiments. The coupling was performed for 1 h at RT on shaker at 400rpm. Excess peptide was removed using 100kDa MWCO amicon centrifuge tubes. The efficiency of the coupling was tested by using SDS-PAGE (Any kD mini-protein TGX precast protein gel, Bio-RAD). The gel was run at 200V for 35 min and stained with Coomassie Blue and then destained as detailed previously. The coupling efficiency was assessed by densitometric analysis of SDS-PAGE of CuMV$_{TT}$-VLP monomer bands compared to CuMV$_{TT}$-VLP monomer plus p33 after coupling.

3.4.6. Depot-effect of MCT adjuvant with confocal microscopy

The confocal microscopy imaging was performed by Prof. Jens V. Stein at the Theodor Kocher Institute, University of Bern.

Whole popliteal LNs images after injection were obtained using a Zeiss 880 confocal microscope with 10 x dry lens objectives. Images were recorded at 1024x1024 resolution. Tile-Scan and z-stack of each LN (every 9 µm) was acquired. 3D reconstruction and maximal view was performed with Black Zen Software by Zeiss.

3.4.7. Measuring p33 specific $CD8^+$ T-cell response in the spleen

Four groups of C57BL/6 mice (6-8 weeks old; Harlan) (*n=3/group*) were vaccinated with a single dose as described in (Table 3.2):

Table 3. 2 The prepared groups, treatment and route of injection

Groups	Treatment	Route of Injection
1	70 µg of $CuMV_{TT}$-p33	s.c.
2	70 µg of $CuMV_{TT}$-p33+15 nmol of B-type CpGs 5″-TCC ATG ACG TTC CTG ATG CT-3″) (20 mer) with phosphorothiate bonds purchased from (Invivogen)	s.c.
3	70 µg of $CuMV_{TT}$-p33 + 4% MCT	s.c.
4	70 µg of $CuMV_{TT}$-p33 + 100 µl Alhydrogel adjuvant 2% (InvivoGen)	s.c.

Formulating $CuMV_{TT}$-p33 with MCT or Alum requires prolonged mixing of both components for 1h at RT in shaker at 400rpm to ensure adequate adsorption of the VLPs on MCT or Alum surface. Seven days later, spleens were collected tetramer staining was carried out as explained earlier in (Methods 2.4.5).

3.4.8. Intra-cellular cytokine (ICS) staining for IFN-γ and TNF-α

Intra-cellular cytokine staining was performed on spleens and TILs of vaccinated mice for measuring IFN-γ and TNF-α cytokines as explained earlier in (Methods 2.4.6).

3.4.9. Tumour experiments

C57BL/6 mice (6-8 weeks old; Harlan) were used for tumour experiments as described in (Method 2.4.14). In the first tumor experiment (*n=5*) (Results 3.5.5) mice were vaccinated as shown hereunder (Table 3.3):

Table 3. 3 The prepared groups, treatment and route of injection

Groups	Treatment	Route of Injection
1	70 µg of $CuMV_{TT}$-VLPs	s.c.
2	70 µg of $CuMV_{TT}$-p33	s.c.
3	70 µg of $CuMV_{TT}$-p33 + 4% MCT	s.c.

MCT was obtained from (Allergy Therapeutics Ltd. Worthing, UK). Formulating $CuMV_{TT}$-p33 with MCT requires prolonged mixing of both components for 1h at RT in shaker at 400rpm to ensure adequate adsorption of the VLPs on MCT surface. In the second tumour experiment (*n=4*) (Results 3.5.6), mice were vaccinated as shown hereunder (Table 3.4):

Table 3. 4 The prepared groups, treatment and route of injection

Groups	Treatment	Route of Injection
1	70 µg of $CuMV_{TT}$-VLPs	s.c.
2	70 µg of $CuMV_{TT}$-p33+15 nmol of B-type CpGs 5′-TCC ATG ACG TTC CTG ATG CT-3′) (20 mer) with phosphorothiate bonds purchased from (Invivogen)	s.c.
3	70 µg of $CuMV_{TT}$-p33 + 4% MCT	s.c.
4	70 µg of $CuMV_{TT}$-p33 + 100 µl Alhydrogel adjuvant 2% (InvivoGen)	s.c.

Formulating $CuMV_{TT}$-p33 vaccine with MCT or Alum required prolonged mixing as described above. Mice were vaccinated 3 times over 14 days. Tumour growth was followed daily and measured using calipers as described in (Method 2.4.14). Tumours were collected and measured on day 14 (mice in the first group vaccinated with $CuMV_{TT}$-VLPs reached the humane end-point at day 14) and TILs were isolated and stained with live/dead, Fc block, anti CD-8α, p33 tetramers mAb (eBioscience) as described in (Method 2.4.5). Analysis

was carried out using flow cytometry.

3.4.10. Statistics

Tumour growth curves were compared by calculating the area-under curve (AUC) and analysed by One-Way ANOVA (Turkey's Multiple Comparison Test). Other data in this chapter has been analysed and presented using Unpaired Student's *t* test. Additionally, One-Way ANOVA was calculated and the significance was added in the figure's legend. GraphPad Prism7 software was used for the analysis. ns = not significant, ***=P value < 0.0001; **=P value < 0.001; *=P value < 0.01.

3.5. Results

3.5.1. CuMV$_{TT}$-VLPs show efficient draining kinetics

The previously engineered CuMV$_{TT}$-VLPs (incorporating tetanus toxoid epitope, tt830-843) have been used as a vaccine platform (Zeltins et al., 2017). CuMV$_{TT}$-VLPs were expressed and produced as described in detail (Zeltins et al., 2017). The morphology and VLPs integrity were assessed by electron microscopy (Figure 3.1 A). In a next step, the draining kinetics of CuMV$_{TT}$-VLPs have been studied using stereomicroscopy imaging techniques. To this end, the accumulative draining of Alexa Fluor 488 (AF488) labelled CuMV$_{TT}$-VLPs have been followed into the popliteal LN after subcutaneous injection in the footpad of mice. As illustrated in Figure 3.1 B, the labelled CuMV$_{TT}$-VLPs reached the popliteal LN in less than 1 minute indicating fast and efficient draining kinetics of these VLPs.

A.

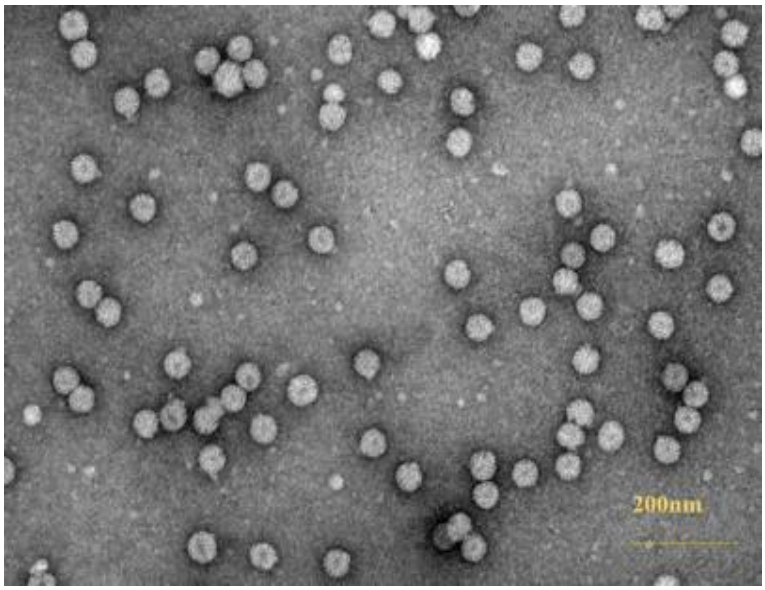

B.

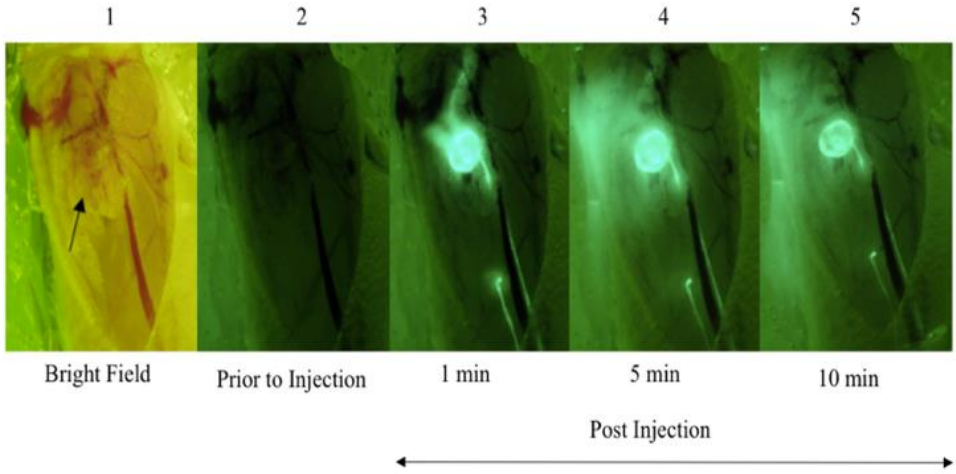

Figure 3. 1 CuMVTT-VLPs exhibit efficient draining kinetics

A, Electron microscopy imaging of $CuMV_{TT}$-VLPs sample (3.5 mg/ml) adsorped on carbon grids and negatively stained with uranyl acetate solution, scale bar 200nm, $CuMV_{TT}$-VLPs sized ~25nm. *B,* Stereomicroscopy images of mice popliteal LN following subcutaneous injection $CuMV_{TT}$-VLPs labelled with AF488. The labelled VLPs accumulated at the popliteal draining LN of C57BL/6 mice. From the left, image 1 bright field image of the popliteal LN (identified by the arrowhead), image 2 fluorescent image prior to injection of AF488 $CuMV_{TT}$-VLPs, images (3-5) 1minute

– 5 minutes and 10 minutes post injection of AF488 $CuMV_{TT}$-VLPs taken with the appropriate fluorescent filters.

3.5.2. $CuMV_{TT}$-VLPs constitute an efficient vaccine platform for displaying target peptides/epitopes

To develop a $CuMV_{TT}$-VLPs vaccine and to study its immunogenecity as a cytotoxic T-cell based vaccine, H2-Db p33 restricted peptide derived from LCMV has been used as a model antigen (Figure 3.2 A). Coupling p33 to $CuMV_{TT}$-VLPs can be carried out using simple chemistry techniques because $CuMV_{TT}$-VLPs express free lysine residues on its outer surface. Previously, different epitopes have been coupled to $CuMV_{TT}$-VLPs using the heterobifunctional cross-linker SMPH "succinimidyl-6 maleimidopropionamido hexanoate". Indeed, this chemistry has shown promising results. However, more recently I have shown that coupling epitopes to VLPs derived from the bacteriophage Qβ, can be more efficient using Cu-free click chemistry (Results 2.5.2). Cu-free click chemistry has also shown to be a faster, safer, less toxic and thus will facilitate GMP production for future translation into humans. The coupling efficiency of p33 epitope to $CuMV_{TT}$-VLPs has been carried out using both chemistry methods (SMPH and Cu-free click chemistry). For SMPH coupling, the model p33 epitope was extended by the addition of GCC amino acids at the C-terminus (Figure 3.2 B), while for DBCO "Cu-free click chemistry" the same p33 peptide was further extended by the addition of N3 azide group at the C-terminus (Figure 3.2 C). Cu-free click chemistry induced clearly more efficient coupling $CuMV_{TT}$-VLPs than SMPH as multiple bands occurred with Click chemistry while only one coupling band occurred with SMPH (Figure 3.2 D-E).

A.

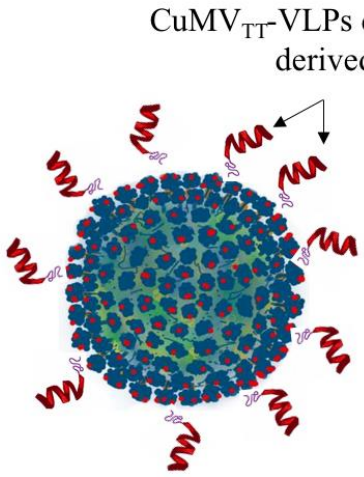
CuMV$_{TT}$-VLPs displaying p33 epitopes
derived from LCMV

B.

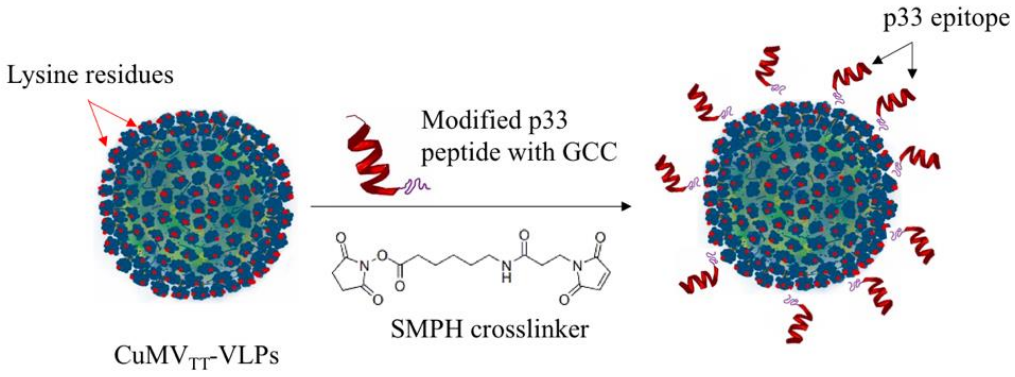
p33 epitope
Lysine residues
Modified p33
peptide with GCC
SMPH crosslinker
CuMV$_{TT}$-VLPs

C.

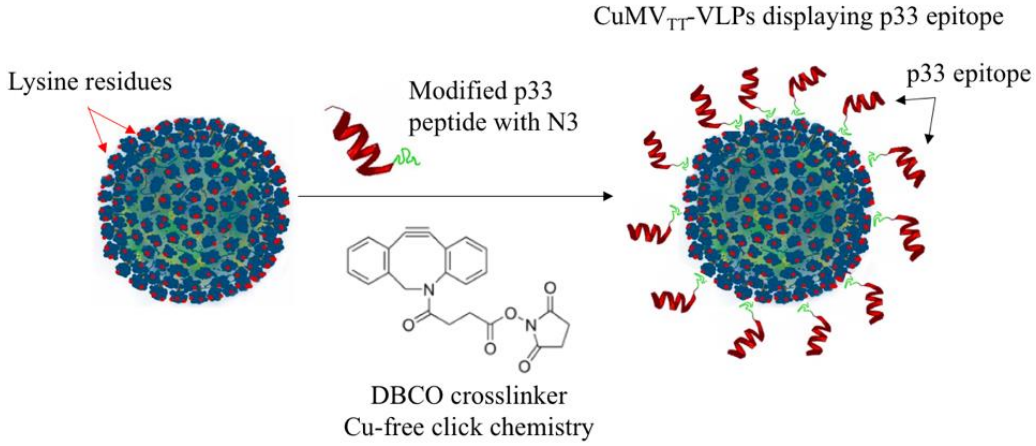
CuMV$_{TT}$-VLPs displaying p33 epitope
Lysine residues
Modified p33
peptide with N3
p33 epitope
DBCO crosslinker
Cu-free click chemistry

D.

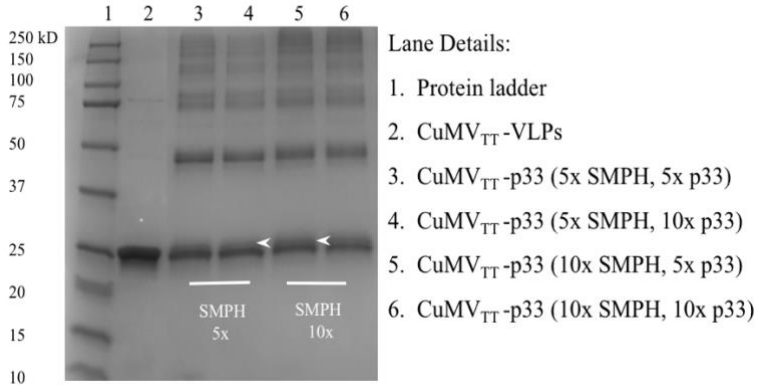

E.

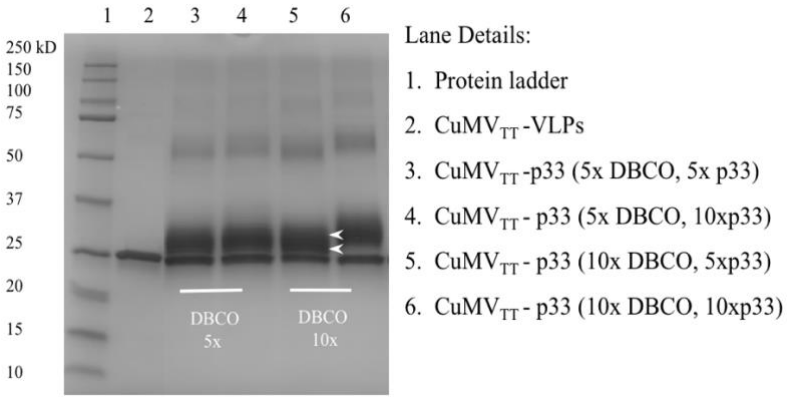

Figure 3. 2 CuMVTT-VLPs constitute an efficient vaccine platform for displaying target peptides

A, A sketch of CuMV$_{TT}$-VLP displaying p33 model antigen on the surface. *B,* CuMV$_{TT}$-VLPs outline illustrating p33 epitope coupling on the surface of the CuMV$_{TT}$-VLP using SMPH chemistry. *C,* CuMV$_{TT}$-VLPs outline illustrating p33 epitope coupling on the surface of the CuMV$_{TT}$-VLP using Cu-free click chemistry. *D,* SDS-PAGE of the generated CuMV$_{TT}$-p33 vaccine using SMPH "succinimidyl-6 maleimidopropionamido hexanoate" cross-linker. Lanes from the left, 1) protein ladder, 2) purified CuMV$_{TT}$-VLP monomer ~25kDa 3) CuMV$_{TT}$-VLP derivatized with 5x molar excess of SMPH and mixed with 5x peptide excess of p33 4) CuMV$_{TT}$-VLP derivatized with 5x molar excess of SMPH and mixed with 10x peptide excess of p33 5) CuMV$_{TT}$-VLP derivatized with 10x molar excess of SMPH and mixed with 5x peptide excess of p33 6) CuMV$_{TT}$-VLP derivatized with 10x molar excess of SMPH

and mixed with 10x peptide excess of p33. *E*, SDS-PAGE of the generated $CuMV_{TT}$-p33 vaccine using DBCO "Dibenzocyclooctyne-*N*-hydroxysuccinimidyl ester" cross-linker. Lanes from the left, 1) protein ladder, 2) purified $CuMV_{TT}$-VLP monomer ~25kDa 3) $CuMV_{TT}$-VLP $CuMV_{TT}$-VLP derivatized with 5x molar excess of DBCO and mixed with 5x peptide excess of p33 4) $CuMV_{TT}$-VLP derivatized with 5x molar excess of DBCO and mixed with 10x peptide excess of p33 5) $CuMV_{TT}$-VLP derivatized with 10x molar excess of DBCO and mixed with 5x peptide excess of p33 6) $CuMV_{TT}$-VLP derivatized with 10x molar excess of DBCO and mixed with 10x peptide excess of p33. One representative experiment of 3 experiments is shown.

3.5.3. MCT adjuvant displays depot effect when combined with $CuMV_{TT}$-p33 vaccine

Microcrystalline tyrosine (MCT) is thought to be a depot-forming adjuvant facilitating the slow release of antigens. Formulating the nano-vaccine $CuMV_{TT}$-p33 with MCT may therefore enhance the slow release of the VLPs displaying the target epitope and extend their exposure to the immune system. To study this hypothesis, $CuMV_{TT}$-p33 nano-vaccine was labelled with AF488 and formulated with MCT adjuvant to carry out confocal microscopy imaging to visualize VLP-binding to MCT crystals (Fig. 3.3A). The results show that the labelled virus-like particles bind and decorate the surface of the micron-sized MCT crystals. Next, *in vivo* experiment was done to image the popliteal LNs of C57BL76 mice by confocal microscopy on different time-points after subcutaneous injection of two different vaccines. The two vaccines were prepared as following; $CuMV_{TT}$-p33 vaccine labelled with AF488 only and $CuMV_{TT}$-p33 vaccine labelled with AF488 and formulated with MCT adjuvant. The prepared vaccines were then injected subcutaneously in C57BL/6 mice footpads as illustrated in Figure 3.3B and popliteal LNs were collected 3 h, 24 h, 48 h and 72 h post-injection. The results (Figure 3.3C) demonstrate that

formulating CuMV$_{TT}$-VLPs with MCT adjuvant results in sustained release of CuMV$_{TT}$-p33 over the 72h. On the other hand, the labeled AF488 CuMV$_{TT}$-VLPs were less observed in the draining LN at 72h. The obtained results correlate with the previous findings (Results 3.5.2) which shows that labelled CuMV$_{TT}$-VLPs reaches the draining lymph node in leass than 1 minute and fades noticeably 10 minutes later as they drain to the next LN. The persistence of the VLPs –alone or formulated with MCT- was also assessed 15 minutes and 1h post injection in mice footpads. The results showed a stronger GFP signal in the group injected with CuMV$_{TT}$-p33+MCT (Figure 3.3 D). Thus, combining the microadjuvant, MCT with CuMV$_{TT}$-VLPs results in a local depot of the nanoparticles.

A.

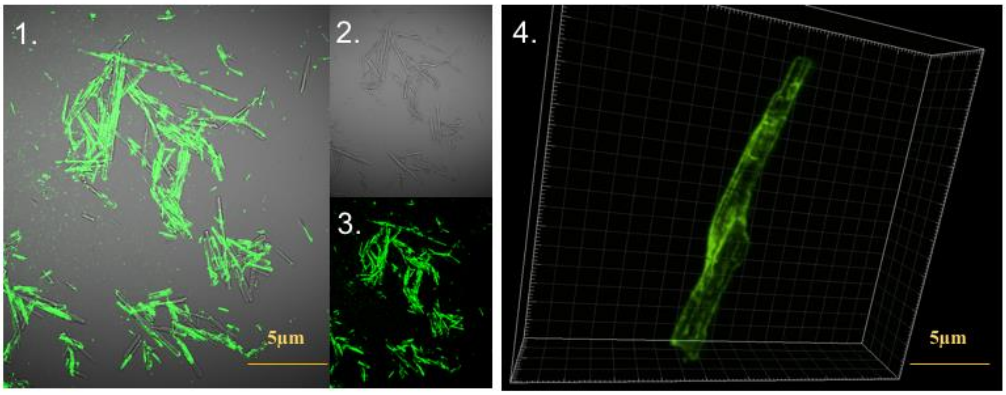

B.

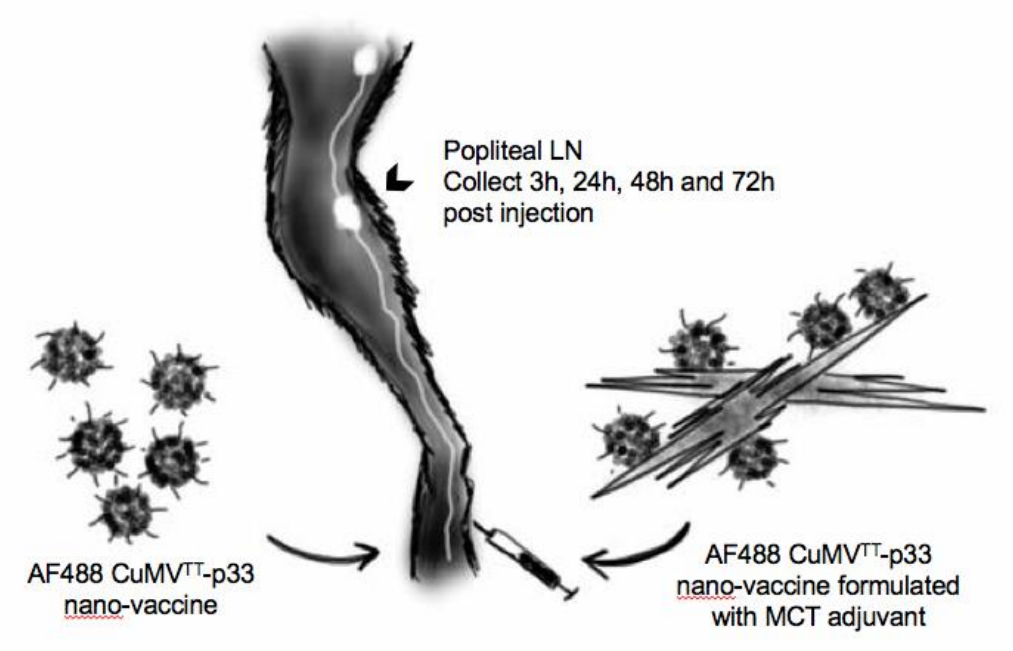
Popliteal LN
Collect 3h, 24h, 48h and 72h
post injection
AF488 CuMV^TT-p33
nano-vaccine
AF488 CuMV^TT-p33
nano-vaccine formulated
with MCT adjuvant

C.

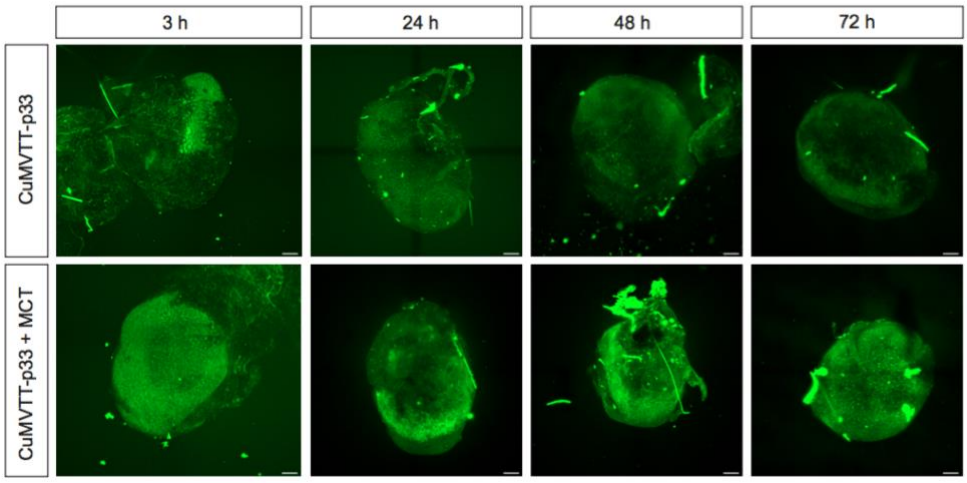
3 h
24 h
48 h
72 h
CuMVTT-p33
CuMVTT-p33 + MCT

D.

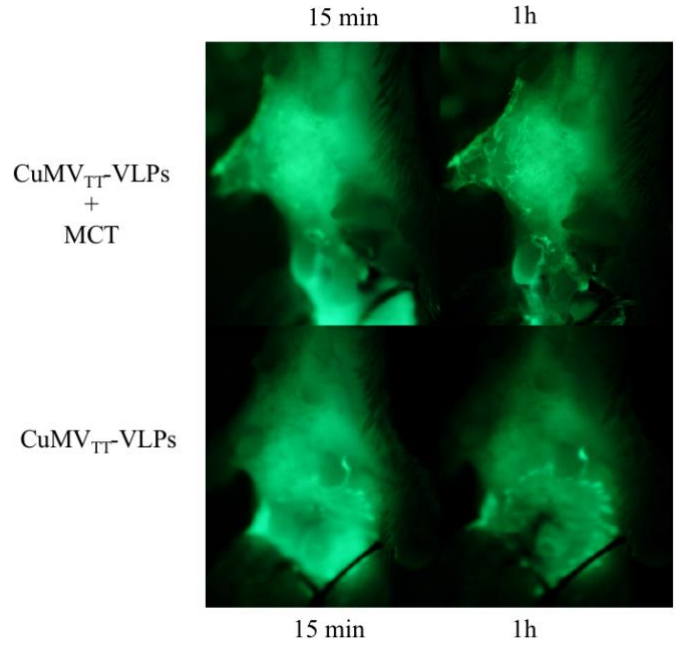

Figure 3. 3 MCT adjuvant displays depot effect when combined with CuMVTT-p33 vaccine

A, Confocal microscopy imaging of AF488 CuMV$_{TT}$-p33 following formulation with MCT adjuvant, 1) GFP signal of AF488 CuMV$_{TT}$-p33 2) bright light field 3) an overlay 4-6 3D images with bright light field. *B,* Two vaccine were prepared to study *in vivo* depot-forming effect of MCT adjuvant. The first vaccine consists of CuMV$_{TT}$-p33 labelled with AF488 alone, while the second vaccine consists of CuMV$_{TT}$-p33 labelled with AF488 and formulated with MCT adjuvant, this was carried out by mixing CuMV$_{TT}$-p33 vaccine with 4% MCT for 1h at RT in shaker at 400rpm to ensure adequate adsorption of the VLPs on MCT surface. The prepared vaccines were injected subcutaneously into the foodpad of C57BL/6 mice (*n=2*/group/time point). Popliteal LNs were collected 3h, 24h, 48h and 72h post-injection and processed for confocal microscopy imaging. *C,* Detecting GFP signal in LNs, whole mount view of z-stacks of popliteal LNs 3h, 24h, 48h and 72h post-injection was acquired using confocal microscopy. *D,* Detecting GFP signal in C57BL/6 mice footpad 15mintutes and 1h post-injection of CuMV$_{TT}$-p33 alone or formulated with MCT. One representative experiment of 3 similar experiments is shown.

3.5.4. Formulating CuMV$_{TT}$-p33 vaccine with MCT adjuvant induces significant p33 specific T-cell response

Next, we asked the question whether formulating CuMV$_{TT}$-p33 vaccine with MCT adjuvant would induce specific T-cell response *in vivo*. To answer this question, 4 vaccine groups were prepared as illustrated in Figure 3.4 A. The first group consists of CuMV$_{TT}$-p33 vaccine alone, while the second is CuMV$_{TT}$-p33 vaccine mixed with the immune-stimulatory B type-CpGs (1668) serving as a positive control. It has been shown previously that B-type CpGs (1668) can be efficiently packaged into Qβ-VLPs derived from Qβ bacteriophage (Gomes, Flace, et al., 2017; Mohsen, Gomes, et al., 2017; Storni et al., 2004). B-type CpGs are potent at activating DCs and inducing cytotoxic T-cell response (Hartmann, Weiner, & Krieg, 1999; Koster et al., 2017; Kranzer et al., 2000; Sluijter et al., 2015; S. Wang et al., 2016). However, packaging CuMV$_{TT}$-VLPs with B-type CpGs was not practically feasible as CuMV$_{TT}$-VLPs are less stable than Qβ-VLPs when digesting the naturally occurring RNA (data not shown). Therefore, in the current work, B-type CpGs were mixed with CuMV$_{TT}$-p33 vaccine prior to injection. The third group contains CuMV$_{TT}$-p33 vaccine formulated with MCT, which requires prolonged mixing of both components for 1h at RT in shaker at 400rpm to ensure adequate adsorption of the VLPs on MCT surface. The last group is CuMV$_{TT}$-VLPs formulated in Alum prepared in a similar way to MCT. The different vaccine formulations were then tested *in vivo* in C57BL/6 mice to assess and compare their immunogenicity by measuring p33 specific $CD8^+$ T-cells and IFN-γ production. C57BL/6 mice were vaccinated once, subcutaneously, and spleens were collected seven days later for tetramer and intra-cellular cytokine staining. The

results showed that mixing CuMV$_{TT}$-p33 vaccine with B-type CpGs induces the highest frequency of p33 specific T-cells (*p* 0.0043) and significant levels of IFN-γ (*p* 0.0369) (Figure 3.4 B-C). Formulating CuMV$_{TT}$-p33 vaccine with MCT also displayed significant increase in p33 specific T-cells (*p* 0.035) as well as IFN-γ production when compared to the first group (*p* 0.035) and to the group formulated with Alum (*p* 0.0183). Combining CuMV$_{TT}$-p33 with Alum did not increase CTL responses when compared to the group treated with CuMV$_{TT}$-p33 alone.

A.

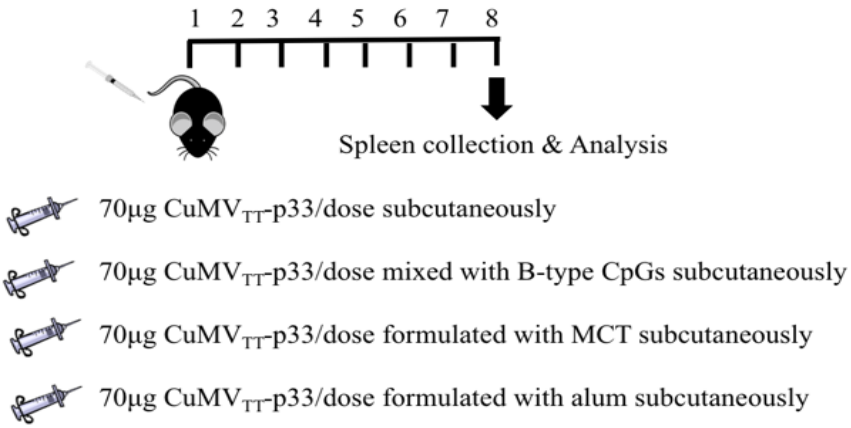

B.

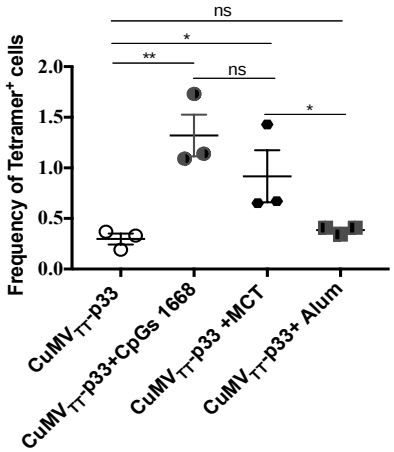

Student's *t* Test	*P* value
CuMV$_{TT}$p33 vs CuMV$_{TT}$p33+CpG(1668)	0.0043 **
CuMV$_{TT}$p33 vs CuMV$_{TT}$p33+MCT	0.035 *
CuMV$_{TT}$p33 vs CuMV$_{TT}$p33+Alum	0.1 ns
CuMV$_{TT}$p33+CpG(1668) vs CuMV$_{TT}$p33+MCT	0.14 ns
CuMV$_{TT}$p33+CpG(1668) vs CuMV$_{TT}$p33+Alum	0.00535 **
CuMV$_{TT}$p33+MCT vs CuMV$_{TT}$p33+Alum	0.05 *

C.

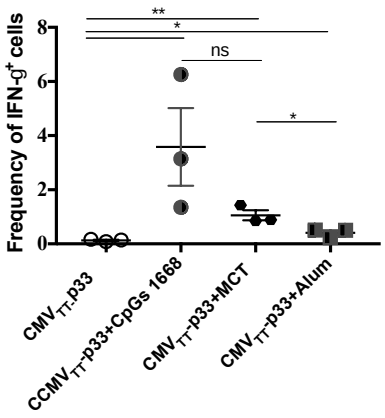

Student's *t* Test	*P* value
CuMV$_{TT}$p33 vs CuMV$_{TT}$p33+CpG(1668)	0.0369 *
CuMV$_{TT}$p33 vs CuMV$_{TT}$p33+MCT	0.004 **
CuMV$_{TT}$p33 vs CuMV$_{TT}$p33+Alum	0.02 *
CuMV$_{TT}$p33+CpG(1668) vs CuMV$_{TT}$p33+MCT	0.077 ns
CuMV$_{TT}$p33+CpG(1668) vs CuMV$_{TT}$p33+Alum	0.046 *
CuMV$_{TT}$p33+MCT vs CuMV$_{TT}$p33+Alum	0.0183 *

Figure 3. 4 Formulating CuMVTT-p33 vaccine with MCT adjuvant induces significant p33 specific T-cell response

A, vaccination scheme for four vaccine groups, CuMV$_{TT}$-p33 alone, CuMV$_{TT}$-p33 mixed with CpG 1668, CuMV$_{TT}$-p33 formulated with MCT and CuMV$_{TT}$-p33 formulated with Alum. *B*, Frequency of CD8$^+$ Tetramer$^+$ cells (means ± SEM) in the spleen in each vaccinated group. Statistical analysis by Student's *t* test (One-tailed). One-Way ANOVA (multiple comparison test) did not show significant difference when compare [CuMV$_{TT}$-p33 vs CuMV$_{TT}$-p33+MCT] or [CuMV$_{TT}$-p33+MCT vs CuMV$_{TT}$-p33+Alum]. *C*, Frequency of CD8$^+$ IFN-γ^+ cells (means ± SEM) in the spleen in each vaccinated group. Statistical analysis by Student's *t* test (One-tailed). One-Way ANOVA for multiple comparison did not show significant difference when compare [CuMV$_{TT}$-p33 vs CuMV$_{TT}$-p33+CpG1668]. (3 mice per group), one representative of 3 similar experiments is shown.

3.5.5. Formulating CuMV$_{TT}$-p33 with MCT adjuvant causes tumour regression and enhances CD8$^+$ and p33 specific CTL infiltration into B16F10p33 tumours

In a next step, the prepared CuMV$_{TT}$-p33 vaccine with or without formulation with MCT adjuvant was tested in C57BL/6 mice bearing transplanted tumours of the aggressive B16F10p33 melanoma cell line transfected with p33 antigen derived from LCMV. The three groups were prepared as illustrated in Figure

3.5A. Using the previously described challenging tumour model in (Results 2.5.6A), I have transplanted about ~2mm^2 sized B16F10p33 melanoma tumours into the flank of C57BL/6 mice. The tumour was then allowed to grow for five days more before starting the vaccination regimen. C57BL/6 mice were vaccinated s.c. with CuMV$_{TT}$-VLPs as a control or with CuMV$_{TT}$-p33 vaccine alone or formulated with MCT adjuvant 3 times over 14 days. Tumour volume was followed and measured with calipers. Tumours were collected on day 14 as the first group reached the ethically defined end-point (Figure 3.5B and C). Tumour-infiltrating lymphocytes (TILs) represent a prognostic factor for effective immune response especially in melanoma (Mihm & Mule, 2015; Rahbar, Naraghi, Mardanpour, & Mardanpour, 2015). Therefore, the tumour-infiltrating cells (TILs) including (total CD8$^+$ T-cells as well as p33 specific T-cells) were analysed in each vaccinated group (Figure 3.5 D, E and F). The obtained results revealed that formulating CuMV$_{TT}$-p33 with MCT would significantly hinder B16F10p33 tumour progression (p <0.0001) when compared to the control group or the group vaccinated with CuMV$_{TT}$-p33 (p 0.0055). Formulating CuMV$_{TT}$-p33 with MCT has also increased the filtration of CD8$^+$ T-cells as well as p33 specific CTL measured by Tetramers, compared to mice vaccinated with CuMV$_{TT}$-VLPs or CuMV$_{TT}$-p33 vaccine. IFN-γ^+ production was significantly enhanced when formulating CuMV$_{TT}$-p33 with MCT (Figure 3.5 G) compared to the control group (p <0.0001) or the group vaccinated with CuMV$_{TT}$-p33 alone (p 0.0210).

A.

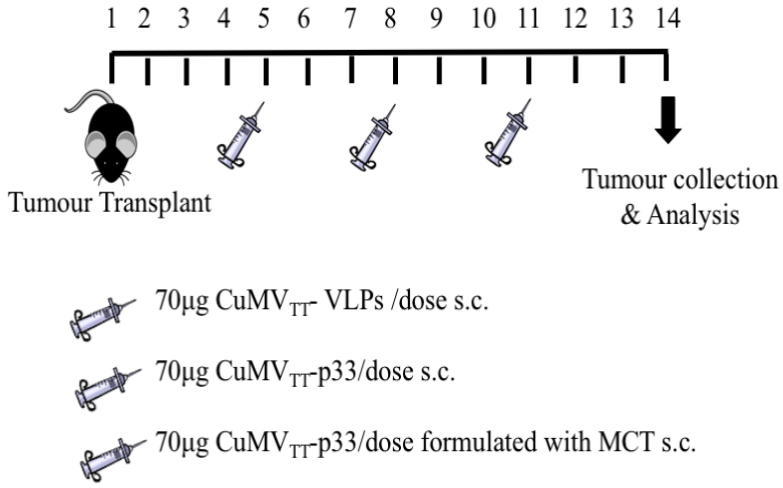

B.

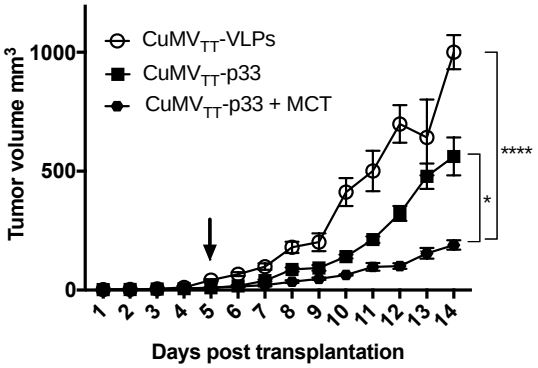

One-Way ANOVA (Turkey's Multiple Comparison Test)	*P* value
CuMV$_{TT}$-VLPs vs CuMV$_{TT}$p33	0.0015 **
CuMV$_{TT}$-VLPs vs CuMV$_{TT}$p33+MCT	<0.0001 ****
CuMV$_{TT}$-p33 vs CuMV$_{TT}$p33+MCT	0.0323 *

C.

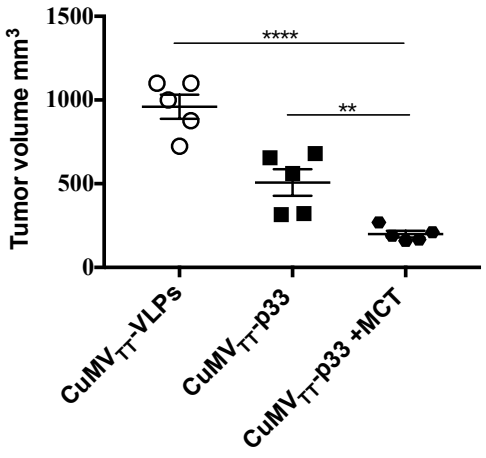

Student's *t* Test	*P* value
CuMV$_{TT}$-VLPs vs CuMV$_{TT}$p33	0.0029 **
CuMV$_{TT}$-VLPs vs CuMV$_{TT}$p33+MCT	<0.0001 ****
CuMV$_{TT}$-p33 vs CuMV$_{TT}$p33+MCT	0.0055 **

D.

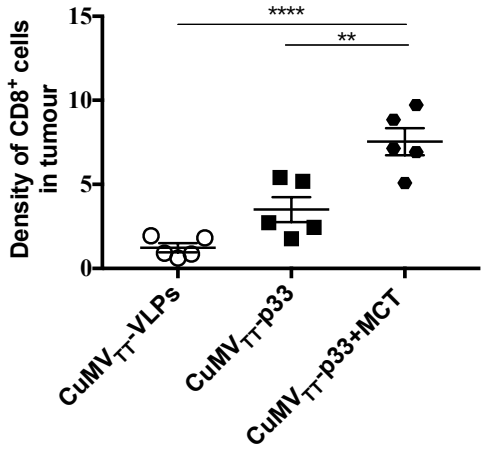

Student's *t* test	*P* value
$CuMV_{TT}$-VLPs vs $CuMV_{TT}$p33	0.0211 *
$CuMV_{TT}$-VLPs vs $CuMV_{TT}$p33+MCT	<0.0001 ****
$CuMV_{TT}$-p33 vs $CuMV_{TT}$p33+MCT	0.0063 **

E.

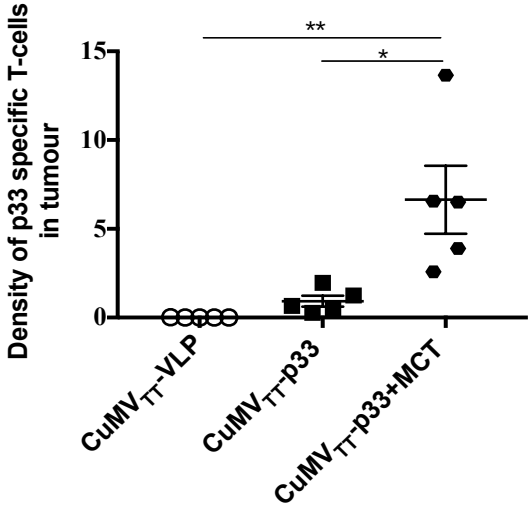

Student's *t* test	*P* value
$CuMV_{TT}$-VLPs vs $CuMV_{TT}$p33	0.0166 *
$CuMV_{TT}$-VLPs vs $CuMV_{TT}$p33+MCT	0.0085 **
$CuMV_{TT}$-p33 vs $CuMV_{TT}$p33+MCT	0.0185 *

F.

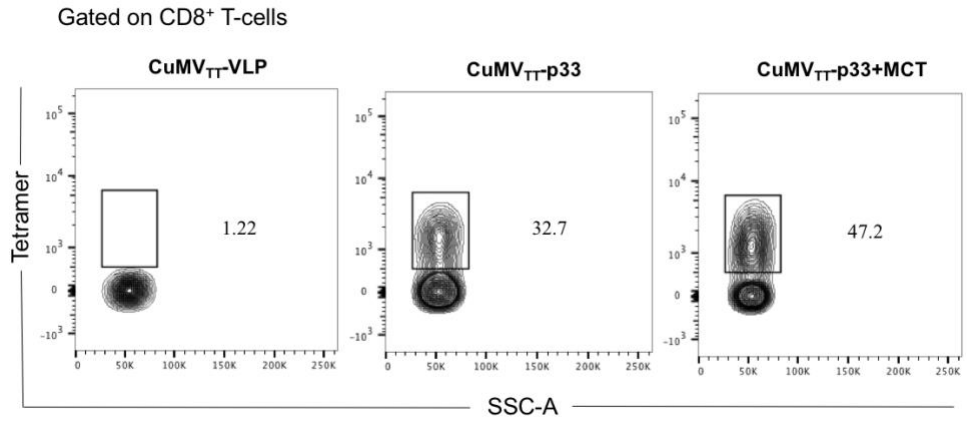

G.

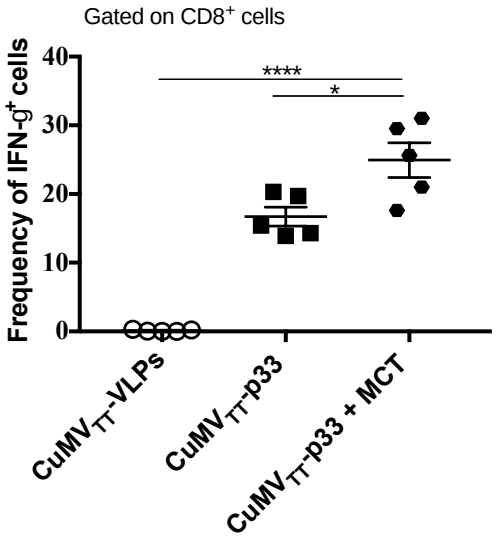

Student's *t* test	*P* value
$CuMV_{TT}$-VLPs vs $CuMV_{TT}$p33	<0.0001 ****
$CuMV_{TT}$-VLPs vs $CuMV_{TT}$p33+MCT	<0.0001 ****
$CuMV_{TT}$-p33 vs $CuMV_{TT}$p33+MCT	0.0210 *

Figure 3. 5 Formulating CuMVTT-p33 with MCT adjuvant causes tumour regression and enhances $CD8^+$ and p33 specific CTL infiltration into B16F10p33 tumours

A, Vaccination regimen post tumour transplantation and the prepared groups (*n*=5/group). From the top; the first group was vaccinated with $CuMV_{TT}$-VLPs, the second group was vaccinated with $CuMV_{TT}$-p33 vaccine alone, the third group was vaccinated with $CuMV_{TT}$-p33 vaccine formulated with 4% MCT. All vaccinated groups received 3 doses of the vaccine formulation over 14 days. At day 14 the tumours were collected (the group vaccinated with $CuMV_{TT}$-VLPs reached humane-end point) and TILs were isolated for further analysis. *B*, Tumour growth curve of subcutaneous B16F10p33 melanomas vaccinated with $CuMV_{TT}$-VLPs, $CuMV_{TT}$-p33 or $CuMV_{TT}$-p33 formulated with MCT, mice were euthanized when the tumour reached ~1000mm^3. The arrow indicates beginning of vaccination. Statistical analysis by measuring AUC analyzed by One-Way ANOVA (multiple comparison test). *C*, Tumour volume mm^3 (mean ± SEM) measured at day 14 post tumour collection in each designated group, each dot represents a tumour. Statistical analysis by Student's *t* test. One-Way ANOVA (multiple comparison test) showed comparable results. *D*, Density of $CD8^+$ T-cells (means ± SEM) in each group, "measured by dividing the number of $CD8^+$ cells by tumour volume $mm^{3"}$. Statistical analysis by Student's *t* test. One-Way ANOVA (multiple comparison test) showed comparable results. *E*, Density of p33 specific $CD8^+$ T-cells (means ± SEM) in each group, "measured by dividing the number of p33 $tetramer^+$ CTL by tumour volume $mm^{3"}$. Statistical analysis by Student's *t* test. One-Way ANOVA (multiple comparison test) showed comparable

results. *F*, Representative flow cytometry dot plots showing the frequency of p33 tetramer$^+$ cells in each group, gated on CD8$^+$ T-cells. *G*, Frequency of IFN-γ^+ (means ± SEM) in each vaccinated tumour, gated on CD8$^+$ T-cells. Statistical analysis by Student's *t* test. One-Way ANOVA (multiple comparison test) showed comparable results. (5 mice per group), one representative of 3 similar experiments is shown.

3.5.6. MCT shows comparable activity to B-type CpGs and is superior to Alum in driving protection against B16F10p33 melanoma

The immunogenecity of MCT adjuvant was then compared to the immune-stimulatory B-type CpGs and the widely used Alum using the same B16F10p33 tumour model when formulated with CuMV$_{TT}$-p33 vaccine. Four groups were prepared as illustrated in Figure 3.6 A, tumours were transplanted and allowed to grow for five days before starting vaccination. C57BL/6 mice were vaccinated with CuMV$_{TT}$-VLPs or with 70 µg CuMV$_{TT}$-p33 vaccine mixed with B-type CpGs or formulated with MCT or Alum 3 times over 14 days. Tumour volume was followed and measured with calipers (Figure 3.6 B). Tumours were collected on day 14 (the group vaccinated with CuMV$_{TT}$-VLPs reached humane-end point). Tumour-infiltrating cells were collected and total CD8$^+$ T-cells as well as p33 specific T-cells were analysed. The results once again revealed that formulating CuMV$_{TT}$-p33 with B-type CpGs or MCT would significantly (*p* 0.0072, 0.0129 respectively) hinder B16F10p33 tumour progression, which was not the case when formulating CuMV$_{TT}$-p33 with Alum (*p* 0.4188). When comparing MCT with Alum, MCT showed tumour protection while Alum did not (Figure 3.6 B). When calculating the density of CD8$^+$ and tetramer$^+$ T-cells in the tumour, there was a general increase in the groups mixed with CpGs or formulated with MCT or Alum (Figure 3.6 C, D, E and F).

Formulating CuMV$_{TT}$-p33 with MCT showed comparable results to the group where CuMV$_{TT}$-VLPs were mixed with B-type CpGs, the gold standard adjuvant in mice. Furthermore, MCT adjuvant increased infiltration of total $CD8^+$ and p33 specific T-cells into the tumour microenvironment when compared to formulating the vaccine with Alum.

A.

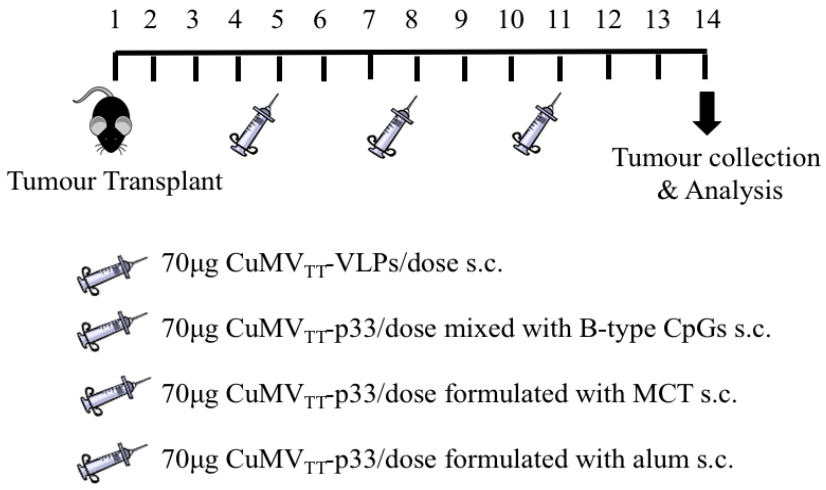

B.

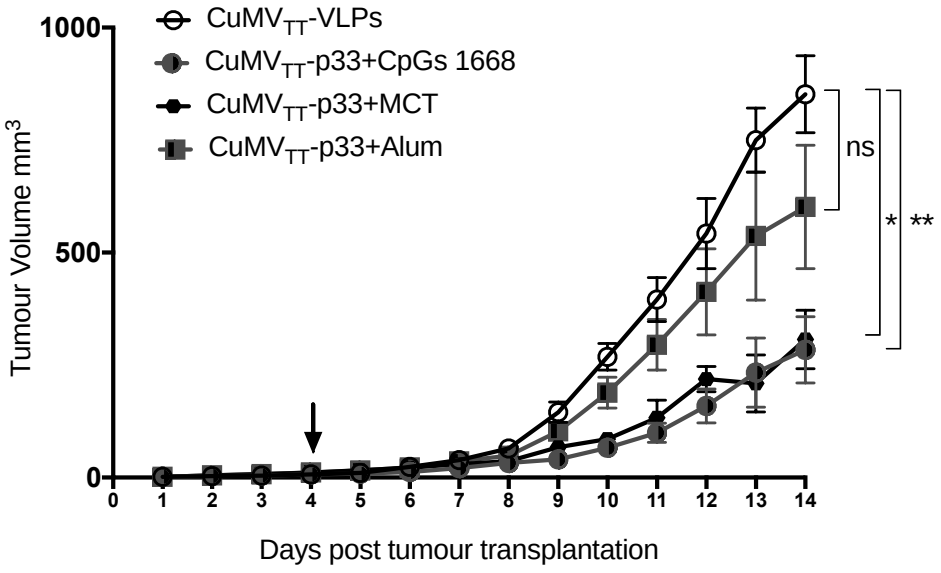

One-Way ANOVA (Turkey's Multiple Comparison Test)	*P* value
$CuMV_{TT}$-VLPs vs $CuMV_{TT}$p33+CpGs1668	0.0072 **
$CuMV_{TT}$-VLPs vs $CuMV_{TT}$p33+MCT	0.0129 *
$CuMV_{TT}$-VLPs vs $CuMV_{TT}$p33+Alum	0.4188 ns
$CuMV_{TT}$p33+CpGs 1668 vs $CuMV_{TT}$p33+MCT	0.9864 ns
$CuMV_{TT}$p33+CpGs 1668 vs $CuMV_{TT}$p33+Alum	0.1127 ns
$CuMV_{TT}$p33+MCT vs $CuMV_{TT}$p33+Alum	0.1918 ns

C.

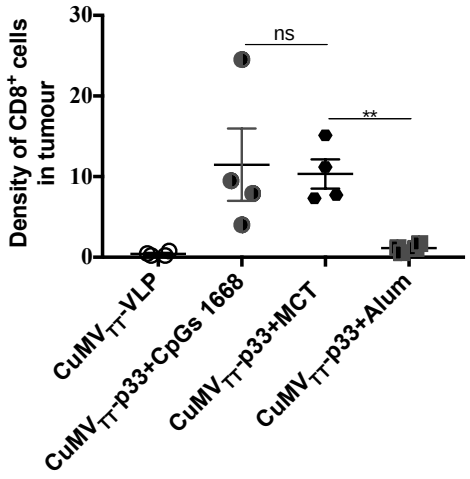

Student's *t* Test	*P* value
$CuMV_{TT}$-VLPs vs $CuMV_{TT}$p33+CpGs1668	0.0491 *
$CuMV_{TT}$-VLPs vs $CuMV_{TT}$p33+MCT	0.0016 **
$CuMV_{TT}$-VLPs vs $CuMV_{TT}$p33+Alum	0.0359 *
$CuMV_{TT}$p33+CpGs 1668 vs $CuMV_{TT}$p33+MCT	0.8211 ns
$CuMV_{TT}$p33+CpGs 1668 vs $CuMV_{TT}$p33+Alum	0.0612 ns
$CuMV_{TT}$p33+MCT vs $CuMV_{TT}$p33+Alum	0.0024 **

D.

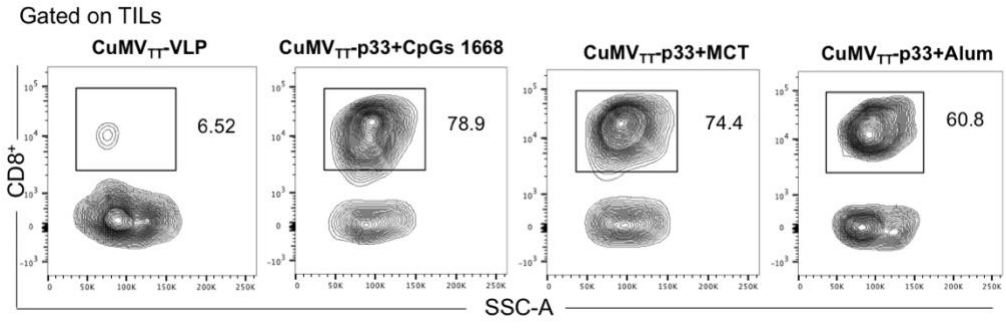

E.

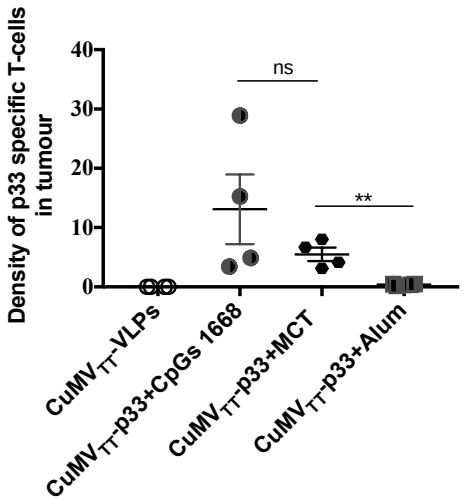

Student's *t* Test	*P* value
CuMV$_{TT}$-VLPs vs CuMV$_{TT}$p33+CpGs1668	0.0674 ns
CuMV$_{TT}$-VLPs vs CuMV$_{TT}$p33+MCT	0.0028 **
CuMV$_{TT}$-VLPs vs CuMV$_{TT}$p33+Alum	0.0023 **
CuMV$_{TT}$p33+CpGs 1668 vs CuMV$_{TT}$p33+MCT	0.2501 ns
CuMV$_{TT}$p33+CpGs 1668 vs CuMV$_{TT}$p33+Alum	0.0735 ns
CuMV$_{TT}$p33+MCT vs CuMV$_{TT}$p33+Alum	0.004 **

F.

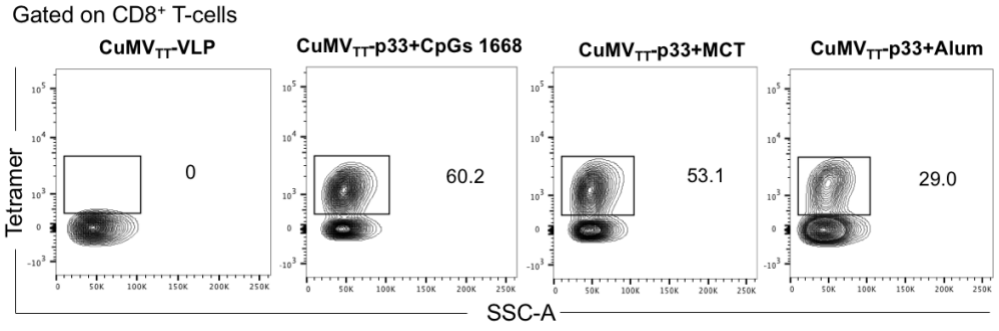

Figure 3. 6 MCT shows comparable activity to B-type CpGs and is superior to Alum in driving protection against B16F10p33 melanoma

A, Vaccination regimen post tumour transplantation and the prepared groups (*n=4*/group). From the top; the first group was vaccinated with CuMV$_{TT}$-VLPs, the second group was vaccinated with CuMV$_{TT}$-p33 vaccine mixed with B-type CpGs, the next group was vaccinated with CuMV$_{TT}$-p33 vaccine formulated with 4% MCT and the last group received CuMV$_{TT}$-p33 vaccine formulated in Alum. All vaccinated groups received 3 doses of mentioned vaccine formulation over 14 days (the group vaccinated with CuMV$_{TT}$-VLPs reached humane-end point). At day 14 the tumours were collected and TILs were isolated for further analysis. *B*, Tumour growth curve of subcutaneous B16F10p33 melanomas vaccinated with CuMV$_{TT}$-VLPs, CuMV$_{TT}$-p33 mixed with CpG 1668, CuMV$_{TT}$-p33 formulated with MCT or CuMV$_{TT}$-p33 formulated alum. Mice were euthanized when the tumour reached ~1000mm^3. The

arrow indicates beginning of vaccination. Statistical analysis by measuring AUC analysed by One-Way ANOVA. *C*, Density of $CD8^+$ (means ± SEM) in each group, "measured by dividing the number of $CD8^+$ cells by tumour volume mm^3". Statistical analysis by Student's *t* test. One-Way ANOVA for multiple comparison did not show significant difference between $CuMV_{TT}$-VLPs vs $CuMV_{TT}$-p33+MCT or between $CuMV_{TT}$-p33+MCT vs $CuMV_{TT}$-p33+Alum. *D*, Representative flow cytometry dot plots showing the frequency of $CD8^+$ T-cells in each vaccinated group. *E*, Density of p33 specific CD8 T-cells (means ± SEM) in each group, "measured by dividing the number of p33 $tetramer^+$ cells by tumour volume mm^3". Statistical analysis by Student's *t* test. One-Way ANOVA for multiple comparison did not show significant difference between $CuMV_{TT}$-VLPs vs $CuMV_{TT}$-p33+MCT or between $CuMV_{TT}$-p33+MCT vs $CuMV_{TT}$-p33+Alum. *F*, Representative flow cytometry dot plots showing the frequency of p33 $tetramer^+$ CTL in each vaccinated group. (4 mice per group), one representative of 3 similar experiments is shown.

3.5.7. MCT shows comparable production of cytokines to B-type CpGs in B16F10p33 melanoma.

Production of IFN-γ and TNF-α cytokines by TILs was also assessed in the tumours after vaccination with $CuMV_{TT}$-p33 mixed with B-type CpGs or formulated with MCT or Alum 3 times over 14 days. $CuMV_{TT}$-p33 mixed with B-type CpGs or formulated in MCT induced higher frequencies of IFN-γ or TNF-α in TILs than Alum (Figure 3.7 A and B) or TNF-α (Figure 3.7 C and D). The difference between $CuMV_{TT}$-p33 mixed with B-type CpGs or formulated with MCT was not statistically significant (*p* 0.3986 and 0.3433). However, there was a significant difference when comparing $CuMV_{TT}$-p33 mixed with B-type CpGs or $CuMV_{TT}$-p33 formulated with MCT to Alum in regard to IFN-γ production (*p* 0.0144 and 0.0187) or TNF-α production (p 0.0042 and 0.0179).

A.

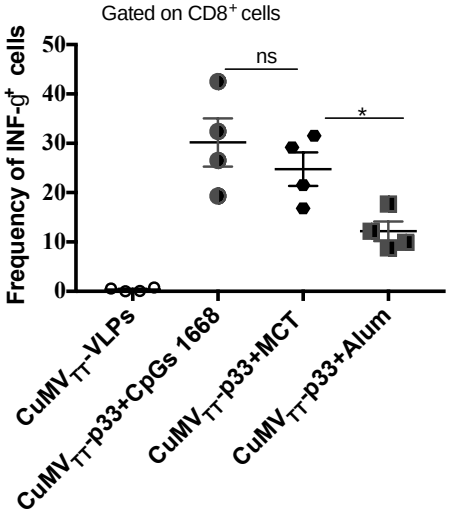

Student's *t* Test	*P* value
$CuMV_{TT}$-VLPs vs $CuMV_{TT}$p33+CpGs1668	<0.0009 ***
$CuMV_{TT}$-VLPs vs $CuMV_{TT}$p33+MCT	0.0004 ***
$CuMV_{TT}$-VLPs vs $CuMV_{TT}$p33+Alum	0.001 ***
$CuMV_{TT}$p33+CpGs 1668 vs $CuMV_{TT}$p33+MCT	0.3986 ns
$CuMV_{TT}$p33+CpGs 1668 vs $CuMV_{TT}$p33+Alum	0.0144 *
$CuMV_{TT}$p33+MCT vs $CuMV_{TT}$p33+Alum	0.0187 *

B.

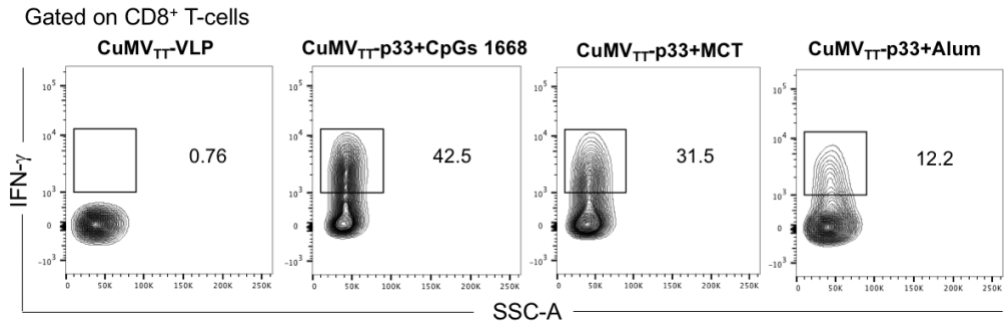

C.

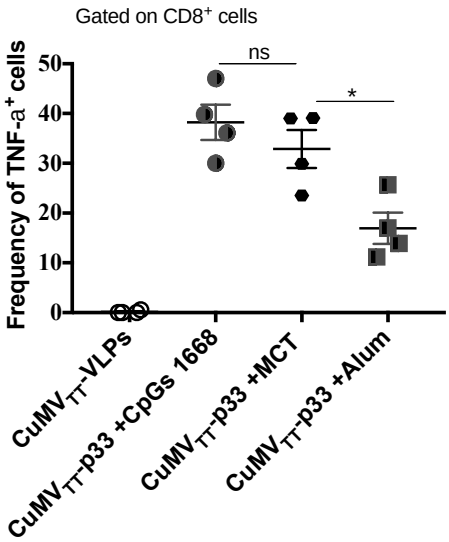

Student's *t* Test	*P* value
$CuMV_{TT}$-VLPs vs $CuMV_{TT}$p33+CpGs1668	<0.0001 ****
$CuMV_{TT}$-VLPs vs $CuMV_{TT}$p33+MCT	0.0001 ***
$CuMV_{TT}$-VLPs vs $CuMV_{TT}$p33+Alum	0.0018 **
$CuMV_{TT}$p33+CpGs 1668 vs $CuMV_{TT}$p33+MCT	0.3433 ns
$CuMV_{TT}$p33+CpGs 1668 vs $CuMV_{TT}$p33+Alum	0.0042 **
$CuMV_{TT}$p33+MCT vs $CuMV_{TT}$p33+Alum	0.0179 *

D.

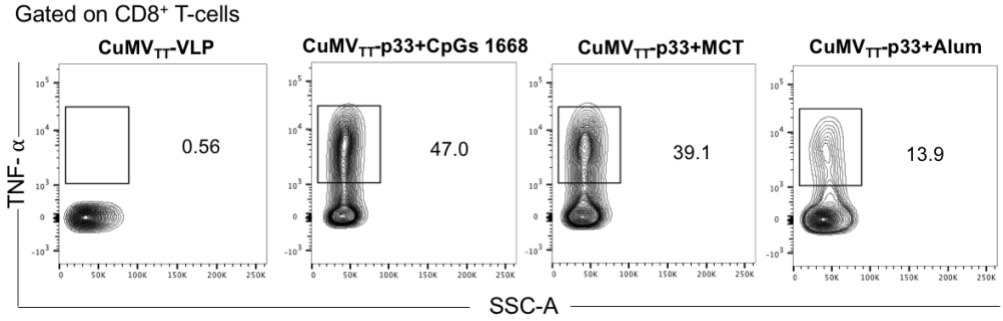

Figure 3. 7 MCT shows comparable production of cytokines to B-type CpGs in B16F10p33 melanoma

A, Frequency of IFN-γ^+ cells (means ± SEM) in each vaccinated tumour, gated on $CD8^+$ T-cells. Statistical analysis by Student's *t* test. One-Way ANOVA for multiple comparison did not show significant difference between $CuMV_{TT}$-p33+MCT and $CuMV_{TT}$-p33+Alum. *B*, Representative flow cytometry dot plots showing the frequency of IFN-γ^+ cells in each group. *C*, Frequency of TNF-α^+ cells (means ± SEM) in each vaccinated tumour, gated on $CD8^+$ T-cells. Statistical analysis by Student's *t* test. One-Way ANOVA for multiple comparison should comparable results. *D*, Representative flow cytometry dot plots showing the frequency of TNF-α^+ cells in each group. (4 mice per group), one representative of 3 similar experiments is shown.

3.6. Discussion

Several preclinical and clinical studies have indicated that some of the adjuvants used in licensed products are not optimal for developing effective cancer vaccines. Examples are the commonly used Montanide (Incomplete Freund's adjuvant) and Alum (Ammi et al., 2015; Hailemichael et al., 2013; O'Hagan, Friedland, Hanon, & Didierlaurent, 2017; Stills, 2005). Such limitations may include the inadequate ability of these adjuvants to induce cytotoxic T-cells (Temizoz, Kuroda, & Ishii, 2016).

Alum in general has been used as a potent adjuvant for most classical vaccines such as the vaccines against hepatitis A virus, haemophilus Influenzae type B, HPV, Streptococcus pneumonia and the vaccines against diphtheria, tetanus and pertussis (Gavin et al., 2006). In addition to stimulating the inflammasome (Eisenbarth, Colegio, O'Connor, Sutterwala, & Flavell, 2008; H. Li, Willingham, Ting, & Re, 2008; Marichal et al., 2011), Alum is considered a depot adjuvant prolonging antigen presentation time and allowing its gradual release causing sustained induction of antigen-specific T and B-cells (Hutchison et al., 2012). Nevertheless, Alum adjuvant failed to induce strong T_H1 and cellular immune responses and thus its use in cancer vaccines has been limited (Hogenesch, 2012; Kennedy & Celis, 2008).

We have previously developed cucumber mosaic virus-derived like particles genetically fused to the universal T-cell epitope of Tetanus toxin ($CuMV_{TT}$-VLPs). These VLPs constitute a promising vaccine platform as the incorporated Tetanus toxin epitope can enhance their immunogenicity and the production of robust antibody and CTL responses especially in aging populations (Fettelschoss-Gabriel et al., 2018; Zeltins et al., 2017). Displaying epitopes on $CuMV_{TT}$-VLPs exterior surface can be achieved by simple chemical techniques such as the SMPH heterobifunctional cross-linker. This technique has shown good results in many different clinical settings (Ambuhl et al., 2007; Cavelti-Weder et al., 2016; Tissot et al., 2008). However, I have enhanced the coupling efficiency of epitopes to bacteriophage Qβ-VLPs using the biorthogonal Cu-free click chemistry as described in Chapter 2. In general, Cu-free click chemistry is a safe, non-toxic coupling method as the azide moiety attached to the target epitope does not react with any of the body's natural

biological molecules (Baskin et al., 2007; Chang et al., 2010; Mohsen, Zha, et al., 2017). Cu-free click chemistry has been utilized in several applications *in vivo* as well as in vaccine development. (Baskin et al., 2007; Stefanetti et al., 2015; Yoon et al., 2016). To further characterize the 2 chemistries, we have coupled p33 restricted epitope as a model antigen to CuMV$_{TT}$-VLPs using both SMPH and Cu-free click chemistry and found that Cu-free click chemistry was clearly superior to SMPH chemistry. This is an important insight, as use of absolutely non-toxic chemistry will likely facilitate cGMP production of vaccine candidates, in particular for personalized vaccines that may be formulated at bed-side.

Immunostimulatory adjuvants such as synthetic CpGs-oligonucleotides are TLRs agonists and have shown promising therapeutic potentials by activating both the innate and adaptive immune system (Kakwere et al., 2017; Koster et al., 2017; Lai et al., 2018). CpGs have also been successfully used clinically to adjuvant cancer vaccines (Baumgaertner et al., 2016; Speiser et al., 2005). However, CpGs have some drawbacks including their unfavourable pharmacokinetics and their propensity to cause splenomegaly, at least in mice. It has shown previously that packaging CpGs into VLPs such as Qβ or HBcAg can improve the pharmacokinetics and dynamics of the DNA oligomers (Storni et al., 2004). Nevertheless, it is not always feasible to package VLPs with CpGs as some VLPs are unstable and packaging with reassembly processes may be time consuming when targeting translational approaches. Furthermore, TLR-9 agonists have been widely used with VLP-based vaccine to enhance T and B-cell responses mostly in mice and more rarely in humans (Goldinger et al., 2012). In mice, TLR-9 ligand is expressed by all DCs while in human it is

mainly expressed by pDCs in the LNs but not by conventional DCs (Krieg, 2006). pDCs, however, respond much efficiently to A-type CpGs rather than B-type CpGs as only the former induce strong production of IFN-α (Bachmann & Jennings, 2010). Hence, it may be difficult to directly translate findings with B-type CpGs from mice to humans.

MCT® is a micron-sized adjuvant ~5μM that forms crystals that readily adsorb proteins including protein-based nanoparticles such as VLPs. MCT is well known in the world of allergy immunotherapy, as it has been used for decades in registered products for the treatment of allergies. However, the knowledge about its mechanism of action and its potential in different fields of vaccinology is only expanding now. In a recent study, MCT was shown to be an effective adjuvant in allergen-specific immunotherapy. Protection against IgE-mediated allergic response was achieved in mouse models, independently of inflammasome and TLR signalling *in vivo*. As has been seen for Alum the adjuvants activity of MCT was independent of the inflammasome despite its ability to activate the inflammasome *in vitro* and *in vivo* (Leuthard et al., 2018). In malaria, MCT has been shown to consistently enhance protective IgG responses resulting in enhanced protection against malaria and similar observations were made for influenza vaccine candidates (Cabral-Miranda, Heath, Gomes, et al., 2017; Cabral-Miranda, Heath, Mohsen, et al., 2017; Heath et al., 2017).

Here, we have studied the draining kinetics of $CuMV_{TT}$-VLPs alone or when formulated with MCT adjuvant. Our results indicate that the free $CuMV_{TT}$-VLPs can drain fast into the lymphatic capillaries and would reach the draining lymph node in less than 1 minute. However, formulating $CuMV_{TT}$-

VLPs with the microcrystalline tyrosine adjuvant prolonged the release of the VLPs in the draining LN. Previous studies have shown the importance of the depot forming adjuvants in vaccine development as they delay the clearance of the vaccine which result in enhacing the generation of effective antigen-specitic T-cell response (Brewer et al., 2018; Khong & Overwijk, 2016).

We have also studied the immunogenicity of the developed $CuMV_{TT}$-VLP based vaccine when formulated with MCT adjuvant. To this end, the protective capacity of the induced CTL-responses was assessed in the aggressive B16F10 melanoma murine model transfected with H2-Db restricted p33 epitope derived from LCMV. The results show that formulating $CuMV_{TT}$-p33 vaccine with MCT was more potent (p <0.0001) in causing tumour regression that using the vaccine alone (p 0.0029). The protective capacity of the $CuMV_{TT}$-p33 in MCT is remarkable, as we have used a very challenging model based on transplanting ~2mm^3 B16F10p33 melanoma tumours into the flank of C57BL/6 mice. This model is well-defined and the vascularized tumours rapidly grow to lethal size. Previous studies have indicated that melanoma tumours exhibiting increased numbers of tumour infiltrating $CD8^+$ T-cells have better prognosis. TILs have led to a better understating of the interaction between hosts and tumours, mainly because their study allowed better characterization of effective therapeutic responses (Lee, Zakka, Mihm, & Schatton, 2016; Mihm & Mule, 2015). TILs isolated from the vaccinated groups have been assessed for the presence of p33 specific T-cells by means of tetramer- and intracellular cytokine staining. $CuMV_{TT}$-p33 vaccine formulated with MCT adjuvant has significantly enhanced the infiltration of $CD8^+$ (p <0.0001) and p33 specific T-cells (p 0.0085) into the tumour. The production

of IFN- has also been significantly increased (p <0.0001). These results indicate the effectiveness of MCT as a promising cancer adjuvant. When comparing MCT adjuvant to the potent B type CpGs or the widely used Alum, the overall adjuvants activity of MCT was comparable to CpGs and superior to Alum. "please note that p33 specific T-cell density was not significant when comparing $CuMV_{TT}$-VLPs with $CuMV_{TT}$-p33+CpGs (p 0.0674)".

It has been previously seen that Alum may increase overall IgG responses at least as good as MCT. In contrast to Alum, however, MCT induced superior IgG2a responses, which is usually associated with T_H1 responses and/or TLR activity (Cabral-Miranda, Heath, Mohsen, et al., 2017). This may be compatible with the observed ability of MCT to enhance CTL-responses, which Alum failed to do. Further work will be required to elucidate the mechanism of this difference, as both Alum and MCT form a depot and may activate the inflammasome pathway. Obvious hypothesis is that Alum induces a T_H2-driving pathway in addition to the inflammasome or vice versa, MCT may activate a T_H1-driving pathway. As other amino-acids, such as tryptophan or arginine serve as immune-modulators, this may be a currently unknown function for tyrosine as well (Mellor, Lemos, & Huang, 2017; Rath, Muller, Kropf, Closs, & Munder, 2014).

Taken together, this study shows that MCT is a potent enhancer of CTL responses and may be viewed as a novel multi-purpose adjuvant. As such, its effectiveness and compatibility in a mix- and match adjuvant systems approach should be further tested in preclinical and human immunotherapy trials. Combination of MCT with nanoparticles appears particularly attractive, as the micron-sized adjuvants will form a local depot at the injection site with

concomitant activation of skin-resident antigen-presenting cells. Nanoparticles will be released over time, draining to local LNs for extended time-periods, causing an optimal immune reaction.

Future Directions:

- Other VLPs types can be tested in combination with MCT adjuvant.
- The combination of (VLPs + MCT) can be tested in other types of cancer such as breast cancer or colorectal cancer which has less mutation burden than melanoma.
- The injection route can influence the effectiveness of such combination (VLPs + MCT), our preliminary data has shown that intra-tumoural injection may be an effective route. Further research is needed.
- The addition of checkpoint inhibitors to the combination (VLPs + MCT) may also be tested and the results can be compared.
- The systemic protection may also be assessed.

Challenges in Combining VLPs with MCT

- The size of MCT adjuvant may be uncomfortable for subcutaneous injection.
- MCT warms the tumour by inducing inflammation, the exact mechanism is currently under study and needs more investigation.
- Injecting MCT with VLPs intra-tumour may not always be feasible as some tumours may be inaccessible.

4. Delivering adjuvants and antigens in separate nanoparticles eliminates the need of physical linkage for effective vaccination

Published: M.O. Mohsen et al. / Journal of Controlled Release 251 (2017) 92–100

To whom it may concern

We are the co-authors of the published paper entitled: **Delivering adjuvants and antigens in separate nanoparticles eliminates the need of physical linkage for effective vaccination**

Mona O. Mohsen, Ariane C. Gomes, Gustavo Cabral-Miranda, Caroline C. Krueger, Fabiana MS Leoratti, Jens V. Stein, Martin F. Bachmann

Published on: Journal of Controlled Release 251 (2017) 92–100

http://dx.doi.org/10.1016/j.jconrel.2017.02.031

We confirm that the data and materials including (text and figures) in this paper have been authored and produced by the first author (Mona O. Mohsen).

We confirm that we have no issues or conflict of interest that (Mona O. Mohsen) uses the data, text and figures from this paper in her DPhil thesis as a chapter at the University of Oxford.

Co-author Name	Signature
Ariane C. Gomes	
Gustavo Cabral-Miranda	
Caroline C. Krueger	
Fabiana MS Leoratti	
Jens V. Stein	
Martin F. Bachmann	

4.1. Introduction

4.1.1. Adjuvanting VLP-based vaccines

Successful therapeutic vaccination aims at producing a large pool of effective T-cells usually starts with a small number of naive T-cells (Abbas, Lichtman, & Pillai, 2007). Effective vaccination is based mainly on several essentials steps including successful stimulation of the innate immune system, in particular dendritic cells (DCs) (Speiser et al., 2010; S. Wang et al., 2016). VLPs have been known as good inducers of Abs and cellular responses due to their special characteristics which have been discussed earlier. However, for effective induction of cellular responses, VLPs should be armed with adjuvants (Gomes, Mohsen, et al., 2017). VLP-based vaccines have been widely adjuvanted with the immune-stimulators CpGs "TLR-9 ligands that have augmented the antigen-specific T-cell response when compared to VLPs containing RNA (TLR7/8 ligands) or without any TLR-ligands (Schwarz et al., 2005).

Clinical trials in melanoma have shown that loading VLPs with CpGs would enhance the induction of melanoma-specific T-cell response (Goldinger et al., 2012; Speiser et al., 2010). Another example of VLPs loaded and encapsulated with A-type CpGs is CMP-001 vaccine. CMO-001 vaccine is currently in phase-I clinical trial for melanoma patients ("Warming "Cold" Melanoma with TLR9 Agonists," 2018).

4.1.2. Non-methylated CpGs as potent adjuvant for T-cell vaccines

A classic example of such adjuvants is CpGs, which are oligonucleotides rich in CpG motifs (R. S. Chu, Targoni, Krieg, Lehmann, & Harding, 1997; Speiser et al., 2005). Prokaryotes are rich in non-methylated CpG motifs, but not

mammalian DNA, therefore their presence in mammalian systems may be considered a danger signal indicating the presence of bacteria or other types of pathogen-associated molecular patterns (PAMPs). Consequently, the innate immune system reacts by initiating innate and adaptive immune responses to eliminate the threat (Krieg et al., 1995).

Non-methylated CpGs are primarily recognized by the Toll-Like Receptor 9 (TLR-9) conserved family expressed in the endosomal compartment of APCs (Bode, Zhao, Steinhagen, Kinjo, & Klinman, 2011; Hornung et al., 2002). TLR-9 is mainly expressed by plasmacytoid DCs (pDCs) and B-cells in humans, while in mice it is also expressed by macrophages, monocytes and conventional DCs (cDCs) (Kadowaki et al., 2001). As has been alluded to in earlier chapters, CpGs can be divided into different classes including A-type CpGs and B-type CpGs. A-type CpGs have a regular DNA backbone and are considered potent inducers of INF-α *in vitro*. Conversely, production of INF-α *in vivo* is less efficient due to degradation of the CpGs by host DNase activity (Kerkmann et al., 2003). However, this obstacle can be overcome by packaging A-type CpGs into VLPs, thereby protecting them from degradation and enhancing their activity (Storni et al., 2004). B-type CpGs have thioester backbone and thus are more stable (Hartmann et al., 1999; Klinman, 2004; Martinson et al., 2007), and have shown good results in clinical trials (Higgins, Marshall, Traquina, Van Nest, & Livingston, 2007; Schlom, 2012; Speiser et al., 2010). However, administering free form B-type CpGs *in vivo* has shown serious systemic side effects in mice such as splenomegaly and toxic shock (Hemmi et al., 2000; Storni et al., 2004). Furthermore, the presence of the phosphorothioate backbone in B-type CpGs increases their half-life *in vivo*,

which may result in unspecific reactions with the proteins (Christensen et al., 2014; Stein & Cheng, 1993). These obstacles can also be overcome by packaging B-type CpGs into VLPs. Generally packaging CpGs in VLPs ensures their effective deposition into the endosomal compartments of APCs (Storni et al., 2004) as well as effective activation of APCs, predominantly DCs (Gomes, Mohsen, et al., 2017). B-type CpGs have shown promising results in inducing potent immune responses in human (Speiser et al., 2010) and mice (Mohsen, Zha, et al., 2017; Storni et al., 2004).

The standard consensus when developing VLP-based vaccines is to deliver both antigen and adjuvant in the same VLP (Bauer et al., 2001; Storni et al., 2004). Means that both components should be in close proximity (*i.e.* physically linked) for effective vaccination (Bode et al., 2011; Eckl-Dorna & Batista, 2009; Storni et al., 2004). Relatively little is known about the approach of delivering antigens and adjuvants in separate virus-like particles (VLPs).

4.1.3. Experimental approach

The aim of this chapter is to study whether antigens and adjuvants should always be physically linked to the same VLP for effective vaccination, or is it possible to package adjuvants in one batch of VLPs and separately mix with other VLPs displaying CTL epitopes. Vaccines using the standard conventional method (antigen and adjuvants linked in the same VLP) and the new method (a VLP packaging adjuvant mixed with another VLP displaying the antigen) were prepared and tested (Figure 4.1). The two approaches were compared for their ability of inducing specific T-cell response as well as pro-inflammatory cytokines. CFSE *in vivo* cytotoxicity assay was used to study the cytolytic

toxicity. Characterization of APCs uptake of the vaccines by both methods were also assessed.

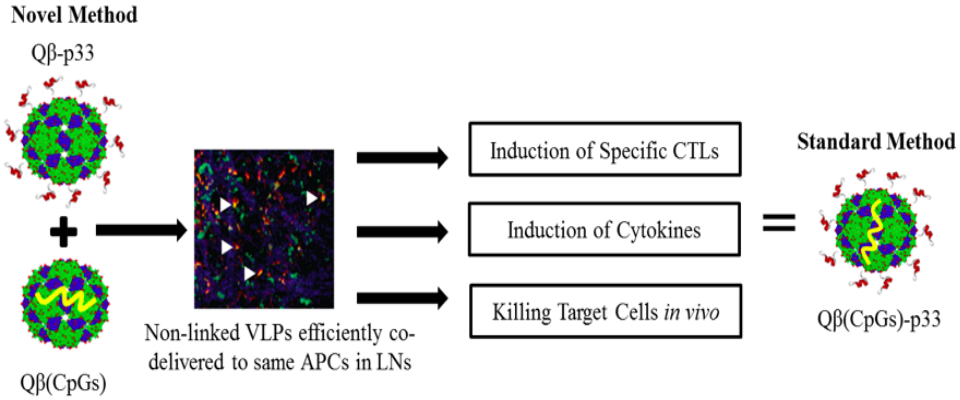

Figure 4. 1 A diagram illustrating the experimental approach of the current study

Packaging adjuvant in a separate VLP and mix it with another VLP displaying the antigen would induce similar results as the standard method which implies that adjuvant and antigen should be in close proximity when using VLP-based vaccine.

4.2. Research questions and objectives

4.2.1. Research questions

1. Can Qβ-VLPs efficiently be packaged with B-type CpGs, and is the packaging stable?
2. Can the new vaccine formulation Qβ(CpGs) mixed with Qβ(Ø)-p33 charge same APCs in the LN?
3. Can the new vaccine formulation of Qβ(CpGs) mixed with Qβ(Ø)-p33 induce CTL response comparable to the standard conventional method?
4. What are the APCs subset that take-up and process both mixed VLPs?
5. Can the new vaccine formulation Qβ(CpGs) mixed with Qβ(Ø)-p33 induce similar lytic activity *in vivo* comparable to the standard conventional method?

4.2.2. Research objectives

1. To test the hypothesis whether Qβ-VLPs can be efficiently and stably package B-type CpGs even when mixed with another Qβ-VLPs displaying the antigen.
2. To test whether Qβ(CpGs) and Qβ displaying P33 would be taken up simultaneously by the same APCs.
3. To test if the new proposed vaccine formulation would induce comparable specific CTLs response to the standard method where both adjuvants and antigens are linked to the same VLP.
4. To analyse which APC subsets would mainly be involved in the process of taking up and processing the Qβ(CpGs) and Qβ(Ø)-p33 simultaneously.
5. To test the *in vivo* lytic activity of the new vaccine formulation and compare it to the standard method.

4.3. Reagents and materials

Table 4. 1 Name, supplier and catalog number of Peptides, reagents and materials

Reagent	Supplier	Catalogue Number
SMPH (succinimidyl-6-(X-maleimidopropionamido) hexanoate NHS ester)	Thermo Fisher SCIENTIFIC	22363
DMSO	Sigma-Aldrich	M81802
DMEM Medium	Sigma-Aldrich	D6046
Fc Block antibody	eBioscience	553142
CD8α mAb/anti-mouse/PerCP-Cyanine 5.5	eBioscience	45-0081-80
CD11c mAb/anti-mouse/ PE Cyanine7	eBioscience	25-0116-41
CD11b mAb/anti-mouse/PE	eBioscience	12-0112-81

F4/80 mAb/anti-mouse/PerCP-Cyanine 5.5	eBioscience	45-4801-80
CD45R/B220 mAb/anti-mouse/PE Cyanine7	eBioscience	25-0452-82
MHC-II mAb/anti-mouse/APC Cy7	eBioscience	47-5321-80
IFN-γ mAb/anti-mouse/APC	eBioscience	554413
TNF-α mAb/anti-mouse/PE	eBioscience	12-7321-81
Tetramers H2-Db (KAVYNFATM) APC/PE	TCMetrix	Custom made
Monensin	BD Bioscience	554724
BrefeldinA	BD Bioscience	555029
IC Fixation Buffer	Fisher-Scientific SCIENTIFIC	00-8222-49
Permeabilization Buffer 10x	Fisher-Scientific SCIENTIFIC	00-8333-56
Alexa Fluor 647 NHS ester dye	Thermo Fisher SCIENTIFIC	A20006
Alexa Fluor 488 NHS ester dye	Thermo Fisher SCIENTIFIC	A20000
Alexa Fluor 594 NHS ester dye	Thermo Fisher SCIENTIFIC	A20004
Collagenase D	Roche	11 088 858 001
DNase I	Sigma-Aldrich	0000000047 16728001
RNase I	Merck	70498624
CellTrace-CFSE proliferation kit	Thermo Fisher SCIENTIFIC	C34554
P33 (NH2-KAVYNFATMGCC-H2)	Pepscan PRESTO	Custom made

B-type CpGs 5″-TCC ATG ACG TTC CTG ATG CT-3″	Iba	Tlrl-1668c
SYBR Safe DNA gel stain	Thermo Fisher Scientific	S33102
Brilliant Blue R Staining Solution	Sigma-Aldrich	6104-59-2
Materials	**Supplier**	**Catalogue Number**
Amicon centrifuge tubes 100 kDa MWCU	Thermo Fisher Scientific	UFC501008
Tissue-Tek O.C.T. compound	Sakura	25608-930
Fluoromount G solution	Thermo Fisher SCIENTIFIC	00-4958-02
Any kD mini-protein TGX precast protein gel	Bio-RAD	4569033
70 μM filters	BD Bioscience	352350

4.4. Methods

4.4.1. Qβ-VLPs expression and production

Qβ-VLPs expression and production was performed and provided by the core lab facility at University of Bern.

Qβ-VLPs expression and production is described in detail in (Kozlovska et al., 1996).

4.4.2. Qβ(RNA)-p33 vaccine generation

Qβ naturally packaging RNA was derivatized using SMPH heterobifunctional for 1 h at RT. Excess SMPH cross-linker was removed using Amicon centrifuge tubes of 100kDa MWCO. Modified version of p33 model peptide was purchased from (Pepscan PRESTO) and has been synthesized by adding GCC amino acids to the C terminus of the peptide to facilitate its coupling to SMPH

cross-linker. The modified peptide was reconstituted in DMSO. 10-fold molar excess of the modified peptide was added over Qβ-VLPs monomer. The mixture was incubated at RT for 2 h and excess peptide was removed using Amicon centrifuge tubes. The efficiency of the coupling was tested by using SDS-PAGE (Any kD mini-protein TGX precast protein gel, Bio-Rad). The gel was run at 200V for 35 min and stained with Coomassie Blue and destained as previously described. The coupling efficiency was assessed by densitometric analysis of SDS-PAGE of Qβ-VLP monomer bands compared to Qβ-VLP monomer plus p33 after coupling.

4.4.3. Qβ(Ø)-p33 vaccine generation

The naturally packaged RNA in Qβ-VLPs was digested with 1.2 mg/ ml RNase for 3 mg/ ml Qβ-VLPs, digestion was done for 3 h at 37°C on shaker 350rpm and RNA depletion was confirmed by 1% agarose gel stained with SYBRsafe stain. Derivatization of Qβ-VLPs was carried afterwards using SMPH cross-linker as explained above for Qβ(RNA)-p33 vaccine generation.

4.4.4. Packaging B-type CpGs into Qβ-VLPs

Packaging of B-type CpGs into Qβ-VLPs was described in (Methods 2.4.2).

4.4.5. Measuring p33 specific $CD8^+$ T-cells by tetramer staining

C57BL/6, 9-12 weeks old mice (Harlan) were used to measure p33 specific T-cell response by tetramer staining. Mice were vaccinated s.c. with 50 μg of the developed vaccine. Tetramer staining procedure has been described in detail in (Method 2.4.5).

4.4.6. Intra-cellular cytokine (ICS) staining for IFN-γ and TNF-α

Intra-cellular cytokine staining was performed on spleens of immunized mice for measuring IFN-γ and TNF-α cytokines as explained earlier in (Methods

2.4.6).

4.4.7. Lymph node trafficking experiment

Qβ(RNA)-p33 and Qβ(Ø)-p33 were labelled with AF647 while Qβ(CpGs) was labelled with AF488 according to manufacturer instructions. C57BL/6 mice (9-12 weeks old; Harlan) were injected in the footpad under isoflurane anesthesia with total 25 μg of Qβ(RNA)-p33 mixed with Qβ(CpGs) or Qβ(Ø)-p33 mixed with Qβ(CpGs). Twenty-four h later the popliteal LNs were collected and treated with DNaseI and collagenase D for 30 min at 37°C. The cells were stained with anti CD11c, CD11b, F4/80, CD45R/B220 mAb and MHC-I and analysed by flow cytometry.

4.4.8. Immunohistochemistry

C57BL/6 mice (9-12 weeks old; Harlan) were injected in the footpad with Qβ(Ø)-p33 labelled with AF647 and Qβ(CpGs) labelled with AF488. Twenty-four h later the popliteal LNs were collected and embedded in tissue-tek O.C.T. and flash-frozen immediately in liquid nitrogen. Next, 8 μm sections were prepared and dried over-night before staining. The sections were then fixed with 100% acetone and allowed to dry in air. Sections were then pre-wet in PBS for 5 min and blocked with 1% BSA and normal mouse serum for about 20 min. The sections were then stained with anti-CD11b for 1 h. Sections were then washed and mounted by fluoromount G solution. Imaging was done using Zeiss Axio Imager A2 microscope with Plan-NEOFLUAR 20×/ 0,5 objective.

4.4.9. Imaging of popliteal lymph nodes by stereomicroscope

The stereomicroscopic imaging was performed by Prof. Jens V. Stein at the Theodor Kocher Institute, University of Bern.

The stereomicroscopic imaging of the popliteal LNs was done as a collaboration

with Prof. Jens V. Stein at Theodor Kocher Institute, University of Bern, Switzerland. C57BL/6 mice (9-12 weeks old; Harlan) were used and prepared for imaging by shaving their right leg and removing the skin and adipose tissue under terminal anesthesia to expose the popliteal LN. A customized imaging platform was then used to stabilize the mice. Several bright field illumination images were then acquired to allocate the popliteal LN. Qβ(Ø)-p33 labelled with AF594 or Qβ(CpGs) labelled with AF488 were prepared and 25 µg of either VLPs was injected in the right mice footpad to visualize the VLPs trafficking. This was done using a CCD camera (Nikon) and fluorescent light illumination.

4.4.10. Imaging using 2-photon microscopy

2-photon microscopy imaging of the popliteal LNs was performed by Prof. Jens V. Stein at Theodor Kocher Institute, University of Bern, Switzerland.

C57BL/6 mice (9-12 weeks old; Harlan) were injected with Qβ(Ø)-p33 labelled with AF594 and Qβ(CpGs) labelled with AF488 in the right footpad. Twenty-four h later the popliteal LNs were surgically prepared and exposed as explained earlier. TrimeScope 2PM system equipped with tunable laser Ti:Sa (Spectraphysics) was used to excite the labelled VLPs, the laser was set to 840nm excitation 0-80 um below the LN surface and identified by collagen capsule SHG signal. The harmonic signal and emitted light were detected by 593/40, 525/50 and 447/55 nm using non-descanned detectors (Boscacci et al., 2010).

4.4.11. CFSE *in vivo* cytotoxicity assay

CFSE *in vivo* cytotoxicity assay was described in detail in (Method 2.4.7).

4.4.12. Statistics

Data was analysed and compared by One-Way ANOVA (Turkey's Multiple Comparison Test). ns = not significant, ***=P value < 0.0001; **=P value < 0.001; *=P value < 0.01.

4.5. Results:

4.5.1. B-type CpGs can efficiently be packaged into Qβ -VLPs

It has previously been shown that Qβ-VLPs do naturally package RNA derived from E. *coli* during the expression and production process in host cells. These naturally packaged RNA can be enzymatically digested from the interior facet of VLPs leaving a positively charged inner surface which then can be repackaged with a range of adjuvants including B-type CpGs. Qβ-VLPs have pores of ~2 nm allowing the passive diffusion of RNase enzyme into the capsids and thus effectively digest the naturally packaged RNA. Likewise, B-type CpGs can also diffuse into the empty VLP shell and will bind to the positively charged arginine residues on the inner surface. A titration experiment has been first carried out to optimize packaging of B-type CpGs into Qβ-VLPs after digesting the naturally packaged RNA (Figure 4.2A). The titration results indicated that Qβ-VLPs can be effectively packaged with 1.125 µg/ 20 µg Qβ-VLPs. This indicates that low concentrations of B-type CpGs have limited aggregation and thus facilitate diffusion into the empty shell of Qβ-VLPs. The p33 derived from LCMV was used as a model antigen, and is a H2-Db restricted peptide that has been extended by the addition of GCC amino acids at the C terminus. P33 was then coupled to Qβ-VLPs using SMPH cross-linker (Figure 4.2B). SDS-PAGE in Figure 4.2C illustrates the coupling efficiency of p33 to Qβ-VLPs, with about

360 peptides apparently coupled to one VLP as estimated from the densitometric analysis.

Immunizing the mice with Qβ(CpGs)-p33 vaccine is capable of inducing strong CTL response measured by tetramer staining (Storni et al., 2004). In this experiment, RNA-loaded Qβ-VLP or an empty Qβ-VLP are planned to be mixed with another Qβ-VLP packaged with B-type CpGs. Therefore, it is important to test that the B-type CpGs would not pass from the packaged VLP into the empty VLP once mixed together. To test this, Qβ(B-type CpGs) was mixed with empty Qβ(Ø)-p33 for 10 min, 1 h and 2 h, then we ran the mixture on agarose gel stained with SYBRsafe stain and Coomassie Blue stain to visualize the DNA and the protein, respectively. The results of this experiment indicate that no CpGs were apparently passed from the packaged Qβ-VLPs to the empty Qβ(Ø)-p33 since the DNA and protein bands did not change in density (Figure 4.2 D).

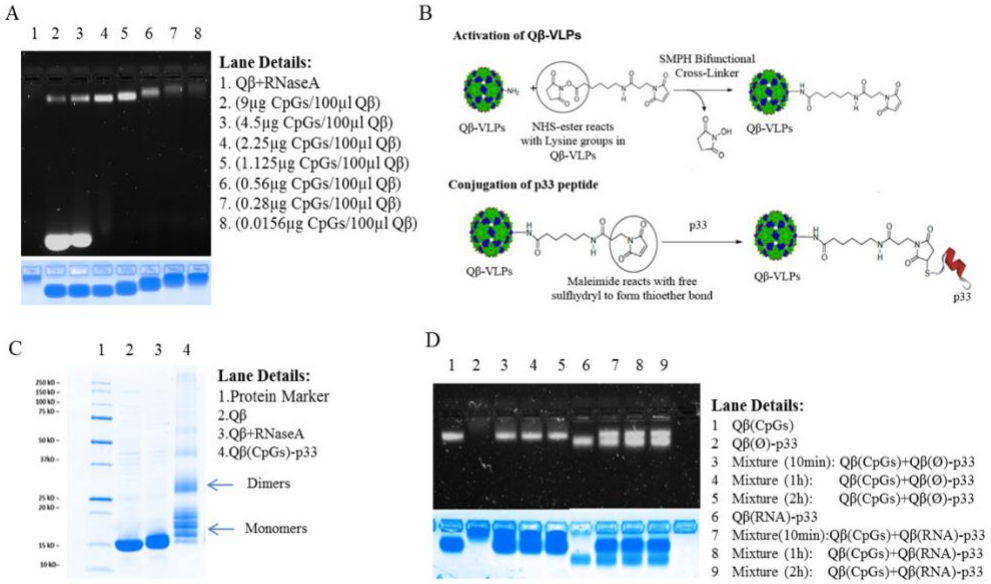

Figure 4. 2 B-type CpGs can efficiently be packaged into Qβ –VLPs

A, loading Qβ-VLPs with different concentration of B-type CpGs, top: 1% agarose gel stained by SYBRsafe stain for visualizing RNA and DNA, bottom: same 1% agarose

gel stained with Coomassie Blue stain to visualize Qβ-VLPs protein. Lane 1: Qβ after digestion with RNaseA, Lanes: 2, 3, 4, 5, 6,7 and 8: packaging Qβ-VLPs with 9 μg CpGs, 4.5 μg CpGs, 2.25 μg CpGs, 1.125 ug CpG, 0.56 μg CpGs, 0.28 μg CpGs or 0.0156 μg CpGs respectively in 100 μl Qβ-VLPs of (3 mg/ ml). *B,* Schematic diagram of p33 coupling process to Qβ-VLPs using bifunctional SMPH crosslinker. *C,* SDS-PAGE with Coomassie Blue stain, Lane 1: protein marker, Lane 2: Qβ-VLPs monomers of 14kD, Lane 3: Qβ-VLPs after digestion of RNA, Lane 4: Qβ-VLPs after packaging with B-type CpGs and coupling to p33 using SMPH crosslinker, arrows indicate the monomers and dimers of Qβ-VLPs. *D,* confirming stability of packaging B-type CpGs into empty Qβ-VLPs, top: 1% agarose gel stained by SYBRsafe stain for visualizing RNA and DNA, bottom: same 1% agarose gel stained with Coomassie Blue stain to visualize Qβ-VLPs protein. Qβ(Ø)-p33 or Qβ(RNA)-p33 was mixed with Qβ(CpGs) for different time points 30 min, 1 h and 2 h.

4.5.2 Mixing Qβ-VLPs packaging B-type CpGs with Qβ-VLPs displaying the antigen can efficiently reach draining lymph node and activate the resident APCs *in vivo*

A trafficking experiment has been performed to test whether Qβ(CpGs) mixed with Qβ(Ø)-p33 would efficiently reach the same draining LN and charge the same resident APCs. To this end, I injected the mixed VLPs into the popliteal draining LN of C57BL6 mice and visualized the accumulation of both VLPs (Figure 4.2A). To perform this experiment, I have labelled Qβ(CpGs) with AF488 and Qβ(Ø)-p33 with AF594 and co-injected them into the mouse' footpad (Figure 4.2B). Both labelled VLPs efficiently reached the popliteal draining LN with fast kinetics. To test whether both VLPs were simultaneously taken by the same APCs and what cell types would mainly uptake the VLPs,

flow cytometry hs been performed 24h post injection in the mice footpads. Different types of APCs managed to efficiently take up the VLPs, with a large fraction of APCs identified as double positive for both VLPs (Figure 4.2C). This observation indicates that the physical linkage between adjuvants and antigens to the same VLP may not be necessary. Further analysis showed that the most predominant APCs taking up both VLPs were cDCs including $CD8^{-}CD11b^{+}$, $CD8^{-}CD11c^{+}$ and $CD8^{+}CD11c^{+}$, monocyte derived DCs $CD11c^{+}CD11b^{+}$ and macrophages $CDF4/80^{+}CD11b^{+}$. B cells characterized by $CD45/B220^{+}$ were less efficient in binding VLPs (Figure 4.2C). The expression of MHC-II molecules on $CD11c^{+}$ cells was also measured as an activation marker. MHC-II expression was increased on those $CD11c^{+}$ cells that took up both VLPs in comparison with $CD11c^{+}$ from naïve mice. This indicates that VLPs packaged with B-type CpGs can effectively activate $CD11c^{+}$ APCs (Figure 4.2D). Interestingly, APCs residing in the popliteal LN and that did not take up both VLPs also exhibited increased MHC-II expression (Figure 4.2D). This result is consistent with the finding that soluble IFN-β mediates the up-regulation of activation markers by TLRs (Uematsu & Akira, 2007). The co-localization of both VLPs in the popliteal LNs has been further studied by immunohistochemistry staining 24h post injection with Qβ(CpGs) AF488 and Qβ(Ø)-p33 AF495, $CD11b^{+}$ staining was also used to visualize APCs. Immunohistochemistry results have shown that $CD11b^{+}$ APCs in the sub-capsular and paracortex regions have efficiently taken up both labelled VLPs (Figure 4.2E). Further assessment of the co-localization of both labelled VLPs was performed by 2 photon-microscopy. The results confirmed the immunohistochemistry results and have shown that both VLPs were

simultaneously taken up by APCs in the popliteal LN of the injected mice (Figure 4.2F).

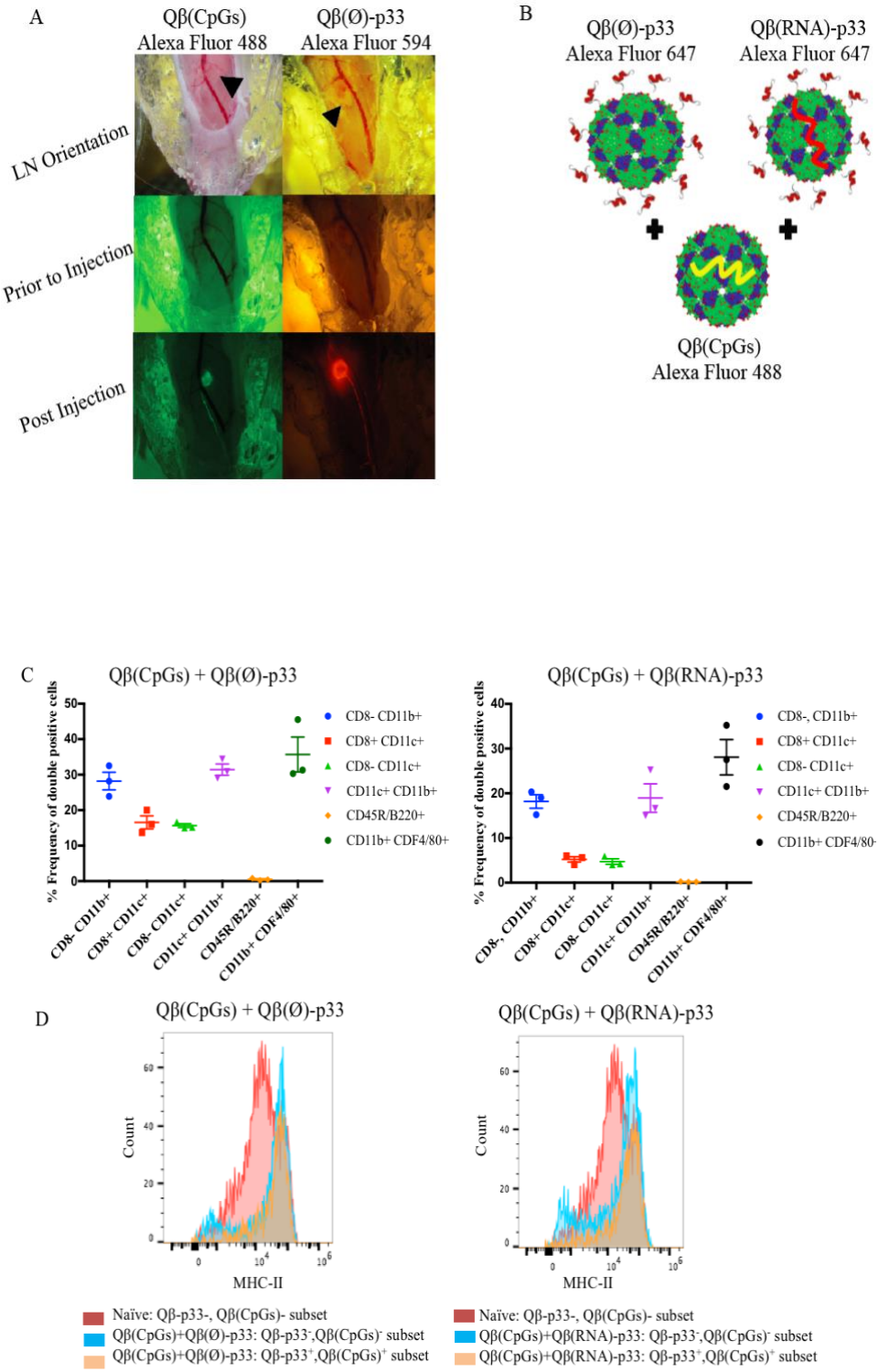

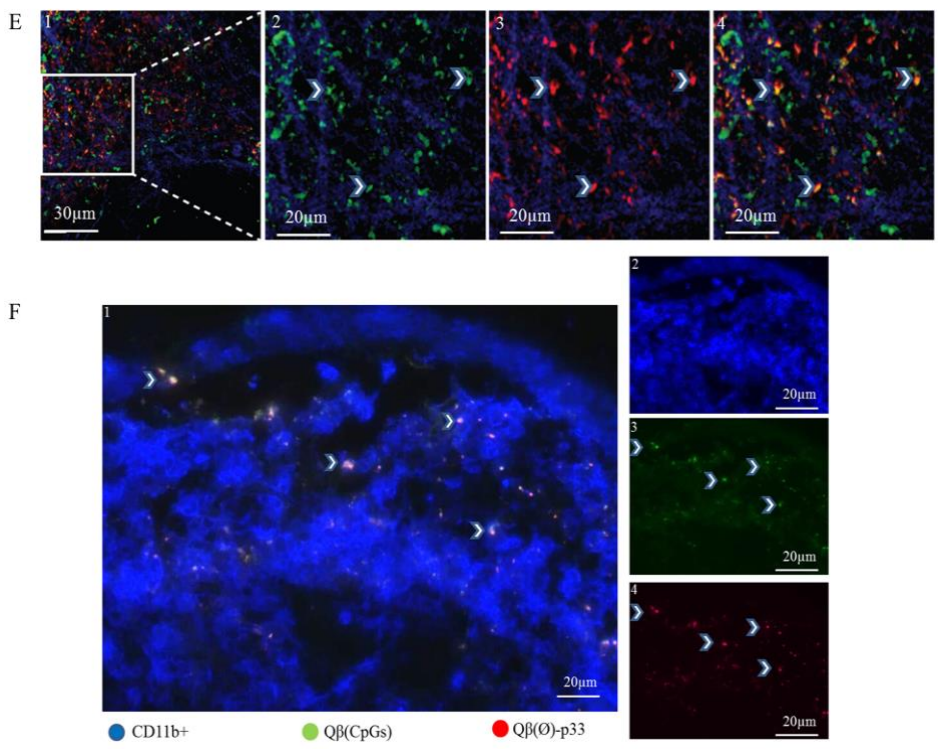

Figure 4. 3 Mixing Qβ-VLPs packaging B-type CpGs with Qβ-VLPs displaying the antigen can efficiently reach draining lymph node and activate the resident APCs *in vivo*

A, Stereomicroscopic imaging in live C57BLK6 mice for the right popliteal LN showing the fast accumulation of Qβ(Ø)-p33 labelled with AF594 or Qβ(CpGs) labelled with AF488 in the popliteal LN 10 min post injection in the mice footpad. Top: bright field image of popliteal LN, middle: fluorescent image before injection, bottom: fluorescent image 10 min post injection using appropriate filters. *B*, diagram illustrating the vaccination groups, Qβ(Ø)-p33 or Qβ(RNA)-p33 labelled with AF647 and mixed with Qβ(CpGs) labelled with AF488.*C*, C57BLK6 mice were injected according to the diagram illustrated in B, popliteal LN were collected, and frequency of cell subsets taken up both VLPs (double positive) were analysed by flow cytometry. Three mice per group, one representative of 3 similar experiments is shown. *D*, MHC-II histogram count expression for $CD11c^+$ cells in both naïve and vaccinated groups with Qβ(Ø)-p33 or Qβ(RNA)-p33 labelled with AF647 and mixed with Qβ(CpGs) labelled with AF488. The histogram was analysed for 3 different subsets (red histogram: double (-) cells in naïve mice, blue histogram: double (-) cells in vaccinated mice, orange: double (+) cells in vaccinated mice). *E*, maximum intensity projections of the popliteal LN using 2-photon microscopy

imaging in live C57BLK6 mice demonstrating the co-localization of both Qβ(Ø)-p33 labelled with AF647 and mixed with Qβ(CpGs) labelled with AF488 24 h after injection in the mice foot pad. The collagen fibers of the popliteal LN were visualized by second harmonic generation (blue SHG). Image 1: overview 30 µm scale, 2-4 magnified images from the circled area illustrating (2) green Qβ(CpGs) and SHG blue signal (3) red Qβ(Ø)-p33 and SHG blue signal (4) overlay of both VLPs. Arrowheads show exemplary double positive VLPs; presumably DCs 20 µm scale. *F*, immunohistochemistry staining of the popliteal LNs 24 h after injecting in the footpad with Qβ(Ø)-p33 labelled with AF647 and mixed with Qβ(CpGs) labelled with AF488 and probed with $CD11b^+$ antibodies to assess the uptake and co-localization of both VLPs.

4.5.3 Qβ(CpGs) mixed with Qβ(Ø)-p33 can significantly induce p33 specific $CD8^+$ T-cell response *in vivo*

APCs mainly DCs should be activated for optimal induction of specific T-cell response, this activation can be done using CpGs. The standard consensus in vaccinology with VLPs is that CpGs need to be physically linked with the VLP, *i.e.* CpGs packaged inside VLP displaying the antigen of interest. I have shown above that Qβ(CpGs) and Qβ(Ø)-p33 are taken up and presented by the same APC in the popliteal draining LN. The next step was to test whether this formulation is capable of inducing p33 specific T-cell response comparable to the standard method.

To address this question, seven groups have been produced as illustrated in Figure 4.3A. The produced vaccines were also designed to compare the adjuvant activity of the naturally packaged RNA in comparison to B-type CpGs. Groups 1 and 2 present the control groups without antigen, groups 3 and 4 present Qβ coupled to p33 with/without RNA and were not mixed with Qβ (CpGs). These 2 groups have been designed to assess the importance of CpGs as adjuvants. However, groups 5 and 6 were mixed with CpGs packaged VLPs.

The last group 7 is the standard method where Qβ is coupled to p33 and loaded with CpGs, this group also served as a positive control and reference. The resultant vaccine formulations were tested *in vivo* to assess p33 specific T-cell response. A single injection of 50µg of the produced vaccine was injected subcutaneously into C57BL/6 mice and 7 days later the spleens were collected for p33 tetramer staining and ICS. The naturally packaged RNA was less efficient (*p* 0.0016) in inducing immunogenicity *in vivo* when compared with CpGs (*p* 0.0008), this observation confirms earlier data (Storni & Bachmann, 2004). Furthermore, groups 3 Qβ(Ø)-p33 and 4 Qβ(RNA)-p33 were less efficient in inducing specific T-cell response when compared to groups 5 [Qβ(Ø)-p33 + Qβ(CpGs)], group 6 [Qβ(RNA)-p33 + Qβ(CpGs)] and the reference group 7 Qβ(CpGs)-p33. This clearly indicates the importance of using adjuvants such as B-type CpGs for effective T-cell response. Intra cellular staining for IFN-γ and TNF-α mirrored the responses obtained with tetramer staining and showed that groups 5 and 7 performed best (Figure 4.3 B-D).

A.

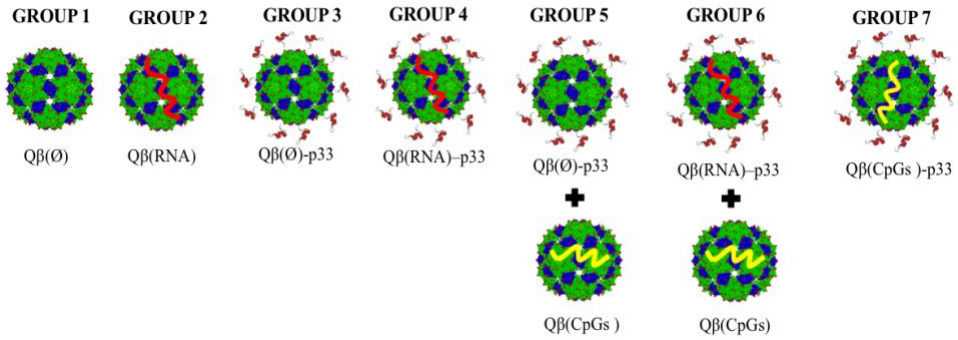

B.

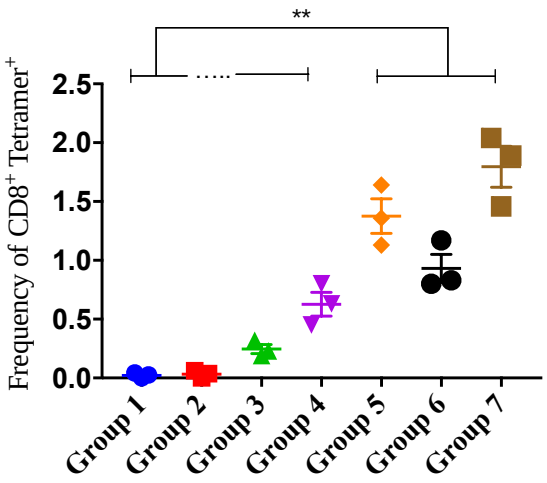

Group	Description
1	Qβ(Ø)
2	Qβ(RNA)
3	Qβ(Ø)-p33
4	Qβ(RNA)-p33
5	Qβ(Ø)-p33 + Qβ(CpGs)
6	Qβ(RNA)-p33 + Qβ(CpGs)
7	Qβ(CpGs)-p33

One-Way ANOVA (Turkey's Multiple Comparison Test)	***P* value**	**One-Way ANOVA (Turkey's Multiple Comparison Test)**	***P* value**
Group 1 vs Group 2	Ns	Group 3 vs Group 4	*
Group 1 vs Group 3	**	Group 3 vs Group 5	*
Group 1 vs Group 4	**	Group 3 vs Group 6	ns
Group 1 vs Group 5	***	Group 3 vs Group 7	**
Group 1 vs Group 6	**	Group 4 vs Group 5	**
Group 1 vs Group 7	***	Group 4 vs Group 6	**
Group 2 vs Group 3	**	Group 4 vs Group 7	***
Group 2 vs Group 4	**	Group 5 vs Group 6	ns
Group 2 vs Group 5	***	Group 5 vs Group 7	ns
Group 2 vs Group 6	**	Group 6 vs Group 7	*
Group 2 vs Group 7	***		

C.

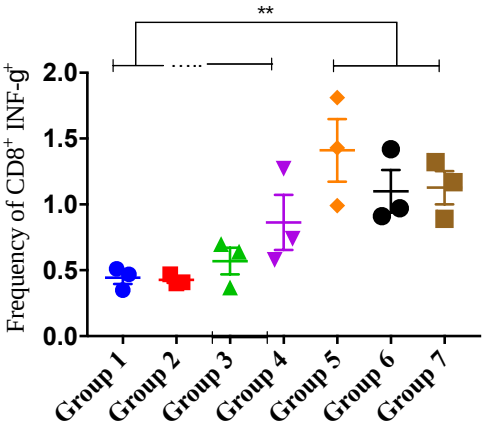

Group	Description
1	Qβ(Ø)
2	Qβ(RNA)
3	Qβ(Ø)-p33
4	Qβ(RNA)-p33
5	Qβ(Ø)-p33 + Qβ(CpGs)
6	Qβ(RNA)-p33 + Qβ(CpGs)
7	Qβ(CpGs)-p33

One-Way ANOVA (Turkey's Multiple Comparison Test)	*P* value	One-Way ANOVA (Turkey's Multiple Comparison Test)	*P* value
Group 1 vs Group 2	ns	Group 3 vs Group 4	ns
Group 1 vs Group 3	ns	Group 3 vs Group 5	ns
Group 1 vs Group 4	ns	Group 3 vs Group 6	ns
Group 1 vs Group 5	*	Group 3 vs Group 7	ns
Group 1 vs Group 6	*	Group 4 vs Group 5	*
Group 1 vs Group 7	**	Group 4 vs Group 6	*
Group 2 vs Group 3	ns	Group 4 vs Group 7	*
Group 2 vs Group 4	ns	Group 5 vs Group 6	ns
Group 2 vs Group 5	*	Group 5 vs Group 7	ns
Group 2 vs Group 6	*	Group 6 vs Group 7	ns
Group 2 vs Group 7	**		

D.

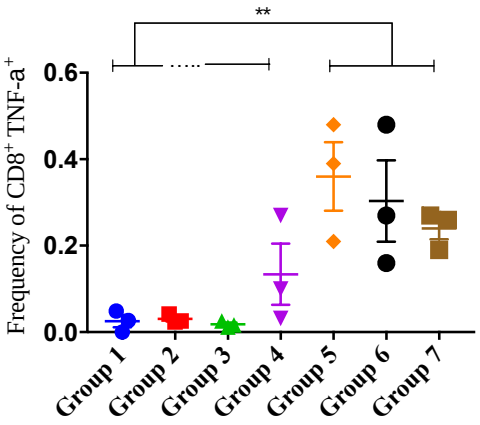

Group	Description
1	Qβ(Ø)
2	Qβ(RNA)
3	Qβ(Ø)-p33
4	Qβ(RNA)-p33
5	Qβ(Ø)-p33 + Qβ(CpGs)
6	Qβ(RNA)-p33 + Qβ(CpGs)
7	Qβ(CpGs)-p33

One-Way ANOVA (Turkey's Multiple Comparison Test)	*P* value	One-Way ANOVA (Turkey's Multiple Comparison Test)	*P* value
Group 1 vs Group 2	ns	Group 3 vs Group 4	ns
Group 1 vs Group 3	ns	Group 3 vs Group 5	ns
Group 1 vs Group 4	ns	Group 3 vs Group 6	ns
Group 1 vs Group 5	*	Group 3 vs Group 7	ns
Group 1 vs Group 6	*	Group 4 vs Group 5	*
Group 1 vs Group 7	**	Group 4 vs Group 6	*
Group 2 vs Group 3	ns	Group 4 vs Group 7	***
Group 2 vs Group 4	ns	Group 5 vs Group 6	ns
Group 2 vs Group 5	*	Group 5 vs Group 7	ns
Group 2 vs Group 6	*	Group 6 vs Group 7	ns
Group 2 vs Group 7	**		

Figure 4. 4 Qβ (CpGs) mixed with Qβ (Ø)-p33 can significantly induce p33 specific CD8$^+$ T-cell response *in vivo*

A, seven groups were designed and developed, left: Group 1 Qβ(Ø) after digesting RNA, Group 2 Qβ(RNA) with RNA, Group 3 Qβ(Ø)-p33 using, Group 4 Qβ(RNA)-p33, Group 5 Qβ(Ø)-p33 + Qβ(CpGs), Group 6 Qβ(RNA)-p33 + Qβ(CpGs), Group 7 Qβ(CpGs)-p33 represents the standard method. *B*, frequency of CD8$^+$ Tetramer$^+$ cells in each developed group after s.c. injection of 50µg vaccine in C57BLK6 mice. *C*, Frequency of CD8$^+$ IFN-γ $^+$ cells in each developed group by ICS. *D*, Frequency of CD8$^+$ TNF-α $^+$ cells in each developed group by ICS. Statistical analysis by one-way ANOVA (Turkey's multiple comparison test). 3 mice per group, 1 representative of 3 similar experiments is shown.

4.5.4 Qβ (CpGs) mixed with Qβ (Ø)-p33 induce p33 lytic CTL response *in vivo*

I have then examined the *in vivo* lytic activity of p33 CTL by performing CFSE cytotoxicity assay where naïve splenocytes unpulsed or pulsed with p33 have been labelled with different CFSE concentrations. Both unpulsed and pulsed populations have been mixed in 1:1 ratio and co-injected i.v. into recipient previously immunized mice seven days earlier as illustrated in Figure 4.4A. After 4 h later the spleens were harvested and the percentage of both CFSE^{low} and p33-pulsed CFSE^{high} cells were analysed. The lytic activity of groups 1, 5, 6 and 7 are shown in (Figure 4.4B) where p33 pulsed population was efficiently depleted in groups 5, 6 and 7 but not in the control group 1. The percentage of p33 specific lytic activity of all the groups have been calculated and plotted in (Figure 4.4C).

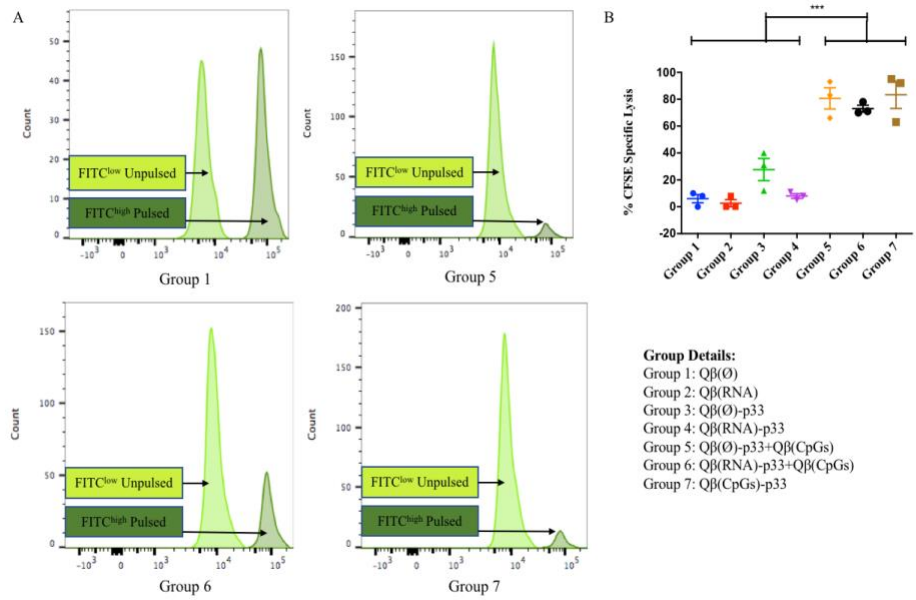

One-Way ANOVA (Turkey's Multiple Comparison Test)	*P* value	One-Way ANOVA (Turkey's Multiple Comparison Test)	*P* value
Group 1 vs Group 2	ns	Group 3 vs Group 4	Ns
Group 1 vs Group 3	ns	Group 3 vs Group 5	**
Group 1 vs Group 4	ns	Group 3 vs Group 6	**
Group 1 vs Group 5	***	Group 3 vs Group 7	*
Group 1 vs Group 6	****	Group 4 vs Group 5	***
Group 1 vs Group 7	**	Group 4 vs Group 6	****
Group 2 vs Group 3	*	Group 4 vs Group 7	**
Group 2 vs Group 4	ns	Group 5 vs Group 6	Ns
Group 2 vs Group 5	***	Group 5 vs Group 7	Ns
Group 2 vs Group 6	****	Group 6 vs Group 7	Ns
Group 2 vs Group 7	**		

Figure 4. 5 Qβ (CpGs) mixed with Qβ (Ø)-p33 induce p33 lytic CTL response *in vivo* *A*, flow cytometry data showing the frequency of splenocytes un-pulsed population labelled with low CFSE concentration 2 µM and p33 pulsed population labelled with CFSE high concentration of 10 µm in: group 1 Qβ(Ø) control, group 5 Qβ (Ø)-p33 + Qβ (CpGs), group 6 Qβ (RNA)-p33 + Qβ (CpGs) and group 7 Qβ(CpGs)-p33. *B*, the calculated % of specific lysis in each vaccinated group 100 X (1– CFSE ^{high} pulsed / CSFE ^{low} un-pulsed). Statistical analysis by One-Way ANOVA (Turkey's multiple comparison test). 3 mice per group, one experiment is shown and is representative of 3 similar experiments.

4.6 Discussion:

CpGs are effective and potent stimulators of the innate immune system, they activate APCs by engaging TLR-9. Such binding enhances the upregulation of different costimulatory molecules and increases APCs and B-cells production of chemokines and cytokines ((Bode et al., 2011; Hartmann et al., 1999; Mohsen, Gomes, et al., 2017). This initial innate response will then be augmented to adaptive response in the presence of immunogenic antigen. CpGs have previously been shown to improve DCs and macrophage antigen presenting function, they also enhance NK cells via secretion of different cytokines (Hartmann et al., 1999; Higgins et al., 2007). Therefore, CpGs can be considered as an effective vaccine adjuvant which can be administered mucosally or systemically for mounting stronger, faster and long lasting immune response (Higgins et al., 2007).

Previous studies have shown the drawbacks of administering CpGs in the free form, such as increasing auto-antibodies formation, inflammation or toxic shock (Gilkeson, Ruiz, Howell, Lefkowith, & Pisetsky, 1993; Steinberg, Krieg, Gourley, & Klinman, 1990). These obstacles can be overcome by packaging the synthetic CpGs into VLPs which should increase the adjuvants' potency and facilitate their delivery to the endosomal compartments in APCs. In addition, such packaging would prevent the exposure of CpGs to other cells such as B-cells which will not recognize the packaged CpGs through their B-cell receptors and thus preventing the induction of anti CpGs antibodies (Storni et al., 2004). Taken all together, immunization with VLPs packaging CpGs would result in efficient and strong CTL responses in mice without causing any toxicity (Storni et al., 2004).

The current consensus in VLP-based vaccines is that both adjuvants and antigens should be in close proximity (physically linked) for optimal immune response (Senti et al., 2009; Speiser et al., 2010; Storni et al., 2004). In the current study, we have shown a novel strategy for delivering adjuvants when using VLP-based vaccines. The idea is based on packaging synthetic oligonucleotides in VLPs and mix them with another VLP vaccine only prior to administration *in vivo*. In the current project, we have mainly focused on packaging B-type CpGs into Qβ-VLPs due to their favorable characteristics. These characteristics include being small, single strands that can easily diffuse into the 2 nm pores of Qβ-VLPs capsid and bind to the positively charged inner Arginine residues (Conway et al., 2003; Crowther et al., 1994; Storni et al., 2004).

The trafficking kinetics of the two different VLPs in mice were generated earlier and the results indicated that both VLPs can reach the popliteal LN surprisingly fast in less than 10 minutes (Manolova et al., 2008). Normally DCs can internalise up to 50 VLPs upon immunization (Keller et al., 2010), therefore it may be expected that Qβ(CpGs) and Qβ(O)-p33 would also be taken up simultaneously by the same APCs. To address this, we have performed a trafficking experiment to study the drainage kinetics and the uptake of both VLPs after labelling each with a different fluorophore. The results have shown efficient drainage of both VLPs via the lymphatic system to the popliteal LN where they will be simultaneously taken up by different subsets of APCs, this would ensure potent activation of the same cells that present the antigen. Two lymphoid resident APCs subsets ($CD8^{-}CD11c^{+}$ and $CD8^{+}CD11c^{+}$) have been shown to have different functions (Dudziak et al., 2007), with both subsets

having the ability to take up VLPs and upregulate MHC-II presentation. However, only $CD8^+$ subsets located mainly in the T-cell zone of the LN can cross present VLP-derived antigens to T-cells (Keller et al., 2010). There is an important point to keep in mind for any future vaccine application in humans, principally that TLR-9 is not expressed on cDCs and therefore, it will be important to employ additional adjuvants to activate all DC types and/ or target pDCs in LN. Immunohistochemistry of the popliteal LN cryosections have been performed to confirm the efficient up take of both VLPs by the same APCs. The obtained results confirmed the findings and suggested the up-take of both VLPs by the same APC. The naturally packaged RNA packaged in Qβ-VLPs did not increase VLP immunogenicity when compared to CpGs. The reduced CTL response by RNA is not due to RNA degradation before cellular uptake, as VLPs naturally packaging RNA have shown strong and equal IgG and IgA responses as VLPs packaged with CpGs (Bessa et al., 2009). This is markedly different from empty VLPs. This observation demonstrates the ability of RNA naturally packaged in VLPs to activate TLR7/8 *in vivo* (Bessa et al., 2009). Furthermore, *in vivo* immunization using Qβ-VLPs cross-linked to p33 without administration CpGs was less efficient in producing specific T-cell population, mirroring the importance of activating TLR-9 in APCs for enhancing adaptive immune responses. For the induction of T-cell response, the formulated vaccines have induced similar response to the reference standard vaccine. This was also observed when performing intra cellular cytokine staining for IFN-γ and TNF-α as groups 5 [Qβ(Ø)-p33 + Qβ(CpGs)] (p 0.0161) and group 6 [Qβ(RNA)-p33 + Qβ(CpGs)] (p 0.0143) showed significant increase comparable to group 7 Qβ(CpGs)-p33 (p 0.0071).

CFSE *in vivo* cytotoxic assay was carried out to assess the lytic activity of the induced CTLs. Groups 5 and 6 induced similar lysis as the standard group 7. This indicates that both conjugated and un-conjugated VLPs vaccine preparations induce CTLs response at a similar level. The lytic activity of other vaccines was not more than what is seen in the control group, also low tetramer frequency was induced by groups 1, 2, 3 and 4. These findings have interesting potential implications in the fields of cancer immunology and autoimmunity. Cell debris from dying cells or naturally occurring exosomes could be taken up by host APCs leading to self-antigen presentation, behaving like our empty VLPs loaded with antigens. During infection APCs that simultaneously take up bacteria or viral antigens may become activated in a similar way to those taken up VLPs packaged with CpGs in this project. Hence, in analogy this process may lead to specific T-cell response against self-antigens, causing autoimmunity. On the other hand, injecting VLPs packaged with CpGs intra-tumoural may be sufficient to induce anti-tumour immunity since local APCs may be charged with antigens derived from the tumour. Therefore, we believe that this novel method of delivering adjuvants and antigens in separate VLPs may be important and beneficial in several ways. First, when designing personalized VLP-based vaccines it may be helpful to have single adjuvanted VLPs which can be formulated with patient specific antigens bearing VLPs. Second, this method would allow to easily adjuvant VLPs that do not naturally carry DNA or RNA such as Influenza-derived VLPs, HPV or HBsAg VLPs.

5. Concluding remarks

Ideal therapeutic cancer vaccine should be patients' specific and use general technologies that are compatible with cGMP production. Yet at the same time it should be flexible enough to produce a personalized vaccine that will likely differ between every patient. Even though it might be possible to have a few off-the-shelf vaccines that are compatible with the idea of precision medicine, the true goal will be the generation of a different vaccine cocktail for each patient. Here we outlined such a procedure and demonstrated in mice that immunogenecity based on individual vaccine cocktails may be sufficiently potent and equivalent to using one of the strongest T-cell epitopes known in mice, the peptide p33 derived from Lymphocytic Choriomeningitis Virus (LCMV).

By combining immunopeptidomics, which reveals all peptides actually presented by a given tumour with whole exome sequencing which yields all mutations in the tumour, we were able to identify two sets of tumour vaccine epitopes. The germ-line epitopes generally associated with tumours and the mutated neo-epitopes that are specific for this very tumour only. *In silico* analysis and in-depth literature study allowed to identify a set of germ-line and neo-epitopes of potential value. To further prioritize the peptides, we used tumour-infiltrating cells (TILs) and stimulated them with the different peptides to identify epitopes with pre-existing immunity, which are usually considered to be more protective, in particular in the presence of check-point inhibitors (Gubin et al., 2014; Rizvi et al., 2015). The top 6 germ-line and the 2 best mutated neo-epitopes where then used to generate personalized multi-target VLP-based vaccines. To facilitate cGMP production, we used Cu-free Click

chemistry which is an efficient, safe and fast method for coupling epitopes to VLPs. Indeed, as we show, Cu-free Click chemistry is more efficient than the classical SMPH method. The bio-orthogonal chemistry does not have the ability to react with any components of the body and thus is preferable as it is completely non-toxic. Accordingly, it is not necessary to undergo elaborate processing to purify all uncoupled components away. Thereby supporting the approach of coupling selected peptides to VLPs at the bedside while remaining compliant with cGMP. By testing neoepitopes versus germline epitopes, we could demonstrate that both vaccine cocktails could induce protection against the aggressive, transplanted B16F10 melanoma murine model. Most interestingly, the combination of both vaccine cocktails resulted in optimal protection. That is to say, protection as good as that achieved with a maximally immunogenic model peptide p33. Protection not only resulted in radically smaller tumour, but also in changing the myeloid cell composition of the tumours rendering the local milieu more receptive to immune responses.

The choice of adjuvants and check-point inhibitors is key for the success of a potential cancer vaccine. It is known that blocking PD-1 is of limited efficiency in the B16 model. We have however found that depleting Tregs using anti-CD25 antibodies was highly efficacious in enhancing vaccine's induced protection. This is of high interest, as in humans, anti-CD25 antibodies have not been very efficacious so far. This may be explained by the fact that Daclizumab was developed as an immunosuppressant to allow organ-transplantation. Hence our data strongly support the re-evaluation of anti-CD25 antibodies as check-point inhibitors in humans.

There is only a very limited number of adjuvants available for use in humans and none of them are good at inducing cytotoxic T-cells in humans. Here we demonstrate that MCT, a biodegradable adjuvant that is already licensed for use in humans and has been used in millions of people, is a strong stimulator of killer cells in mice and clearly enhances vaccine immunogenecity. Thus, combining our personalized vaccine platform with MCT may lead to optimal clinical results. For these reasons, we are currently performing additional experiments to support entry in to clinical trials 2019/2020.

Finally, we have shown that adjuvants such as the potent immune-stimulators can be packaged in a separate VLPs and mixed with the other VLPs displaying the peptide of interest prior to injection *in vivo*. This modified novel method showed a similar immunogenecity to the standard method where the adjuvant and antigen are in close proximity (*i.e.* physically linked). This would be of high importance when designing a personalized VLP-based vaccine as it would be handy to have a ready adjuvanted VLP that can be easily formulated with the patient-specific vaccine at the bed-side.

Challenges in VLP-based vaccine

As the case in every vaccine platform development, there are several obstacles should be taken into account for the successful development of VLP-based vaccines. These obstacles or challenges can be divided into 1) challenges in VLP-platform technology and 2) challenges in individual VLP-based vaccine (Mohsen et al., 2018).

1) ***Challenges in VLP-platform technology***

- Despite the fact that several VLP-based vaccines are currently in the market "mainly prophylactic VLP-based vaccines", some recent ones are struggling with stability.
- So far, no VLP-based vaccine displaying foreign epitope has been successful in reaching the market. Hence, a real proof of concept for such vaccine is still missing.
- Most VLPs derived from RNA viruses do package RNA during assembly in host cells. Such obstacle may require additional Quality Control.
- Fusing epitopes into VLPs may create some issues concerning the assembly of VLPs.

2) ***Challenges in individual VLP-based vaccine***

- The selected, coupled antigen of interest or epitope may not confer protection.
- The induced immune response may be low.
- Selected indication may be attractive, nevertheless it may not attract the attention of end-users or industry.

6. References

(CDER), (2007). Commonly used efficacy endpoints in oncology clinical trials: advantages and limitations.

Abad, J. D., Wrzensinski, C., Overwijk, W., De Witte, M. A., Jorritsma, A., Hsu, C., Morgan, R. A. (2008). T-cell receptor gene therapy of established tumors in a murine melanoma model. *Journal of Immunotherapy, 31*(1), 1-6. doi:10.1097/CJI.0b013e31815c193f

Abbas, A. K., Lichtman, A. H., & Pillai, S. (2007). *Cellular and molecular immunology* (6th ed.). Philadelphia: Saunders Elsevier.

Ahi, Y. S., Bangari, D. S., & Mittal, S. K. (2011). Adenoviral vector immunity: its implications and circumvention strategies. *Curr Gene Ther, 11*(4), 307-320.

Akira, S., Uematsu, S., & Takeuchi, O. (2006). Pathogen recognition and innate immunity. *Cell, 124*(4), 783-801. doi:10.1016/j.cell.2006.02.015

Allan, R. S., Waithman, J., Bedoui, S., Jones, C. M., Villadangos, J. A., Zhan, Y., Carbone, F. R. (2006). Migratory dendritic cells transfer antigen to a lymph node-resident dendritic cell population for efficient CTL priming. *Immunity, 25*(1), 153-162. doi:10.1016/j.immuni.2006.04.017

Alsaab, H. O., Sau, S., Alzhrani, R., Tatiparti, K., Bhise, K., Kashaw, S. K., & Iyer, A. K. (2017). PD-1 and PD-L1 Checkpoint Signaling Inhibition for Cancer Immunotherapy: Mechanism, Combinations, and Clinical Outcome. *Front Pharmacol, 8*, 561. doi:10.3389/fphar.2017.00561

Ambuhl, P. M., Tissot, A. C., Fulurija, A., Maurer, P., Nussberger, J., Sabat, R., Bachmann, M. F. (2007). A vaccine for hypertension based on virus-like particles: preclinical efficacy and phase I safety and immunogenicity. *J Hypertens, 25*(1), 63-72. doi:10.1097/HJH.0b013e32800ff5d6

Ammi, R., De Waele, J., Willemen, Y., Van Brussel, I., Schrijvers, D. M., Lion, E., & Smits, E. L. (2015). Poly(I:C) as cancer vaccine adjuvant: knocking on the door of medical breakthroughs. *Pharmacol Ther, 146*, 120-131. doi:10.1016/j.pharmthera.2014.09.010

Andor, N., Graham, T. A., Jansen, M., Xia, L. C., Aktipis, C. A., Petritsch, C., Maley, C. C. (2016). Pan-cancer analysis of the extent and consequences of intratumor heterogeneity. *Nat Med, 22*(1), 105-113. doi:10.1038/nm.3984

Assessment of adenoviral vector safety and toxicity: report of the National Institutes of Health Recombinant DNA Advisory Committee. (2002). *Hum Gene Ther, 13*(1), 3-13. doi:10.1089/10430340152712629

Aurisicchio, L., & Ciliberto, G. (2012). Genetic cancer vaccines: current status and perspectives. *Expert Opin Biol Ther, 12*(8), 1043-1058. doi:10.1517/14712598.2012.689279

Australia, M. I. (2018). Stages of melanoma. Retrieved from https://www.melanoma.org.au/understanding-melanoma/stages-of-melanoma/

Bachmann, M. F., & Jennings, G. T. (2010). Vaccine delivery: a matter of size, geometry, kinetics and molecular patterns. *Nat Rev Immunol, 10*(11), 787-796. doi:10.1038/nri2868

Bachmann, M. F., Oxenius, A., Pircher, H., Hengartner, H., Ashton-Richardt, P. A., Tonegawa, S., & Zinkernagel, R. M. (1995). TAP1-independent loading of class I molecules by exogenous viral proteins. *Eur J Immunol, 25*(6), 1739-1743. doi:10.1002/eji.1830250637

Bachmann, M. F., Zeltins, A., Kalnins, G., Balke, I., Fischer, N., Rostaher, A., Favrot, C. (2018). Vaccination against IL-31 for the treatment of atopic dermatitis in dogs. *J Allergy Clin Immunol*. doi:10.1016/j.jaci.2017.12.994

Bakker, A. B. H., Schreurs, M. W. J., Deboer, A. J., Kawakami, Y., Rosenberg, S. A., Adema, G. J., & Figdor, C. G. (1994). Melanocyte Lineage-Specific Antigen Gp100 Is Recognized by Melanoma-Derived Tumor-Infiltrating Lymphocytes. *Journal of Experimental Medicine, 179*(3), 1005-1009. doi:DOI 10.1084/jem.179.3.1005

Ball, N. J., Yohn, J. J., Morelli, J. G., Norris, D. A., Golitz, L. E., & Hoeffler, J. P. (1994). Ras mutations in human melanoma: a marker of malignant progression. *J Invest Dermatol, 102*(3), 285-290.

Baluk, P., Fuxe, J., Hashizume, H., Romano, T., Lashnits, E., Butz, S., McDonald, D. M. (2007). Functionally specialized junctions between endothelial cells of lymphatic vessels. *J Exp Med, 204*(10), 2349-2362. doi:10.1084/jem.20062596

Banchereau, J., & Palucka, A. K. (2005). Dendritic cells as therapeutic vaccines against cancer. *Nat Rev Immunol, 5*(4), 296-306. doi:10.1038/nri1592

Banchereau, J., Palucka, A. K., Dhodapkar, M., Burkeholder, S., Taquet, N., Rolland, A., Fay, J. (2001). Immune and clinical responses in patients with metastatic melanoma to CD34(+) progenitor-derived dendritic cell vaccine. *Cancer Res, 61*(17), 6451-6458.

Baskin, J. M., Prescher, J. A., Laughlin, S. T., Agard, N. J., Chang, P. V., Miller, I. A., Bertozzi, C. R. (2007). Copper-free click chemistry for dynamic in vivo imaging. *Proc Natl Acad Sci U S A, 104*(43), 16793-16797. doi:10.1073/pnas.0707090104

Bassani-Sternberg, M., & Coukos, G. (2016). Mass spectrometry-based antigen discovery for cancer immunotherapy. *Curr Opin Immunol, 41*, 9-17. doi:10.1016/j.coi.2016.04.005

Bauer, S., Kirschning, C. J., Hacker, H., Redecke, V., Hausmann, S., Akira, S., Lipford, G. B. (2001). Human TLR9 confers responsiveness to bacterial DNA via species-specific CpG motif recognition. *Proc Natl Acad Sci U S A, 98*(16), 9237-9242. doi:10.1073/pnas.161293498

Baumgaertner, P., Costa Nunes, C., Cachot, A., Maby-El Hajjami, H., Cagnon, L., Braun, M., Jandus, C. (2016). Vaccination of stage III/IV melanoma patients with long NY-ESO-1 peptide and CpG-B elicits robust CD8(+) and CD4(+) T-cell responses with multiple specificities including a novel DR7-restricted epitope. *Oncoimmunology, 5*(10), e1216290. doi:10.1080/2162402X.2016.1216290

Beadling, C., Jacobson-Dunlop, E., Hodi, F. S., Le, C., Warrick, A., Patterson, J., Corless, C. L. (2008). KIT gene mutations and copy number in melanoma subtypes. *Clin Cancer Res, 14*(21), 6821-6828. doi:10.1158/1078-0432.CCR-08-0575

Berger, M., Kreutz, F. T., Horst, J. L., Baldi, A. C., & Koff, W. J. (2007). Phase I study with an autologous tumor cell vaccine for locally advanced or metastatic prostate cancer. *J Pharm Pharm Sci, 10*(2), 144-152.

Bessa, J., Jegerlehner, A., Hinton, H. J., Pumpens, P., Saudan, P., Schneider, P., & Bachmann, M. F. (2009). Alveolar macrophages and lung dendritic cells sense RNA and drive mucosal IgA responses. *Journal of Immunology, 183*(6), 3788-3799. doi:10.4049/jimmunol.0804004

Blair, D. A., Turner, D. L., Bose, T. O., Pham, Q. M., Bouchard, K. R., Williams, K. J., Lefrancois, L. (2011). Duration of antigen availability influences the expansion and memory differentiation of T cells. *Journal of Immunology, 187*(5), 2310-2321. doi:10.4049/jimmunol.1100363

Bloom, M. B., PerryLalley, D., Robbins, P. F., Li, Y., ElGamil, M., Rosenberg, S. A., & Yang, J. C. (1997). Identification of tyrosinase-related protein 2 as a tumor rejection antigen for the B16 melanoma. *Journal of Experimental Medicine, 185*(3), 453-459. doi:DOI 10.1084/jem.185.3.453

Bode, C., Zhao, G., Steinhagen, F., Kinjo, T., & Klinman, D. M. (2011). CpG DNA as a vaccine adjuvant. *Expert Review of Vaccines, 10*(4), 499-511. doi:10.1586/Erv.10.174

Boscacci, R. T., Pfeiffer, F., Gollmer, K., Sevilla, A. I., Martin, A. M., Soriano, S. F., Stein, J. V. (2010). Comprehensive analysis of lymph node stroma-expressed Ig superfamily members reveals redundant and nonredundant roles for ICAM-1, ICAM-2, and VCAM-1 in lymphocyte homing. *Blood, 116*(6), 915-925. doi:10.1182/blood-2009-11-254334

Bowne, W. B., Srinivasan, R., Wolchok, J. D., Hawkins, W. G., Blachere, N. E., Dyall, R., Houghton, A. N. (1999). Coupling and uncoupling of tumor immunity and autoimmunity. *J Exp Med, 190*(11), 1717-1722.

Brahmer, J. R., Tykodi, S. S., Chow, L. Q., Hwu, W. J., Topalian, S. L., Hwu, P., Wigginton, J. M. (2012). Safety and activity of anti-PD-L1 antibody in patients with advanced cancer. *N Engl J Med, 366*(26), 2455-2465. doi:10.1056/NEJMoa1200694

Braun, M., Jandus, C., Maurer, P., Hammann-Haenni, A., Schwarz, K., Bachmann, M. F., Romero, P. (2012). Virus-like particles induce robust human T-helper cell responses. *Eur J Immunol, 42*(2), 330-340. doi:10.1002/eji.201142064

Brewer, K. D., Weir, G. M., Dude, I., Davis, C., Parsons, C., Penwell, A., Stanford, M. M. (2018). Unique depot formed by an oil based vaccine facilitates active antigen uptake and provides effective tumour control. *J Biomed Sci, 25*(1), 7. doi:10.1186/s12929-018-0413-9

Brinkman, M., Walter, J., Grein, S., Thies, M. J., Schulz, T. W., Herrmann, M., Hess, J. (2005). Beneficial therapeutic effects with different particulate structures of murine polyomavirus VP1-coat protein carrying self or non-self CD8 T cell epitopes against murine melanoma. *Cancer Immunol Immunother, 54*(6), 611-622. doi:10.1007/s00262-004-0655-0

Bronte, V., Brandau, S., Chen, S. H., Colombo, M. P., Frey, A. B., Greten, T. F., Gabrilovich, D. I. (2016). Recommendations for myeloid-derived suppressor cell nomenclature and characterization standards. *Nat Commun, 7*, 12150. doi:10.1038/ncomms12150

Brown, A. D., Naves, L., Wang, X., Ghodssi, R., & Culver, J. N. (2013). Carboxylate-directed in vivo assembly of virus-like nanorods and tubes for the display of functional peptides and residues. *Biomacromolecules, 14*(9), 3123-3129. doi:10.1021/bm400747k

Brown, S. D., Fiedler, J. D., & Finn, M. G. (2009). Assembly of hybrid bacteriophage Qbeta virus-like particles. *Biochemistry, 48*(47), 11155-11157. doi:10.1021/bi901306p

Brune, K. D., Leneghan, D. B., Brian, I. J., Ishizuka, A. S., Bachmann, M. F., Draper, S. J., Howarth, M. (2016). Plug-and-Display: decoration of Virus-Like Particles via isopeptide bonds for modular immunization. *Sci Rep, 6*, 19234. doi:10.1038/srep19234

Cabral-Miranda, G., Heath, M. D., Gomes, A. C., Mohsen, M. O., Montoya-Diaz, E., Salman, A. M., Bachmann, M. F. (2017). Microcrystalline Tyrosine (MCT((R))): A Depot Adjuvant in Licensed Allergy Immunotherapy Offers New Opportunities in Malaria. *Vaccines (Basel), 5*(4). doi:10.3390/vaccines5040032

Cabral-Miranda, G., Heath, M. D., Mohsen, M. O., Gomes, A. C., Engeroff, P., Flaxman, A., Bachmann, M. F. (2017). Virus-Like Particle (VLP) Plus Microcrystalline Tyrosine (MCT) Adjuvants Enhance Vaccine Efficacy Improving T and B Cell Immunogenicity and Protection against Plasmodium berghei/vivax. *Vaccines (Basel), 5*(2). doi:10.3390/vaccines5020010

Cancer Genome Atlas, N. (2015). Genomic Classification of Cutaneous Melanoma. *Cell, 161*(7), 1681-1696. doi:10.1016/j.cell.2015.05.044

cancer, I. A. f. R. o. (2012). GLOBOCAN 2012: Estimated Cancer Incidence, Mortality and Prevalence Worldwide in 2012.

Caron, E., Aebersold, R., Banaei-Esfahani, A., Chong, C., & Bassani-Sternberg, M. (2017). A Case for a Human Immuno-Peptidome Project Consortium. *Immunity, 47*(2), 203-208. doi:10.1016/j.immuni.2017.07.010

Carralot, J. P., Weide, B., Schoor, O., Probst, J., Scheel, B., Teufel, R., Pascolo, S. (2005). Production and characterization of amplified tumor-derived cRNA libraries to be used as vaccines against metastatic melanomas. *Genet Vaccines Ther, 3*, 6. doi:10.1186/1479-0556-3-6

Castle, J. C., Kreiter, S., Diekmann, J., Lower, M., van de Roemer, N., de Graaf, J., Sahin, U. (2012). Exploiting the mutanome for tumor vaccination. *Cancer Res, 72*(5), 1081-1091. doi:10.1158/0008-5472.CAN-11-3722

Cavelti-Weder, C., Timper, K., Seelig, E., Keller, C., Osranek, M., Lassing, U., Bachmann, M. F. (2016). Development of an Interleukin-1beta Vaccine in Patients with Type 2 Diabetes. *Mol Ther, 24*(5), 1003-1012. doi:10.1038/mt.2015.227

Chae, Y. K., Arya, A., Iams, W., Cruz, M. R., Chandra, S., Choi, J., & Giles, F. (2018). Current landscape and future of dual anti-CTLA4 and PD-1/PD-L1 blockade immunotherapy in cancer; lessons learned from clinical trials with melanoma and non-small cell lung cancer (NSCLC). *J Immunother Cancer, 6*(1), 39. doi:10.1186/s40425-018-0349-3

Chang, P. V., Prescher, J. A., Sletten, E. M., Baskin, J. M., Miller, I. A., Agard, N. J., Bertozzi, C. R. (2010). Copper-free click chemistry in living animals. *Proc Natl Acad Sci U S A, 107*(5), 1821-1826. doi:10.1073/pnas.0911116107

Chapman, P. B., Hauschild, A., Robert, C., Haanen, J. B., Ascierto, P., Larkin, J., Group, B.-S. (2011). Improved survival with vemurafenib in melanoma with BRAF V600E mutation. *N Engl J Med, 364*(26), 2507-2516. doi:10.1056/NEJMoa1103782

Chatterji, A., Ochoa, W., Shamieh, L., Salakian, S. P., Wong, S. M., Clinton, G., Johnson, J. E. (2004). Chemical conjugation of heterologous proteins on the surface of Cowpea mosaic virus. *Bioconjug Chem, 15*(4), 807-813. doi:10.1021/bc0402888

Chen, D. S., & Mellman, I. (2013). Oncology meets immunology: the cancer-immunity cycle. *Immunity, 39*(1), 1-10. doi:10.1016/j.immuni.2013.07.012

Chen, L., & Flies, D. B. (2013). Molecular mechanisms of T cell co-stimulation and co-inhibition. *Nat Rev Immunol, 13*(4), 227-242. doi:10.1038/nri3405

Chen, P., Huang, Y., Bong, R., Ding, Y., Song, N., Wang, X., Luo, Y. (2011). Tumor-associated macrophages promote angiogenesis and melanoma growth via adrenomedullin in a paracrine and autocrine manner. *Clin Cancer Res, 17*(23), 7230-7239. doi:10.1158/1078-0432.CCR-11-1354

Chen, P., Liu, X., Sun, Y., Zhou, P., Wang, Y., & Zhang, Y. (2016). Dendritic cell targeted vaccines: Recent progresses and challenges. *Hum Vaccin Immunother, 12*(3), 612-622. doi:10.1080/21645515.2015.1105415

Chen, Q., & Lai, H. (2013). Plant-derived virus-like particles as vaccines. *Hum Vaccin Immunother, 9*(1), 26-49. doi:10.4161/hv.22218

Chen, Y. J., Chalouni, C., Tan, C., Clark, R., Venook, R., Ohri, R., Polakis, P. (2012). The Melanosomal Protein PMEL17 as a Target for Antibody Drug Conjugate Therapy in Melanoma. *Journal of Biological Chemistry, 287*(29), 24082-24091. doi:10.1074/jbc.M112.361485

Cherobin, A., Wainstein, A. J. A., Colosimo, E. A., Goulart, E. M. A., & Bittencourt, F. V. (2018). Prognostic factors for metastasis in cutaneous melanoma. *An Bras Dermatol, 93*(1), 19-26. doi:10.1590/abd1806-4841.20184779

Chiocca, E. A., & Rabkin, S. D. (2014). Oncolytic viruses and their application to cancer immunotherapy. *Cancer Immunol Res, 2*(4), 295-300. doi:10.1158/2326-6066.CIR-14-0015

Christensen, J., Litherland, K., Faller, T., van de Kerkhof, E., Natt, F., Hunziker, J., Swart, P. (2014). Biodistribution and metabolism studies of lipid nanoparticle-formulated internally [3H]-labeled siRNA in mice. *Drug Metab Dispos, 42*(3), 431-440. doi:10.1124/dmd.113.055434

Chu, R. S., Targoni, O. S., Krieg, A. M., Lehmann, P. V., & Harding, C. V. (1997). CpG oligodeoxynucleotides act as adjuvants that switch on T helper 1 (Th1) immunity. *J Exp Med, 186*(10), 1623-1631.

Chu, W., Pak, B. J., Bani, M. R., Kapoor, M., Lu, S. J., Tamir, A., Ben-David, Y. (2000). Tyrosinase-related protein 2 as a mediator of melanoma specific resistance to cis-diamminedichloroplatinum(II): therapeutic implications. *Oncogene, 19*(3), 395-402. doi:DOI 10.1038/sj.onc.1203315

Cielens, I., Ose, V., Petrovskis, I., Strelnikova, A., Renhofa, R., Kozlovska, T., & Pumpens, P. (2000). Mutilation of RNA phage Qbeta virus-like particles: from icosahedrons to rods. *FEBS Lett, 482*(3), 261-264.

Comellas-Aragones, M., de la Escosura, A., Dirks, A. J., van der Ham, A., Fuste-Cune, A., Cornelissen, J. J. L. M., & Nolte, R. J. M. (2009). Controlled Integration of Polymers into Viral Capsids. *Biomacromolecules, 10*(11), 3141-3147. doi:10.1021/bm9007953

Conway, J. F., Watts, N. R., Belnap, D. M., Cheng, N., Stahl, S. J., Wingfield, P. T., & Steven, A. C. (2003). Characterization of a conformational epitope on hepatitis B virus core antigen and quasiequivalent variations in antibody binding. *J Virol, 77*(11), 6466-6473.

Cortes-Perez, N. G., Kharrat, P., Langella, P., & Bermudez-Humaran, L. G. (2009). Heterologous production of human papillomavirus type-16 L1 protein by a lactic acid bacterium. *BMC Res Notes, 2*, 167. doi:10.1186/1756-0500-2-167

Cox, J. C., & Coulter, A. R. (1997). Adjuvants - A classification and review of their modes of action. *Vaccine, 15*(3), 248-256. doi:Doi 10.1016/S0264-410x(96)00183-1

Crick, F. H., & Watson, J. D. (1956). Structure of small viruses. *Nature, 177*(4506), 473-475.

Crowther, R. A., Kiselev, N. A., Bottcher, B., Berriman, J. A., Borisova, G. P., Ose, V., & Pumpens, P. (1994). Three-dimensional structure of hepatitis B virus core particles determined by electron cryomicroscopy. *Cell, 77*(6), 943-950.

Cubas, R., Zhang, S., Li, M., Chen, C., & Yao, Q. (2011). Chimeric Trop2 virus-like particles: a potential immunotherapeutic approach against pancreatic cancer. *J Immunother, 34*(3), 251-263. doi:10.1097/CJI.0b013e318209ee72

Curtin, J. A., Fridlyand, J., Kageshita, T., Patel, H. N., Busam, K. J., Kutzner, H., Bastian, B. C. (2005). Distinct sets of genetic alterations in melanoma. *N Engl J Med, 353*(20), 2135-2147. doi:10.1056/NEJMoa050092

D'Aloia, M. M., Zizzari, I. G., Sacchetti, B., Pierelli, L., & Alimandi, M. (2018). CAR-T cells: the long and winding road to solid tumors. *Cell Death Dis, 9*(3), 282. doi:10.1038/s41419-018-0278-6

Davies, H., Bignell, G. R., Cox, C., Stephens, P., Edkins, S., Clegg, S., Futreal, P. A. (2002). Mutations of the BRAF gene in human cancer. *Nature, 417*(6892), 949-954. doi:10.1038/nature00766

Desmet, C., Lurquin, C., Vanderbruggen, P., Deplaen, E., Brasseur, F., & Boon, T. (1994). Sequence and Expression Pattern of the Human Mage2 Gene. *Immunogenetics, 39*(2), 121-129. doi:Doi 10.1007/Bf00188615

Dick, J. E. (2008). Stem cell concepts renew cancer research. *Blood, 112*(13), 4793-4807. doi:10.1182/blood-2008-08-077941

Dilthey, A. T., Gourraud, P. A., Mentzer, A. J., Cereb, N., Iqbal, Z., & McVean, G. (2016). High-Accuracy HLA Type Inference from Whole-Genome Sequencing Data Using Population Reference Graphs. *PLoS Comput Biol, 12*(10), e1005151. doi:10.1371/journal.pcbi.1005151

Ding, F. X., Wang, F., Lu, Y. M., Li, K., Wang, K. H., He, X. W., & Sun, S. H. (2009). Multiepitope peptide-loaded virus-like particles as a vaccine against hepatitis B virus-related hepatocellular carcinoma. *Hepatology, 49*(5), 1492-1502. doi:10.1002/hep.22816

Donaldson, B., Al-Barwani, F., Pelham, S. J., Young, K., Ward, V. K., & Young, S. L. (2017). Multi-target chimaeric VLP as a therapeutic vaccine in a model of colorectal cancer. *J Immunother Cancer, 5*(1), 69. doi:10.1186/s40425-017-0270-1

Dudziak, D., Kamphorst, A. O., Heidkamp, G. F., Buchholz, V. R., Trumpfheller, C., Yamazaki, S., Nussenzweig, M. C. (2007).

Differential antigen processing by dendritic cell subsets in vivo. *Science, 315*(5808), 107-111. doi:10.1126/science.1136080

Eckl-Dorna, J., & Batista, F. D. (2009). BCR-mediated uptake of antigen linked to TLR9 ligand stimulates B-cell proliferation and antigen-specific plasma cell formation. *Blood, 113*(17), 3969-3977. doi:10.1182/blood-2008-10-185421

Eggermont, A. M., & Robert, C. (2011). New drugs in melanoma: it's a whole new world. *Eur J Cancer, 47*(14), 2150-2157. doi:10.1016/j.ejca.2011.06.052

Eisenbarth, S. C., Colegio, O. R., O'Connor, W., Sutterwala, F. S., & Flavell, R. A. (2008). Crucial role for the Nalp3 inflammasome in the immunostimulatory properties of aluminium adjuvants. *Nature, 453*(7198), 1122-1126. doi:10.1038/nature06939

Emery, C. M., Vijayendran, K. G., Zipser, M. C., Sawyer, A. M., Niu, L., Kim, J. J., . . . Garraway, L. A. (2009). MEK1 mutations confer resistance to MEK and B-RAF inhibition. *Proc Natl Acad Sci U S A, 106*(48), 20411-20416. doi:10.1073/pnas.0905833106

Espuelas, S., Roth, A., Thumann, C., Frisch, B., & Schuber, F. (2005). Effect of synthetic lipopeptides formulated in liposomes on the maturation of human dendritic cells. *Mol Immunol, 42*(6), 721-729. doi:10.1016/j.molimm.2004.09.022

Fang, P. Y., Gomez Ramos, L. M., Holguin, S. Y., Hsiao, C., Bowman, J. C., Yang, H. W., & Williams, L. D. (2017). Functional RNAs: combined assembly and packaging in VLPs. *Nucleic Acids Res, 45*(6), 3519-3527. doi:10.1093/nar/gkw1154

Faridi, P., Purcell A. W., Croft, N. P. (2018). In Immunopeptidomics We Need a Sniper Instead of a Shotgun. *Proteomics, 18*(12). doi:doi.org/10.1002/pmic.201700464

Fesnak, A. D., June, C. H., & Levine, B. L. (2016). Engineered T cells: the promise and challenges of cancer immunotherapy. *Nature Reviews Cancer, 16*(9), 566-581. doi:10.1038/nrc.2016.97

Fettelschoss-Gabriel, A., Fettelschoss, V., Thoms, F., Giese, C., Daniel, M., Olomski, F., Bachmann, M. F. (2018). Treating insect-bite hypersensitivity in horses with active vaccination against IL-5. *J Allergy Clin Immunol*. doi:10.1016/j.jaci.2018.01.041

Fifis, T., Gamvrellis, A., Crimeen-Irwin, B., Pietersz, G. A., Li, J., Mottram, P. L., Plebanski, M. (2004). Size-dependent immunogenicity: therapeutic and protective properties of nano-vaccines against tumors. *J Immunol, 173*(5), 3148-3154.

Forsea, A. M., Del Marmol, V., de Vries, E., Bailey, E. E., & Geller, A. C. (2012). Melanoma incidence and mortality in Europe: new estimates, persistent disparities. *Br J Dermatol, 167*(5), 1124-1130. doi:10.1111/j.1365-2133.2012.11125.x

Fotin-Mleczek, M., Zanzinger, K., Heidenreich, R., Lorenz, C., Thess, A., Duchardt, K. M., & Kallen, K. J. (2012). Highly potent mRNA based cancer vaccines represent an attractive platform for combination therapies supporting an improved therapeutic effect. *J Gene Med, 14*(6), 428-439. doi:10.1002/jgm.2605

Fritsch, E. F., Hacohen, N., & Wu, C. J. (2014). Personal neoantigen cancer vaccines: The momentum builds. *Oncoimmunology, 3*, e29311. doi:10.4161/onci.29311

Fritsch, E. F., Rajasagi, M., Ott, P. A., Brusic, V., Hacohen, N., & Wu, C. J. (2014). HLA-binding properties of tumor neoepitopes in humans. *Cancer Immunol Res, 2*(6), 522-529. doi:10.1158/2326-6066.CIR-13-0227

Gabrilovich, D. I. (2017). Myeloid-Derived Suppressor Cells. *Cancer Immunol Res, 5*(1), 3-8. doi:10.1158/2326-6066.CIR-16-0297

Gabrilovich, D. I., Ostrand-Rosenberg, S., & Bronte, V. (2012). Coordinated regulation of myeloid cells by tumours. *Nat Rev Immunol, 12*(4), 253-268. doi:10.1038/nri3175

Gajewski, T. F. (2007). Failure at the effector phase: Immune barriers at the level of the melanoma tumor microenvironment. *Clinical Cancer Research, 13*(18), 5256-5261. doi:10.1158/1078-0432.Ccr-07-0892

Gavin, A. L., Hoebe, K., Duong, B., Ota, T., Martin, C., Beutler, B., & Nemazee, D. (2006). Adjuvant-enhanced antibody responses in the absence of toll-like receptor signaling. *Science, 314*(5807), 1936-1938. doi:10.1126/science.1135299

Geoerger, B., Bergeron, C., Gore, L., Sender, L., Dunkel, I. J., Herzog, C., Pappo, A. (2017). Phase II study of ipilimumab in adolescents with unresectable stage III or IV malignant melanoma. *Eur J Cancer, 86*, 358-363. doi:10.1016/j.ejca.2017.09.032

Gide, T. N., Wilmott, J. S., Scolyer, R. A., & Long, G. V. (2018). Primary and Acquired Resistance to Immune Checkpoint Inhibitors in Metastatic Melanoma. *Clin Cancer Res, 24*(6), 1260-1270. doi:10.1158/1078-0432.CCR-17-2267

Gilkeson, G. S., Ruiz, P., Howell, D., Lefkowith, J. B., & Pisetsky, D. S. (1993). Induction of immune-mediated glomerulonephritis in normal mice immunized with bacterial DNA. *Clin Immunol Immunopathol, 68*(3), 283-292.

Gold, J. S., Ferrone, C. R., Guevara-Patino, J. A., Hawkins, W. G., Dyall, R., Engelhorn, M. E., Houghton, A. N. (2003). A single heteroclitic epitope determines cancer immunity after xenogeneic DNA immunization against a tumor differentiation antigen. *J Immunol, 170*(10), 5188-5194.

Goldinger, S. M., Dummer, R., Baumgaertner, P., Mihic-Probst, D., Schwarz, K., Hammann-Haenni, A., Speiser, D. E. (2012). Nano-particle vaccination combined with TLR-7 and -9 ligands triggers memory and effector CD8(+) T-cell responses in melanoma patients. *Eur J Immunol, 42*(11), 3049-3061. doi:10.1002/eji.201142361

Goldstein, A. M., & Tucker, M. A. (2013). Dysplastic nevi and melanoma. *Cancer Epidemiol Biomarkers Prev, 22*(4), 528-532. doi:10.1158/1055-9965.EPI-12-1346

Gomes, A. C., Flace, A., Saudan, P., Zabel, F., Cabral-Miranda, G., Turabi, A. E., Bachmann, M. F. (2017). Adjusted Particle Size Eliminates the Need of Linkage of Antigen and Adjuvants for Appropriated T Cell Responses in Virus-Like Particle-Based Vaccines. *Front Immunol, 8*, 226. doi:10.3389/fimmu.2017.00226

Gomes, A. C., Mohsen, M., & Bachmann, M. F. (2017). Harnessing Nanoparticles for Immunomodulation and Vaccines. *Vaccines (Basel), 5*(1). doi:10.3390/vaccines5010006

Gong, J., Chehrazi-Raffle, A., Reddi, S., & Salgia, R. (2018). Development of PD-1 and PD-L1 inhibitors as a form of cancer immunotherapy: a comprehensive review of registration trials and future considerations. *Journal for Immunotherapy of Cancer, 6*. doi:ARTN 8

10.1186/s40425-018-0316-z

Grabstald, H. (1965). Unproved Methods of Cancer Treatment: Coley's Mixed Toxins. *CA Cancer J Clin, 15*, 139-140.

Greenwald, R. J., Freeman, G. J., & Sharpe, A. H. (2005). The B7 family revisited. *Annu Rev Immunol, 23*, 515-548. doi:10.1146/annurev.immunol.23.021704.115611

Gubin, M. M., Zhang, X., Schuster, H., Caron, E., Ward, J. P., Noguchi, T., Schreiber, R. D. (2014). Checkpoint blockade cancer immunotherapy targets tumour-specific mutant antigens. *Nature, 515*(7528), 577-581. doi:10.1038/nature13988

Guermonprez, P., Valladeau, J., Zitvogel, L., Thery, C., & Amigorena, S. (2002). Antigen presentation and T cell stimulation by dendritic cells. *Annu Rev Immunol, 20*, 621-667. doi:10.1146/annurev.immunol.20.100301.064828

Guo, C., Manjili, M. H., Subjeck, J. R., Sarkar, D., Fisher, P. B., & Wang, X. Y. (2013). Therapeutic cancer vaccines: past, present, and future. *Adv Cancer Res, 119*, 421-475. doi:10.1016/B978-0-12-407190-2.00007-1

Gupta, P. B., Kuperwasser, C., Brunet, J. P., Ramaswamy, S., Kuo, W. L., Gray, J. W., Weinberg, R. A. (2005). The melanocyte differentiation program predisposes to metastasis after neoplastic transformation. *Nat Genet, 37*(10), 1047-1054. doi:10.1038/ng1634

Hacohen, N., Fritsch, E. F., Carter, T. A., Lander, E. S., & Wu, C. J. (2013). Getting personal with neoantigen-based therapeutic cancer vaccines. *Cancer Immunol Res, 1*(1), 11-15. doi:10.1158/2326-6066.CIR-13-0022

Hailemichael, Y., Dai, Z. M., Jaffarzad, N., Ye, Y., Medina, M. A., Huang, X. F., Overwijk, W. W. (2013). Persistent antigen at vaccination sites induces tumor-specific CD8(+) T cell sequestration, dysfunction and deletion. *Nature Medicine, 19*(4), 465-+. doi:10.1038/nm.3105

Hamid, O., Robert, C., Daud, A., Hodi, F. S., Hwu, W. J., Kefford, R., Ribas, A. (2013). Safety and tumor responses with lambrolizumab (anti-PD-1) in melanoma. *N Engl J Med, 369*(2), 134-144. doi:10.1056/NEJMoa1305133

Hamid, O., Sosman, J. A., Lawrence, D. P., Sullivan, R. J. I., N., Kluger, H. M., Boasberg, P. D., Hodi, S. (2013). Clinical activity, safety, and biomarkers of MPDL3280A, an engineered PD-L1 antibody in patients with locally advanced or metastatic melanoma (mM). *Journal of Clinical Oncology, 31*, 9010-9010.

Handolias, D., Salemi, R., Murray, W., Tan, A., Liu, W., Viros, A., McArthur, G. A. (2010). Mutations in KIT occur at low frequency in melanomas arising from anatomical sites associated with chronic and intermittent sun exposure. *Pigment Cell Melanoma Res, 23*(2), 210-215. doi:10.1111/j.1755-148X.2010.00671.x

Hanna, M. G., Jr., & Peters, L. C. (1978). Specific immunotherapy of established visceral micrometastases by BCG-tumor cell vaccine alone or as an adjunct to surgery. *Cancer, 42*(6), 2613-2625.

Harland, M., Cust, A. E., Badenas, C., Chang, Y. M., Holland, E. A., Aguilera, P., Puig, S. (2014). Prevalence and predictors of germline CDKN2A mutations for melanoma cases from Australia, Spain and the United Kingdom. *Hered Cancer Clin Pract, 12*(1), 20. doi:10.1186/1897-4287-12-20

Hartmann, G., Weiner, G. J., & Krieg, A. M. (1999). CpG DNA: a potent signal for growth, activation, and maturation of human dendritic cells. *Proc Natl Acad Sci U S A, 96*(16), 9305-9310.

Hawkins, W. G., Gold, J. S., Dyall, R., Wolchok, J. D., Hoos, A., Bowne, W. B., Lewis, J. J. (2000). Immunization with DNA coding for gp100 results in CD4 T-cell independent antitumor immunity. *Surgery, 128*(2), 273-280. doi:10.1067/msy.2000.107421

Hayward, N. K. (2003). Genetics of melanoma predisposition. *Oncogene, 22*(20), 3053-3062. doi:10.1038/sj.onc.1206445

Heath, M. D., Swan, N. J., Marriott, A. C., Silman, N. J., Hallis, B., Prevosto, C., Skinner, M. A. (2017). Comparison of a novel microcrystalline tyrosine adjuvant with aluminium hydroxide for enhancing vaccination against seasonal influenza. *BMC Infect Dis, 17*(1), 232. doi:10.1186/s12879-017-2329-5

Hemmi, H., Takeuchi, O., Kawai, T., Kaisho, T., Sato, S., Sanjo, H., Akira, S. (2000). A Toll-like receptor recognizes bacterial DNA. *Nature, 408*(6813), 740-745. doi:10.1038/35047123

Hershkovitz, L., Schachter, J., Treves, A. J., & Besser, M. J. (2010). Focus on adoptive T cell transfer trials in melanoma. *Clin Dev Immunol, 2010*, 260267. doi:10.1155/2010/260267

Higgins, D., Marshall, J. D., Traquina, P., Van Nest, G., & Livingston, B. D. (2007). Immunostimulatory DNA as a vaccine adjuvant. *Expert Rev Vaccines, 6*(5), 747-759. doi:10.1586/14760584.6.5.747

Hodge, J. W., Chakraborty, M., Kudo-Saito, C., Garnett, C. T., & Schlom, J. (2005). Multiple costimulatory modalities enhance CTL avidity. *J Immunol, 174*(10), 5994-6004.

Hodi, F. S., Butler, M., Oble, D. A., Seiden, M. V., Haluska, F. G., Kruse, A., Dranoff, G. (2008). Immunologic and clinical effects of antibody blockade of cytotoxic T lymphocyte-associated antigen 4 in previously vaccinated cancer patients. *Proc Natl Acad Sci U S A, 105*(8), 3005-3010. doi:10.1073/pnas.0712237105

Hodi, F. S., O'Day, S. J., McDermott, D. F., Weber, R. W., Sosman, J. A., Haanen, J. B., Urba, W. J. (2010). Improved survival with ipilimumab in patients with metastatic melanoma. *N Engl J Med, 363*(8), 711-723. doi:10.1056/NEJMoa1003466

Hodis, E., Watson, I. R., Kryukov, G. V., Arold, S. T., Imielinski, M., Theurillat, J. P., Chin, L. (2012). A landscape of driver mutations in melanoma. *Cell, 150*(2), 251-263. doi:10.1016/j.cell.2012.06.024

Hofmann, K. J., Cook, J. C., Joyce, J. G., Brown, D. R., Schultz, L. D., George, H. A., Jansen, K. U. (1995). Sequence determination of human papillomavirus type 6a and assembly of virus-like particles in

Saccharomyces cerevisiae. *Virology, 209*(2), 506-518. doi:10.1006/viro.1995.1283

Hofmann, O., Caballero, O. L., Stevenson, B. J., Chen, Y. T., Cohen, T., Chua, R., Hide, W. (2008). Genome-wide analysis of cancer/testis gene expression. *Proc Natl Acad Sci U S A, 105*(51), 20422-20427. doi:10.1073/pnas.0810777105

Hogenesch, H. (2012). Mechanism of immunopotentiation and safety of aluminum adjuvants. *Front Immunol, 3*, 406. doi:10.3389/fimmu.2012.00406

Hornung, V., Rothenfusser, S., Britsch, S., Krug, A., Jahrsdorfer, B., Giese, T., Hartmann, G. (2002). Quantitative expression of Toll-like receptor 1-10 mRNA in cellular subsets of human peripheral blood mononuclear cells and sensitivity to CpG oligodeoxynucleotides. *Journal of Immunology, 168*(9), 4531-4537.

Hu, Z., Ott, P. A., & Wu, C. J. (2017). Towards personalized, tumour-specific, therapeutic vaccines for cancer. *Nat Rev Immunol*. doi:10.1038/nri.2017.131

Hu, Z., Ott, P. A., & Wu, C. J. (2018). Towards personalized, tumour-specific, therapeutic vaccines for cancer. *Nat Rev Immunol, 18*(3), 168-182. doi:10.1038/nri.2017.131

Huang, M., Shen, A., Ding, J., & Geng, M. (2014). Molecularly targeted cancer therapy: some lessons from the past decade. *Trends Pharmacol Sci, 35*(1), 41-50. doi:10.1016/j.tips.2013.11.004

Humphrey, L. J., Boehm, B., Jewell, W. R., & Boehm, O. R. (1972). Immunologic response of cancer patients modified by immunization with tumor vaccine. *Ann Surg, 176*(4), 554-558.

Hutchison, S., Benson, R. A., Gibson, V. B., Pollock, A. H., Garside, P., & Brewer, J. M. (2012). Antigen depot is not required for alum adjuvanticity. *FASEB J, 26*(3), 1272-1279. doi:10.1096/fj.11-184556

Hwang, D. J., Roberts, I. M., & Wilson, T. M. (1994). Expression of tobacco mosaic virus coat protein and assembly of pseudovirus particles in Escherichia coli. *Proc Natl Acad Sci U S A, 91*(19), 9067-9071.

Inaba, K., Inaba, M., Romani, N., Aya, H., Deguchi, M., Ikehara, S., Steinman, R. M. (1992). Generation of large numbers of dendritic cells from mouse bone marrow cultures supplemented with granulocyte/macrophage colony-stimulating factor. *Journal of Experimental Medicine, 176*(6), 1693-1702.

Institute, N. C. (2015). Melanoma Treatment–for health professionals Retrieved from https://www.cancer.gov/types/skin/hp/melanoma-treatment-pdq

Ito, A. K., S.; Kim, Y.; Inoue, M., Fuse, M.; et al. (2015). Cancer Neoantigens: A Promising Source of Immunogens for Cancer Immunotherapy. *J Clin Cell Immunol, 6*(322). doi:10.4172/2155-9899.1000322

Janeway, C. A., Jr., & Medzhitov, R. (2002). Innate immune recognition. *Annu Rev Immunol, 20*, 197-216. doi:10.1146/annurev.immunol.20.083001.084359

Janik, J. E., Morris, J. C., O'Mahony, D., Pittaluga, S., Jaffe, E. S., Redon, C. E., Waldmann, T. A. (2015). 90Y-daclizumab, an anti-CD25 monoclonal antibody, provided responses in 50% of patients with relapsed Hodgkin's lymphoma. *Proc Natl Acad Sci U S A, 112*(42), 13045-13050. doi:10.1073/pnas.1516107112

Jazirehi, A. R., Lim, A., & Dinh, T. (2016). PD-1 inhibition and treatment of advanced melanoma-role of pembrolizumab. *Am J Cancer Res, 6*(10), 2117-2128.

Jemon, K., Young, V., Wilson, M., McKee, S., Ward, V., Baird, M., Hibma, M. (2013). An enhanced heterologous virus-like particle for human papillomavirus type 16 tumour immunotherapy. *PLoS One, 8*(6), e66866. doi:10.1371/journal.pone.0066866

Jen, J., & Wang, Y. C. (2016). Zinc finger proteins in cancer progression. *J Biomed Sci, 23*(1), 53. doi:10.1186/s12929-016-0269-9

Jewett, J. C., & Bertozzi, C. R. (2010). Cu-free click cycloaddition reactions in chemical biology. *Chem Soc Rev, 39*(4), 1272-1279.

Jia, R., Guo, J. H., & Fan, M. W. (2012). The effect of antigen size on the immunogenicity of antigen presenting cell targeted DNA vaccine. *Int Immunopharmacol, 12*(1), 21-25. doi:10.1016/j.intimp.2011.08.016

Joffre, O. P., Segura, E., Savina, A., & Amigorena, S. (2012). Cross-presentation by dendritic cells. *Nat Rev Immunol, 12*(8), 557-569. doi:10.1038/nri3254

Johansen, P., Mohanan, D., Martinez-Gomez, J. M., Kundig, T. M., & Gander, B. (2010). Lympho-geographical concepts in vaccine delivery. *J Control Release, 148*(1), 56-62. doi:10.1016/j.jconrel.2010.05.019

Johnston, R. J., Comps-Agrar, L., Hackney, J., Yu, X., Huseni, M., Yang, Y., Grogan, J. L. (2014). The immunoreceptor TIGIT regulates antitumor and antiviral CD8(+) T cell effector function. *Cancer Cell, 26*(6), 923-937. doi:10.1016/j.ccell.2014.10.018

Kadowaki, N., Ho, S., Antonenko, S., Malefyt, R. W., Kastelein, R. A., Bazan, F., & Liu, Y. J. (2001). Subsets of human dendritic cell precursors express different toll-like receptors and respond to different microbial antigens. *Journal of Experimental Medicine, 194*(6), 863-869.

Kafri, T., Morgan, D., Krahl, T., Sarvetnick, N., Sherman, L., & Verma, I. (1998). Cellular immune response to adenoviral vector infected cells does not require de novo viral gene expression: implications for gene therapy. *Proc Natl Acad Sci U S A, 95*(19), 11377-11382.

Kakwere, H., Ingham, E. S., Allen, R., Mahakian, L. M., Tam, S. M., Zhang, H., Ferrara, K. W. (2017). Toward Personalized Peptide-Based Cancer Nanovaccines: A Facile and Versatile Synthetic Approach. *Bioconjug Chem, 28*(11), 2756-2771. doi:10.1021/acs.bioconjchem.7b00502

Kantoff, P. W., Schuetz, T. J., Blumenstein, B. A., Glode, L. M., Bilhartz, D. L., Wyand, M., Godfrey, W. R. (2010). Overall survival analysis of a phase II randomized controlled trial of a Poxviral-based PSA-targeted immunotherapy in metastatic castration-resistant prostate cancer. *J Clin Oncol, 28*(7), 1099-1105. doi:10.1200/JCO.2009.25.0597

Karachaliou, N., Gonzalez-Cao, M., Sosa, A., Berenguer, J., Bracht, J. W. P., Ito, M., & Rosell, R. (2017). The combination of checkpoint immunotherapy and targeted therapy in cancer. *Ann Transl Med, 5*(19), 388. doi:10.21037/atm.2017.06.47

Kaufman, H. L., & Bines, S. D. (2010). OPTIM trial: a Phase III trial of an oncolytic herpes virus encoding GM-CSF for unresectable stage III or IV melanoma. *Future Oncol, 6*(6), 941-949. doi:10.2217/fon.10.66

Kawakami, Y., Eliyahu, S., Sakaguchi, K., Robbins, P. F., Rivoltini, L., Yannelli, J. R., Rosenberg, S. A. (1994). Identification of the

immunodominant peptides of the MART-1 human melanoma antigen recognized by the majority of HLA-A2-restricted tumor infiltrating lymphocytes. *Journal of Experimental Medicine, 180*(1), 347-352.

Kazaks, A., Balmaks, R., Voronkova, T., Ose, V., & Pumpens, P. (2008). Melanoma vaccine candidates from chimeric hepatitis B core virus-like particles carrying a tumor-associated MAGE-3 epitope. *Biotechnol J, 3*(11), 1429-1436. doi:10.1002/biot.200800160

Keller, S. A., Bauer, M., Manolova, V., Muntwiler, S., Saudan, P., & Bachmann, M. F. (2010). Cutting edge: limited specialization of dendritic cell subsets for MHC class II-associated presentation of viral particles. *J Immunol, 184*(1), 26-29. doi:10.4049/jimmunol.0901540

Kelly, F. J., Miller, C. R., Buchsbaum, D. J., Gomez-Navarro, J., Barnes, M. N., Alvarez, R. D., & Curiel, D. T. (2000). Selectivity of TAG-72-targeted adenovirus gene transfer to primary ovarian carcinoma cells versus autologous mesothelial cells in vitro. *Clin Cancer Res, 6*(11), 4323-4333.

Kennedy, R., & Celis, E. (2008). Multiple roles for CD4+ T cells in anti-tumor immune responses. *Immunological Reviews, 222*, 129-144. doi:10.1111/j.1600-065X.2008.00616.x

Kerkmann, M., Rothenfusser, S., Hornung, V., Towarowski, A., Wagner, M., Sarris, A., Hartmann, G. (2003). Activation with CpG-A and CpG-B oligonucleotides reveals two distinct regulatory pathways of type I IFN synthesis in human plasmacytoid dendritic cells. *Journal of Immunology, 170*(9), 4465-4474.

Khong, H., & Overwijk, W. W. (2016). Adjuvants for peptide-based cancer vaccines. *J Immunother Cancer, 4*, 56. doi:10.1186/s40425-016-0160-y

Kirn, D., Martuza, R. L., & Zwiebel, J. (2001). Replication-selective virotherapy for cancer: Biological principles, risk management and future directions. *Nat Med, 7*(7), 781-787. doi:10.1038/89901

Kissenpfennig, A., Henri, S., Dubois, B., Laplace-Builhe, C., Perrin, P., Romani, N., Malissen, B. (2005). Dynamics and function of Langerhans cells in vivo: dermal dendritic cells colonize lymph node areas distinct from slower migrating Langerhans cells. *Immunity, 22*(5), 643-654. doi:10.1016/j.immuni.2005.04.004

Klinman, D. M. (2004). Immunotherapeutic uses of CpG oligodeoxynucleotides. *Nat Rev Immunol, 4*(4), 249-258. doi:10.1038/nri1329

Koster, B. D., van den Hout, M., Sluijter, B. J. R., Molenkamp, B. G., Vuylsteke, R., Baars, A., de Gruijl, T. D. (2017). Local Adjuvant Treatment with Low-Dose CpG-B Offers Durable Protection against Disease Recurrence in Clinical Stage I-II Melanoma: Data from Two Randomized Phase II Trials. *Clin Cancer Res, 23*(19), 5679-5686. doi:10.1158/1078-0432.CCR-17-0944

Kozlovska, T. M., Cielens, I., Vasiljeva, I., Strelnikova, A., Kazaks, A., Dislers, A., Pumpens, P. (1996). RNA phage Q beta coat protein as a carrier for foreign epitopes. *Intervirology, 39*(1-2), 9-15.

Kranzer, K., Bauer, M., Lipford, G. B., Heeg, K., Wagner, H., & Lang, R. (2000). CpG-oligodeoxynucleotides enhance T-cell receptor-triggered interferon-gamma production and up-regulation of CD69 via induction

of antigen-presenting cell-derived interferon type I and interleukin-12. *Immunology, 99*(2), 170-178.

Kreiter, S., Vormehr, M., van de Roemer, N., Diken, M., Lower, M., Diekmann, J., Sahin, U. (2015). Mutant MHC class II epitopes drive therapeutic immune responses to cancer. *Nature, 520*(7549), 692-696. doi:10.1038/nature14426

Krieg, A. M. (2006). Therapeutic potential of Toll-like receptor 9 activation. *Nat Rev Drug Discov, 5*(6), 471-484. doi:10.1038/nrd2059

Krieg, A. M., Yi, A. K., Matson, S., Waldschmidt, T. J., Bishop, G. A., Teasdale, R., Klinman, D. M. (1995). CpG motifs in bacterial DNA trigger direct B-cell activation. *Nature, 374*(6522), 546-549. doi:10.1038/374546a0

Kroemer, G., & Zitvogel, L. (2012). Can the exome and the immunome converge on the design of efficient cancer vaccines? *Oncoimmunology, 1*(5), 579-580. doi:10.4161/onci.20730

Kruit, W. H., Suciu, S., Dreno, B., Mortier, L., Robert, C., Chiarion-Sileni, V., Keilholz, U. (2013). Selection of immunostimulant AS15 for active immunization with MAGE-A3 protein: results of a randomized phase II study of the European Organisation for Research and Treatment of Cancer Melanoma Group in Metastatic Melanoma. *Journal of Clinical Oncology, 31*(19), 2413-2420. doi:10.1200/JCO.2012.43.7111

Lacasse, P., Denis, J., Lapointe, R., Leclerc, D., & Lamarre, A. (2008). Novel plant virus-based vaccine induces protective cytotoxic T-lymphocyte-mediated antiviral immunity through dendritic cell maturation. *J Virol, 82*(2), 785-794. doi:10.1128/JVI.01811-07

Lai, C., Duan, S., Ye, F., Hou, X., Li, X., Zhao, J., Lu, X. (2018). The enhanced antitumor-specific immune response with mannose- and CpG-ODN-coated liposomes delivering TRP2 peptide. *Theranostics, 8*(6), 1723-1739. doi:10.7150/thno.22056

Lamm, D. L., Blumenstein, B. A., Crawford, E. D., Montie, J. E., Scardino, P., Grossman, H. B., et al. (1991). A randomized trial of intravesical doxorubicin and immunotherapy with bacille Calmette-Guerin for transitional-cell carcinoma of the bladder. *N Engl J Med, 325*(17), 1205-1209. doi:10.1056/NEJM199110243251703

Larkin, J., Hodi, F. S., & Wolchok, J. D. (2015). Combined Nivolumab and Ipilimumab or Monotherapy in Untreated Melanoma. *N Engl J Med, 373*(13), 1270-1271. doi:10.1056/NEJMc1509660

Lawrence, M. S., Stojanov, P., Polak, P., Kryukov, G. V., Cibulskis, K., Sivachenko, A., Getz, G. (2013). Mutational heterogeneity in cancer and the search for new cancer-associated genes. *Nature, 499*(7457), 214-218. doi:10.1038/nature12213

Le, D. T., Uram, J. N., Wang, H., Bartlett, B. R., Kemberling, H., Eyring, A. D., Diaz, L. A., Jr. (2015). PD-1 Blockade in Tumors with Mismatch-Repair Deficiency. *N Engl J Med, 372*(26), 2509-2520. doi:10.1056/NEJMoa1500596

Lebel, M. E., Chartrand, K., Leclerc, D., & Lamarre, A. (2015). Plant Viruses as Nanoparticle-Based Vaccines and Adjuvants. *Vaccines (Basel), 3*(3), 620-637. doi:10.3390/vaccines3030620

Lee, N., Zakka, L. R., Mihm, M. C., Jr., & Schatton, T. (2016). Tumour-infiltrating lymphocytes in melanoma prognosis and cancer

immunotherapy. *Pathology*, *48*(2), 177-187. doi:10.1016/j.pathol.2015.12.006

Lester, S. N., & Li, K. (2014). Toll-like receptors in antiviral innate immunity. *J Mol Biol*, *426*(6), 1246-1264. doi:10.1016/j.jmb.2013.11.024

Lesterhuis, W. J., de Vries, I. J., Schreibelt, G., Lambeck, A. J., Aarntzen, E. H., Jacobs, J. F., Figdor, C. G. (2011). Route of administration modulates the induction of dendritic cell vaccine-induced antigen-specific T cells in advanced melanoma patients. *Clin Cancer Res*, *17*(17), 5725-5735. doi:10.1158/1078-0432.CCR-11-1261

Lesueur, F., de Lichy, M., Barrois, M., Durand, G., Bombled, J., Avril, M. F., Zattara, H. (2008). The contribution of large genomic deletions at the CDKN2A locus to the burden of familial melanoma. *Br J Cancer*, *99*(2), 364-370. doi:10.1038/sj.bjc.6604470

Letavernier, E., Dansou, B., Lochner, M., Perez, J., Bellocq, A., Lindenmeyer, M. T., Baud, L. (2011). Critical role of the calpain/calpastatin balance in acute allograft rejection. *Eur J Immunol*, *41*(2), 473-484. doi:10.1002/eji.201040437

Leuthard, D. S., Duda, A., Freiberger, S. N., Weiss, S., Dommann, I., Fenini, G., Johansen, P. (2018). Microcrystalline Tyrosine and Aluminum as Adjuvants in Allergen-Specific Immunotherapy Protect from IgE-Mediated Reactivity in Mouse Models and Act Independently of Inflammasome and TLR Signaling. *J Immunol*, *200*(9), 3151-3159. doi:10.4049/jimmunol.1800035

Levenson, A. S., Thurn, K. E., Simons, L. A., Veliceasa, D., Jarrett, J., Osipo, C., Gartenhaus, R. B. (2005). MCT-1 oncogene contributes to increased in vivo tumorigenicity of MCF7 cells by promotion of angiogenesis and inhibition of apoptosis. *Cancer Res*, *65*(23), 10651-10656. doi:10.1158/0008-5472.CAN-05-0845

Li, H. (2013). Aligning sequence reads, clone sequences and assembly contigs with BWA-MEM. *Quantitative Biology Genomics, v2*(may 26, 2013).

Li, H., Handsaker, B., Wysoker, A., Fennell, T., Ruan, J., Homer, N., Genome Project Data Processing, S. (2009). The Sequence Alignment/Map format and SAMtools. *Bioinformatics*, *25*(16), 2078-2079. doi:10.1093/bioinformatics/btp352

Li, H., Willingham, S. B., Ting, J. P., & Re, F. (2008). Cutting edge: inflammasome activation by alum and alum's adjuvant effect are mediated by NLRP3. *J Immunol*, *181*(1), 17-21.

Li, M., Bharadwaj, U., Zhang, R., Zhang, S., Mu, H., Fisher, W. E., Yao, Q. (2008). Mesothelin is a malignant factor and therapeutic vaccine target for pancreatic cancer. *Mol Cancer Ther*, *7*(2), 286-296. doi:10.1158/1535-7163.MCT-07-0483

Li, W., Joshi, M. D., Singhania, S., Ramsey, K. H., & Murthy, A. K. (2014). Peptide Vaccine: Progress and Challenges. *Vaccines (Basel)*, *2*(3), 515-536. doi:10.3390/vaccines2030515

Liao, J. C., Gregor, P., Wolchok, J. D., Orlandi, F., Craft, D., Leung, C., Bergman, P. J. (2006). Vaccination with human tyrosinase DNA induces antibody responses in dogs with advanced melanoma. *Cancer Immun*, *6*, 8.

Liao, W., Lin, J. X., & Leonard, W. J. (2013). Interleukin-2 at the crossroads of effector responses, tolerance, and immunotherapy. *Immunity, 38*(1), 13-25. doi:10.1016/j.immuni.2013.01.004

Liau, L. M., Black, K. L., Martin, N. A., Sykes, S. N., Bronstein, J. M., Jouben-Steele, L., Cloughesy, T. F. (2000). Treatment of a patient by vaccination with autologous dendritic cells pulsed with allogeneic major histocompatibility complex class I-matched tumor peptides. Case Report. *Neurosurg Focus, 9*(6), e8.

Lipson, E. J., & Drake, C. G. (2011). Ipilimumab: an anti-CTLA-4 antibody for metastatic melanoma. *Clin Cancer Res, 17*(22), 6958-6962. doi:10.1158/1078-0432.CCR-11-1595

Liu, M. A., & Ulmer, J. B. (2005). Human clinical trials of plasmid DNA vaccines. *Adv Genet, 55*, 25-40. doi:10.1016/S0065-2660(05)55002-8

Liu, Y., Jang, S., Xie, L., & Sowa, G. (2014). Host deficiency in caveolin-2 inhibits lung carcinoma tumor growth by impairing tumor angiogenesis. *Cancer Res, 74*(22), 6452-6462. doi:10.1158/0008-5472.CAN-14-1408

Liu, Y., & Sowa, G. (2014). Role of caveolin-2 in subcutaneous tumor growth and angiogenesis associated with syngeneic mouse Lewis lung carcinoma and B16 melanoma models. *Cancer Cell Microenviron, 1*(6). doi:10.14800/ccm.439

Lopez, J. E., & Peppas, N. A. (2004). Effect of poly (ethylene glycol) molecular weight and microparticle size on oral insulin delivery from P(MAA-g-EG) microparticles. *Drug Dev Ind Pharm, 30*(5), 497-504. doi:10.1081/DDC-120037480

Lovly, C. M., Dahlman, K. B., Fohn, L. E., Su, Z., Dias-Santagata, D., Hicks, D. J., Pao, W. (2012). Routine multiplex mutational profiling of melanomas enables enrollment in genotype-driven therapeutic trials. *PLoS One, 7*(4), e35309. doi:10.1371/journal.pone.0035309

Lutzky, J. A., S. J.; Blake-Haskins, A.; Li X.; Robbins, P.B.; Shalabi, A.M. . (2014). A phase 1 study of MEDI4736, an anti-PD-L1 antibody, in patients with advanced solid tumors. *J Clin Oncol, 32*(%s).

Maecker, H. T., Umetsu, D. T., DeKruyff, R. H., & Levy, S. (1998). Cytotoxic T cell responses to DNA vaccination: dependence on antigen presentation via class II MHC. *J Immunol, 161*(12), 6532-6536.

Mahoney, K. M., Rennert, P. D., & Freeman, G. J. (2015). Combination cancer immunotherapy and new immunomodulatory targets. *Nat Rev Drug Discov, 14*(8), 561-584. doi:10.1038/nrd4591

Makkouk, A., & Weiner, G. J. (2015). Cancer immunotherapy and breaking immune tolerance: new approaches to an old challenge. *Cancer Res, 75*(1), 5-10. doi:10.1158/0008-5472.CAN-14-2538

Malvezzi, M., Carioli, G., Bertuccio, P., Boffetta, P., Levi, F., La Vecchia, C., & Negri, E. (2017). European cancer mortality predictions for the year 2017, with focus on lung cancer. *Ann Oncol, 28*(5), 1117-1123. doi:10.1093/annonc/mdx033

Manolova, V., Flace, A., Bauer, M., Schwarz, K., Saudan, P., & Bachmann, M. F. (2008). Nanoparticles target distinct dendritic cell populations according to their size. *Eur J Immunol, 38*(5), 1404-1413. doi:10.1002/eji.200737984

Marichal, T., Ohata, K., Bedoret, D., Mesnil, C., Sabatel, C., Kobiyama, K., Desmet, C. J. (2011). DNA released from dying host cells mediates

aluminum adjuvant activity. *Nat Med, 17*(8), 996-1002. doi:10.1038/nm.2403

Marshall, J. L., Hawkins, M. J., Tsang, K. Y., Richmond, E., Pedicano, J. E., Zhu, M. Z., & Schlom, J. (1999). Phase I study in cancer patients of a replication-defective avipox recombinant vaccine that expresses human carcinoembryonic antigen. *J Clin Oncol, 17*(1), 332-337. doi:10.1200/JCO.1999.17.1.332

Marshall, J. L., Hoyer, R. J., Toomey, M. A., Faraguna, K., Chang, P., Richmond, E., Schlom, J. (2000). Phase I study in advanced cancer patients of a diversified prime-and-boost vaccination protocol using recombinant vaccinia virus and recombinant nonreplicating avipox virus to elicit anti-carcinoembryonic antigen immune responses. *J Clin Oncol, 18*(23), 3964-3973. doi:10.1200/JCO.2000.18.23.3964

Martin Caballero, J., Garzon, A., Gonzalez-Cintado, L., Kowalczyk, W., Jimenez Torres, I., Calderita, G., von Kobbe, C. (2012). Chimeric infectious bursal disease virus-like particles as potent vaccines for eradication of established HPV-16 E7-dependent tumors. *PLoS One, 7*(12), e52976. doi:10.1371/journal.pone.0052976

Martinez-Lostao, L., Anel, A., & Pardo, J. (2015). How Do Cytotoxic Lymphocytes Kill Cancer Cells? *Clin Cancer Res, 21*(22), 5047-5056. doi:10.1158/1078-0432.CCR-15-0685

Martinson, J. A., Tenorio, A. R., Montoya, C. J., Al-Harthi, L., Gichinga, C. N., Krieg, A. M., Landay, A. L. (2007). Impact of class A, B and C CpG-oligodeoxynucleotides on in vitro activation of innate immune cells in human immunodeficiency virus-1 infected individuals. *Immunology, 120*(4), 526-535. doi:10.1111/j.1365-2567.2007.02530.x

Marusyk, A., & Polyak, K. (2010). Tumor heterogeneity: causes and consequences. *Biochim Biophys Acta, 1805*(1), 105-117. doi:10.1016/j.bbcan.2009.11.002

Mathe, G., Amiel, J. L., Schwarzenberg, L., Schneider, M., Cattan, A., Schlumberger, J. R., De Vassal, F. (1969). Active immunotherapy for acute lymphoblastic leukaemia. *Lancet, 1*(7597), 697-699.

Maximiano, S., Magalhaes, P., Guerreiro, M. P., & Morgado, M. (2016). Trastuzumab in the Treatment of Breast Cancer. *BioDrugs, 30*(2), 75-86. doi:10.1007/s40259-016-0162-9

McCarter, M. D., Baumgartner, J., Escobar, G. A., Richter, D., Lewis, K., Robinson, W., Gonzalez, R. (2007). Immunosuppressive dendritic and regulatory T cells are upregulated in melanoma patients. *Ann Surg Oncol, 14*(10), 2854-2860. doi:10.1245/s10434-007-9488-3

McCarthy, E. F. (2006). The toxins of William B. Coley and the treatment of bone and soft-tissue sarcomas. *Iowa Orthop J, 26*, 154-158.

McDermott, D., Haanen, J., Chen, T. T., Lorigan, P., O'Day, S., & Investigators, M.-. (2013). Efficacy and safety of ipilimumab in metastatic melanoma patients surviving more than 2 years following treatment in a phase III trial (MDX010-20). *Annals of Oncology, 24*(10), 2694-2698. doi:10.1093/annonc/mdt291

McDermott, D. F., Drake, C. G., Sznol, M., Choueiri, T. K., Powderly, J. D., Smith, D. C., Atkins, M. B. (2015). Survival, Durable Response, and Long-Term Safety in Patients With Previously Treated Advanced Renal

Cell Carcinoma Receiving Nivolumab. *J Clin Oncol, 33*(18), 2013-2020. doi:10.1200/JCO.2014.58.1041

McLaren, W., Gil, L., Hunt, S. E., Riat, H. S., Ritchie, G. R., Thormann, A., .Cunningham, F. (2016). The Ensembl Variant Effect Predictor. *Genome Biol, 17*(1), 122. doi:10.1186/s13059-016-0974-4

Meacham, C. E., & Morrison, S. J. (2013). Tumour heterogeneity and cancer cell plasticity. *Nature, 501*(7467), 328-337. doi:10.1038/nature12624

Medjitna, T. D., Stadler, C., Bruckner, L., Griot, C., & Ottiger, H. P. (2006). DNA vaccines: safety aspect assessment and regulation. *Dev Biol (Basel), 126*, 261-270; discussion 327.

Mehnert, J. M., & Kluger, H. M. (2012). Driver mutations in melanoma: lessons learned from bench-to-bedside studies. *Curr Oncol Rep, 14*(5), 449-457. doi:10.1007/s11912-012-0249-5

Mellor, A. L., Lemos, H., & Huang, L. (2017). Indoleamine 2,3-Dioxygenase and Tolerance: Where Are We Now? *Front Immunol, 8*, 1360. doi:10.3389/fimmu.2017.01360

Mempel, T. R., Henrickson, S. E., & Von Andrian, U. H. (2004). T-cell priming by dendritic cells in lymph nodes occurs in three distinct phases. *Nature, 427*(6970), 154-159. doi:10.1038/nature02238

Mendez, R., Ruiz-Cabello, F., Rodriguez, T., Del Campo, A., Paschen, A., Schadendorf, D., & Garrido, F. (2007). Identification of different tumor escape mechanisms in several metastases from a melanoma patient undergoing immunotherapy. *Cancer Immunol Immunother, 56*(1), 88-94. doi:10.1007/s00262-006-0166-2

Mihm, M. C., Jr., & Mule, J. J. (2015). Reflections on the Histopathology of Tumor-Infiltrating Lymphocytes in Melanoma and the Host Immune Response. *Cancer Immunol Res, 3*(8), 827-835. doi:10.1158/2326-6066.CIR-15-0143

Mingozzi, F., & High, K. A. (2013). Immune responses to AAV vectors: overcoming barriers to successful gene therapy. *Blood, 122*(1), 23-36. doi:10.1182/blood-2013-01-306647

Miranda Poma, J., Ostios Garcia, L., Villamayor Sanchez, J., & D'Errico, G. (2018). What do we know about cancer immunotherapy? Long-term survival and immune-related adverse events. *Allergol Immunopathol (Madr)*. doi:10.1016/j.aller.2018.04.005

Mohsen, M. O., Gomes, A. C., Cabral-Miranda, G., Krueger, C. C., Leoratti, F. M., Stein, J. V., & Bachmann, M. F. (2017). Delivering adjuvants and antigens in separate nanoparticles eliminates the need of physical linkage for effective vaccination. *J Control Release, 251*, 92-100. doi:10.1016/j.jconrel.2017.02.031

Mohsen, M. O., Gomes, A. C., Vogel, M., & Bachmann, M. F. (2018). Interaction of Viral Capsid-Derived Virus-Like Particles (VLPs) with the Innate Immune System. *Vaccines (Basel), 6*(3). doi:10.3390/vaccines6030037

Mohsen, M. O., Zha, L., Cabral-Miranda, G., & Bachmann, M. F. (2017). Major findings and recent advances in virus-like particle (VLP)-based vaccines. *Semin Immunol, 34*, 123-132. doi:10.1016/j.smim.2017.08.014

Moorthy, V. S., & Ballou, W. R. (2009). Immunological mechanisms underlying protection mediated by RTS,S: a review of the available data. *Malar J, 8*, 312. doi:10.1186/1475-2875-8-312

Morton, D. L., Foshag, L. J., Hoon, D. S., Nizze, J. A., Famatiga, E., Wanek, L. A., et al. (1992). Prolongation of survival in metastatic melanoma after active specific immunotherapy with a new polyvalent melanoma vaccine. *Ann Surg, 216*(4), 463-482.

Morton, D. L., Hsueh, E. C., Essner, R., Foshag, L. J., O'Day, S. J., Bilchik, A., Elashoff, R. M. (2002). Prolonged survival of patients receiving active immunotherapy with Canvaxin therapeutic polyvalent vaccine after complete resection of melanoma metastatic to regional lymph nodes. *Ann Surg, 236*(4), 438-448; discussion 448-439. doi:10.1097/01.SLA.0000029242.77191.D6

Moynihan, K. D., Opel, C. F., Szeto, G. L., Tzeng, A., Zhu, E. F., Engreitz, J. M., Irvine, D. J. (2016). Eradication of large established tumors in mice by combination immunotherapy that engages innate and adaptive immune responses. *Nat Med, 22*(12), 1402-1410. doi:10.1038/nm.4200

Murphy M. K., W. C. (2016). *Janeway's Immunobiology* (8 ed.).

Murray, A. A., Wang, C., Fiering, S., & Steinmetz, N. F. (2018). In Situ Vaccination with Cowpea vs Tobacco Mosaic Virus against Melanoma. *Mol Pharm*. doi:10.1021/acs.molpharmaceut.8b00316

Naddafi, F., & Davami, F. (2015). Anti-CD19 Monoclonal Antibodies: a New Approach to Lymphoma Therapy. *Int J Mol Cell Med, 4*(3), 143-151.

Naftzger, C., Takechi, Y., Kohda, H., Hara, I., Vijayasaradhi, S., & Houghton, A. N. (1996). Immune response to a differentiation antigen induced by altered antigen: a study of tumor rejection and autoimmunity. *Proc Natl Acad Sci U S A, 93*(25), 14809-14814.

Naidoo, J., Page, D. B., Li, B. T., Connell, L. C., Schindler, K., Lacouture, M. E., Wolchok, J. D. (2015). Toxicities of the anti-PD-1 and anti-PD-L1 immune checkpoint antibodies. *Ann Oncol, 26*(12), 2375-2391. doi:10.1093/annonc/mdv383

Nair, S. K., Morse, M., Boczkowski, D., Cumming, R. I., Vasovic, L., Gilboa, E., & Lyerly, H. K. (2002). Induction of tumor-specific cytotoxic T lymphocytes in cancer patients by autologous tumor RNA-transfected dendritic cells. *Ann Surg, 235*(4), 540-549.

Neefjes, J., Jongsma, M. L., Paul, P., & Bakke, O. (2011). Towards a systems understanding of MHC class I and MHC class II antigen presentation. *Nat Rev Immunol, 11*(12), 823-836. doi:10.1038/nri3084

Neelapu, S. S., & Sharma, P. (2015). Targeting the tumor niche to treat cancer. *Proc Natl Acad Sci U S A, 112*(42), 12907-12908. doi:10.1073/pnas.1517389112

Nestle, F. O., Alijagic, S., Gilliet, M., Sun, Y., Grabbe, S., Dummer, R., Schadendorf, D. (1998). Vaccination of melanoma patients with peptide- or tumor lysate-pulsed dendritic cells. *Nat Med, 4*(3), 328-332.

Niikura, K., Matsunaga, T., Suzuki, T., Kobayashi, S., Yamaguchi, H., Orba, Y., Sawa, H. (2013). Gold nanoparticles as a vaccine platform: influence of size and shape on immunological responses in vitro and in vivo. *ACS Nano, 7*(5), 3926-3938. doi:10.1021/nn3057005

Nikolaev, S. I., Rimoldi, D., Iseli, C., Valsesia, A., Robyr, D., Gehrig, C., Antonarakis, S. E. (2011). Exome sequencing identifies recurrent

somatic MAP2K1 and MAP2K2 mutations in melanoma. *Nat Genet, 44*(2), 133-139. doi:10.1038/ng.1026

Nuzzaci, M., Piazzolla, G., Vitti, A., Lapelosa, M., Tortorella, C., Stella, I., Piazzolla, P. (2007). Cucumber mosaic virus as a presentation system for a double hepatitis C virus-derived epitope. *Arch Virol, 152*(5), 915-928. doi:10.1007/s00705-006-0916-7

O'Hagan, D. T., Friedland, L. R., Hanon, E., & Didierlaurent, A. M. (2017). Towards an evidence based approach for the development of adjuvanted vaccines. *Curr Opin Immunol, 47*, 93-102. doi:10.1016/j.coi.2017.07.010

O'Hagan, D. T., & Valiante, N. M. (2003). Recent advances in the discovery and delivery of vaccine adjuvants. *Nat Rev Drug Discov, 2*(9), 727-735. doi:10.1038/nrd1176

O'Neill, D. W., Adams, S., & Bhardwaj, N. (2004). Manipulating dendritic cell biology for the active immunotherapy of cancer. *Blood, 104*(8), 2235-2246. doi:10.1182/blood-2003-12-4392

Oehen, S., & Brduscha-Riem, K. (1998). Differentiation of naive CTL to effector and memory CTL: correlation of effector function with phenotype and cell division. *J Immunol, 161*(10), 5338-5346.

Okuyama, R., Aruga, A., Hatori, T., Takeda, K., & Yamamoto, M. (2013). Immunological responses to a multi-peptide vaccine targeting cancer-testis antigens and VEGFRs in advanced pancreatic cancer patients. *Oncoimmunology, 2*(11), e27010. doi:10.4161/onci.27010

Olotu, A., Lusingu, J., Leach, A., Lievens, M., Vekemans, J., Msham, S., Bejon, P. (2011). Efficacy of RTS,S/AS01E malaria vaccine and exploratory analysis on anti-circumsporozoite antibody titres and protection in children aged 5-17 months in Kenya and Tanzania: a randomised controlled trial. *Lancet Infect Dis, 11*(2), 102-109. doi:10.1016/S1473-3099(10)70262-0

Ong, H. K., Tan, W. S., & Ho, K. L. (2017). Virus like particles as a platform for cancer vaccine development. *PeerJ, 5*, e4053. doi:10.7717/peerj.4053

Ostrand-Rosenberg, S. (2010). Myeloid-derived suppressor cells: more mechanisms for inhibiting antitumor immunity. *Cancer Immunol Immunother, 59*(10), 1593-1600. doi:10.1007/s00262-010-0855-8

Ott, P. A., Hu, Z., Keskin, D. B., Shukla, S. A., Sun, J., Bozym, D. J., Wu, C. J. (2017). An immunogenic personal neoantigen vaccine for patients with melanoma. *Nature, 547*(7662), 217-221. doi:10.1038/nature22991

Palucka, K., & Banchereau, J. (2013). Dendritic-cell-based therapeutic cancer vaccines. *Immunity, 39*(1), 38-48. doi:10.1016/j.immuni.2013.07.004

Pan, Y., Zhang, Y., Jia, T., Zhang, K., Li, J., & Wang, L. (2012). Development of a microRNA delivery system based on bacteriophage MS2 virus-like particles. *FEBS J, 279*(7), 1198-1208. doi:10.1111/j.1742-4658.2012.08512.x

Park, J. H., Geyer, M. B., & Brentjens, R. J. (2016). CD19-targeted CAR T-cell therapeutics for hematologic malignancies: interpreting clinical outcomes to date. *Blood, 127*(26), 3312-3320. doi:10.1182/blood-2016-02-629063

Parkhurst, M. R., Fitzgerald, E. B., Southwood, S., Sette, A., Rosenberg, S. A., & Kawakami, Y. (1998). Identification of a shared HLA-A*0201-

restricted T-cell epitope from the melanoma antigen tyrosinase-related protein 2 (TRP2). *Cancer Res, 58*(21), 4895-4901.

Pashine, A., Valiante, N. M., & Ulmer, J. B. (2005). Targeting the innate immune response with improved vaccine adjuvants. *Nat Med, 11*(4 Suppl), S63-68. doi:10.1038/nm1210

Patel, S. P., Kim, D. W., Lacey, C. L., & Hwu, P. (2016). GNA11 Mutation in a Patient With Cutaneous Origin Melanoma: A Case Report. *Medicine (Baltimore), 95*(4), e2336. doi:10.1097/MD.0000000000002336

Phelps, J. P., Dang, N., & Rasochova, L. (2007). Inactivation and purification of cowpea mosaic virus-like particles displaying peptide antigens from Bacillus anthracis. *Journal of Virological Methods, 141*(2), 146-153. doi:10.1016/j.jviromet.2006.12.008

Phelps, J. P., Dao, P., Jin, H., & Rasochova, L. (2007). Expression and self-assembly of cowpea chlorotic mottle virus-like particles in Pseudomonas fluorescens. *J Biotechnol, 128*(2), 290-296. doi:10.1016/j.jbiotec.2006.10.005

Piazzolla, G., Nuzzaci, M., Tortorella, C., Panella, E., Natilla, A., Boscia, D., Antonaci, S. (2005). Immunogenic properties of a chimeric plant virus expressing a hepatitis C virus (HCV)-derived epitope: new prospects for an HCV vaccine. *J Clin Immunol, 25*(2), 142-152. doi:10.1007/s10875-005-2820-4

Pleckaityte, M., Bremer, C. M., Gedvilaite, A., Kucinskaite-Kodze, I., Glebe, D., & Zvirbliene, A. (2015). Construction of polyomavirus-derived pseudotype virus-like particles displaying a functionally active neutralizing antibody against hepatitis B virus surface antigen. *BMC Biotechnol, 15*, 85. doi:10.1186/s12896-015-0203-3

Postow, M. A., Chesney, J., Pavlick, A. C., Robert, C., Grossmann, K., McDermott, D., Hodi, F. S. (2015). Nivolumab and ipilimumab versus ipilimumab in untreated melanoma. *N Engl J Med, 372*(21), 2006-2017. doi:10.1056/NEJMoa1414428

Prosniak, M., Dierov, J., Okami, K., Tilton, B., Jameson, B., Sawaya, B. E., & Gartenhaus, R. B. (1998). A novel candidate oncogene, MCT-1, is involved in cell cycle progression. *Cancer Research, 58*(19), 4233-4237.

Pumpens, P. (2008). *Construction of novel vaccines on the basis of the virus-like particles: Hepatitis B virus proteins as vaccine carriers* (1st ed.): CRC Press, Taylor & Francis Group, Boca Raton London, New York.

Pumpens, P. (2016). *Viral Nanotechnology*. USA: Taylor and Francis Group

Qian, Y., Qiao, S., Dai, Y., Xu, G., Dai, B., Lu, L., Zhang, Z. (2017). Molecular-Targeted Immunotherapeutic Strategy for Melanoma via Dual-Targeting Nanoparticles Delivering Small Interfering RNA to Tumor-Associated Macrophages. *ACS Nano, 11*(9), 9536-9549. doi:10.1021/acsnano.7b05465

Rahbar, M., Naraghi, Z. S., Mardanpour, M., & Mardanpour, N. (2015). Tumor-Infiltrating CD8+ Lymphocytes Effect on Clinical Outcome of Muco-Cutaneous Melanoma. *Indian J Dermatol, 60*(2), 212. doi:10.4103/0019-5154.152571

Raimbourg, Q., Perez, J., Vandermeersch, S., Prignon, A., Hanouna, G., Haymann, J. P., Letavernier, E. (2013). The Calpain/Calpastatin System

Has Opposing Roles in Growth and Metastatic Dissemination of Melanoma. *PLoS One, 8*(4). doi:ARTN e60469

10.1371/journal.pone.0060469

Raman, R., & Vaena, D. (2015). Immunotherapy in Metastatic Renal Cell Carcinoma: A Comprehensive Review. *Biomed Res Int, 2015*, 367354. doi:10.1155/2015/367354

Randolph, G. J., Angeli, V., & Swartz, M. A. (2005). Dendritic-cell trafficking to lymph nodes through lymphatic vessels. *Nat Rev Immunol, 5*(8), 617-628. doi:10.1038/nri1670

Rath, M., Muller, I., Kropf, P., Closs, E. I., & Munder, M. (2014). Metabolism via Arginase or Nitric Oxide Synthase: Two Competing Arginine Pathways in Macrophages. *Front Immunol, 5*, 532. doi:10.3389/fimmu.2014.00532

Rech, A. J., Mick, R., Martin, S., Recio, A., Aqui, N. A., Powell, D. J., Jr., Vonderheide, R. H. (2012). CD25 blockade depletes and selectively reprograms regulatory T cells in concert with immunotherapy in cancer patients. *Sci Transl Med, 4*(134), 134ra162. doi:10.1126/scitranslmed.3003330

Reddy, B. Y., Miller, D. M., & Tsao, H. (2017). Somatic driver mutations in melanoma. *Cancer, 123*(S11), 2104-2117. doi:10.1002/cncr.30593

Redman, J. M., Gibney, G. T., & Atkins, M. B. (2016). Advances in immunotherapy for melanoma. *BMC Med, 14*, 20. doi:10.1186/s12916-016-0571-0

Regules, J. A., Cummings, J. F., & Ockenhouse, C. F. (2011). The RTS,S vaccine candidate for malaria. *Expert Rev Vaccines, 10*(5), 589-599. doi:10.1586/erv.11.57

Restifo, N. P., Dudley, M. E., & Rosenberg, S. A. (2012). Adoptive immunotherapy for cancer: harnessing the T cell response. *Nat Rev Immunol, 12*(4), 269-281. doi:10.1038/nri3191

Rhodes, A. R., Weinstock, M. A., Fitzpatrick, T. B., Mihm, M. C., Jr., & Sober, A. J. (1987). Risk factors for cutaneous melanoma. A practical method of recognizing predisposed individuals. *JAMA, 258*(21), 3146-3154.

Ribas, A., Kefford, R., Marshall, M. A., Punt, C. J., Haanen, J. B., Marmol, M., Hauschild, A. (2013). Phase III randomized clinical trial comparing tremelimumab with standard-of-care chemotherapy in patients with advanced melanoma. *J Clin Oncol, 31*(5), 616-622. doi:10.1200/JCO.2012.44.6112

Rice, J., Dunn, S., Piper, K., Buchan, S. L., Moss, P. A., & Stevenson, F. K. (2006). DNA fusion vaccines induce epitope-specific cytotoxic CD8(+) T cells against human leukemia-associated minor histocompatibility antigens. *Cancer Res, 66*(10), 5436-5442. doi:10.1158/0008-5472.CAN-05-3130

Rimmer, A., Phan, H., Mathieson, I., Iqbal, Z., Twigg, S. R. F., Consortium, W. G. S., Lunter, G. (2014). Integrating mapping-, assembly- and haplotype-based approaches for calling variants in clinical sequencing applications. *Nat Genet, 46*(8), 912-918. doi:10.1038/ng.3036

Rivoltini, L., Canese, P., Huber, V., Iero, M., Pilla, L., Valenti, R., Parmiani, G. (2005). Escape strategies and reasons for failure in the interaction between tumour cells and the immune system: how can we tilt the

balance towards immune-mediated cancer control? *Expert Opin Biol Ther, 5*(4), 463-476. doi:10.1517/14712598.5.4.463

Rizvi, N. A., Hellmann, M. D., Snyder, A., Kvistborg, P., Makarov, V., Havel, J. J., Chan, T. A. (2015). Cancer immunology. Mutational landscape determines sensitivity to PD-1 blockade in non-small cell lung cancer. *Science, 348*(6230), 124-128. doi:10.1126/science.aaa1348

Robert, C., Long, G. V., Brady, B., Dutriaux, C., Maio, M., Mortier, L., Ascierto, P. A. (2015). Nivolumab in Previously Untreated Melanoma without BRAF Mutation. *New England Journal of Medicine, 372*(4), 320-330. doi:10.1056/NEJMoa1412082

Robert, C., Schachter, J., Long, G. V., Arance, A., Grob, J. J., Mortier, L., investigators, K.-. (2015). Pembrolizumab versus Ipilimumab in Advanced Melanoma. *N Engl J Med, 372*(26), 2521-2532. doi:10.1056/NEJMoa1503093

Rodriguez-Cerdeira, C., Carnero Gregorio, M., Lopez-Barcenas, A., Sanchez-Blanco, E., Sanchez-Blanco, B., Fabbrocini, G., Guzman, R. A. (2017). Advances in Immunotherapy for Melanoma: A Comprehensive Review. *Mediators Inflamm, 2017*, 3264217. doi:10.1155/2017/3264217

Roenigk, H. H., Jr., Deodhar, S., St Jacques, R., & Burdick, K. (1974). Immunotherapy of malignant melanoma with vaccinia virus. *Arch Dermatol, 109*(5), 668-673.

Roldao, A., Mellado, M. C., Castilho, L. R., Carrondo, M. J., & Alves, P. M. (2010). Virus-like particles in vaccine development. *Expert Rev Vaccines, 9*(10), 1149-1176. doi:10.1586/erv.10.115

Romano, E., Rossi, M., Ratzinger, G., de Cos, M. A., Chung, D. J., Panageas, K. S., Young, J. W. (2011). Peptide-loaded Langerhans cells, despite increased IL15 secretion and T-cell activation in vitro, elicit antitumor T-cell responses comparable to peptide-loaded monocyte-derived dendritic cells in vivo. *Clin Cancer Res, 17*(7), 1984-1997. doi:10.1158/1078-0432.CCR-10-3421

Rosenberg, S. A., & Restifo, N. P. (2015). Adoptive cell transfer as personalized immunotherapy for human cancer. *Science, 348*(6230), 62-68. doi:10.1126/science.aaa4967

Rosenblatt, J., Vasir, B., Uhl, L., Blotta, S., Macnamara, C., Somaiya, P., Avigan, D. (2011). Vaccination with dendritic cell/tumor fusion cells results in cellular and humoral antitumor immune responses in patients with multiple myeloma. *Blood, 117*(2), 393-402. doi:10.1182/blood-2010-04-277137

Rubinstein, J. C., Sznol, M., Pavlick, A. C., Ariyan, S., Cheng, E., Bacchiocchi, A., Halaban, R. (2010). Incidence of the V600K mutation among melanoma patients with BRAF mutations, and potential therapeutic response to the specific BRAF inhibitor PLX4032. *J Transl Med, 8*, 67. doi:10.1186/1479-5876-8-67

Ruedl, C., Schwarz, K., Jegerlehner, A., Storni, T., Manolova, V., & Bachmann, M. F. (2005). Virus-like particles as carriers for T-cell epitopes: limited inhibition of T-cell priming by carrier-specific antibodies. *J Virol, 79*(2), 717-724. doi:10.1128/JVI.79.2.717-724.2005

Ruedl, C., Storni, T., Lechner, F., Bachi, T., & Bachmann, M. F. (2002). Cross-presentation of virus-like particles by skin-derived CD8(-) dendritic cells: a dispensable role for TAP. *Eur J Immunol, 32*(3), 818-825.

doi:10.1002/1521-4141(200203)32:3<818::AID-IMMU818>3.0.CO;2-U

Ruttinger, D., van den Engel, N. K., Winter, H., Schlemmer, M., Pohla, H., Grutzner, S., Hatz, R. A. (2007). Adjuvant therapeutic vaccination in patients with non-small cell lung cancer made lymphopenic and reconstituted with autologous PBMC: first clinical experience and evidence of an immune response. *J Transl Med, 5*, 43. doi:10.1186/1479-5876-5-43

Sadelain, M. (2017). CD19 CAR T Cells. *Cell, 171*(7), 1471. doi:10.1016/j.cell.2017.12.002

Sahin, U., Derhovanessian, E., Miller, M., Kloke, B. P., Simon, P., Lower, M., Tureci, O. (2017). Personalized RNA mutanome vaccines mobilize poly-specific therapeutic immunity against cancer. *Nature, 547*(7662), 222-226. doi:10.1038/nature23003

Saito, H., Frleta, D., Dubsky, P., & Palucka, A. K. (2006). Dendritic cell-based vaccination against cancer. *Hematol Oncol Clin North Am, 20*(3), 689-710. doi:10.1016/j.hoc.2006.02.011

Scheel, B., Braedel, S., Probst, J., Carralot, J. P., Wagner, H., Schild, H., Pascolo, S. (2004). Immunostimulating capacities of stabilized RNA molecules. *Eur J Immunol, 34*(2), 537-547. doi:10.1002/eji.200324198

Scheel, B., Teufel, R., Probst, J., Carralot, J. P., Geginat, J., Radsak, M., Pascolo, S. (2005). Toll-like receptor-dependent activation of several human blood cell types by protamine-condensed mRNA. *Eur J Immunol, 35*(5), 1557-1566. doi:10.1002/eji.200425656

Schlom, J. (2012). Therapeutic cancer vaccines: current status and moving forward. *J Natl Cancer Inst, 104*(8), 599-613. doi:10.1093/jnci/djs033

Schuler-Thurner, B., Schultz, E. S., Berger, T. G., Weinlich, G., Ebner, S., Woerl, P., Schuler, G. (2002). Rapid induction of tumor-specific type 1 T helper cells in metastatic melanoma patients by vaccination with mature, cryopreserved, peptide-loaded monocyte-derived dendritic cells. *Journal of Experimental Medicine, 195*(10), 1279-1288.

Schwartzentruber, D. J., Lawson, D. H., Richards, J. M., Conry, R. M., Miller, D. M., Treisman, J., Hwu, P. (2011). gp100 peptide vaccine and interleukin-2 in patients with advanced melanoma. *N Engl J Med, 364*(22), 2119-2127. doi:10.1056/NEJMoa1012863

Schwarz, K., Meijerink, E., Speiser, D. E., Tissot, A. C., Cielens, I., Renhof, R., Bachmann, M. F. (2005). Efficient homologous prime-boost strategies for T cell vaccination based on virus-like particles. *Eur J Immunol, 35*(3), 816-821. doi:10.1002/eji.200425755

Schwarz, K., Storni, T., Manolova, V., Didierlaurent, A., Sirard, J. C., Rothlisberger, P., & Bachmann, M. F. (2003). Role of Toll-like receptors in costimulating cytotoxic T cell responses. *Eur J Immunol, 33*(6), 1465-1470. doi:10.1002/eji.200323919

Segal, N. H., Parsons, D. W., Peggs, K. S., Velculescu, V., Kinzler, K. W., Vogelstein, B., & Allison, J. P. (2008). Epitope landscape in breast and colorectal cancer. *Cancer Res, 68*(3), 889-892. doi:10.1158/0008-5472.CAN-07-3095

Senti, G., Johansen, P., Haug, S., Bull, C., Gottschaller, C., Muller, P., Kundig, T. M. (2009). Use of A-type CpG oligodeoxynucleotides as an adjuvant in allergen-specific immunotherapy in humans: a phase I/IIa clinical

trial. *Clin Exp Allergy, 39*(4), 562-570. doi:10.1111/j.1365-2222.2008.03191.x

Senzer, N. N., Kaufman, H. L., Amatruda, T., Nemunaitis, M., Reid, T., Daniels, G., Nemunaitis, J. J. (2009). Phase II clinical trial of a granulocyte-macrophage colony-stimulating factor-encoding, second-generation oncolytic herpesvirus in patients with unresectable metastatic melanoma. *J Clin Oncol, 27*(34), 5763-5771. doi:10.1200/JCO.2009.24.3675

Servid, A., Jordan, P., O'Neil, A., Prevelige, P., & Douglas, T. (2013). Location of the bacteriophage P22 coat protein C-terminus provides opportunities for the design of capsid-based materials. *Biomacromolecules, 14*(9), 2989-2995. doi:10.1021/bm400796c

Sharma, P., & Allison, J. P. (2015). Immune checkpoint targeting in cancer therapy: toward combination strategies with curative potential. *Cell, 161*(2), 205-214. doi:10.1016/j.cell.2015.03.030

Sharma, P., Hu-Lieskovan, S., Wargo, J. A., & Ribas, A. (2017). Primary, Adaptive, and Acquired Resistance to Cancer Immunotherapy. *Cell, 168*(4), 707-723. doi:10.1016/j.cell.2017.01.017

Shi, B., Hsu, H. L., Evens, A. M., Gordon, L. I., & Gartenhaus, R. B. (2003). Expression of the candidate MCT-1 oncogene in B- and T-cell lymphoid malignancies. *Blood, 102*(1), 297-302. doi:10.1182/blood-2002-11-3486

Shurin, M. R., Naiditch, H., Zhong, H., & Shurin, G. V. (2011). Regulatory dendritic cells: new targets for cancer immunotherapy. *Cancer Biol Ther, 11*(11), 988-992.

Sloan, A. E., Dansey, R., Zamorano, L., Barger, G., Hamm, C., Diaz, F., Wood, G. (2000). Adoptive immunotherapy in patients with recurrent malignant glioma: preliminary results of using autologous whole-tumor vaccine plus granulocyte-macrophage colony-stimulating factor and adoptive transfer of anti-CD3-activated lymphocytes. *Neurosurg Focus, 9*(6), e9.

Sluijter, B. J., van den Hout, M. F., Koster, B. D., van Leeuwen, P. A., Schneiders, F. L., van de Ven, R., de Gruijl, T. D. (2015). Arming the Melanoma Sentinel Lymph Node through Local Administration of CpG-B and GM-CSF: Recruitment and Activation of BDCA3/CD141(+) Dendritic Cells and Enhanced Cross-Presentation. *Cancer Immunol Res, 3*(5), 495-505. doi:10.1158/2326-6066.CIR-14-0165

Snyder, A., & Chan, T. A. (2015). Immunogenic peptide discovery in cancer genomes. *Curr Opin Genet Dev, 30*, 7-16. doi:10.1016/j.gde.2014.12.003

Sober, A. J., Fitzpatrick, T. B., Mihm, M. C., Wise, T. G., Pearson, B. J., Clark, W. H., & Kopf, A. W. (1979). Early recognition of cutaneous melanoma. *JAMA, 242*(25), 2795-2799.

Society, A. C. (2016, Jan 4, 2018). Treatment of Melanoma Skin Cancer, by Stage. Retrieved from https://www.cancer.org/cancer/melanoma-skin-cancer/treating/by-stage.html

Sondak, V. K., Sabel, M. S., & Mule, J. J. (2006). Allogeneic and autologous melanoma vaccines: where have we been and where are we going? *Clin*

Cancer Res, 12(7 Pt 2), 2337s-2341s. doi:10.1158/1078-0432.CCR-05-2555

Speiser, D. E., Lienard, D., Rufer, N., Rubio-Godoy, V., Rimoldi, D., Lejeune, F., Romero, P. (2005). Rapid and strong human CD8+ T cell responses to vaccination with peptide, IFA, and CpG oligodeoxynucleotide 7909. *J Clin Invest, 115*(3), 739-746. doi:10.1172/JCI23373

Speiser, D. E., Schwarz, K., Baumgaertner, P., Manolova, V., Devevre, E., Sterry, W., Bachmann, M. F. (2010). Memory and effector CD8 T-cell responses after nanoparticle vaccination of melanoma patients. *J Immunother, 33*(8), 848-858. doi:10.1097/CJI.0b013e3181f1d614

Steele, J. C., Rao, A., Marsden, J. R., Armstrong, C. J., Berhane, S., Billingham, L. J., Steven, N. M. (2011). Phase I/II trial of a dendritic cell vaccine transfected with DNA encoding melan A and gp100 for patients with metastatic melanoma. *Gene Ther, 18*(6), 584-593. doi:10.1038/gt.2011.1

Stefanetti, G., Saul, A., MacLennan, C. A., & Micoli, F. (2015). Click Chemistry Applied to the Synthesis of Salmonella Typhimurium O-Antigen Glycoconjugate Vaccine on Solid Phase with Sugar Recycling. *Bioconjug Chem, 26*(12), 2507-2513. doi:10.1021/acs.bioconjchem.5b00521

Stein, C. A., & Cheng, Y. C. (1993). Antisense Oligonucleotides as Therapeutic Agents - Is the Bullet Really Magical. *Science, 261*(5124), 1004-1012. doi:DOI 10.1126/science.8351515

Steinberg, A. D., Krieg, A. M., Gourley, M. F., & Klinman, D. M. (1990). Theoretical and Experimental Approaches to Generalized Autoimmunity. *Immunological Reviews, 118*, 129-163. doi:DOI 10.1111/j.1600-065X.1990.tb00815.x

Stewart, J. H. t., & Rosenberg, S. A. (2000). Long-term survival of anti-tumor lymphocytes generated by vaccination of patients with melanoma with a peptide vaccine. *J Immunother, 23*(4), 401-404.

Stills, H. F., Jr. (2005). Adjuvants and antibody production: dispelling the myths associated with Freund's complete and other adjuvants. *ILAR J, 46*(3), 280-293.

Storni, T., & Bachmann, M. F. (2004). Loading of MHC class I and II presentation pathways by exogenous antigens: a quantitative in vivo comparison. *J Immunol, 172*(10), 6129-6135.

Storni, T., Lechner, F., Erdmann, I., Bachi, T., Jegerlehner, A., Dumrese, T., Bachmann, M. F. (2002). Critical role for activation of antigen-presenting cells in priming of cytotoxic T cell responses after vaccination with virus-like particles. *J Immunol, 168*(6), 2880-2886.

Storni, T., Ruedl, C., Schwarz, K., Schwendener, R. A., Renner, W. A., & Bachmann, M. F. (2004). Nonmethylated CG motifs packaged into virus-like particles induce protective cytotoxic T cell responses in the absence of systemic side effects. *J Immunol, 172*(3), 1777-1785.

Sun, Z., Fourcade, J., Pagliano, O., Chauvin, J. M., Sander, C., Kirkwood, J. M., & Zarour, H. M. (2015). IL10 and PD-1 Cooperate to Limit the Activity of Tumor-Specific CD8+ T Cells. *Cancer Res, 75*(8), 1635-1644. doi:10.1158/0008-5472.CAN-14-3016

Svedman, F. C., Pillas, D., Taylor, A., Kaur, M., Linder, R., & Hansson, J. (2016). Stage-specific survival and recurrence in patients with

cutaneous malignant melanoma in Europe - a systematic review of the literature. *Clin Epidemiol, 8*, 109-122. doi:10.2147/CLEP.S99021

Swetter, S. M. (2017). Cutaneous Melanoma.

Sznol, M., Kluger, H. M., Hodi, F. S., McDermott, D. F., Carvajal, R. D., Lawrence, D. P., Sosman, J. A. (2013). Survival and long-term follow-up of safety and response in patients (pts) with advanced melanoma (MEL) in a phase I trial of nivolumab (anti-PD-1; BMS-936558; ONO-4538). *Journal of Clinical Oncology, 31*(18).

Tabeta, K., Georgel, P., Janssen, E., Du, X., Hoebe, K., Crozat, K., Beutler, B. (2004). Toll-like receptors 9 and 3 as essential components of innate immune defense against mouse cytomegalovirus infection. *Proc Natl Acad Sci U S A, 101*(10), 3516-3521. doi:10.1073/pnas.0400525101

Takeda, K., & Akira, S. (2005). Toll-like receptors in innate immunity. *Int Immunol, 17*(1), 1-14. doi:10.1093/intimm/dxh186

Tartour, E., Pere, H., Maillere, B., Terme, M., Merillon, N., Taieb, J., Oudard, S. (2011). Angiogenesis and immunity: a bidirectional link potentially relevant for the monitoring of antiangiogenic therapy and the development of novel therapeutic combination with immunotherapy. *Cancer Metastasis Rev, 30*(1), 83-95. doi:10.1007/s10555-011-9281-4

Tegerstedt, K., Franzen, A., Ramqvist, T., & Dalianis, T. (2007). Dendritic cells loaded with polyomavirus VP1/VP2Her2 virus-like particles efficiently prevent outgrowth of a Her2/neu expressing tumor. *Cancer Immunol Immunother, 56*(9), 1335-1344. doi:10.1007/s00262-007-0281-8

Tegerstedt, K., Lindencrona, J. A., Curcio, C., Andreasson, K., Tullus, C., Forni, G., Ramqvist, T. (2005). A single vaccination with polyomavirus VP1/VP2Her2 virus-like particles prevents outgrowth of HER-2/neu-expressing tumors. *Cancer Res, 65*(13), 5953-5957. doi:10.1158/0008-5472.CAN-05-0335

Temizoz, B., Kuroda, E., & Ishii, K. J. (2016). Vaccine adjuvants as potential cancer immunotherapeutics. *Int Immunol, 28*(7), 329-338. doi:10.1093/intimm/dxw015

Testa, U., Castelli, G., & Pelosi, E. (2017). Melanoma: Genetic Abnormalities, Tumor Progression, Clonal Evolution and Tumor Initiating Cells. *Med Sci (Basel), 5*(4). doi:10.3390/medsci5040028

Thomas, C. E., Schiedner, G., Kochanek, S., Castro, M. G., & Lowenstein, P. R. (2001). Preexisting antiadenoviral immunity is not a barrier to efficient and stable transduction of the brain, mediated by novel high-capacity adenovirus vectors. *Hum Gene Ther, 12*(7), 839-846. doi:10.1089/104303401750148829

Tissot, A. C., Maurer, P., Nussberger, J., Sabat, R., Pfister, T., Ignatenko, S., Bachmann, M. F. (2008). Effect of immunisation against angiotensin II with CYT006-AngQb on ambulatory blood pressure: a double-blind, randomised, placebo-controlled phase IIa study. *Lancet, 371*(9615), 821-827. doi:10.1016/S0140-6736(08)60381-5

Topalian, S. L., Hodi, F. S., Brahmer, J. R., Gettinger, S. N., Smith, D. C., McDermott, D. F., Sznol, M. (2012). Safety, activity, and immune correlates of anti-PD-1 antibody in cancer. *N Engl J Med, 366*(26), 2443-2454. doi:10.1056/NEJMoa1200690

Topalian, S. L., Sznol, M., McDermott, D. F., Kluger, H. M., Carvajal, R. D., Sharfman, W. H., Hodi, F. S. (2014). Survival, durable tumor remission,

and long-term safety in patients with advanced melanoma receiving nivolumab. *J Clin Oncol, 32*(10), 1020-1030. doi:10.1200/JCO.2013.53.0105

Tsao, H., & Sober, A. J. (2005). Melanoma treatment update. *Dermatol Clin, 23*(2), 323-333. doi:10.1016/j.det.2004.09.005

Uematsu, S., & Akira, S. (2007). Toll-like receptors and Type I interferons. *J Biol Chem, 282*(21), 15319-15323. doi:10.1074/jbc.R700009200

UK, C. R. (2016). Melanoma skin cancer stages and types. Retrieved from https://www.cancerresearchuk.org/about-cancer/melanoma/stages-types

Umansky, V., & Sevko, A. (2012). Melanoma-induced immunosuppression and its neutralization. *Semin Cancer Biol, 22*(4), 319-326. doi:10.1016/j.semcancer.2012.02.003

Umansky, V., Sevko, A., Gebhardt, C., & Utikal, J. (2014). Myeloid-derived suppressor cells in malignant melanoma. *J Dtsch Dermatol Ges, 12*(11), 1021-1027. doi:10.1111/ddg.12411

Utaisincharoen, P., Kespichayawattana, W., Anuntagool, N., Chaisuriya, P., Pichyangkul, S., Krieg, A. M., & Sirisinha, S. (2003). CpG ODN enhances uptake of bacteria by mouse macrophages. *Clin Exp Immunol, 132*(1), 70-75.

Valenzuela, P., Medina, A., Rutter, W. J., Ammerer, G., & Hall, B. D. (1982). Synthesis and assembly of hepatitis B virus surface antigen particles in yeast. *Nature, 298*(5872), 347-350.

van 't Veer, L. J., Burgering, B. M., Versteeg, R., Boot, A. J., Ruiter, D. J., Osanto, S., Bos, J. L. (1989). N-ras mutations in human cutaneous melanoma from sun-exposed body sites. *Mol Cell Biol, 9*(7), 3114-3116.

van der Burg, S. H., Arens, R., Ossendorp, F., van Hall, T., & Melief, A. J. M. (2016). Vaccines for established cancer: overcoming the challenges posed by immune evasion. *Nature Reviews Cancer, 16*(4), 219-233. doi:10.1038/nrc.2016.16

van der Burg, S. H., Arens, R., Ossendorp, F., van Hall, T., & Melief, C. J. (2016). Vaccines for established cancer: overcoming the challenges posed by immune evasion. *Nature Reviews Cancer, 16*(4), 219-233. doi:10.1038/nrc.2016.16

van der Meijden, A. P., Sylvester, R. J., Oosterlinck, W., Hoeltl, W., Bono, A. V., & Group, E. G.-U. T. C. (2003). Maintenance Bacillus Calmette-Guerin for Ta T1 bladder tumors is not associated with increased toxicity: results from a European Organisation for Research and Treatment of Cancer Genito-Urinary Group Phase III Trial. *Eur Urol, 44*(4), 429-434.

Van Raamsdonk, C. D., Griewank, K. G., Crosby, M. B., Garrido, M. C., Vemula, S., Wiesner, T., Bastian, B. C. (2010). Mutations in GNA11 in uveal melanoma. *N Engl J Med, 363*(23), 2191-2199. doi:10.1056/NEJMoa1000584

Vasquez, M., Tenesaca, S., & Berraondo, P. (2017). New trends in antitumor vaccines in melanoma. *Ann Transl Med, 5*(19), 384. doi:10.21037/atm.2017.09.09

Vogelstein, B., Papadopoulos, N., Velculescu, V. E., Zhou, S., Diaz, L. A., Jr., & Kinzler, K. W. (2013). Cancer genome landscapes. *Science, 339*(6127), 1546-1558. doi:10.1126/science.1235122

Walsh, S. R., & Dolin, R. (2011). Vaccinia viruses: vaccines against smallpox and vectors against infectious diseases and tumors. *Expert Rev Vaccines, 10*(8), 1221-1240. doi:10.1586/erv.11.79

Wanebo, H. J., Pace, R., Hargett, S., Katz, D., & Sando, J. (1986). Production of and response to interleukin-2 in peripheral blood lymphocytes of cancer patients. *Cancer, 57*(3), 656-662.

Wang, S., Campos, J., Gallotta, M., Gong, M., Crain, C., Naik, E., Guiducci, C. (2016). Intratumoral injection of a CpG oligonucleotide reverts resistance to PD-1 blockade by expanding multifunctional CD8+ T cells. *Proc Natl Acad Sci U S A, 113*(46), E7240-E7249. doi:10.1073/pnas.1608555113

Wang, X. Y., Zuo, D. M., Sarkar, D., & Fisher, P. B. (2011). Blockade of cytotoxic T-lymphocyte antigen-4 as a new therapeutic approach for advanced melanoma. *Expert Opinion on Pharmacotherapy, 12*(17), 2695-2706. doi:10.1517/14656566.2011.629187

Warming "Cold" Melanoma with TLR9 Agonists. (2018). *Cancer Discov, 8*(6), 670. doi:10.1158/2159-8290.CD-ND2018-004

Weber, J. S., D'Angelo, S. P., Minor, D., Hodi, F. S., Gutzmer, R., Neyns, B., . . . Larkin, J. (2015). Nivolumab versus chemotherapy in patients with advanced melanoma who progressed after anti-CTLA-4 treatment (CheckMate 037): a randomised, controlled, open-label, phase 3 trial. *Lancet Oncol, 16*(4), 375-384. doi:10.1016/S1470-2045(15)70076-8

Weber, J. S., Yang, J. C., Atkins, M. B., & Disis, M. L. (2015). Toxicities of Immunotherapy for the Practitioner. *J Clin Oncol, 33*(18), 2092-2099. doi:10.1200/JCO.2014.60.0379

Wheeler, A. W., Marshall, J. S., & Ulrich, J. T. (2001). A Th1-inducing adjuvant, MPL, enhances antibody profiles in experimental animals suggesting it has the potential to improve the efficacy of allergy vaccines. *Int Arch Allergy Immunol, 126*(2), 135-139. doi:10.1159/000049504

Wheeler, A. W., Moran, D. M., Robins, B. E., & Driscoll, A. (1982). l-Tyrosine as an immunological adjuvant. *Int Arch Allergy Appl Immunol, 69*(2), 113-119.

Whiteside, T. L., Demaria, S., Rodriguez-Ruiz, M. E., Zarour, H. M., & Melero, I. (2016). Emerging Opportunities and Challenges in Cancer Immunotherapy. *Clin Cancer Res, 22*(8), 1845-1855. doi:10.1158/1078-0432.CCR-16-0049

Williams, M. L., & Sagebiel, R. W. (1994). Melanoma risk factors and atypical moles. *West J Med, 160*(4), 343-350.

Wilson, J. M. (2009). Lessons learned from the gene therapy trial for ornithine transcarbamylase deficiency. *Mol Genet Metab, 96*(4), 151-157. doi:10.1016/j.ymgme.2008.12.016

Wolchok, J. D., Yuan, J., Houghton, A. N., Gallardo, H. F., Rasalan, T. S., Wang, J., Perales, M. A. (2007). Safety and immunogenicity of tyrosinase DNA vaccines in patients with melanoma. *Mol Ther, 15*(11), 2044-2050. doi:10.1038/sj.mt.6300290

Wu, Z., Chen, K., Yildiz, I., Dirksen, A., Fischer, R., Dawson, P. E., & Steinmetz, N. F. (2012). Development of viral nanoparticles for efficient intracellular delivery. *Nanoscale, 4*(11), 3567-3576. doi:10.1039/c2nr30366c

Wykes, M., Pombo, A., Jenkins, C., & MacPherson, G. G. (1998). Dendritic cells interact directly with naive B lymphocytes to transfer antigen and initiate class switching in a primary T-dependent response. *J Immunol, 161*(3), 1313-1319.

Xagorari, A., & Chlichlia, K. (2008). Toll-like receptors and viruses: induction of innate antiviral immune responses. *Open Microbiol J, 2*, 49-59. doi:10.2174/1874285800802010049

Xiang, R., Luo, Y., Niethammer, A. G., & Reisfeld, R. A. (2008). Oral DNA vaccines target the tumor vasculature and microenvironment and suppress tumor growth and metastasis. *Immunol Rev, 222*, 117-128. doi:10.1111/j.1600-065X.2008.00613.x

Yarchoan, M., Hopkins, A., & Jaffee, E. M. (2017). Tumor Mutational Burden and Response Rate to PD-1 Inhibition. *N Engl J Med, 377*(25), 2500-2501. doi:10.1056/NEJMc1713444

Yildiz, I., Shukla, S., & Steinmetz, N. F. (2011). Applications of viral nanoparticles in medicine. *Curr Opin Biotechnol, 22*(6), 901-908. doi:10.1016/j.copbio.2011.04.020

Ying, H., Zaks, T. Z., Wang, R. F., Irvine, K. R., Kammula, U. S., Marincola, F. M., Restifo, N. P. (1999). Cancer therapy using a self-replicating RNA vaccine. *Nat Med, 5*(7), 823-827. doi:10.1038/10548

Yoon, H. I., Yhee, J. Y., Na, J. H., Lee, S., Lee, H., Kang, S. W., Kim, K. (2016). Bioorthogonal Copper Free Click Chemistry for Labeling and Tracking of Chondrocytes In Vivo. *Bioconjug Chem, 27*(4), 927-936. doi:10.1021/acs.bioconjchem.6b00010

Yoshimoto, T., Takeda, K., Tanaka, T., Ohkusu, K., Kashiwamura, S., Okamura, H., Nakanishi, K. (1998). IL-12 up-regulates IL-18 receptor expression on T cells, Th1 cells, and B cells: synergism with IL-18 for IFN-gamma production. *J Immunol, 161*(7), 3400-3407.

Yu, B., Dong, J., Wang, C., Zhan, Y., Zhang, H., Wu, J., Yu, X. (2013). Characteristics of neutralizing antibodies to adenovirus capsid proteins in human and animal sera. *Virology, 437*(2), 118-123. doi:10.1016/j.virol.2012.12.014

Yuan, J., Ku, G. Y., Adamow, M., Mu, Z., Tandon, S., Hannaman, D., Wolchok, J. D. (2013). Immunologic responses to xenogeneic tyrosinase DNA vaccine administered by electroporation in patients with malignant melanoma. *J Immunother Cancer, 1*, 20. doi:10.1186/2051-1426-1-20

Yue, H., Wei, W., Yue, Z., Lv, P., Wang, L., Ma, G., & Su, Z. (2010). Particle size affects the cellular response in macrophages. *Eur J Pharm Sci, 41*(5), 650-657. doi:10.1016/j.ejps.2010.09.006

Zeltins, A. (2013). Construction and characterization of virus-like particles: a review. *Mol Biotechnol, 53*(1), 92-107. doi:10.1007/s12033-012-9598-4

Zeltins, A., West, J., Zabel, F., El Turabi, A., Balke, I., Haas, S., Bachmann, M. F. (2017). Incorporation of tetanus-epitope into virus-like particles achieves vaccine responses even in older recipients in models of psoriasis, Alzheimer's and cat allergy. *NPJ Vaccines, 2*, 30. doi:10.1038/s41541-017-0030-8

Zhang, H. G., Chen, H. S., Peng, J. R., Shang, X. Y., Zhang, J., Xing, Q., Chen, W. F. (2007). Specific CD8(+)T cell responses to HLA-A2 restricted

MAGE-A3 p271-279 peptide in hepatocellular carcinoma patients without vaccination. *Cancer Immunol Immunother, 56*(12), 1945-1954. doi:10.1007/s00262-007-0338-8

Zhang, J., Fujimoto, J., Zhang, J., Wedge, D. C., Song, X., Zhang, J., Futreal, P. A. (2014). Intratumor heterogeneity in localized lung adenocarcinomas delineated by multiregion sequencing. *Science, 346*(6206), 256-259. doi:10.1126/science.1256930

Zhang, S., Yong, L. K., Li, D., Cubas, R., Chen, C., & Yao, Q. (2013). Mesothelin virus-like particle immunization controls pancreatic cancer growth through CD8+ T cell induction and reduction in the frequency of CD4+ foxp3+ ICOS- regulatory T cells. *PLoS One, 8*(7), e68303. doi:10.1371/journal.pone.0068303

Zhao, Q., Allen, M. J., Wang, Y., Wang, B., Wang, N., Shi, L., & Sitrin, R. D. (2012). Disassembly and reassembly improves morphology and thermal stability of human papillomavirus type 16 virus-like particles. *Nanomedicine, 8*(7), 1182-1189. doi:10.1016/j.nano.2012.01.007

Zhou, Q., Wang, F., Zhang, Y., Yang, F., Wang, Y., & Sun, S. (2011). Down-regulation of Prdx6 contributes to DNA vaccine induced vitiligo in mice. *Mol Biosyst, 7*(3), 809-816. doi:10.1039/c0mb00181c

Zigrino, P., Loffek, S., & Mauch, C. (2005). Tumor-stroma interactions: their role in the control of tumor cell invasion. *Biochimie, 87*(3-4), 321-328. doi:10.1016/j.biochi.2004.10.025

Zuckerman, J. N., Zuckerman, A. J., Symington, I., Du, W., Williams, A., Dickson, B., Group, U. K. H. S. (2001). Evaluation of a new hepatitis B triple-antigen vaccine in inadequate responders to current vaccines. *Hepatology, 34*(4 Pt 1), 798-802. doi:10.1053/jhep.2001.27564

7. Appendices

Supplementary figures and tables for chapter 2

Targeting germline and mutated epitopes enhances the immunogenicity of a preclinical model of personalized VLP-based vaccine

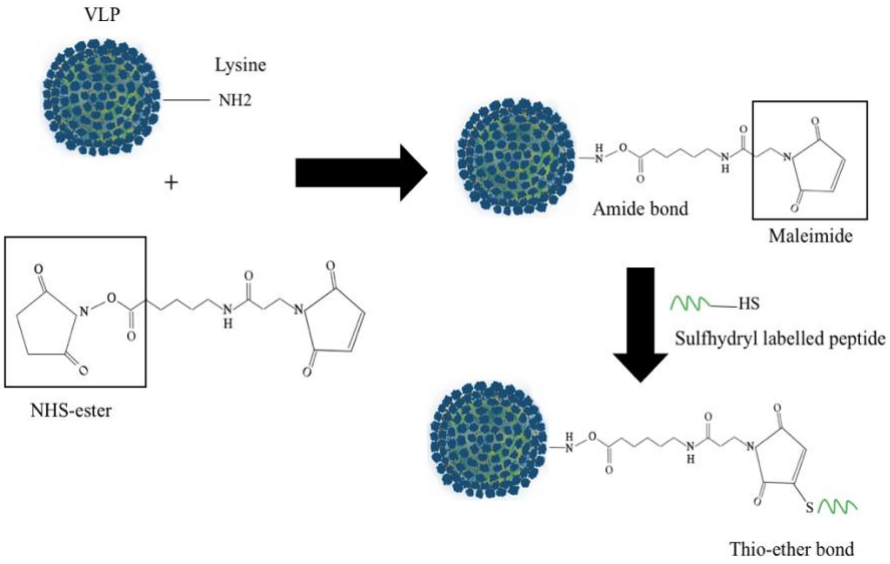

Figure 2.S 1 Schematic diagram illustrating SMPH chemistry

Schematic diagram illustrating the standard coupling method using SMPH cross-linker with NHS at one end and maleimide group on the other end. NHS reacts with Lys residues on VLPs while the maleimide reacts with peptide labelled with HS forming a thio-ether bond.

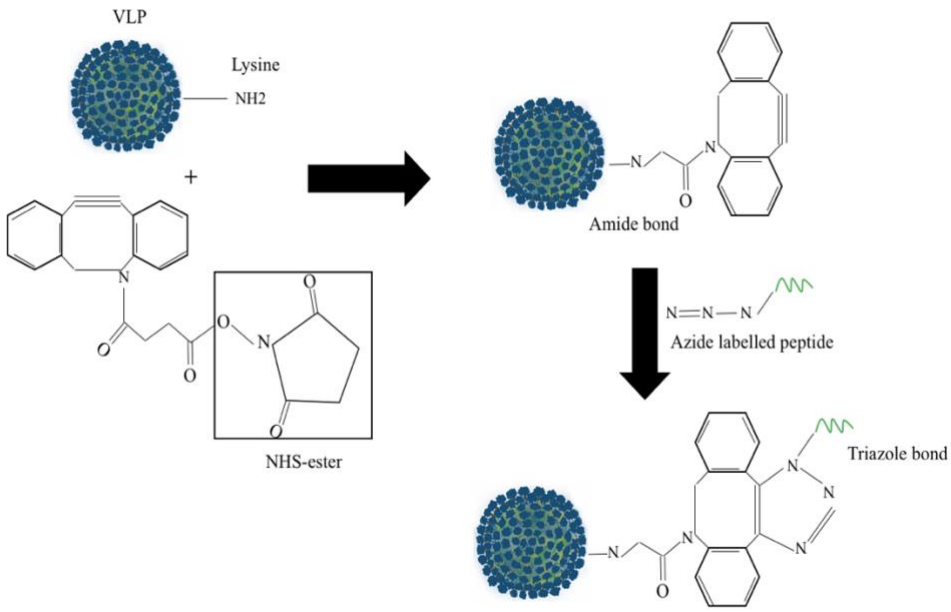

Figure 2.S 2 Schematic diagram illustrating Cu-free click chemistry

Schematic diagram illustrating the standard coupling method using Bio-orthogonal Cu-free click chemistry (dibenzocyclooctyne NHS ester DBCO), NHS ester reacts with Lys residues on VLPs and incorporates a cyclooctyne moiety which reacts with the azide labelled molecule forming a stable triazole linkage.

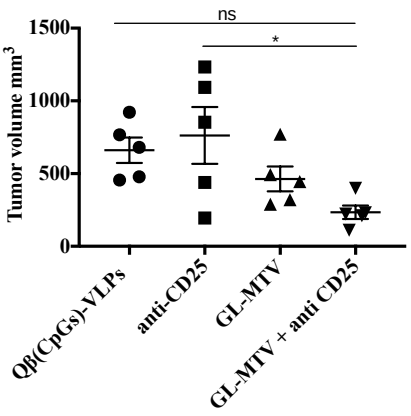

One-Way ANOVA (Turkey's Multiple Comparison Test)	*P* value
Qβ(CpGs)-VLPs vs anti-CD25	0.9272 ns
Qβ(CpGs)-VLPs vs GL-MTV	0.6464 ns
Qβ(CpGs)-VLPs vs GL-MTV+anti-CD25	0.0882 ns
anti-CD25 vs GL-MTV	0.3124 ns
anti-CD25 vs GL-MTV+anti-CD25	0.0274 *
GL vs GL-anti-CD25	0.531 ns

Figure 2.S 3 Combining GL-MTV with anti-CD25 mAb

Tumour volume mm^3 in the following designated groups; 1st group vaccinated with 120µg Qβ(CpGs)-VLPs, 2nd group vaccinated with 10µg anti-CD25 mAb i.v., 3rd group vaccinated with 120µg GL-MTV and the 4th group vaccinated with 120µg GL-MTV+10µg anti-CD25 mAb i.v. The GL-MTV in this experiment consisted of 4 germline peptides (PMEL17, MTC-1, Calpastatin and ZFP518). C57BL/6 mice were vaccinated 3 times over 14dys. Statistical analysis by One-Way ANOVA (Turkey's Multiple Comparison Test). *n=5* mice per group. One representative of 3 similar experiments is shown.

A.

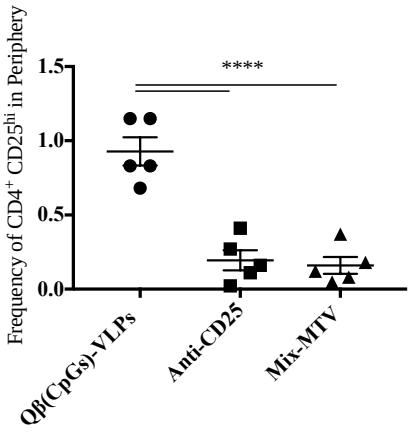

One-Way ANOVA (Turkey's Multiple Comparison Test)	*P* value
Qβ(CpGs)-VLPs vs anti-CD25	<0.0001 ****
Qβ(CpGs)-VLPs vs Mix-MTV	<0.0001 ****
anti-CD25 vs Mix-MTV	0.9422 ns

B.

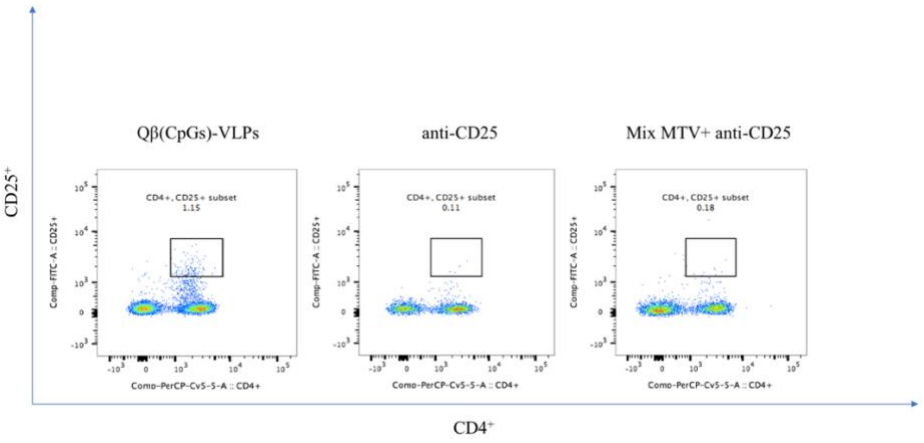

Figure 2.S 4 Tregs depletion in periphery of vaccinated mice

A. Frequency of Tregs ($CD4^{+}CD25^{hi+}$) cells in the periphery of C57BL/6 mice in the groups vaccinated with Qβ(CpGs)-VLPs, anti-CD25 and (Mix-MTV+anti-CD25) on day 6 post tumour transplantation. Statistical analysis by One-Way ANOVA (Turkey's Multiple Comparison Test). *B,* Representative FACS dot plot of frequency of Tregs ($CD4^{+}CD25^{hi+}$) cells in the periphery of C57BL/6 mice in the designated groups. *n=5* mice per group. One representative of 3 similar experiments is shown.

Table 2.S 1 Biological characteristics of the selected peptides from immunopeptidomics for the development of germline multi-target VLP-based vaccine (GL-MTV)

Selected Peptide	Biological Characteristics
Melanocyte protein PMEL (Melanocyte protein Pmel 17) (Premelanosome protein) (Silver locus protein) [Cleaved into: M-alpha; M-beta]	A melanocytes differentiation antigen –ortholog to gp100 in human- often overexpressed in melanoma and therefore constitute a good target in cancer immunotherapy. (Abad et al., 2008; Y. J. Chen et al., 2012)
MTC-1 Malignant T- cell-amplified sequence 1 (MCT-1) (Multiple copies T- cell malignancies 1)	The candidate oncogene MTC-1 promotes the development of lymphoid tumours, such tumours exhibit an increase in growth rate and avoid apoptosis. It has also been shown that overexpression of this protein contributes to breast cancer pathogenesis and progression. (Levenson et al., 2005; Prosniak et al., 1998; Shi, Hsu, Evens, Gordon, & Gartenhaus, 2003)
Calpastatin (Calpain inhibitor)	Calcium-dependent cysteine protease inhibitor (Calpain inhibitor). It has been shown that Calpastatin overexpression can increase the dissemination of B16F10 melanoma to regional LNs since Calpains are essential for the motility of immune cells towards solid tumours. (Letavernier et al., 2011; Raimbourg et al., 2013)
Zinc finger protein 518B	The largest family of transcription factors. Several zinc-finger motif classes have been identified as oncogenes causing tumourigenesis (Jen & Wang, 2016). Overexpression has also been reported in melanoma. https://www.proteinatlas.org/ENSG00000178163-ZNF518B/pathology
L-dopachrome tautomerase (DCT) (DT) (EC 5.3.3.12) (L-dopachrome Delta-isomerase) (SLATY locus	An enzyme participates in the biosynthesis of melanin pigment. Has been shown to be overexpressed in melanoma and therefore constitutes a good target in cancer immunotherapy.

protein) (Tyrosinase-related protein 2) (TRP-2) (TRP2)	(Bloom et al., 1997; Castle et al., 2012; W. Chu et al., 2000; Yuan et al., 2013)
Caveolin2	A protein expressed in stromal cells in tumour microenvironment of B16F10 melanoma. It has been reported that Caveolin2 promotes tumour growth and enhances neovascularization in B16F10. (Y. Liu, Jang, Xie, & Sowa, 2014; Y. Liu & Sowa, 2014)